

Understanding the Crosstalk between Bone and Gamma Delta T lymphocytes In Cancer Patients

By

Ms. Swati Popat Phalke

[LIFE09200904011]

Tata Memorial Centre, Navi Mumbai

*A thesis submitted to the
Board of Studies in Life Sciences
In partial fulfillment of requirements
For the Degree of*

DOCTOR OF PHILOSOPHY

of

HOMI BHABHA NATIONAL INSTITUTE

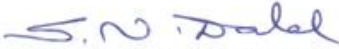


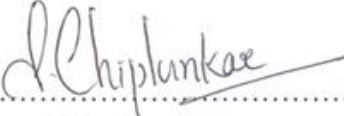
October, 2016

Homi Bhabha National Institute

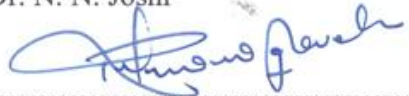
Recommendations of the Viva Voce Committee

As members of the Viva Voce Committee, we certify that we have read the dissertation prepared by Ms. Swati Popat Phalke, entitled "**Understanding the crosstalk between bone and gamma delta T lymphocytes in cancer patients**" and recommend that it may be accepted as fulfilling the thesis requirement for the award of Degree of Doctor of Philosophy.

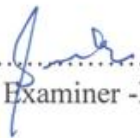

.....
Chairman - Dr. S.N. Dalal Date: 7/10/16


.....
Guide / Convener - Dr. S.V. Chiplunkar Date: 7/10/16


.....
Member 1 - Dr. N. N. Joshi Date: 7.10.16


.....
Member 2 - Dr. R.B. Govekar Date: 7.10.16


.....
Invitee-Dr. M.R. Wani Date: 7.10.16


.....
External Examiner -Dr. S.K. Arora Date: 07.10.2016

Final approval and acceptance of this thesis is contingent upon the candidate's submission of the final copies of the thesis to HBNI.

I hereby certify that I have read this thesis prepared under my direction and recommend that it may be accepted as fulfilling the thesis requirement.

Date:

Place: Navi Mumbai


Prof. S.V. Chiplunkar
(Guide)

STATEMENT BY AUTHOR

This dissertation has been submitted in partial fulfillment of requirements for an advanced degree at Homi Bhabha National Institute (HBNI) and is deposited in the Library to be made available to borrowers under rules of the HBNI.

Brief quotations from this dissertation are allowable without special permission, provided that accurate acknowledgement of source is made. Requests for permission for extended quotation from or reproduction of this manuscript in whole or in part may be granted by the Competent Authority of HBNI when in his or her judgment the proposed use of the material is in the interests of scholarship. In all other instances, however, permission must be obtained from the author.



Ms. Swati Popat Phalke

DECLARATION

I, hereby declare that the investigation presented in the thesis has been carried out by me. The work is original and has not been submitted earlier as a whole or in part for a degree / diploma at this or any other Institution / University.



Ms. Swati Popat Phalke

List of Publications arising from the thesis

Journal

1. “**Activation status of $\gamma\delta$ T cells dictates their effect on osteoclast generation and bone resorption**”, Swati P. Phalke, Shubhada V. Chiplunkar, “Bone Reports” (2015), Vol 3 (95-103)
2. “**Cytokine dynamics of $\gamma\delta$ T cells: A double edged sword in osteoclastogenesis**”, Swati Phalke and Shubhada V. Chiplunkar, “Journal of Cytokine Biology” (2016), Vol 1, issue 3 (In Press)

Chapters in books and lectures notes: Nil

Conferences

1. “*8th National Research Scholars Meet*” held at ACTREC, Mumbai during 21st-22nd December 2012, Swati P. Phalke, Shubhada V. Chiplunkar, “Understanding the crosstalk between $\gamma\delta$ T cells and osteoclasts in patients with breast cancer”
2. “*32nd Annual Convention of Indian Association for Cancer Research*”, held at New Delhi during 13-16th February 2013, Swati Phalke, Vani Parmar, Sudeep Gupta, Rajendra Badwe, Shubhada Chiplunkar, “Understanding the crosstalk between $\gamma\delta$ T cells and osteoclasts in patients with breast cancer”
3. “*Tata Platinum Jubilee Conference*” , held at Mumbai, Italy during -26th - 28th February, 2016, Swati Phalke, Rajendra Badwe, Vani Parmar, Shubhada Chiplunkar, “Zoledronate induced $\gamma\delta$ T cells activation: A potential cell based cancer therapy”
4. “*15th International congress of Immunology*”, held in Milan, Italy during 22nd-27th August 2013, Swati Phalke, Vani Parmar, Sudeep Gupta, Rajendra Badwe, Shubhada Chiplunkar, “Understanding the crosstalk between $\gamma\delta$ T cells and osteoclasts in patients with breast cancer”, Abstract was published in “Frontiers in Immunology”

Others: Nil



Ms. Swati Papat Phalke

This thesis is my small contribution to science.....

Acknowledgement

“It is during our darkest moments that we must focus to see the light - Aristotle Onassis”

This thesis is not only a representation of my work; it is the journey where I got introduced to the field of science. My experience at ACTREC has been nothing short of extraordinary. It has laid a sound foundation for my future in research, a place where I strengthened my scientific prowess. It has also molded me into a person who believes in the value of hard-work, the power of observation, the significance of questioning everything and most significantly into a person who understands the importance of believing in yourself. My time here is always going to be a part of me that I will proudly carry along on my journey ahead. My journey as a PhD student has been a series of professional and personal milestones and at the end of it, I would like to take a moment and thank everyone who made it a memorable experience.

I wish to thank my advisor, **Professor. Shubhada V. Chiplunkar**. She has been the most wonderful guide and I am eternally grateful for her patience during my early days at the lab, her support and encouragement throughout my thesis work. Prof. Chiplunkar's expertise and experience in the field has assisted me in my research work. I thank her for all the wonderful opportunities and for the motivation and freedom in writing this thesis.

I would like to thank the members of my doctoral committee: **Dr. K.B. Sainis, Dr. Rajiv Gude, Lt. Dr. Rajiv Kalraiya, Dr. Narendra Joshi, Dr. Rukmini Govekar** and **Dr. Sorab Dalal** for their insightful comments and encouragement and also for the hard questions which incited me to widen my research perspectives.

My sincere gratitude goes to **Dr. Mohan Wani (NCCS, Pune)** and **Dr. Rukmini Govekar (ACTREC)**, who provided me the opportunity, during the initial stages of my doctoral work, to learn human osteoclast culture work and proteomics work, respectively. I am immensely thankful to **Dr. Sudeep Gupta**, Deputy Director of ACTREC, for helping me in procuring the breast cancer patient samples. I am indebted to all the **breast cancer patients and healthy volunteers**, who voluntarily participated in our study.

I extend my thanks to Flow cytometry facility (Ms. Shamal Vetale, Mrs. Rekha Gaur and Mr. Ravi Joshi), Mass spectrometry facility (Mr. Shashi Dolas, Mrs. Savita Prabhu-Chavan and Mr. Prashant Masane) and imaging facility (Mrs. Vaishali Kailaje and Mrs. Tanuja Dighe) for their tremendous help during my work. I am thankful to the Director's office (Mrs. Pritha Menon and Mrs. Lata Shelar), Programme office (Mrs. Maya Dolas), Administration department (Chitramam, Sujatamam, Seema mam and Lisa), Accounts department (Arunamam) and Dispatch department for their assistance over these years. I would also like to extend my thanks to Mr. Dinesh Pawar (Hostel caretaker) and Anumavashi, who made the hostel stay comfortable.

I acknowledge my gratitude to Department of Biotechnology- Government of India for fellowship and to Tata Memorial Centre for "Seed In Air" grant (Project funding awarded to Dr. S.V.Chiplunkar) for supporting this thesis work.

I am obliged to all the Chiplunkar Lab members (Dr. Kode, Meenatai, Shamalmam, Truptimam, Sawantbhai, Dakave uncle and Ram), my fellow colleagues (Bhairavbhai, Dimpu, Aparna, Asif, Rushikesh, Sajad, Shalini, Sachin and Neha) for their help during the times needed. I would like to remember friends like Arpit, Ayush, Pradipbhau, Babita, Vasanti, Amruta, Kalpesh, Minal and Nirupama for their selfless support and encouragement throughout my stay. The memories we created together will always be special to me. Special thanks to Dr. Amit Fulzele and Dr. Biharilal Soni who helped tremendously during proteomics work.

Most importantly, I take this opportunity to express my profound gratitude to my family (Aai, Pappa, Girish and Supriyavahini) and my best friend Rahul for their support through the hard times. Without them, I would not have completed this journey. I am lucky to have them! I also want to thank "Bhai" and his family members for their love and support. I thank them all a thousand times for not letting me feel alone and being there for me always.

Ms. Swati Popat Phalke

CONTENTS

Page No.

<i>Synopsis</i>	<i>(1-15)</i>
<i>List of figures</i>	<i>(17-19)</i>
<i>List of tables</i>	<i>(20)</i>
<i>Abbreviations</i>	<i>(21-23)</i>
<i>Chapter 1: Introduction</i>	<i>(25-31)</i>
<i>Chapter 2: Review of Literature</i>	<i>(33-60)</i>
[2.1] Breast cancer.....	35
[2.2] Classification of breast cancer.....	36
[2.3] Bone is the preferential site of metastasis.....	40
[2.4] Bone remodeling.....	42
[2.5] Crosstalk between tumor cells, immune cells and bone cells.....	48
[2.6] Vicious cycle.....	51
[2.7] Aminobisphosphonates.....	53
[2.8] $\gamma\delta$ T cells.....	55
<i>Chapter 3: Materials and methods</i>	<i>(61-108)</i>
[3.1] Culture medium.....	63
[3.2] Preparation of buffers.....	63
[3.3] Maintenance of cell lines.....	66
[3.4] Antibodies and recombinant proteins.....	67
[3.5] Study group.....	69
[3.6] Cell separation techniques.....	70
[3.7] Generation and characterization of mouse and human osteoclasts.....	72
[3.8] Flow cytometry.....	78
[3.9] Cytokine estimation in serum sample and cell free supernatants of $\gamma\delta$ T cells.....	82
[3.10] Confocal microscopy.....	83
[3.11] MTT Assay.....	87

CONTENTS

Page No.

[3.12] Identification of differentially expressed protein in MCF7 cells upon Zoledronate treatment by 2D PAGE-MALDI-TOF/TOF.....	88
[3.13] Liquid chromatography-Mass spectrometry.....	100
[3.14] Validation of differentially expressed proteins by western blotting.....	105

Chapter 4: Results-I

<i>To investigate the effect of $\gamma\delta$ T cells on osteoclastogenesis.....</i>	<i>(109-148)</i>
[4.1] Analysis of activation markers on $\gamma\delta$ T cells.....	112
[4.2] Effect of $\gamma\delta$ T cells on human osteoclastogenesis.....	124
[4.3] Cytokine profiling of cell free supernatants of antigen activated $\gamma\delta$ T cells.....	141
[4.4] Effect of IL6 and IFN γ neutralization in cell free supernatants of “unstimulated” $\gamma\delta$ T cells on osteoclast function.....	145

Chapter 5: Results-II

<i>To understand the effect of aminobisphosphonate (Zoledronate) on protein profiles of breast tumor cells.....</i>	<i>(149-196)</i>
[5.1] Determination of sublethal concentration of Zoledronate for treatment of MCF7 cells.....	152
[5.2] Separation of differentially expressed proteins in MCF7 cells upon Zoledronate treatment by 2-dimensional (2D) polyacrylamide gel electrophoresis.....	153
[5.3] Identification of differentially expressed proteins in MCF7 upon Zoledronate treatment by 2D PAGE/MALDI-TOD TOF.....	161
[5.4] Identification of differentially expressed proteins in Zoledronate treated MCF7 cells by liquid chromatography-mass spectrometry (LC-MS).....	163
[5.5] Interactome analysis.....	180
[5.6] Validation of differentially expressed proteins.....	182

CONTENTS

Page No.

Chapter 6: Results-III

Immune profiling of breast cancer patients on Zoledronate treatment.....(197-216)

[6.1] Demographic analysis of breast cancer patients.....200

[6.2] Immune profile of metastatic (Zoledronate treated) and
non-metastatic (untreated) breast cancer patients..... 201

[6.3] Zoledronate treatment activated both $\alpha\beta$ and $\gamma\delta$ T cells in breast cancer
patients.....205

[6.4] Zoledronate treatment activated central memory $\gamma\delta$ T cells.....209

[6.5] Effect of Zoledronate treatment on intracellular cytokines profile of
 $\gamma\delta$ T cells.....211

[6.6] Cytokine profiling of cell free supernatants collected of $\gamma\delta$ T cells isolated from
HI and breast cancer patients (Rx^- and Rx^+).....214

Chapter 7: Discussion.....(217-240)

Chapter 8: Summary and Conclusion.....(241-250)

References.....(251-274)

Publications.....(275)

Homi Bhabha National Institute



SYNOPSIS OF Ph.D. THESIS

- 1. Name of the Student:** Ms. Swati Popat Phalke
- 2. Name of the Constituent Institution:** Advanced Centre for Treatment , Research and Education in Cancer-Tata Memorial Centre
- 3. Enrolment No. :** LIFE09200904011
- 4. Title of the Thesis:** “Understanding the crosstalk between bone and gamma delta T lymphocytes in cancer patients”
- 5. Board of Studies:** Life Sciences

SYNOPSIS

Introduction

Breast cancer is the second most commonly occurring cancer in the world (Globocan 2012). 70% of breast cancer patients show bone metastasis, accounting for death of these patients [1]. Bone is a dynamic structure which undergoes continuous remodeling, which is under the tight control of osteoblasts and osteoclasts. Osteoblasts are derived from mesenchymal cells, secrete bone matrix proteins and promote mineralization. Osteoclasts are large multinucleated cells generated by fusion of monocyte-macrophage precursor cells [2] and are known to decalcify and degrade the bone by secreting the lysosomal proteases [3]. Therapeutic modalities to treat bone metastasis are targeted to modulating the bone microenvironment or to reduce bone resorption [4,5]. Antiresorptive bisphosphonates are used as standard drug treatment for skeletal disorders and

bone metastasis [6,7]. Aminobisphosphonates inhibit farnesyl pyrophosphate synthase in the mevalonate pathway thus inhibit mevalonate pathway [6], upregulate intracellular levels of isopentenyl pyrophosphate (IPP), inhibits osteoclastogenesis [8] and tumor cells [9,10].

Human $\gamma\delta$ T cells are a small subset of immune cells accounting for 5-10% of total T cell population in peripheral blood and possess unique properties like MHC independent antigen recognition, tissue tropism, gene usage and the antigens they recognize [11,12]. Major subtype of $\gamma\delta$ T cells in human peripheral blood expresses V γ 9V δ 2 TCR and secrete copious amount of IFN γ upon stimulation [13,14]. $\gamma\delta$ T cells play an important role in antitumor cytotoxicity [15,16], wound healing and tissue repair [17,18,19]. These cells express natural killer receptors [20,21] and recognize stressed/ tumor cells expressing MICA/B and ULBPs [22]. $\gamma\delta$ T cells recognize unique set of antigens like intermediate products of eukaryotic mevalonate pathway (isopentenyl pyrophosphate or its synthetic analog bromohydrin pyrophosphate) and bacterial Rohmer pathway (HMBPP ((E)-4-Hydroxy-3-methyl-but-2-enylpyrophosphate), alkylamines and aminobisphosphonates [20,23]. Antitumor ability of $\gamma\delta$ T cells against solid tumors and leukemia's has been widely reported [24,25,26,27]. Recent reports have suggested presence of $\gamma\delta$ T cells in the bone [28], but their role in osteoclastogenesis is not well understood.

There is a great interest in understanding how T lymphocytes interact with osteoclasts and influence their function. Activated CD4⁺ T cells secrete pro-osteoclastogenic [29,30] and anti-osteoclastogenic cytokines [31,32], but it is still not understood what dictates their pro and anti-osteoclastogenic behavior. Although the role of CD4⁺ $\alpha\beta$ T cells in osteoclastogenesis has been thoroughly investigated, the role of $\gamma\delta$ T cells is not well understood. We hypothesize that; aminobisphosphonates may have a profound influence on tumor cells that make them susceptible to lysis by $\gamma\delta$ T cells. Simultaneously their anti-resorptive activity on osteoclasts may be

explained by their ability to activate the innate immune cells like $\gamma\delta$ T cells that accelerate the cross talk between immune and skeletal system.

Aim and Objectives

1. To investigate the effect of $\gamma\delta$ T cells on osteoclastogenesis
2. To understand the effect of aminobisphosphonate (Zoledronate) on protein profiles of breast tumor cells
3. Immune profiling of breast cancer patients on Zoledronate treatment

Methodology

Separation of “freshly isolated” and “activated” $\gamma\delta$ T cell from peripheral blood

Peripheral blood mononuclear cells (PBMCs) were separated from heparinized peripheral blood of healthy individuals and breast cancer patients by Ficoll Hypaque density gradient centrifugation. These PBMCs were expanded using α CD3/CD28+ rhIL2 for 12 days and $\gamma\delta$ T cells were immunomagnetically purified using $\gamma\delta$ T cell separation kit and were termed as “activated” $\gamma\delta$ T cells. $\gamma\delta$ T cells separated directly from fresh PBMCs were termed as “freshly isolated” $\gamma\delta$ T cells. Separated $\gamma\delta$ T cells were checked for purity and populations having >95% purity were used for experiments.

Generation and characterization of human osteoclasts

CD14⁺ precursor cells were immunomagnetically purified from PBMCs using CD14⁺ cell separation kit (Milteny Biotech). These CD14⁺ cells (1×10^5) were cultured in complete α MEM (200 μ l) containing recombinant human macrophage colony stimulating factor (rhMCSF, 30ng/ml) and recombinant human receptor activator of nuclear factor kappa B ligand (rhRANKL, 40ng/ml) on thermanox coverslips for 21 days, with intermediate feedings on every 3rd day. On 21st days, osteoclasts were characterized by staining them for multinucleation,

tartarate resistant acid phosphatase (TRAP) or vitronectin receptor (23c6 or CD51/61). Cells showing multinucleation (>3 nuclei) and TRAP positivity or vitronectin receptor positivity were considered as mature osteoclasts.

CD14⁺: $\gamma\delta$ T cell coculture assay

CD14⁺ cells (1×10^5) were cocultured with autologous unstimulated “activated” or “freshly isolated” $\gamma\delta$ T cells (1×10^4) in complete α MEM (200 μ l) containing rhMCSF, rhRANKL and rhIL2 (0.5IU). As a positive control, osteoclasts were generated from CD14⁺ cells in the presence of rhMCSF and rhRANKL only. Effect of phosphoantigen stimulated “freshly isolated” $\gamma\delta$ T cells on osteoclastogenesis was analyzed by adding BrHPP (200nM) to cocultures along with rhMCSF and rhRANKL on Day 0. CD14⁺: $\gamma\delta$ T cells (10:1) were fed with rhMCSF, rhRANKL and rhIL2 for 21 days, with intermediate feedings on every 3rd day. On 21st day, number of osteoclasts (multinucleated, 23c6⁺ cells) generated in an entire well were quantified and the effect of $\gamma\delta$ T cells on osteoclastogenesis was determined by analyzing increase or decrease in the total number of osteoclast generated per well as compared to control wells.

Generation of human osteoclast in the presence of cells free supernatants of $\gamma\delta$ T cells

“Activated” and “freshly isolated” $\gamma\delta$ T cells were stimulated with rhIL2 or BrHPP+rhIL2 for 24 hrs and cell free supernatants were collected. Osteoclast precursor cells (OPCs) were generated from CD14⁺ precursor cells (1×10^5) in the presence of rhMCSF and rhRANKL for 12 days in osteoclast activity assay substrate module (OAAS, synthetic Ca₂PO₄ coated slides). From 12th day onwards, every 3rd day, the cultures were supplemented with pretitrated volumes of cell free supernatant of stimulated “activated” and “freshly isolated” $\gamma\delta$ T cells along with rhMCSF and rhRANKL. Osteoclasts generated in the presence of rhMCSF and rhRANKL were kept as positive control. On 21st day, cells were bleached out using 6% sodium hypochlorite and 5.2%

sodium chloride. OAAS plates were air dried and resorption area/pits generated by mature resorbing osteoclasts were imaged and quantitated using ImageJ software. Effect of $\gamma\delta$ T cells on resorptive ability of osteoclasts was assessed by comparing the total resorbed area generated by osteoclasts in the presence of cell free supernatant of $\gamma\delta$ T cells compared to positive control.

IL6-IFN γ neutralization assay

Role of IFN γ and IL6 on osteoclastogenesis were analyzed by neutralizing these cytokines in cell free supernatants of $\gamma\delta$ T cells used for resorption assays. Osteoclasts were generated from CD14⁺ cells (1×10^5) in the presence of rhMCSF and rhRANKL for 12 days in OAAS module as described earlier. From 12th day onwards, every 3rd day, the cells were supplemented with rhMCSF, rhRANKL and cell free supernatant of unstimulated “activated” and “non-activated/freshly isolated” $\gamma\delta$ T cells, with or without antihuman α IFN γ or α IL6 neutralization antibody (10 μ g/ml) respectively. Osteoclasts generated in the presence of rhMCSF and rhRANKL were kept as positive control. On 21st day, the cultures were terminated and resorption area generated by mature resorbing osteoclasts in OAAS well was calculated using ImageJ software.

2D-PAGE-MS

MCF7 cells were treated with Zoledronate (100 μ M) or left untreated for 24 hrs at 37°C. Lysates were prepared using urea based lysis buffer (8M urea, 2M thiourea, 1% CHAPS, 1% DTT) and protein estimation was done by TCA method. Two dimensional profiles of the Zoledronate treated and untreated MCF7 cells were generated using 3-10 nonlinear, 17cm IPG strip according to Laemmli [33] and gels were silver stained for visualization of the proteins. Protein profiles of untreated and Zoledronate treated MCF7 cells were compared using PDQuest software for differential protein expression. Proteins spots showing quantitative /qualitative changes were separated, destained and were subjected for *in gel digestion* with trypsin (HPLC grade). Tryptic

peptides were reconstituted in 10% acetonitrile with 0.1% TFA. Reconstituted peptides were acquired on MALDI TOF-TOF Ultraflex-II (Brucker Daltonics) and data was analyzed using MASCOT search engine.

LC-MS

iTRAQ labeling followed by LC-MS was used to analyze quantitative differences between zoledronate treated and untreated MCF7 cells. Zoledronate (100 μ M) treated and untreated MCF7 cells lysed in NP-40 based lysis buffer and protein estimation was done by TCA method. Proteins from untreated and Zoledronate treated MCF7 lysates were digested *in solution* using trypsin at 37°C. These trypsin digested peptides were, delipidated, purified and concentrated using Zip-tip and were vacuum dried. iTRAQ labeling of peptides was carried out using kit as per the kit instructions. Samples were acquired using Nano LC-ESI-Q TOF (Triple TOF 5600+, AB SCIEX, USA). The data was analyzed using Protein PilotTM Software.

Multicolor flow cytometry

Multicolor flow cytometry was used to analyze immune cell subsets, their activation status, intracellular cytokines, memory status of healthy individuals and breast cancer patients. PBMCs (1x10⁶/50 μ l) were stained with combination of fluochrome labeled monoclonal antibodies (1 μ g/1x10⁶ cells) for 30 min at 4°C in dark. The cells were washed with 1X PBS, fixed in 1% paraformaldehyde for 15 min at 4°C in dark. Atleast 50000 events were acquired on FACS Aria and data was analyzed using FlowJo software.

Cytokine estimation by Cytometric bead array CBA

“Freshly isolated” or “activated” $\gamma\delta$ T cells from healthy individuals or breast cancer patients were stimulated with rhIL2, BrHPP+rhIL2, Zoledronate+rhIL2 or were kept unstimulated (incubated in medium only/ control) for 24 hrs. After 24 hrs, cell free supernatants were

collected and analyzed for Th1/Th2/Th17 cytokines (IL2, IL4, IL6, IL10, TNF α , IFN γ and IL17) using CBA kit (BD Biosciences) as per the kit instructions.

Results

Objective 1: To investigate the effect of $\gamma\delta$ T cells in osteoclastogenesis

Analysis of activation markers on “freshly isolated” $\gamma\delta$ T cells (directly separated from PBMCs) and “activated” $\gamma\delta$ T cells (separated from α CD3/CD28+rhIL2 expanded PBMCs) was carried out. “Freshly isolated” $\gamma\delta$ T cells showed low levels of activation markers (CD69, CD25 and RANKL), while “activated” $\gamma\delta$ T cells showed higher expression of activation markers on them. Antigenic stimulation of both “freshly isolated” and “activated” $\gamma\delta$ T cells with rhIL2, BrHPP+rhIL2 and Zoledronate+rhIL2 showed significant increase in expression of these activation markers. To study the direct effect of $\gamma\delta$ T cells on osteoclastogenesis, osteoclasts were generated from CD14⁺ cells in the presence of autologous “freshly isolated” and “activated” $\gamma\delta$ T cells. CD14⁺ cells cultured in the presence of “activated” $\gamma\delta$ T cells showed significant reduction in total number of generated osteoclasts, while “freshly isolated” $\gamma\delta$ T cells significantly increased total number of osteoclasts compared to positive control. Long term stimulation of “freshly isolated” $\gamma\delta$ T cells with BrHPP during coculture, showed reduction in osteoclast generation. Similarly, generation of osteoclasts in the presence of cell free supernatants of rhIL2 or BrHPP+rhIL2 stimulated “activated” $\gamma\delta$ T cells showed reduction of osteoclast function (resorption area generated by mature osteoclast). Contrary to that, cell free supernatants of “freshly isolated” $\gamma\delta$ T cells, stimulated with rhIL2 or BrHPP+rhIL2 showed significant increase in resorption area. Cytokine profile of cell free supernatant of unstimulated “freshly isolated” and “activated” $\gamma\delta$ T cells showed major differences in IL6 and IFN γ levels. At

baseline level, “activated” $\gamma\delta$ T cells produced higher levels of anti-osteoclastogenic IFN γ , while “freshly isolated” $\gamma\delta$ T cells were major producers of pro-osteoclastogenic cytokine IL6. Stimulation of both “freshly isolated” and “activated” $\gamma\delta$ T cells with rhIL2, BrHPP or Zoledronate upregulated IFN γ levels, but levels of IL6 remained higher in case of “freshly isolated” $\gamma\delta$ T cells. Pro and anti –osteoclastogenic effect of $\gamma\delta$ T cells on osteoclastogenesis through IFN γ and IL6 was further validated by neutralizing these cytokines using blocking antibodies. Blocking of IFN γ in cell free supernatants of “activated” $\gamma\delta$ T cells reverted its anti-osteoclastogenic effect, while blocking of IL6 from cell free supernatants of “freshly isolated” $\gamma\delta$ T cells showed reduction in resorption area. Our results suggests that the dynamics of IFN γ and IL6 play a major role in mediating the pro and antiosteoclastogenic effects of “activated” $\gamma\delta$ T cells and “freshly isolated” $\gamma\delta$ T cells respectively.

Objective 2: To understand the effect of aminobisphosphonate Zoledronate on protein profiles of breast tumor cells

Comparative analysis of 2D profiles of Zoledronate treated and untreated MCF7 cells showed quantitative and qualitative changes in proteins expression. Among the proteins identified by MALDI-TOF TOF, most of the proteins were cytoskeletal elements (Keratin 7,8,18 and β tubulin) and enzymes (α -enolase, Phosphoglycerate mutase1, Triosephosphate isomerase, Peroxiredoxin 1). A more sensitive approach, iTRAQ labeling followed by LC-MS was used to analyze quantitative differences between Zoledronate treated and untreated MCF7 cells. Total 2222 proteins were identified. Out of that, 148 proteins were upregulated (Treated/untreated=1.5), and 26 proteins showed downregulation (Treated/untreated=0.5). PANTHER analysis showed major changes in cellular and metabolic processes in MCF7 cells upon Zoledronate treatment. A significant upregulation in “diphosphomevalonate decarboxylase/

phosphomevalonate decarboxylase” enzyme, which catalyzes last step of isopentenyl pyrophosphate generation from mevalonate (IPP, potent $\gamma\delta$ T cell antigen) was observed, along with other $\gamma\delta$ T cells recruiting (S100A8, IPP) and activating (HSP60) proteins. Zoledronate treatment caused upregulation of tumor antigens (mellanotransferrins and melanoma antigen D2). Proteins involved in immune synapse formation between T cells and antigen presenting cells (dynamins, CD2AP, phocein, clusterins) were found upregulated. Zoledronate upregulated expression of proteins involved in apoptosis, copper toxicity, EGFR degradation, glycolytic enzymes, while proteins involved in cytoskeletal reorganization, vesicular trafficking, protein degradation and cell adhesion were found downregulated. Zoledronate also downregulated the proteins involved in DNA repair and chromatin remodeling, arresting breast tumor cells in S-phase (validated by cell cycle experiment).

Objective 3: Immune profiling of breast cancer patients on Zoledronate treatment

Comparative immune profiling of breast cancer patients on Zoledronate treatment (n=21), without Zoledronate treatment (n =28) and healthy individuals (n=32) was carried out. Total CD3⁺ T cells in peripheral blood of breast cancer patients (both Zoledronate treated and Zoledronate untreated) were reduced as compared to healthy individuals. Zoledronate treatment in breast cancer patients showed significant increase in cytotoxic T cells (CD8⁺), natural killer cells and B cells, while percentages of regulatory T cells, monocytes (osteoclast precursor cells) were reduced compared to Zoledronate untreated breast cancer patients and healthy individuals. $\gamma\delta$ T cell percentages in peripheral blood of breast cancer patients on Zoledronate treatment were reduced but these cells were in highly activated state (high CD25, RANKL and increased IFN γ production). Analysis of memory status of $\gamma\delta$ T cells showed significant increase in effector memory cells with concomitant decrease in central memory cells. Zoledronate activated $\gamma\delta$ T

cells showed increased IFN γ secretion upon antigenic stimulation. Cytokine profiling of cell free supernatants of unstimulated $\gamma\delta$ T cells of Zoledronate treated breast cancer patient showed reduced IL6 (pro-osteoclastogenic and pro-tumorogenic) levels compared to Zoledronate untreated breast cancer patient and healthy individuals. This showed correlation with our *in vitro* data that, upon antigenic stimulation, secretion of IL6 by $\gamma\delta$ T cells reduces while IFN γ levels increases, which has a potent anti-osteoclastogenic effect.

Summary and Conclusion

The present study has shown that activation status and cytokine dynamics of $\gamma\delta$ T cells determines their effect on osteoclastogenesis. Non-activated $\gamma\delta$ T cells are major producers of pro-osteoclastogenic cytokine IL6 and enhance osteoclastogenesis. Activated $\gamma\delta$ T cells show higher levels of IFN γ (anti-osteoclastogenic) secretion and potentially inhibit osteoclast generation and function. Detailed proteome analysis of untreated and Zoledronate treated breast tumor cells (MCF7) showed elevated expression of proteins involved in recruitment of $\gamma\delta$ T cells and those involved in immune synapse formation between $\gamma\delta$ T cells and breast tumor cells. Zoledronate also affected multiple metabolic processes involved in apoptosis of breast tumor cells. *In vivo* effect of Zoledronate treatment on the immune scenario was investigated in breast cancer patients. It was observed that Zoledronate treatment activated both innate ($\gamma\delta$ T cells, NK cells) and adaptive (CD8) immune cells; while percentages of regulatory cells (CD4⁺CD25⁺127⁻FOXP3⁺) and macrophages were reduced. $\gamma\delta$ T cells percentages in peripheral blood were reduced in Zoledronate treated breast cancer patients, but these cells were in highly activated state, expressing increased levels of activation markers (CD25, RANKL) and IFN γ . $\gamma\delta$ T cells from Zoledronate treated breast cancer patients were of effector memory phenotype

($\gamma\delta^+$ CD45RA⁻ CD27⁻). Zoledronate treated breast cancer patients also showed reduced levels of IL6 secretion, which is a potent pro-osteoclastogenic and pro-tumorigenic cytokine.

In conclusion, the present study has demonstrated that aminobisphosphonates facilitate the crosstalk between the immune and skeletal system. The study has also highlighted the mechanism of action of aminobisphosphonates in breast cancer patients that extends its role beyond the well defined anti-resorptive function to the treatment of malignancies.

References

1. Ahn SG, Lee HM, Cho SH, Lee SA, Hwang SH, et al. (2013) Prognostic factors for patients with bone-only metastasis in breast cancer. *Yonsei Med J* 54: 1168-1177.
2. Soysa NS, Alles N, Aoki K, Ohya K (2012) Osteoclast formation and differentiation: an overview. *J Med Dent Sci* 59: 65-74.
3. Teitelbaum SL (2007) Osteoclasts: what do they do and how do they do it? *Am J Pathol* 170: 427-435.
4. Zheng Y, Zhou H, Dunstan CR, Sutherland RL, Seibel MJ (2013) The role of the bone microenvironment in skeletal metastasis. *J Bone Oncol* 2: 47-57.
5. Soki FN, Park SI, McCauley LK (2012) The multifaceted actions of PTHrP in skeletal metastasis. *Future Oncol* 8: 803-817.
6. Fournier PG, Stresing V, Ebetino FH, Clezardin P (2010) How do bisphosphonates inhibit bone metastasis in vivo? *Neoplasia* 12: 571-578.
7. Drake MT, Clarke BL, Khosla S (2008) Bisphosphonates: mechanism of action and role in clinical practice. *Mayo Clin Proc* 83: 1032-1045.
8. Kimachi K, Kajiya H, Nakayama S, Ikebe T, Okabe K (2011) Zoledronic acid inhibits RANK expression and migration of osteoclast precursors during osteoclastogenesis. *Naunyn Schmiedebergs Arch Pharmacol* 383: 297-308.
9. Green JR (2003) Antitumor effects of bisphosphonates. *Cancer* 97: 840-847.

10. Jagdev SP, Coleman RE, Shipman CM, Rostami HA, Croucher PI (2001) The bisphosphonate, zoledronic acid, induces apoptosis of breast cancer cells: evidence for synergy with paclitaxel. *Br J Cancer* 84: 1126-1134.
11. Chiplunkar S, Dhar S, Wesch D, Kabelitz D (2009) gammadelta T cells in cancer immunotherapy: current status and future prospects. *Immunotherapy* 1: 663-678.
12. Hayday AC (2000) [gamma][delta] cells: a right time and a right place for a conserved third way of protection. *Annu Rev Immunol* 18: 975-1026.
13. Caccamo N, Todaro M, Sireci G, Meraviglia S, Stassi G, et al. (2013) Mechanisms underlying lineage commitment and plasticity of human gammadelta T cells. *Cell Mol Immunol* 10: 30-34.
14. Beetz S, Marischen L, Kabelitz D, Wesch D (2007) Human gamma delta T cells: candidates for the development of immunotherapeutic strategies. *Immunol Res* 37: 97-111.
15. Konigshofer Y, Chien YH (2006) Gammadelta T cells - innate immune lymphocytes? *Curr Opin Immunol* 18: 527-533.
16. Kabelitz D, Kalyan S, Oberg HH, Wesch D (2013) Human Vdelta2 versus non-Vdelta2 gammadelta T cells in antitumor immunity. *Oncoimmunology* 2: e23304.
17. Sharp LL, Jameson JM, Cauvi G, Havran WL (2005) Dendritic epidermal T cells regulate skin homeostasis through local production of insulin-like growth factor 1. *Nat Immunol* 6: 73-79.
18. Jameson JM, Cauvi G, Sharp LL, Witherden DA, Havran WL (2005) Gammadelta T cell-induced hyaluronan production by epithelial cells regulates inflammation. *J Exp Med* 201: 1269-1279.
19. Havran WL, Jameson JM, Witherden DA (2005) Epithelial cells and their neighbors. III. Interactions between intraepithelial lymphocytes and neighboring epithelial cells. *Am J Physiol Gastrointest Liver Physiol* 289: G627-630.
20. Born WK, Reardon CL, O'Brien RL (2006) The function of gammadelta T cells in innate immunity. *Curr Opin Immunol* 18: 31-38.
21. Hayday AC (2009) Gammadelta T cells and the lymphoid stress-surveillance response. *Immunity* 31: 184-196.
22. Wu YL, Ding YP, Tanaka Y, Shen LW, Wei CH, et al. (2014) gammadelta T cells and their potential for immunotherapy. *Int J Biol Sci* 10: 119-135.

23. Wesch D, Marx S, Kabelitz D (1997) Comparative analysis of alpha beta and gamma delta T cell activation by Mycobacterium tuberculosis and isopentenyl pyrophosphate. *Eur J Immunol* 27: 952-956.
24. Gomes AQ, Correia DV, Grosso AR, Lanca T, Ferreira C, et al. (2010) Identification of a panel of ten cell surface protein antigens associated with immunotargeting of leukemias and lymphomas by peripheral blood gammadelta T cells. *Haematologica* 95: 1397-1404.
25. Gertner-Dardenne J, Castellano R, Mamessier E, Garbit S, Kochbati E, et al. (2012) Human Vgamma9Vdelta2 T cells specifically recognize and kill acute myeloid leukemic blasts. *J Immunol* 188: 4701-4708.
26. Dhar S, Chiplunkar SV (2010) Lysis of aminobisphosphonate-sensitized MCF-7 breast tumor cells by Vgamma9Vdelta2 T cells. *Cancer Immun* 10: 10.
27. Thomas ML, Samant UC, Deshpande RK, Chiplunkar SV (2000) gammadelta T cells lyse autologous and allogenic oesophageal tumours: involvement of heat-shock proteins in the tumour cell lysis. *Cancer Immunol Immunother* 48: 653-659.
28. Pollinger B, Junt T, Metzler B, Walker UA, Tyndall A, et al. (2011) Th17 cells, not IL-17+ gammadelta T cells, drive arthritic bone destruction in mice and humans. *J Immunol* 186: 2602-2612.
29. Kotake S, Udagawa N, Hakoda M, Mogi M, Yano K, et al. (2001) Activated human T cells directly induce osteoclastogenesis from human monocytes: possible role of T cells in bone destruction in rheumatoid arthritis patients. *Arthritis Rheum* 44: 1003-1012.
30. Lee SJ, Nam KI, Jin HM, Cho YN, Lee SE, et al. (2011) Bone destruction by receptor activator of nuclear factor kappaB ligand-expressing T cells in chronic gouty arthritis. *Arthritis Res Ther* 13: R164.
31. Walsh MC, Kim N, Kadono Y, Rho J, Lee SY, et al. (2006) Osteoimmunology: interplay between the immune system and bone metabolism. *Annu Rev Immunol* 24: 33-63.
32. Sato K, Takayanagi H (2006) Osteoclasts, rheumatoid arthritis, and osteoimmunology. *Curr Opin Rheumatol* 18: 419-426.
33. Laemmli UK (1970) Cleavage of structural proteins during the assembly of the head of bacteriophage T4. *Nature* 227: 680-685.

Publications in Refereed Journal:**a. Published**

Swati P. Phalke, Shubhada V. Chiplunkar, “Activation status of $\gamma\delta$ T cells dictates their effect on osteoclast generation and bone resorption”, Bone Reports, Vol 3, (2015) 95-103.

b. Manuscripts under preparation:

1) **Swati P. Phalke**, Rukmini B. Govekar, Shubhada V. Chiplunkar, Proteomic analysis of breast cancer cells treated with Zoledronate

2) **Swati P. Phalke**, Shubhada V. Chiplunkar, Immune profiling of breast cancer patients on Zoledronate treatment

c. Other Publications/ Presentations:*1) National Conferences*

- “8th National Research Scholars Meet” held at ACTREC, Mumbai during 21st-22nd December 2012, Swati P. Phalke, Shubhada V. Chiplunkar, “Understanding the crosstalk between $\gamma\delta$ T cells and osteoclasts in patients with breast cancer”

- “32nd Annual Convention of Indian Association for Cancer Research” , held at New Delhi during 13-16th February 2013, Swati Phalke, Vani Parmar, Sudeep Gupta, Rajendra Badwe, Shubhada Chiplunkar, “Understanding the crosstalk between $\gamma\delta$ T cells and osteoclasts in patients with breast cancer”

- “Tata Platinum Jubilee” Conference , held at Mumbai, Italy during -26th - 28th February, 2016, Swati Phalke, Rajendra Badwe, Vani Parmar, Shubhada Chiplunkar,

“Zoledronate induced $\gamma\delta$ T cells activation: A potential cell based cancer therapy”

2) *International Conferences*

- “15th International Congress of Immunology”, held at Milan, Italy during 22nd-27th August 2013, Swati Phalke, Vani Parmar, Sudeep Gupta, Rajan Badwe, Shubhada Chiplunkar, “Understanding the crosstalk between $\gamma\delta$ T cells and osteoclasts in patients with breast cancer”, Abstract was published in “Frontiers in immunology”

Signature of Student:

phalke

Date: 25/04/2016

Doctoral Committee:

Sr. No.	Name	Designation	Signature	Date
1	Dr. Sorab N. Dalal	Chairman	<i>S. N. Dalal</i>	25/4/2016
2	Prof. Shubhada V. Chiplunkar	Guide/ Convener	<i>S. V. Chiplunkar</i>	25/4/16
3	Dr. Narendra N. Joshi	Member	<i>N. N. Joshi</i>	25/4/16
4	Dr. Rukmini B. Govekar	Member	<i>R. B. Govekar</i>	25/4/16
5	Dr. Mohan R. Wani	Invitee	<i>M. R. Wani</i>	25/4/16

S. V. Chiplunkar
25/4/16
Dr. S.V. Chiplunkar
Director, ACTREC
Chairperson,
Academic & training Program, ACTREC

K. S. Sharma
Prof. K. Sharma
Director, Academics
T.M.C.

PROF. K. S. SHARMA

DIRECTOR (ACADEMICS)
TATA MEMORIAL CENTRE
PAREL, MUMBAI

Version approved during the meeting of Standing Committee of Deans held during 29-30 Nov 2013.
Dr. S. V. Chiplunkar
Director
Advanced Centre for Treatment, Research &
Education in Cancer (ACTREC)
Tata Memorial Centre
Kharghar, Navi Mumbai 410210.

List of Figures

<i>Figure No.</i>	<i>Title</i>	<i>Page No.</i>
Figure 1	Chemical structure of bisphosphonate.....	28
Figure 2	Histological classification of breast cancer.....	38
Figure 3	Molecular classification of breast cancer.....	39
Figure 4	Osteoclast structure.....	44
Figure 5	The process of bone remodeling.....	47
Figure 6	Mechanism of aminobisphosphonates action.....	54
Figure 7	Principle of MTT assay.....	87
Figure 8	Principle of Folin-Lowry's method of protein estimation.....	90
Figure 9	Immunomagnetic separation of "freshly isolated" and "activated" $\gamma\delta$ T cells.....	114
Figure 10	Analysis of activation markers (CD69, CD25 and RANKL) on "freshly isolated (FI)" $\gamma\delta$ T cells.....	120
Figure 11	Analysis of activation markers (CD69, CD25 and RANKL) on "activated (ACT)" $\gamma\delta$ T cells.....	122
Figure 12	Comparative analysis of activation markers on antigen activated "freshly isolated" and "activated" $\gamma\delta$ T cells.....	123
Figure 13	Generation of osteoclasts form mouse macrophage cell line – RAW264.7.....	126
Figure 14	Generation of mouse osteoclasts from bone marrow precursor cells.....	128
Figure 15	Generation of human osteoclasts from CD14 ⁺ precursor cells.....	130
Figure 16	Characterization of human osteoclasts.....	132
Figure 17	Differentiation of human osteoclasts form macrophages.....	133
Figure 18	Direct effect of "activated" and "freshly isolated" $\gamma\delta$ T cells on generation of human osteoclasts.....	136
Figure 19	Effect of soluble factors secreted by "activated" $\gamma\delta$ T cells on function of human osteoclasts.....	139

List of Figures

<i>Figure No.</i>	<i>Title</i>	<i>Page No.</i>
Figure 20	Effect of soluble factors secreted by “freshly isolated” $\gamma\delta$ T cells on function of human osteoclasts.....	140
Figure 21	Estimation of Th1/Th2/Th17 cytokines in cell free supernatants of “activated” (ACT) and “freshly isolated” (FI) $\gamma\delta$ T cells.....	143
Figure 22	Effect of IFN γ and IL6 neutralization in cell free supernatants of “activated” (ACT) and “freshly isolated” (FI) $\gamma\delta$ T cells on osteoclast function.....	146
Figure 23	Determination of sublethal concentration of Zoledronate for <i>in vitro</i> assays using MTT Assay.....	152
Figure 24	Images of silver stained 2D gels generated using pH 3-10 NL,17cm IPG strip.....	154
Figure 25	Comparative analysis of 2D profiles of untreated and Zoledronate treated MCF7 cells using PDQuest software.....	156
Figure 26	Schematic presentation of <i>in gel</i> digestion of proteins.....	157
Figure 27	Diagrammatic representation of identified proteins in untreated MCF7 cell lysate using MALDI-TOF/ TOF.....	158
Figure 28	Classification of upregulated proteins by gene ontology based on their biological processes, molecular function and protein class in MCF7 upon Zoledronate treatment.....	171
Figure 29	Classification of downregulated proteins by gene ontology based on their biological processes, molecular function and protein class in MCF7 upon Zoledronate treatment.....	172
Figure 30	Interactome analysis of differentially expressed proteins in MCF7 upon Zoledronate treatment	181
Figure 31	Effect of Zoledronate treatment on reorganization and expression of cytoskeletal elements in MCF7	186
Figure 32	Effect of Zoledronate treatment on expression of heat shock proteins in MCF7 cells.....	189

List of Figures

<i>Figure No.</i>	<i>Title</i>	<i>Page No.</i>
Figure 33	Effect of Zoledronate treatment on expression of epidermal growth factor receptor (EGFR) in MCF7 cells.....	192
Figure 34	Effect of Zoledronate treatment on cell cycle of breast tumor cells.....	195
Figure 35	Immune profile of breast cancer patients on Zoledronate treatment and untreated breast cancer patients.....	204
Figure 36	Effect of Zoledronate treatment on activation status of $\alpha\beta$ and $\gamma\delta$ T cells.....	207
Figure 37	Effect of Zoledronate treatment on memory status of $\gamma\delta$ T cells	210
Figure 38	Intracellular cytokine profiling of Zoledronate treated breast cancer patients.....	213
Figure 39	Estimation of Th1/Th2/Th17 cytokines in cell free supernatants of HI and breast cancer patients $\gamma\delta$ T cells.....	215
Figure 40	Crosstalk between bone and $\gamma\delta$ T lymphocytes in breast cancer patients mediated by Zoledronate	248

List of Tables

<i>Figure No.</i>	<i>Title</i>	<i>Page No.</i>
Table 1	Major differences between $\alpha\beta$ and $\gamma\delta$ T cells.....	56
Table 2	Phenotypic heterogeneity and functional package organization of human $\gamma\delta$ T cells.....	56
Table 3	Percent yield of “freshly isolated” $\gamma\delta$ T cells from healthy individuals.....	115
Table 4	Percent yield of “activated” $\gamma\delta$ T cells from healthy individuals.....	116
Table 5	Percent yield of CD14 ⁺ cells from healthy individuals (HI).....	131
Table 6	Cytokine profiling of cell free supernatants of antigen activated $\gamma\delta$ T cells.....	144
Table 7	Identification of <i>in gel</i> digested proteins separated from 2D silver stained gel by MALDI-TOF/TOF.....	159
Table 8	Differentially expressed proteins in 2D-PAGE identified by MS/MS.....	162
Table 9	List of upregulated proteins in MCF7 upon Zoledronate treatment.....	165
Table 10	List of downregulated proteins in MCF7 upon Zoledronate treatment.....	167
Table 11	List of differentially expressed proteins in MCF7 involved in immune cell activation.....	175
Table 12	List of differentially expressed proteins in MCF7 involved in important cellular processes.....	177
Table 13	List of differentially expressed proteins in MCF7 related to cytoskeletal elements.....	184
Table 14	List of differentially expressed proteins in MCF7 involved in EGFR signaling.....	191
Table 15	List of differentially expressed proteins in MCF7 involved in cell cycle.....	194
Table 16	Inclusion- Exclusion criteria for breast cancer patients.....	201
Table 17	Median fluorescent intensity of activation markers (CD69, CD25 and RANKL) on $\alpha\beta$ and $\gamma\delta$ T cells.....	208
Table 18	Cytokine profiling of cell free supernatants of activated $\gamma\delta$ T cells.....	216

Abbreviations

ACN	Acetonitrile
ADCC	Antibody dependent cellular cytotoxicity
Ab	Antibody
Ag	Antigen
APCs	Antigen presenting cells
BrHPP	Bromohydrin pyrophosphate
BC	Breast cancer
BSA	Bovine serum albumin
CD	Cluster of differentiation
CTL	Cytotoxic T lymphocyte
CBA	Cytometric bead array
DTT	Dithiothretol
DMSO	Dimethyl sulphoxide
DAPI	4,6 diamidino 2 phenylindole
EDTA	Ethylene diamine tetraacetic acid
EGFR	Epidermal growth factor receptor
FCS	Fetal calf serum
FH	Ficoll Hypaque
FACS	Fluorescence activated cell sorting
FPPS	Farnesyl pyrophosphate synthase
FBS	Fetal bovine serum
FITC	Fluoresecein isothiocyanate
GAM	Goat anti mouse
GAR	Goat anti rabbit
Hr	Hour
HSPs	Heat shock proteins
HI	Healthy individual
HMBPP	(E)-4-hydroxy-3-methyl-but-2-enyl pyrophosphate
IDO	Indoleamine 2,3-dioxygenase
IEF	Isoelectric focusing
IFN	Interferon
IPP	Isopentenyl pyrophosphate
IL	Interleukin
IPG	Immobilized pH gradient
iTRAQ	Isobaric tags for relative and absolute quantification
KDa	Kilodalton
LPS	Lipopolysaccharide
ml	Millilitre
Min	Minute

MEP	2-C-methyl-D-erythritol 4-phosphate
MHC	Major histocompatibility complex
MICA	MHC class I chain related molecules
mAbs	Monoclonal antibodies
MACS	Magnetic Assisted Cell Sorting
MTT	3-(4,5-dimethylthiazol-2-yl)-2,5-diphenyltetrazolium bromide
MALDI	Matrix assisted laser desorption assay
MS	Mass spectrometry
NS	Normal saline
NK	Natural Killer
NKT	Natural Killer T
NF κ B	Nuclear factor kappa B
NBP	Nitrogen containing bisphosphonates
NKG2D	Natural Killer Group 2D receptor
OPG	Osteoprotegerin
OPCs	Osteoclast Precursor Cells
OAAS	Osteoclast Activity Assay Substrate
PAGE	Polyacrylamide gel electrophoresis
PBMCs	Peripheral blood mononuclear cells
PE	Phycoerythrin
PBS	Phosphate Buffered saline
PFA	Paraformaldehyde
PI	Propidium iodide
Ppm	Parts per million
RAGE	Receptor for advanced glycation end products
rmMCSF	Recombinant mouse macrophage colony stimulating factor
rmRANKL	Recombinant mouse receptor activator of nuclear factor kappa B ligand
rhMCSF	Recombinant human macrophage colony stimulating factor
rhRANKL	Recombinant human receptor activator of nuclear factor kappa B ligand
RT	Room temperature
RPMI	Roswell Park Memorial Institute
rhIL2	Recombinant human interleukin 2
RPM	Rotations per minute
RCF	Relative centrifugal force
SDS	Sodium dodecyl sulphate
TCR	T cell receptor
Th	T helper
Tregs	Regulatory T cells
TAA	Tumor associated antigen
TGF	Transforming growth factor
TNF	Tumor necrosis factor

TLR	Toll like receptor
TALL	T cell acute lymphoblastic leukemia/lymphoma
TRAP	Tartarate resistant acid phosphatase
TOF	Time of flight
ULBP	UL16 binding protein
VHrs	Volt Hours
WHO	World Health Organization
$\gamma\delta$	Gamma delta
$\alpha\beta$	Alpha beta
α MEM	Minimum essential medium with alpha modification
μ g	Microgram
μ l	Microlitre
μ M	Micromolar

Chapter 1

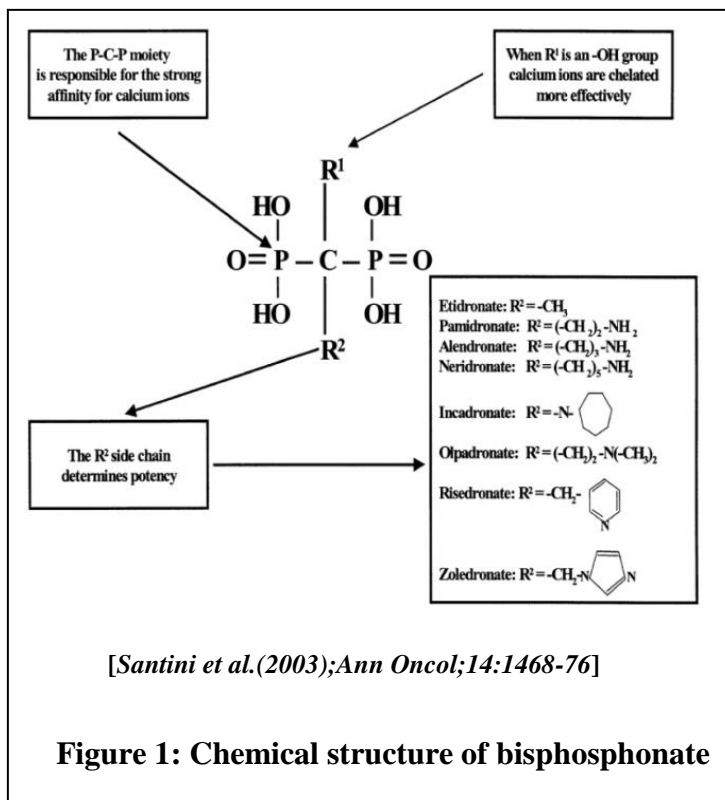
Introduction

Breast cancer is the 2nd most common cancer in the world and the most frequent cancer among women, with an estimate of 1.67 million new cancer cases diagnosed in 2012 (25% of all cancers). Breast cancer ranks as the 5th cause of death from cancer overall and it is the most frequent cause of cancer death in women in less developed regions (14.3% of total). It is now the 2nd cause of cancer death in more developed regions (15.4%) after lung cancer (GLOBOCAN 2012).

Breast cancer cells metastasize preferentially to the bone, while other sites include lungs, regional lymph nodes, liver and brain [34,35,36]. 80% of patients with advanced breast cancer show bone metastasis [37]. Bone microenvironment plays essential role in metastasis of the tumor cells [38]. Bone undergoes continuous remodeling during entire life to attain and preserve skeletal size, shape, and structural integrity and regulate mineral homeostasis [3,39]. Bone remodeling is essentially carried out by two cells-osteoclasts and osteoblasts in a highly coordinated manner. Osteoclasts are large multinucleated cells generated by fusion of monocyte-macrophage precursor cells [2] and are known to decalcify and degrade the bone by secreting the lysosomal proteases [3]. Osteoblasts are derived from mesenchymal cells, secrete bone matrix proteins and promote mineralization. Imbalance in bone remodeling results in pathological conditions such as osteoporosis, rheumatoid arthritis (RA), Paget's disease and osteoporosis [40]. Breast cancer cells show osteolytic metastasis, which causes severe and progressive pain, hypercalcemia, fragile bone, pathological fractures, spinal cord compression, other nerve compression syndromes, erythema over the affected bone and swelling [41]. The mechanism responsible for tumor growth in bone involves complex events. Breast tumor cells enhance osteoclastogenesis by stimulation of osteoclast and osteoblast [42,43]. Increased bone resorption releases growth factors and TGF β from bone and provides nutrition to tumor cells,

creating a vicious cycle. Tumor cells also recruit immune cells in the bone microenvironment. Immune system and skeletal system share number of common cytokines, chemokines, signaling molecules and transcription factors [31,44]. Activated T lymphocytes have been shown to stimulate osteoclast differentiation and bone resorption through cytokines, such as receptor activator of nuclear factor (NF)-kB ligand (RANKL), interleukin (IL)-6, IL7, IL17 and TNF α [45,46,47,48,49,50,51].

Bisphosphonates (BPs) are chemically stable analogs of inorganic pyrophosphates, which are characterized by two pyrophosphate groups linked to a central carbon atom, forming a P-C-P structure. Two side chains (referred to as R1 and R2) are covalently bound to the carbon atom of the common P-C-P structure (Figure 1). The P-C-P backbone and the R1 side chain allow the



bisphosphonates to bond avidly to hydroxyapatite on the bone surface and are preferentially delivered to sites of increased bone formation or resorption. The first generation bisphosphonates were non-nitrogen containing and exerted their effect by replacing terminal phosphate of adenosine pyrophosphates (ATP). These non-hydrolysable ATP analogs likely promoted apoptosis by inhibiting ATP dependent cellular enzymes [52]. The more potent second and third generation nitrogen containing bisphosphonates (NBPs) inhibit the farnesyl pyrophosphate

synthase (FPPS) enzyme in the mammalian mevalonate pathway [53]. This arrests the prenylation or geranylation of crucial GTPases such as Ras, Rho, Rac that are vital for cell survival, subsequently leading to tumor cell apoptosis. Aminobisphosphonates and anti-RANKL antibodies (Denosumab) are commonly used to prevent bone loss in osteoporosis and for the treatment of bone disease in solid cancer (breast and prostate cancer) and multiple myeloma [54,55,56,57,58,59,60,61]. Inhibition of FPPS by aminobisphosphonates leads to upregulation of intracellular isopentenyl pyrophosphate (IPP) levels in cell and these are recognized by $\gamma\delta$ T cell through $\gamma\delta$ TCR, resulting in direct activation of $\gamma\delta$ T cells [62,63].

$\gamma\delta$ T cells are unique subset of immune cells and represent ~1-10% of total T cell population in peripheral blood of humans [22]. Unlike $\alpha\beta$ T cells, $\gamma\delta$ T cells are unique with respect to their T-cell receptor (TCR) gene usage, tissue tropism and MHC independent antigen recognition [11,12]. Major population of $\gamma\delta$ T cells (>90%) express V γ 9V δ 2 TCR (also called as V γ 2V δ 2) and are present in human peripheral blood, while 10% population express V γ 9V δ 1 TCR [16]. $\gamma\delta$ T cells are Th1 type cells and secrete copious amount of IFN γ upon stimulation [13,14]. $\gamma\delta$ T cells are highly plastic and can differentiate into Th2 [64,65], Th17 [66,67], Tfh [13] and T regulatory [68] type. $\gamma\delta$ T cells play an important role in antitumor cytotoxicity [15,16], wound healing and tissue repair [17,18,19]. $\gamma\delta$ T cells express natural killer receptors [20,21] and recognize stressed/ tumor cells expressing MICA/B and ULBPs [22]. $\gamma\delta$ T cells are increased in bacterial, viral and parasitic infections [20]. Antitumor ability of $\gamma\delta$ T cells against a broad panel of solid tumors and leukemia's has been widely reported [24,25,26,27,69,70,71]. There are three major subclasses of nonpeptide compounds that stimulate $\gamma\delta$ T cells: prenyl pyrophosphates, aminobisphosphonates and alkylamines [22,63,72]. Prenyl pyrophosphates and alkylamines are natural antigens that are produced by bacteria and other human pathogens during

infections [73]. A unique set of antigens recognized by $\gamma\delta$ T cells include intermediate products of eukaryotic mevalonate pathway (isopentenyl pyrophosphate or its synthetic analog bromohydrin pyrophosphate) and bacterial Rohrer pathway (HMBPP [E]-4-Hydroxy-3-methyl-but-2-enylpyrophosphate) [20]. Emerging data suggests that NBPs have immunomodulatory properties. Some NBPs can induce expansion of human $\gamma\delta$ T cells (V γ 9V δ 2) [11,74,75]. It is known that aminobisphosphonate recognition is $\gamma\delta$ TCR mediated [26,76], but the exact mechanism of activation of $\gamma\delta$ T cells induced by aminobisphosphonates is still unclear.

Aminobisphosphonates, apart from acting as antigens for $\gamma\delta$ T cells also bear potent anti tumor effects [9]. *In vitro* studies have shown that, Zoledronate inhibits growth of tumor cells and induces apoptosis [77,78]. They are known to induce apoptosis in myelomas, lymphomas and in some solid tumors. Further, aminobisphosphonates have been shown to interfere with angiogenesis and target endothelial cell adhesion and migration [79]. Earlier studies from our lab and others have shown that aminobisphosphonate treated tumor cells are sensitized to efficient lysis by $\gamma\delta$ T cells [26,80,81,82]. Thus, it is important to investigate the mechanisms by which aminobisphosphonates sensitize tumor cells to $\gamma\delta$ T cell mediated lysis and also directly augment their anti-tumor effector functions. It is therefore perceived that understanding the immunomodulatory effects of aminobisphosphonates on $\gamma\delta$ T cells would enable inclusion of these aminobisphosphonates in designing protocols for efficient expansion of $\gamma\delta$ T cells for immunotherapy. Therefore, it becomes both interesting and imperative to analyze the role of endogenous phosphate metabolites contributed by a dysregulated mevalonate pathway in tumor cells; that could potentiate the activation of human $\gamma\delta$ T cells. Dual effect of aminobisphosphonates in curtailing bone loss and activating V γ 9V δ 2 T cells opens an exciting area of research that has clinical implications.

With this background, the present thesis aims at investigating the crosstalk between breast tumor cells, $\gamma\delta$ T cells and osteoclasts, mediated by aminobisphosphonates (Zoledronate).

The objectives of the present thesis are:

1. To investigate the effect of $\gamma\delta$ T cells on osteoclastogenesis
2. To understand the effect of aminobisphosphonate (Zoledronate) on protein profiles of breast tumor cells
3. Immune profiling of breast cancer patients on Zoledronate treatment

Chapter 2

Review of literature

2.1) Breast cancer

Breast cancer is the most commonly occurring cancer in women and 2nd most frequent cancer worldwide, with more than 1.7 million cases diagnosed in 2012 (GLOBOCAN 2012). GLOBOCAN 2012 statistics suggests that compared to 2008, there is 20% increase in BC incidence and 14% increase in mortality worldwide. Frequency of young females diagnosed with breast cancer is higher. In total patients diagnosed with breast cancer, around 6.6% are below 40 years of age, 2.5% are below 35 and 0.65% are below 30 years of age [83,84]. In Asian countries, the age of females at which the incidence of breast cancer peaks is 40s, whereas in European countries and USA it peaks at the age of 60s [85]. More than 80% of Indian breast cancer patients are less than 60 years of age.

Multiple risk factors are associated with breast cancer; those are broadly divided into two groups- modifiable as well as nonmodifiable factors. Modifiable risk factors include late age at first child birth, use of oral contraceptives and hormone replacement therapy, postmenopausal obesity, cigarette smoking and alcohol consumption, whereas nonmodifiable risk factors include sex, increasing age, family history of breast or ovarian cancer, germ line mutation in a high-risk breast cancer susceptibility gene, benign breast disease with atypical hyperplasia, early age at menarche, late age at menopause and dense mammary tissue [86,87,88]. Postmenopausal women with higher level of endogenous hormones (estrogen and testosterone) show increased risk of breast cancer compared to women with lower hormonal levels [89]. There are two important genes which predispose the individual to breast cancer are BRCA1 (breast cancer 1) and BRCA2. These genes code for BRCA1 and BRCA2 proteins, which acts as tumor suppressors and play essential role in DNA repair. Individuals with these mutations have 15-20 fold increased risk of having breast cancer as compared to normal individuals [90]. Another gene

TP53, which code for P53 proteins, has a major role in regulation of cell cycle and induction of cell growth arrest/ apoptosis in response to injury. Mutations in gene TP53 results in reduced levels of active P53 and thus have higher chances of many cancers including breast cancer [90]. Breast cancer usually arises as ductal hyperproliferation and evolves into ductal carcinoma *in situ* (DCIS), into invasive carcinoma and finally metastatic disease [91].

Techniques such as mammography, biopsies [fine needle aspiration (FNA) biopsy, core biopsy, vacuum assisted breast biopsy, excisional and incisional surgical biopsy], magnetic field, sound waves or radioactive tracers are used for diagnosis of breast cancer [92].

2.2) Classification of breast cancer

Based on tumor size, invasiveness, lymph node involvement and metastatic status, the stage of the breast cancer is determined. Breast cancer staging helps to understand the prognosis and to determine the treatment strategies. Breast cancer classification is done on the basis of TNM (Tumor, Node and Metastasis) staging, histology, hormone receptor status and molecular markers.

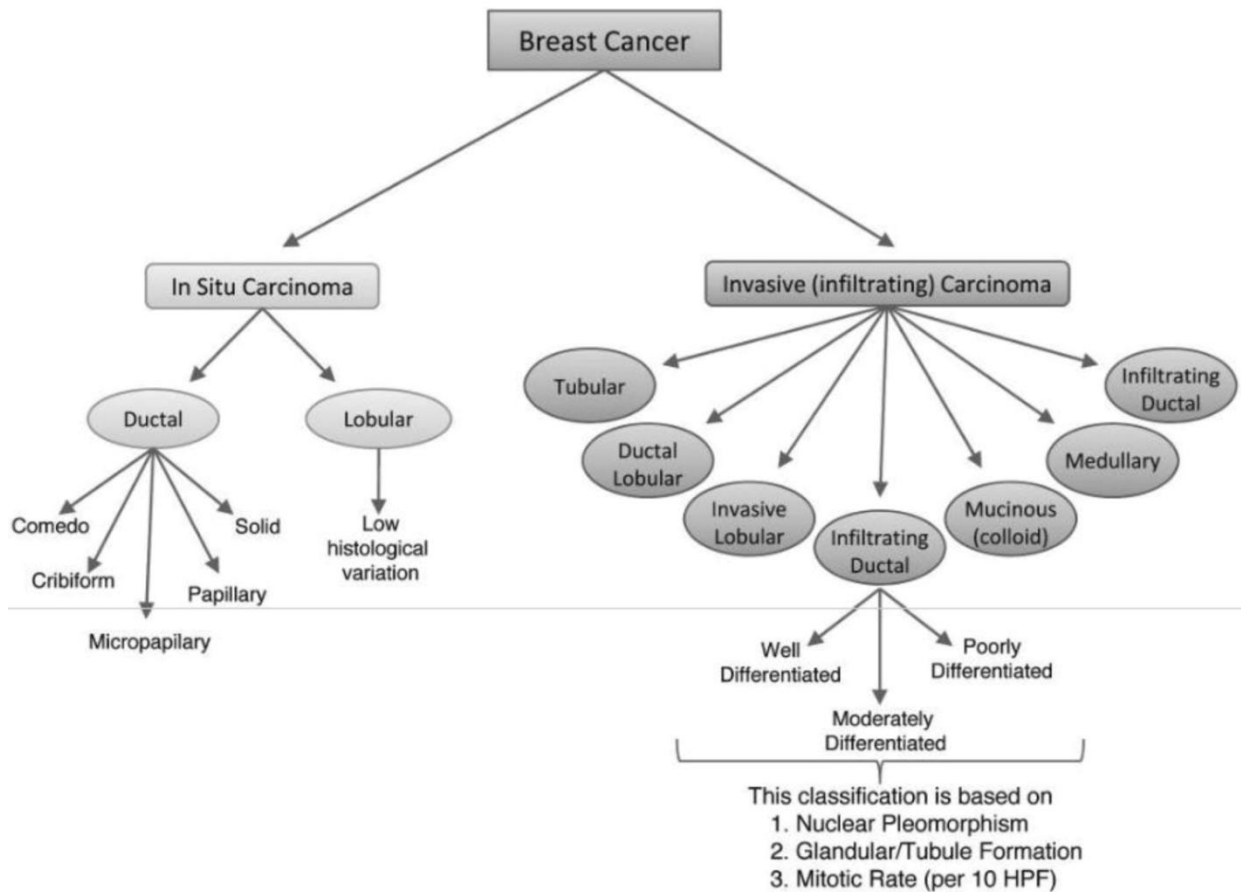
[2.2.1] TNM classification of breast cancer:

Stage 0	Tis, N0, M0	<i>Ductal carcinoma in situ (DCIS)</i> :Cancer cells are still within a duct and haven't invaded deeper into the surrounding fatty breast tissue. <i>Lobular carcinoma in situ (LCIS)</i> Paget disease of the nipple (without an underlying tumor mass) is also stage 0. In all cases the cancer has not spread to lymph nodes or distant sites.
Stage IA	T1, N0, M0	Tumor is 2 cm or less across (T1) and has not spread to lymph nodes (N0) or distant sites (M0).
Stage IB	T0 or T1, N1mi, M0	Tumor is 2 cm or less across (or is not found) (T0 or T1) with micrometastases in 1 to 3 axillary lymph nodes (the cancer in the underarm lymph nodes is greater than 0.2mm across and/or more than 200 cells but is not larger than 2 mm)(N1mi). The cancer has not spread to distant sites (M0).
Stage IIA	T0 or T1, N1 (but not N1mi), M0	The tumor is 2 cm or less across (or is not found) (T1 or T0) and either: It has spread to 1 to 3 axillary (underarm) lymph nodes, with the cancer in the lymph nodes larger than 2 mm across (N1a) OR Tiny amounts of cancer are found in internal mammary lymph nodes (nodes near the breast bone) on sentinel lymph node biopsy (N1b) OR It has spread to 1 to 3 axillary lymph nodes and to internal mammary lymph nodes (found on sentinel lymph node biopsy) (N1c). The cancer has not spread to distant sites (M0).
	T2, N0, M0	The tumor is larger than 2 cm but less than 5 cm (about 2 inches) across (T2) but hasn't spread to the lymph nodes (N0). The cancer has not spread to distant sites (M0).
Stage IIB	T2, N1, M0	The tumor is larger than 2 cm but less than 5 cm across (T2). It has spread to 1 to 3 axillary lymph nodes and/or tiny amounts of cancer are found in internal mammary lymph nodes on sentinel lymph node biopsy (N1). The cancer hasn't spread to distant sites (M0).
	T3, N1 or N2, M0	The tumor is larger than 5 cm across but does not grow into the chest wall or skin (T3). It has spread to 1 to 9 axillary nodes, or to internal mammary nodes (N1 or N2). The cancer hasn't spread to distant sites (M0).
Stage IIB	T4, N0 to N2, M0	The tumor has grown into the chest wall or skin (T4), and one of the following applies: It has not spread to- lymph nodes (N0) OR to 1 to 3 axillary lymph nodes and/or tiny amounts of cancer are found in internal mammary lymph nodes on sentinel lymph node biopsy (N1) OR 4 to 9 axillary lymph nodes, or it has enlarged the internal mammary lymph nodes (N2). The cancer hasn't spread to distant sites (M0). Inflammatory breast cancer is classified as T4d and is at least stage IIB. If it has spread too many nearby lymph nodes (N3) it could be stage IIIC, and if it has spread to distant lymph nodes or organs (M1) it would be stage IV.
Stage IIIC	any T, N3, M0	The tumor is any size (or can't be found), and one of the following applies: Cancer has spread - 10 or more axillary lymph nodes (N3) OR to lymph nodes under the collar bone (infraclavicular nodes) (N3) OR to lymph nodes above the collar bone (supraclavicular nodes) (N3) OR 4 or more axillary lymph nodes, and tiny amounts of cancer are found in internal mammary lymph nodes on sentinel lymph node biopsy (N3) OR it involves axillary lymph nodes and has enlarged the internal mammary lymph nodes (N3). Cancer has spread to The cancer hasn't spread to distant sites (M0).
Stage IV	any T, any N, M1	The cancer can be any size (any T) and may or may not have spread to nearby lymph nodes (any N). It has spread to distant organs or to lymph nodes far from the breast (M1). The most common sites of spread are the bones, liver, brain, or lungs.

[93] <http://www.cancer.org/cancer/breastcancer/detailedguide/breast-cancer-staging>

[2.2.2] Histological classification of breast cancer:

Breast cancer is broadly categorized into *in situ* carcinoma and invasive (infiltrating) carcinoma. Breast carcinoma *in situ* is further sub-classified into two groups- either ductal or lobular, on the basis of growth patterns and cytological features (Figure 2). Ductal carcinoma *in situ* (DCIS) is considerably more common than its lobular carcinoma *in situ* (LCIS). Similarly, invasive carcinomas are also categorized into several subgroups- infiltrating ductal, invasive lobular, ductal/lobular, mucinous (colloid), tubular, medullary and papillary carcinomas. Both DCIS and IDC are comprised of heterogeneous group of tumors [94].

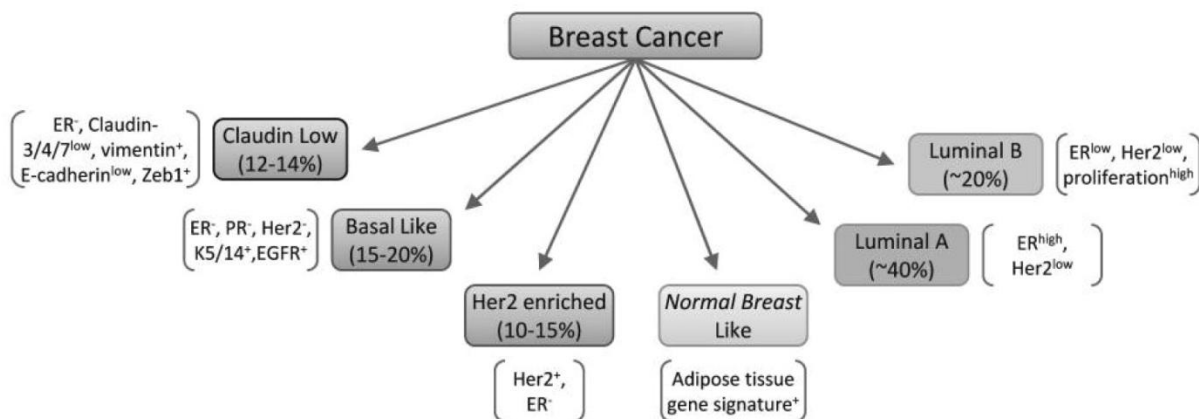


[Malhotra et al (2010), Cancer Biol Ther. 10 (10): 955–960]

Figure 2: Histological classification of breast cancer

[2.2.3] Molecular classification of breast cancer:

More intrinsic classification of breast cancer is carried out using microarray-based gene expression analysis and unbiased hierarchical clustering (Figure 3). It is based on expression of hormone receptors- estrogen receptor (ER), progesterone receptor (PR), epidermal growth factor receptor (ErbB2, Cerb2 or Her2) and is classified as luminal subtype A and luminal subtype B, basal-like, Her²⁺ enriched, claudine low and normal breast like [95,96,97,98,99,100]. Hormone receptor positive tumors usually fall in luminal A/B type and have positive prognosis as they respond to hormonal therapy. While “triple negative” tumors (ER⁻PR⁻Her2⁻) belong to basal subtype, have poor prognosis and are most likely to metastasize [96,97].



[Malhotra et al (2010), *Cancer Biol Ther.* 10 (10): 955–960]

Figure 3: Molecular classification of breast cancer

Majority of the breast cancer patients show metastasis to distant sites (bone, brain, lung and liver) and it is the main cause of breast cancer related deaths [101]. Common risk factors for metastasis include presence of tumor in lymph node, larger tumor size, loss of

histopathological differentiation and vessel invasion in patients with negative tumor in axillary lymph node [102,103,104]. Vast heterogeneity of the disease makes it difficult to predict the prognostic markers and risk factors for development of metastasis. However, Her2 is used as a prognostic marker [104].

Breast cancer disease treatment includes surgery (breast-conserving surgery, mastectomy, axillary lymph node dissection), radiotherapy (whole or partial breast irradiation with X-rays or γ -rays), and chemotherapy (use of cytotoxic drugs, such as cyclophosphamide, methotrexate, doxorubicin, and paclitaxel), endocrine therapy (use of anti-estrogens, estrogen inhibitors, aromatase inhibitors, ovarian ablation or ovarian suppression) or a combinatorial approach. For the treatment of metastatic breast cancer, bisphosphonates (antiresorptive drugs) are used as a standard treatment modality [105]. In Her2 positive metastatic breast cancer patients, addition of trastuzumab (also known as herceptin and is monoclonal antibody against Her2 receptor) to chemotherapy have significantly increased patients survival [106].

2.3) Bone is the preferential site of metastasis

Breast cancer cells frequently metastasize to bone and in many patients with advanced disease the skeleton is the site of the most significant tumor burden [107]. In 1989, Stephan Paget presented “seed and soil” hypothesis, explaining that properties of cancer cells and complementary properties of the particular organ microenvironment provide an advantage to the cancer cells [108]. It was stated that, chemoattractant factors and adhesion molecules that are produced by the target organ in combination with the proper counter-receptors expressed on the tumor cells determine homing of tumor cells to specific organs [109,110]. Bone metastasis is aided by fenestrated structure of the bone marrow sinusoid capillaries, high blood flow in the

areas of red marrow and receptors expressed by tumor cells, which bind to the bone cells and bone matrix [43,111]. Chemokine receptors, adhesion molecules and cell surface receptors expressed by tumor cells allow them to adhere to bone matrix and establish themselves. Human breast cancer cells, malignant tumor cells and metastasized tumor cells express higher levels of CXCR4, while CXCR12/ SDF1 (CXCR4 ligand) is abundantly expressed by bone marrow cells [112]. Apart from that, tumor cells also express $\alpha 4\beta 1$ / $\alpha 2\beta 1$ integrins, while VCAM1 and type 1 collagen are expressed on bone stromal cells [113]. During the process of bone formation, osteoblast incorporate multiple growth factors like TGF β , fibroblast growth factor, insulin growth factor and bone morphogenic protein -2 along with Collagen type-1[113]. These factors are released upon bone resorption and have been reported to stimulate the growth of metastasized tumor cells and induce them to produce osteoclastogenic factors [113]. Bone metastasis could be of osteolytic or osteoblastic or mixed type [114,115]. Most of the solid tumors (breast cancer, prostate cancer, thyroid cancer, lung cancer, and renal cancer) cause osteolytic metastasis [113], among which multiple myeloma (90%) and breast cancer (70 %) have highest frequency. The most common sites of bone metastases are the spine, ribs, pelvis, proximal femur and skull. Breast cancer cells preferentially metastasize to the bones and lungs, while prostate cancer cells almost exclusively metastasize to the bones [116]. Metastasized tumor cells (breast cancer, prostate cancer, thyroid cancer, lung cancer, and renal cancer) induce osteolytic bone destruction, through which they remove bone as a physical barrier for their expansion and acquire factors released upon resorption of bone matrix [117]. Osteolytic metastasis is associated with increased osteoclast activity, resulting in destruction of bone. Patients often suffer with sever bone pain and fractures [113]. Crosstalk between bone microenvironment and cancer cells play important role in osteolytic metastasis [118]. Osteoblastic metastasis notably occurs in prostate cancer and

rarely in breast cancer (15-20%). During osteoblastic metastasis, formation of bone is succeeded over bone resorption, generating poor quality bone.

2.4) Bone remodeling

Bone is a dynamic tissue, which undergoes continuous remodeling to maintain mineral homeostasis and structural integrity. Almost 10% of the entire bone is replaced every year [119]. Bone remodeling (coupling) is a sequential and cyclic procedure also referred as “activation-resorption-formation (ARF) cycle”. This process is under the tight regulation of bone cells-osteoclasts and osteoblasts. Cortical bone provides strength and protection, while trabecular bone is most metabolically active, which undergoes turnover in normal and diseased condition [120].

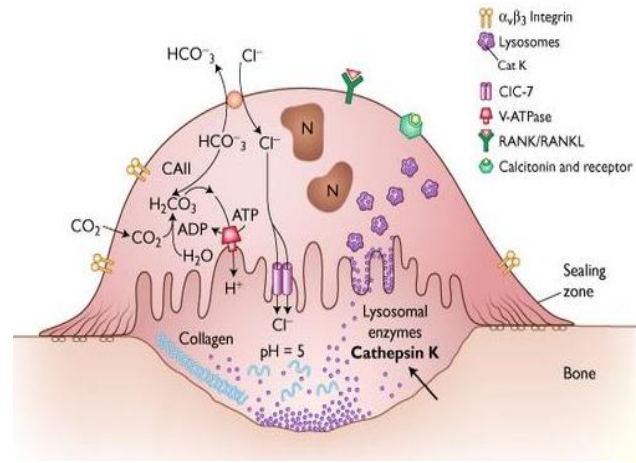
[2.4.1] Osteoblasts are bone forming cells, which regulate bone architecture by secretion of extracellular matrix and also play an important role in regulation of osteoclastogenesis. Osteoblasts are mononuclear cells, which originate from mesenchymal stem cells (MSCs) and are not fully differentiated [121]. MSCs also give rise to progenitors of myoblasts, adipocytes and chondrocytes [121]. In bone remodeling, “ossification (or osteogenesis)” is the process of laying down new bone material by osteoblast. There are two distinct types of ossification processes: Endochondreal and intramembranous ossification. Intramembranous ossification mainly occurs in flat bones, mandible, maxilla and clavicle. In this type of ossification, MSCs condense and ossification centre is created and osteoblasts directly differentiate into bone forming cells. While endochondreal ossification occurs in bone of mesodermal origins which forms axial skeleton, long bone, skull, ribs, vertebrae. This process involves formation of mineralized cartilage template, which gets degraded by osteoclasts and then osteoblasts form new bone matrix. Differentiation and function of osteoblasts is controlled by bone morphogenic

factors (BMPs) and Wnt signaling in association with Hedgehog signaling pathway [122,123]. NOTCH signaling pathway negatively regulates osteoblastogenesis [124]. Smad proteins are recruited and activated following BMP signaling, which controls osteoblast specific transcription factor Runt—related transcription factor 2 (Runx-2)/ core binding factor alpha 1 (cbfa1) [125]. Runx2 regulated expression of zinc finger containing transcription factor “osterix” interacts with NFATc and collectively controls expression of osteoblast specific genes osteocalcin, osteopontin, osteonectin, collagen type-I. Wnt signaling pathways play indispensable role in osteoblast differentiation and maturation. Osteoblasts are the major producers of macrophage colony stimulating factor (MCSF) and receptor activator of nuclear factor kappa B ligand (RANKL). MSCs once committed to osteoprogenitors upregulate expression of hormone receptors, receptors for growth factors and cytokines such as parathyroid hormone, prostaglandin E₂, IL11, insulin growth factor-1 and TGFβ. Following this osteoprogenitors differentiate into pro-osteoblasts, which have limited proliferative capacity and secrete extracellular matrix proteins (collagen type-I, bone sialoproteins, osteopontin) and RANKL. Mature osteoblasts don't proliferate but secrete collagen type-I, bone sialoproteins, osteopontin and OPG. Osteoblasts anchor to bone surface with the help of cadherin-11 and N-cadherins. Osteoblasts secrete collagen-proteoglycan matrix, which binds to calcium, making pre-bone (osteoid) mineralized. Osteoblasts also form tight junctions with nearby osteoblasts. Plasma membrane of osteoblasts is specialized for vesicular trafficking and secretion. Osteoblasts are separate from the calcification region of osteoid layer which they have secreted. Eventually, osteoblast gets trapped into its own secreted matrix and become osteocyte, which doesn't secrete osteoid further.

[2.4.2] Osteoclasts are large, multinucleated cells, generated by fusion of monocyte-macrophage precursor cells of hematopoietic lineage and resorb bone [39,126]. Osteoblasts/ stromal cells secrete macrophage colony stimulating factor

(MCSF); which binds to c-fms receptor expressed by osteoclast precursor cells and

induces fusion of osteoclast precursor cells (OPCs) [126]. MCSF regulates initial stages of osteoclastogenesis such as proliferation, differentiation and fusion of osteoclast precursor cells. MCSF has also been reported to affect osteoclast function at later stages of osteoclastogenesis [127]. Resorptive ability of mononucleated osteoclasts is lower than multinucleated osteoclasts [128]. Binding of MCSF to c-fms also induces expression of RANK on OPCs [129]. RANKL, produced by osteoblasts and stromal cells in response to parathyroid hormone (PTH) and vitamin D3 [130], binds to RANK on osteoclasts and causes differentiation of osteoclasts [39]. Co-stimulatory signals during osteoclastogenesis include (immunoreceptor tyrosine-based activation motif)-containing adaptors DAP12 (DNAX-activating protein of 12kDa) and FcR γ (Fc receptor γ chain). Collectively this leads to activation of the transcription factors nuclear factor κ B (NF- κ B), activator protein-1 (AP-1) and nuclear factor of activated T-cells cytoplasmic 1 (NFATc1) [131], which transcribes osteoclast specific genes (dendritic cell-specific transmembrane protein (DC-STAMP), tartarate resistant acid phosphatase (TRAcP), cathepsin K, matrix metalloproteinase 9 (MMP9) and α V β 3 integrin [132]. Mature osteoclasts get polarized and have the ability to resorb bone matrix [132]. Polarized osteoclasts have



[Wilson et al, (2009), J Bio Chem 284: 2584-92]

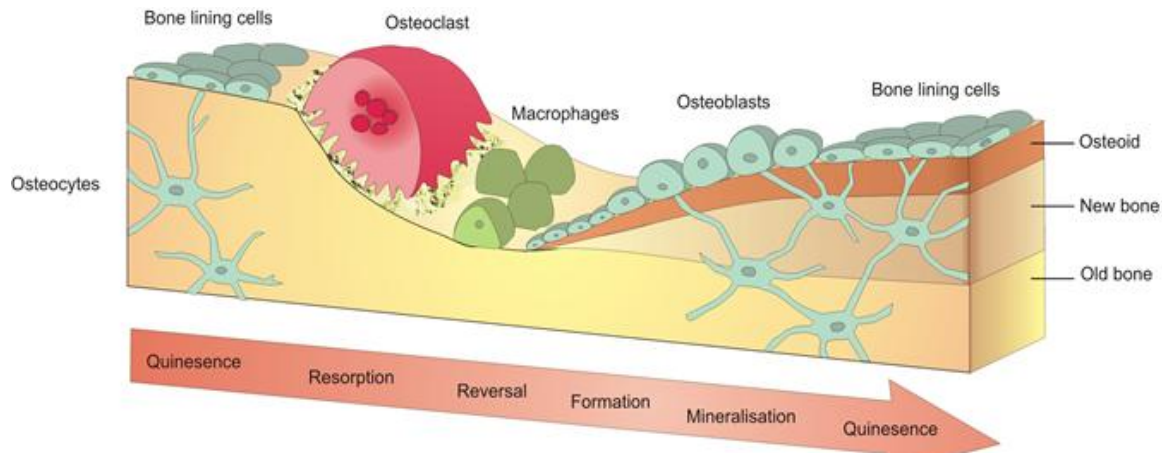
Figure 4: Osteoclast structure

distinct membrane domains- sealing zone, ruffled border and functional secretory domains [133]. Podosomes are attached to extracellular matrix through $\alpha V\beta 3$ integrins / vitronectin receptors. During polarization, a continuous dense highly dynamic podosomes containing F-actin ring is generated by actin reorganization, which isolates area of membrane that develops into ruffled border [134]. Ruffled borders are generated by osteoclasts only when they come in contact with mineralized bone matrix and not on glass during *in vitro* culture [135]. Ruffled borders are the highly convoluted membrane resulted from direct transport of late endosomes and lysosomes and function to deliver proteins during resorption process. Beneath the ruffled borders, vacuolated-type H⁺-ATPases channels are present, which creates acidic zones (pH 3-4.5) required for dissolution of bone minerals. Cysteine protease cathepsin K degrades type I collagen. The chloride-proton antiporter ClC-7 [136] function together with V-ATPase at the ruffled border by transporting chloride ions into the resorption lacuna [137]. Through the process of bone resorption, a very high concentration of calcium, phosphate and degraded collagen accumulates in resorption pit/ lacunae, which is endocytosed by osteoclast, transported through cell, released at functional secretory domain and finally in the blood stream [138,139]. During transcytosis collagen-I is further degraded by cathepsin-K and TRAP (activated by cathepsin-K). RANKL and MCSF are essential for osteoclast survival. Osteoclasts die by apoptosis which involves BCL-XL, Bim and MCL1 from ERK, AKT and mTOR pathway [140,141]. Bone resorption is dependent on polarization and vesicular trafficking, which is regulated by small GTPases like Ras, Rho, Rac, Rab [142]. Isoprenylation of these GTPases is essential for their proper localization at membrane and function, which is targeted by bisphosphonates [143].

[2.4.3] Osteocytes compose 90-95% of all bone cells in adult bone and plays important role in both phosphate metabolism and calcium availability and can remodel perilacunar matrix. Osteocyte is a source of soluble factors for bone cells as well as other distant tissues of kidney, muscle. Osteocytes are often termed as “mechanosensor cells” due to their localization in bone and their complex dendritic network through which they sense the load. Osteocytes originate from mesenchymal stem cells during the process of osteoblast differentiation [144] and are the longest lived bone cells (upto decades within the mineralized environment). Oxygen deprivation, glucocorticoid treatment or estrogen deficiency induces osteocytes apoptosis [144]. Estrogen deficiency also induces osteocytes apoptosis by enhancing TNF α and IL11 levels [145]. However, estrogen, estrogen receptor modulators, bisphosphonates, calcitonin, CD40 ligand, MCP1 and 3 inhibit osteocytes apoptosis [144]. Mechanical stress/ microdamages are also among inducers of apoptosis. Both healthy and apoptosing osteocytes recruit osteoclasts at the site of bone remodeling. In response to shear stress, osteocytes release nitric oxide (NO), ATP and prostaglandins [146]. NO inhibits bone resorption and promotes bone formation [144]. With age, osteocytes get apoptosized and leave behind empty lacunae which get micropetrose.

[2.4.4] Process of bone remodeling

As shown in Figure 5, the process of bone remodeling involves activation phase, reversal phase and formation phase and is known as “ARF cycle”.



[<http://imueos.blogspot.in/2010/09/bone-physiology.html>]

Figure 5: The process of bone remodeling

Activation Phase is a sequential process, where death/ apoptosis of osteocytes (due to mechanical stress or microcracks in the bone) induces activation of bone resorption [147]. Apoptosis of osteocytes leads to the recruitment of osteoclasts. Osteocytes are the major producers of TGF β , which acts as anti-osteoclastogenic factor and levels of TGF β deplete upon osteocyte apoptosis [124]. Estrogen protects osteocytes from apoptosis [148], thus maintains TGF β levels and keeps check on osteoclasts generation and function, explaining enhanced osteoclastogenesis in postmenopausal women [145].

This phase is followed by **reversal phase**. Several independent reports suggest that resorbed surfaces contain signals that regulate recruitment of bone cells/ osteoblasts. After resorption, pre-conditioning of the resorbed area is an essential step which is carried out by cells of mononuclear cells (47). Though these cells belong to osteoblastic lineage, these cells have

been confirmed as bone lining cells and are not osteoblasts [149]. These cells move to the resorption pits and degrade the remaining demineralized collagen matrix. New bone formation occurs in resorption pits and requires complete clearance of resorption pits [149]. Studies indicate that, pre-osteoblasts / bone lining cells mediate cleaning of resorption pits before getting differentiated into mature osteoblasts, which restore resorbed bone matrix (47,70,73,74).

Bone formation phase is influenced by osteoclasts, as reports suggest that mature osteoclasts secrete factors which activate nodule formation by osteoblasts (122). Cardiothrophin-1 produced by osteoclasts activates bone formation by osteoblasts (123). Osteoblasts secrete bone matrix proteins and deposit minerals. Collagen type I α 1 (COL1) is expressed in all stages of osteoblast differentiation and is main structural component of bone matrix. Osteopontin (OPN) is a non-collagenous matrix protein, while alkaline phosphatase is important in stabilizing the matrix. Osteocalcin is another non-collagenous protein, which is almost exclusively expressed in bone and is up-regulated in the late differentiation stage. It is expressed at the same time of mineralization stage indicating its role in the regulation of matrix mineralization [150]. After formation of new bone the process is terminated.

2.5) Crosstalk between tumor cells, immune cells and bone cells

The process of bone remodeling is affected by multiple factors contributed by tumor cells and lymphocytes. Role of T cells in bone remodeling is very well reported [28,50,51,151,152]. T cells originate from hematopoietic stem cells in bone marrow and get activated in thymus. Bone marrow serves as a central organ in mature T cells-traffic, acts as preferential homing site to memory T cells and contribute to their long term cytotoxic memory [153]. T cells regulate bone resorption in inflammation and osteoporosis [154]. T cells have been shown to localize near

osteoclasts [28]. Cancer cells produce multiple factors that recruit T cells to bone microenvironment. PTHrP is one of the important factor abundantly secreted by breast cancer cells under the influence of TGF β (released from resorbed bone) [117]. PTHrP activates secretion of RANKL by osteoblasts [155] and has possibly been predicted to activate T cells. PTH and PTHrP both can bind to PTHR1. T cells express PTHR1 and are activated by PTH [156,157]. Number of surface molecules and membrane proteins on T cells assist them to interact with bone cells, such as LFA1, TCR and CD6⁺ T cells interact with ICAM1, MHC-II and CD166 respectively on osteoblasts [158]. Osteoclasts and osteoblasts behave like antigen presenting cells and activate T cells [159]. Peripheral blood T cells from cancer patients have been shown to secrete potent pro-osteoclastogenic factors like TNF α and sRANKL, which spontaneously induce osteoclastogenesis [160,161,162]. Activated CD8⁺ T cells express higher levels of RANKL as compared to activated CD4⁺ T cells *in vitro* [162]. T cells secrete TNF-related apoptosis-inducing ligand (TRAIL), which blocks OPG action (decoy receptor of RANKL and thus antiosteoclastogenic) and also protects breast cancer cells from TRAIL induced apoptosis [163]. Bone marrow of breast cancer patients [164] and multiple myeloma [162] patients have been reported to show increased IL7 levels as compared to normal tissues. IL7, a key player in lymphocyte generation and T cell homeostasis, induces RANKL and TNF- α secretion in T cells [162,165]. Higher level of IL7 increases T cell proliferation, activation and has been associated with upregulated antigen presentation [166]. Elevated levels of circulating IL7 levels increased T cells migration from thymus in mice [166]. Another cytokine secreted by tumor cells is IL8 (CXCL-8), which activates osteoclastogenesis in RANK-RANKL independent manner [167]. Cytotoxic CD8⁺ T cells express IL8 receptors (CXCR1 and CXCR2), which upon binding to IL8 activates T cells to induce potent cytotoxic reaction (production and release of perforin,

granzyme B and IFN γ) [168]. Inhibition of IL8 receptors showed reduced migration of thymic T cells in mice [168]. Though IL7 has an immunostimulatory effect, bone microenvironment contains elevated levels of TGF- β . TGF- β is a potent immunosuppressive cytokine, which inhibits T cell proliferation, NK-cells and antigen presentation by T cells [169]. TGF- β inhibits expression of IFN- γ induced transcription factors, IFN regulatory factor -1 and T-bet, factors involved in differentiation of naive T cells to Th1 subtype [169] and also downregulates IFN- γ signaling by preventing phosphorylation of JAK1 and STAT1 by increasing Shp-1 phosphatase [170], which ultimately inhibits development of Th1 cell types. TGF β is essential for induction of expansion and function of regulatory T-cells *in vivo* [171]. TGF- β induces expression of transcription factor FoxP3 in CD4⁺CD25⁻ T cells [172]. TGF- β has been shown to suppress cytotoxicity of CD8⁺ T lymphocytes (CTLs) by specifically inhibiting the expression of five cytolytic genes- perforin, granzyme A, granzyme B, FasL, and IFN γ , through binding of TGF- β induced smad and ATF1 to promoters of these genes [173]. Cytokines secreted by T cells influence the process of osteoclastogenesis. Immune cells secrete an array of cytokines like IL6, IL17, TGF β , TNF α and RANKL, which are known to induce osteoclast formation and function, while cytokines like IL4, IL10, IL12, IL13, IL18 and IFN γ inhibit the process of osteoclastogenesis [126]. Conventional CD4⁺ T cells upon activation increase expression of RANKL and are known to be pro-osteoclastogenic [174]. IL17 producing CD4⁺T cells cause bone destruction by inducing RANKL expression on synovial fibroblasts and osteoblasts. IL6, TNF α and IL1 β work in a synergistic manner to stimulate osteoclast differentiation [175]. IL6 together with IL11 supports osteoclast formation and resorption [176]. TNF α is a proinflammatory cytokine, which directly and indirectly enhances osteoclast generation and its resorptive activity [177,178]. TNF along with RANKL increases expression of RANK on

osteoclast precursor cells [179]. $\text{TNF}\alpha$ and $\text{TGF}\beta$ synergistically induce osteoclastogenesis in the absence of TRAF6 or RANK, which explains potential role of $\text{TNF}\alpha$ in bone pathologies [177]. TNF and $\text{IL1}\beta$ synergistically promote expression of osteoprotegerin ligand (osteoprotegerin is a decoy receptor for RANKL) in osteoblasts [180], upregulate expression of RANKL on osteoblasts and stromal cells, stimulate differentiation of osteoclast precursor cells and increase activity and survival of osteoclasts by preventing apoptosis [145]. $\text{TNF}\alpha$ stimulates production of IL6 in osteoblasts and osteoblast-like osteosarcoma cells [181]. IL4 inhibits $\text{TNF}\alpha$ mediated osteoclast formation by inhibition of RANKL expression in $\text{TNF}\alpha$ activated stromal cells and direct inhibition of $\text{TNF}\alpha$ -activated osteoclast precursors via a T-cell-independent mechanism *in vivo* [182]. IL10 exerts a reciprocal action on the differentiation of osteoclasts and macrophages from their shared precursor by substantial reduction in the ratio of calcitonin receptor-positive cells to macrophages [183]. $\text{IFN}\gamma$ is a potent inhibitor of osteoclastogenesis as it degrades TRAF adaptor protein involved in RANK-RANKL signaling [51].

2.6) Vicious Cycle

Primary tumor cells release factors before dissemination and create a pre-metastatic niche, which is supported by bone marrow. Bone remodeling is controlled by osteoblasts through changes in expression of RANKL and OPG [184]. Cancer cells mimic the physiological pathways that maintain bone remodeling and secrete factors which enhance osteoclastogenesis [117]. Breast cancer cells share number of phenotypes with bone cells, such as, expression of calcitonin receptors, bone sialoproteins, cathepsin-K and osteopontin which might be contributing in their establishment and growth in bone [185,186]. Breast cancer produce IL1, IL6, LIF, prostaglandin E2, $\text{TNF}\alpha$ and these factors are known to increase RANKL expression on osteoblasts and

activate them [187]. Most importantly, breast cancer cells produce PTHrP, which plays pivotal role in bone metastasis and increase in osteoclastogenesis [188]. PTHrP positive breast cancer patients are more likely to develop bone metastases [113] and is considered as a good prognostic factor [189]. PTHrP has even been proposed as a potent antigen for cancer immunotherapy in many cancers [190,191]. PTHrP is secreted by breast and prostate cancer cells and functions like Ca^+ regulating hormone PTH [192]. PTHrP plays crucial role in metastasis of breast cancer cells, as reports suggest that PTHrP produced by breast cancer cells can induce generation of osteoclasts in bone marrow cultures with osteoblast in the absence of vitamin D3, PGE2 or IL11 [193,194]. PTHrP secreted by breast cancer cells act in autocrine and paracrine manner on osteoblasts [195], induce RANKL expression in osteoblasts (with reduction in OPG expression) [195,196] and stromal cells [113]. RANKL is essential for survival and differentiation of osteoclasts [197]. RANKL induces expression of factors involved in migration, invasion and angiogenesis like matrix metalloproteinases 1 and 9, matrix metalloproteinase inducer EMMPRIN/CD147, intercellular adhesion molecule-1 (ICAM-1), interleukin 6 and 8 and vascular endothelial growth factor. RANKL also enhances breast cancer-induced osteolytic lesions through upregulation of extracellular matrix metalloproteinase inducer/CD147, while suppresses expression of metastasis suppressor serpin 5b/maspin [198]. TGF- β is a potent stimulator of PTHrP production. It stabilizes PTHrP mRNA during and post transcription [199,200]. Also, breast cancer cells express higher levels of PTHrP at bone metastatic site (92%) compared to primary tumor site (50%) / non-bone metastasis (17%) [113]. Metastatic tumor cells interact with both osteoclast and osteoblasts and alter the process of bone remodeling. Metastatic breast tumor cells induce osteoblasts to release osteoclastogenesis enhancing factors such as RANKL, monocyte chemoattractant protein-1, IL6 and cyclooxygenase 2 [201,202,203]. IL6, a

proinflammatory cytokine, works synergistically with PTHrP to enhance bone resorption [204]. In turn, tumor cells get nourishment through factors like IGF1 and II, TGF β and bone morphogenic proteins, which are embedded in bone otherwise and are released upon bone resorption by osteoclasts [205,206]. These cancer cells further support and enhance osteoclastogenesis, creating a vicious cycle. Thus osteoclastogenesis-directed therapy has proven to be a potential therapy to reduce osteolysis and inhibit tumor growth at metastatic sites [207]. Drugs inhibiting MCSF receptor signaling through cFms in osteoclasts have been found to suppress bone metastasis in breast cancer [208]. Denosumab (anti RANKL mAb) therapy was found effective in bone metastatic breast cancer patients [209,210,211]. Aminobisphosphonates are also potent antiresorptive drugs which are used for the treatment of patients with skeletal disorders and metastasis associated skeletal disorders.

2.7) Aminobisphosphonates

Bisphosphonates (BPs) are synthetic analogues of the naturally occurring pyrophosphate molecule (PPi) but have a greater stability than PPi and are resistant to enzymatic hydrolysis. Two side chains (R1 and R2) are covalently bound to the carbon atom of the common P–C–P structure [52]. This common backbone and R1 chain allow BPs to bind to bone minerals such as calcium, whereas the R2 chain determines the potency of the drug. Depending on R2 group, bisphosphonates are categorized into two groups- non-nitrogen containing and nitrogen containing bisphosphonates. 1st generation bisphosphonate (etidronate, clodronate or tiludronate) are non-nitrogen containing bisphosphonates and inhibit essential ATP-dependent intracellular enzymes which leads to an intracellular accumulation of cytotoxic ATP-analogues. 2nd and 3rd generation bisphosphonates contain nitrogen containing group at R2 side chain and are known as

aminobisphosphonates (pamidronate, risedronate, alendronate, minodronate, ibandronate and Zoledronate). As shown in Figure 6, aminobisphosphonates inhibit a key enzyme in the mevalonate pathway known as farnesyl pyrophosphate synthase (FPPS) and thus inhibits generation of farnesyl pyrophosphates and geranylgeranyl pyrophosphate. Several intermediates in this pathway including farnesyl pyrophosphate and geranylgeranylpyrophosphate are

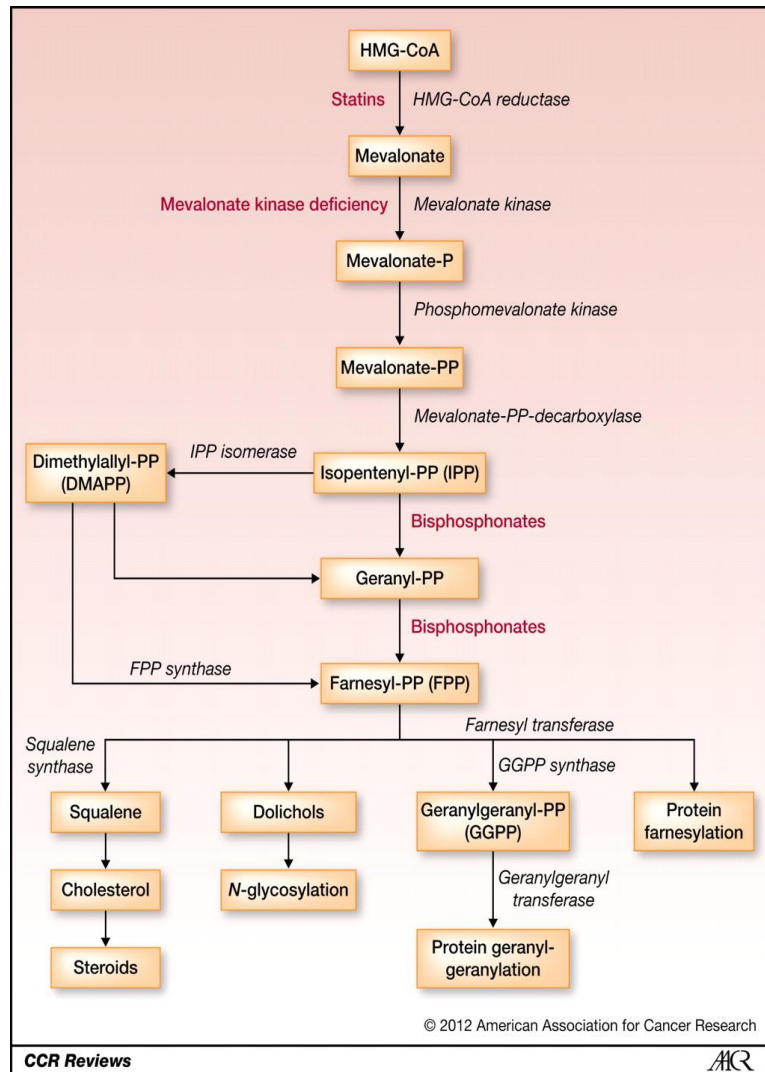


Figure 6: Mechanism of aminobisphosphonates action

required for the post translational modification (i.e. prenylation) of guanosine triphosphate binding proteins such as Ras, Rho, and Rac. These signaling molecules are involved in the regulation of cell proliferation, cell survival and cytoskeletal organization [212,213]. Zoledronate, the most potent 3rd generation aminobisphosphonate, is the only bisphosphonate currently approved for the prevention and treatment of skeletal complications in patients with bone metastases due to all solid tumor [214]. Zoledronate have attraction for elemental calcium, thus get targeted to bone surface and are actively resorbed by osteoclasts [53,215], resulting in

their apoptosis [216]. Zoledronate does not affect the differentiation of osteoblasts [217]. Apart from inhibiting mevalonate pathway, Zoledronate have been shown to inhibit angiogenesis (endothelial cell proliferation, adhesion and capillary formation), decrease tumor cell adhesion to bone, inhibit tumor cells proliferation, induce apoptosis and also acts as an immunomodulator [218]. Inhibition of FPPS enzyme by aminobisphosphonates (Zoledronate) causes accumulation of IPP, which acts as an antigen for $\gamma\delta$ T cells. Proteomic approaches are being used to decipher the effect of bisphosphonates on functional subunits (proteins) of tumor cells [219,220]. In hepatocellular carcinoma cell line, Alendronate treatment upregulated HSP90 expression [219]. In an another study, expression of Fas and Fas associated protein death domain (FADD) was found to be upregulated upon Alendronate treatment on hepatocellular carcinoma cells line [221]. Target cells receive extrinsic apoptosis signals through Fas and FADD [222].

2.8) $\gamma\delta$ T cells

$\gamma\delta$ T cells represent the minor subset of peripheral blood representing ~1-10% of total T cell population in human, but can rise upto 50% in some mucosal sites [223]. They have different properties compared to conventional $\alpha\beta$ T cells (Table 1). Major population of $\gamma\delta$ T cells are present in peripheral blood and express V γ 9V δ 2 TCR (also known as V γ 2V δ 2, 90-95%), while the subset that resides in mucosal tissues express V γ 9V δ 1 TCR (~10%). $\gamma\delta$ T cells harbor properties of both innate and adaptive immune cells. $\gamma\delta$ T cells are typical Th1 type cells but like $\alpha\beta$ T cells, are highly plastic and can differentiate into different subsets like Th2, Th17, T-follicular helper and T-regulatory cells under different conditions [13]. This explains their capacity to influence the nature of immune responses in different challenges (Table 2).

Table 1: Major differences between $\alpha\beta$ and $\gamma\delta$ T cells

Feature	$\alpha\beta$ T cells	$\gamma\delta$ T cells
Frequency in blood	65%–75% of PBMC	<10% of PBMC (25%–60% gut)
MHC restriction	CD4 ⁺ : MHC class II CD8 ⁺ : MHC class I	No MHC restriction Possible roles of CD1 and MICA/B
CD4/CD8 expression	• ~60% CD4 ⁺ ; ~30% CD8 ⁺ <1% double positive; <1% double negative;	Majority (>70) double negative; <1% CD4 ⁺ ; ~30% CD8 ⁺ $\alpha\alpha$ (as intraepithelial lymphocytes in gut)
Antigen recognition	Processed peptide/MHC	Unprocessed, not peptides
TCR V gene germ line repertoire	Large	Small
TCR diversity	Very diverse	Relatively restricted expression despite high potential for junctional diversity; expression variance dictated by tissue localization
Function	Adaptive immunity	Immune regulation, surveillance and homeostasis

[Kalyan et al (2013), *Cellular and molecular immunology*, 10:21-29]

Table 2: Phenotypical heterogeneity and functional package organization of human $\gamma\delta$ T cells

Subset	$\gamma\delta 1$	$\gamma\delta 2$	$\gamma\delta 17$	$\gamma\delta 22$	$\gamma\delta FH$	$\gamma\delta reg$
Polarizing cytokine	IL-12	IL-4	IL-1- β , IL-6, IL-23, TGF- β	?	IL-21	IL-15, TGF- β
Transcription factor	T-bet, Eomes	GATA-3	RORC, AHR	?	Bcl-6	Foxp3?
Homing receptors	CXCR3, CCR5	?	CCR6	?	CXCR5	?
Effector molecules	TNF- α , IFN- γ	IL-4	IL-17	IL-22	IL-4, IL-10	?
Target cells	Macrophages, Dendritic cells	?	Neutrophils, Epithelial cells	?	B cells	T cells
Function	Intracellular bacteria	?	Extracellular bacteria	?	Antibody production	Regulation

[Caccamo et al (2013), *Cellular and molecular immunology*, 10: 30-34]

$\gamma\delta$ T cells possess unique properties with respect to antigen recognition, tissue tropism, MHC-independent antigen recognition and antitumor response. Unlike $\alpha\beta$ T cells, $\gamma\delta$ T cells do not require major histocompatibility complex (MHC) class I and II for antigen recognition [12]. $\gamma\delta$ T cells do not require antigen to be processed and recognize whole antigen [224]. $\gamma\delta$ T cells directly recognize the antigens through TCR. The unique antigens recognized by $\gamma\delta$ T cells include small phosphoantigens such as isopentenyl pyrophosphate (IPP) and (E)-4-Hydroxy-3-methyl-but-2-enyl pyrophosphate (HMBPP), phospholipids, heat shock proteins, alkylamines and aminobisphosphonates [11,74]. IPP is a non-proteinaceous molecule and an intermediate molecule in eukaryotic mevalonate/ cholesterol pathway. HMBPP is an intermediate molecule in bacterial non- mevalonate/ rohmer pathway. Synthetic analog of IPP [bromohydrin pyrophosphate (BrHPP)] and HMBPP (picostim) also stimulates $\gamma\delta$ T cells. Alkylamines are naturally occurring plant and bacterial products and function in a similar manner to aminobisphosphonates [225]. Activation of $\gamma\delta$ T cells through aminobisphosphonates need antigen presenting cells. Aminobisphosphonate treated tumor cells upregulate IPP levels, which recruits $\gamma\delta$ T cells by chemotaxis and activates $\gamma\delta$ T cells. $\gamma\delta$ T cells also recognize transformed tumor cells by upregulation of self heat shock proteins. $\gamma\delta$ T cells recognize stressed cells/ tumor cells / virus infected cells through NKG2D, which binds to non-classical MHC molecule of MHC class I chain related molecule (MICA) and UL16 binding proteins (ULBPs) on affected cells [226,227,228]. ULBPs are expressed on leukemia, lymphoma, ovarian and colon carcinomas [229,230]. $\gamma\delta$ T cells also get activated by mitochondrial protein ATP synthase/ F1ATPase, which shows structural similarity to IPP. Binding of MICA to NKG2D activates $\gamma\delta$ T cells, which upregulates expression of CD25 and release of cytolytic granules (granzyme and perforin), TNF α and IFN γ [227]. $\gamma\delta$ T cells can kill stressed or transformed cells

through engagement of death inducing receptors, such as CD95 (Fas) and TNF-related apoptosis inducing ligand receptor (TRAILR) and release of cytolytic granules granzyme and perforin [231,232]. Crosstalk between $\gamma\delta$ T cells and dendritic cells (DCs) induced maturation of DCs, which further induce proliferation and polarization of $\alpha\beta$ T cells and promote B cell responses and antibody switching [233].

$\gamma\delta$ T cells mediate immune responses against bacteria, viruses and tumor cells [14]. $\gamma\delta$ T cells recognize pathogen associated molecular patterns (PAMPS) and elicit a strong immune responses in salmonellosis, brucellosis, legionellosis, tularemia and listeriolysis [234,235]. In *Mycobacterium tuberculosis* infections, a rapid expansion and activation of $\gamma\delta$ T cells is noted [236]. $\gamma\delta$ T cells initiate effective adaptive immune responses through processing and presenting influenza virus derived peptides to CD4⁺ and CD8⁺ T cells [237]. $\gamma\delta$ T cells have been reported to kill different types of tumor cells *in vivo* and *in vitro*, which include breast cancer, bladder cancer, glioblastoma multiforme, neuroblastoma, carcinoma, hematological malignancies and multiple myeloma [70,238,239,240]. Apart from its direct cytotoxic activity, $\gamma\delta$ T cells secrete proinflammatory cytokines (TNF α , IFN γ and IL17), which clear the bacterial infections [235].

Potent antitumor activity and broad reactivity of $\gamma\delta$ towards different types of cancer cells has generated great interest for their use as immunotherapy [241]. $\gamma\delta$ T cell-based immunotherapy are currently focusing on two main approaches: (a) adoptive transfer of *ex vivo* activated and expanded $\gamma\delta$ T cells, and (b) *in vivo* activation of $\gamma\delta$ T cells using therapeutic agents, such as IL-2, bisphosphonates or tumor-directed monoclonal antibodies (e.g. rituximab and trastuzumab) specifically aimed at the recruitment and expansion of $\gamma\delta$ T cells [242]. Clinical trials involving the adoptive transfer of autologous, *ex vivo*-expanded $\gamma\delta$ T cells into cancer patients has found to be effective [243]. Activated $\gamma\delta$ T cells in cancer patients had given

positive outcome [244,245,246]. Use of $\gamma\delta$ T cell as a vaccine for cancer immunotherapy is considered as a new approach, where tumor antigen loaded $\gamma\delta$ T cells will interact with endogenous, tumor-specific $\alpha\beta$ T cells in secondary lymphoid tissues [247].

Chapter 3

Materials and methods

3.1) Culture medium

Powdered RPMI-1640 medium (Invitrogen Life-Technologies, Grand Island, N.Y), Dulbecco's Minimum essential medium (Invitrogen Life-Technologies, Grand Island, N.Y) or minimum essential medium with alpha modification (Sigma Aldrich, USA) was dissolved in deionized water and as per manufacturer's instructions, was supplemented with 2.8gram sodium bicarbonate (Sarabhai Chemicals, India). The medium was sterilized by membrane filtration (0.45mM, Millipore Co, USA). To prepare complete medium, plain RPMI/ IMDM/ α MEM was supplemented with 10% heat inactivated human AB serum or fetal calf serum (FCS, Invitrogen Life Technologies, USA), penicillin (100 IU/ml; Alembic Chemicals India), streptomycin (100 mg/ml; Alembic chemicals India), mycostatin (5 mg/ml, Sigma, USA), gentamycin (40mg/ml; Schering Corporation, India), L-Glutamine (2mM, Hi Media, India) and β -mercaptoethanol (10^5 ; Sigma USA).

3.2 Preparation of buffers

3.2.1) Normal Saline (NS)

0.85 gram sodium chloride (NaCl) was dissolved in 100 ml of deionized water and sterilized by autoclaving and was stored at 4°C.

3.2.2) L-Glutamine

3 grams of L-glutamine was dissolved in 100ml NS. It was autoclaved and was stored at 0°C.

3.2.3) PSGM

10^6 units of penicillin (against gram positive bacteria), 1gram of streptomycin (against gram negative bacteria), 5ml of gentamycin (against gram positive and gram negative bacteria) and

1ml of prepared stock of mycostatin (antifungal) were added in 400 ml of sterile NS, were aliquoted in sterile 100 ml glass bottles and were stored at -20° C in deep freezer.

3.2.4) Thioglycolate broth (Sterility medium)

14.9 grams of thioglycolate powder was dissolved in 500ml of deionized water completely. The solution was boiled till color turned yellow and was then poured (8ml/tube) in sterile glass tube containing a pinch of calcium carbonate. It was autoclaved at 121°C for 18 min at 15psi.

3.2.5) Ficoll-Hypaque

24 parts of 9% Ficoll 400 (Sigma Aldrich, USA) + 10 parts 33.3% sodium diatrizoate (Sigma Aldrich, USA) were mixed together and specific gravity was adjusted to 1.077 ± 0.001 .

3.2.6) Trypan blue

0.4 gram Trypan Blue powder (Fluke AG, Buchs SG, Switzerland) was dissolved in 100ml NS and was mixed thoroughly. To this, 0.01gram thiomersal was added, mixed well and was filtered by whatmann filter paper no.1. It was aliquoted and stored at 4°C.

3.2.7) 10X Phosphate Buffered Saline (PBS, pH 7.5)

Solution A: 0.2M $\text{NaH}_2\text{PO}_4 \cdot 2\text{H}_2\text{O}$: 5.616 gram $\text{NaH}_2\text{PO}_4 \cdot 2\text{H}_2\text{O}$ was dissolved in 180ml deionized water.

Solution B: 0.2M $\text{Na}_2\text{HPO}_4 \cdot 2\text{H}_2\text{O}$: 32.03 gram $\text{Na}_2\text{HPO}_4 \cdot 2\text{H}_2\text{O}$ was dissolved in 900ml deionized water.

160 ml Solution A and 840ml Solution B was mixed properly and pH was adjusted to 7.5. To this, 170 grams NaCl was added, dissolved properly and volume was made up to 2000 ml. The solution was stored at 4°C.

3.2.8) MACS Buffer

5 gram BSA was added to 2mM EDTA containing 1000 ml 1X PBS (pH 7.5). It was deoxygenated; filter sterilized and was stored at -20 till use.

3.2.9) Trypsin – EDTA

3 grams trypsin (Sigma Aldrich, USA) was dissolved in 100ml 1X PBS and it was filter sterilized. 0.02 gram EDTA (MP Biomedical) was dissolved in 100 ml 1X PBS and sterilized by autoclaving. The working solution was prepared by mixing Trypsin: EDTA (1:9, V/V).

3.2.10) FACS Buffer

2 ml fetal calf serum and 0.02 gram sodium azide (NaN_3 , Sigma Aldrich, USA) was added to 98ml 1X PBS (pH 7.5).

3.2.11) 1% Paraformaldehyde

1 gram paraformaldehyde (Sigma, USA) was dissolved in 70 ml 1X PBS by heating the solution in a microwave till it was dissolved completely. Final volume was made up to 100 ml and after cooling, solution was stored at 4°C.

3.2.12) Saponin Buffer

2ml FCS, 0.02 gram sodium azide (NaN_3 , Sigma Aldrich, USA) and 0.1% saponin (Reagent grade, Amersham Life science) was added to 98 ml 1X PBS (pH 7.5).

3.3) Maintenance of cell lines

The following cell lines were used-

S.No.	Cell line	Origin, (Cell type)	Characteristic features	Type	Medium
1	MCF 7	Breast Cancer, (epithelial)	ER ⁺ PR ^{+/-} HER2 ⁻	Adherent	RPMI
2	MDAMB 231	Breast Cancer, (epithelial)	ER ⁻ PR ⁻ HER2 ⁻	Adherent	DMEM
3	PC3	Prostate Cancer, (epithelial)	-	Adherent	RPMI
4	HeLa	Cervical Cancer, (epithelial)	-	Adherent	DMEM
5	Jurkat	Acute T cell Leukemia, (T-lymphocyte)	-	Suspension	RPMI
6	THP 1	Acute monocytic Leukemia (Monocyte)	-	Suspension	RPMI
7	Raw 264.7	Mouse macrophage,(Monocyte)	-	Adherent	αMEM

(Note: All the complete culture medium were supplemented with 10% FCS)

3.3.1) Revival of the cell lines

The frozen cells, stored in liquid nitrogen (-196°C) were received on ice and were thawed immediately vial by gentle agitation in a water bath at 37°C. Thawed cells were collected and thoroughly washed twice with plain medium to remove DMSO (toxic to cells).

3.3.2) Maintenance and subculturing of cell lines

Upon revival, the cells were washed twice with plain medium and were suspended in complete medium (1×10^6 cells/ 5 ml). These cells were cultured in sterile 25mm² culture flasks (Nunc, Denmark) at 37°C in 5% CO₂ incubator. Adherent cells, upon attaining 70-80% confluency, were trypsinized using 0.3% trypsin prepared in 0.02% EDTA. The cells were collected, washed twice with plain medium and then sub cultured ($0.3\text{-}0.5 \times 10^6$ cell/ 5ml) in 25mm² tissue culture flask. In case of suspension cultures, upon confluency, single cell suspension was prepared by mixing the cells properly using pasture pipette and cells were sub cultured.

3.3.3) Freezing of cell lines

Adherent cells (collected by trypsinization) or non-adherent cells (suspension cultures) were washed twice with plain medium and pelleted by centrifugation at 400g (1200rpm) for 10 min at room temperature. Chilled freezing solution (FCS: DMSO =9:1)) was added (2×10^6 cells/ml) drop by drop with constant mixing to the pellet. $2-3 \times 10^6$ cells/ml of freezing mixture were transferred to cryovials (Nunc, Denmark) and were frozen in liquid nitrogen (-196°C).

(DMSO: Dimethyl Sulphoxide, MP Biomedicals, India)

3.4) Antibodies and recombinant proteins

3.4.1) Conjugated/ Labeled Antibodies

S.No.	Name of the Antibody	Company
1	Mouse- Anti Human CD3-FITC	B.D.Pharmingen, USA
2	Mouse- Anti Human CD3-Phycoerithin	B.D.Pharmingen, USA
3	Mouse- Anti Human CD3-PECF 594	B.D.Pharmingen, USA
4	Mouse- Anti Human CD3-Pascific Blue	B.D.Pharmingen, USA
5	Mouse- Anti Human CD3-PeCy7	B.D.Pharmingen, USA
6	Mouse- Anti Human CD3-PerCP	B.D.Pharmingen, USA
7	Mouse- Anti Human CD3-APC Cy7	B.D.Pharmingen, USA
8	Mouse- Anti Human CD4-APC	B.D.Pharmingen, USA
9	Mouse- Anti Human CD4-PECF 594	B.D.Pharmingen, USA
10	Mouse- Anti Human CD4-Alexafluor700	B.D.Pharmingen, USA
11	Mouse- Anti Human CD8-Pascific Blue	B.D.Pharmingen, USA
12	Mouse- Anti Human CD11b-AF488	B.D.Pharmingen, USA
13	Mouse- Anti Human CD14-FITC	B.D.Pharmingen, USA
14	Mouse- Anti Human IL17-AF488	B.D.Pharmingen, USA
15	Mouse- Anti Human CD19-PE	B.D.Pharmingen, USA
16	Mouse- Anti Human CD25-PE	B.D.Pharmingen, USA
17	Mouse- Anti Human CD25-PeCy5	B.D.Pharmingen, USA
18	Mouse- Anti Human CD25-PeCy7	B.D.Pharmingen, USA
19	Mouse- Anti Human CD27-APC	B.D.Pharmingen, USA
20	Mouse- Anti Human CD27-AF700	B.D.Pharmingen, USA
21	Mouse- Anti Human CD45RA-PeCy5	B.D.Pharmingen, USA
22	Mouse- Anti Human CD45RO-PeCy7	B.D.Pharmingen, USA
23	Mouse- Anti Human CD51/61-AF488	Biolegend, USA
24	Mouse- Anti Human CD54-PB (ICAM1)	Biolegend, USA
25	Mouse- Anti Human CD56-PE	B.D.Pharmingen, USA

26	Mouse- Anti Human CD62L-APC (LECAM-1)	B.D.Pharmingen, USA
27	Mouse- Anti Human CD69-FITC	B.D.Pharmingen, USA
28	Mouse- Anti Human CD127-AF647 (IL-7R)	B.D.Pharmingen, USA
29	Mouse- Anti Human CD178-PE (FasL)	Biolegend, USA
30	Mouse- Anti Human CD254-PE (RANKL)	B.D.Pharmingen, USA
31	Mouse- Anti Human CD314-PE (NKG2D)	Biolegend, USA
32	Mouse- Anti Human CD314-APC (NKG2D)	Milteney Biotech, Germany
33	Mouse- Anti Human $\alpha\beta$ -PE	B.D.Pharmingen, USA
34	Mouse- Anti Human $\gamma\delta$ -FITC	B.D.Pharmingen, USA
35	Mouse- Anti Human $\gamma\delta$ -PE	B.D.Pharmingen, USA
36	Mouse- Anti Human $\gamma\delta$ -APC	B.D.Pharmingen, USA
37	Mouse- Anti Human V δ 1-FITC	Thermo Scientific USA
38	Mouse- Anti Human V δ 2-PE	B.D.Pharmingen, USA
39	Mouse- Anti Human V γ 9-PE	B.D.Pharmingen, USA
40	Mouse- Anti Human MICA-APC	R & D Systems, USA
41	Mouse- Anti Human FOXP3-AF488	B.D.Pharmingen, USA
42	Mouse- Anti Human IFN γ -PECy7	B.D.Pharmingen, USA
43	Mouse- Anti Human HSP 60-AF647	B.D.Pharmingen, USA
44	Mouse- Anti Human HSP 70-PE	Santacruz biotechnologies, USA
45	Mouse- Anti Human HLADR-PE	B.D.Pharmingen, USA
46	Mouse- Anti Human Annexin-FITC	B.D.Pharmingen, USA
47	Goat anti mouse-FITC	Sigma Aldrich, USA
48	Goat anti mouse-PE	Sigma Aldrich, USA
49	Phalloidin-TRITC (Phalloidin-Tetramethyl rhodamine B isothiocyanate)	Sigma Aldrich, USA

3.4.2) Purified Antibodies

S.No.	Name of the Antibody	Company
1	Mouse- Anti Human HSP60	Santa Cruz Biotechnology, USA
2	Mouse- Anti Human HSP70	B.D.Pharmingen, USA
3	Mouse- Anti Human HSP90	B.D.Pharmingen, USA
4	Goat- Anti Human α Tubulin	Abcam, USA
5	Mouse- Anti Human Keratin 8	Sigma, USA
6	Rabbit- Anti Human EGFR	Cell Signaling, USA
7	Mouse- Anti Human β -Actin	Sigma Aldrich, USA
8	Goat anti mouse-HRPO	Sigma Aldrich, USA
9	Goat anti rabbit-HRPO	Cell Signaling, USA
10	Mouse- Anti human CD3	BD Biosciences USA
11	Mouse- Anti human CD28	BD Biosciences, USA
12	Mouse- Anti Human IFN γ	B.D.Pharmingen, USA
13	Mouse- Anti human IL6	R & D Systems, USA

3.4.3) Recombinant proteins

S.No.	Name of the protein	Company
1	Recombinant human interleukin 2 (rhIL2)	Peptotech, USA
2	Recombinant mouse macrophage colony stimulating factor (rmMCSF)	R & D Systems, USA
3	Recombinant mouse receptor activator of nuclear factor kappa B (rmRANKL)	R & D Systems, USA
4	Recombinant human macrophage colony stimulating factor (rhMCSF)	R & D Systems, USA
5	Recombinant human receptor activator of nuclear factor kappa B (rhRANKL)	R & D Systems, USA

3.4.4) Other Chemicals

S.No.	Name of the chemical	Company
1	Bromohydrin Pyrophosphate (BrHPP)	Innate Pharma, France
2	Isopentenyl Pyrophosphate (IPP)	Sigma Aldrich, USA
3	Picostim	Innate Pharma, France
4	Zoledronate (Zometa)	Novartis, Switzerland
5	Brefeldin A	Sigma Aldrich, USA
6	Phorbol 12-myristate 13-acetate (PMA)	Sigma Aldrich, USA
7	Ionomycin Calcium salt	Sigma Aldrich, USA

3.5) Study group

~20 ml heparinized blood was collected from breast cancer patients (n=36, stage I to IV, age 28-77 years) and healthy individuals (n=38, age 23-48 years). For the present study, blood samples were collected from breast cancer patients (a) who had bone metastasis and (b) patients without bone metastasis. All the patients with bone metastasis received Zoledronate treatment for at least 3 months. Zoledronate was given as intravenous infusion over 15 minutes (total 4mg dose), once every 4 weeks. The present study was approved by the Institutional Ethics Committee and informed consents were taken from the breast cancer patients and healthy volunteers before collecting the blood sample.

3.6) Cell separation techniques

3.6.1) Separation of peripheral blood mononuclear cell

Peripheral blood mononuclear cells (PBMCs) were separated from heparinized peripheral blood of healthy individuals or breast cancer patients by ficoll-hypaque density gradient centrifugation. In brief, peripheral blood from healthy individuals or breast cancer patients was collected in heparin (Sigma, USA; 100IU/ml) or EDTA containing vacutainers. The blood was diluted with equal quantity of normal saline. 7-8 ml of diluted blood was loaded on 2.5ml Ficoll-Hypaque and centrifuged at 500g (1500 rpm) for 20 min at RT using a swing-out rotor in Beckman centrifuge. Buffy coat (PBMCs) was collected from interface between ficoll-hypaque and blood plasma. PBMCs were washed twice with normal saline at 400g (1200rpm) 10 min at RT. Viability of the cells was checked by trypan blue dye exclusion method.

3.6.2) Enrichment and purification of $\gamma\delta$ T cells from PBMCs of healthy individuals and breast cancer patient

3.6.2.1) Enrichment of $\gamma\delta$ T cells using α CD3/CD28/rhIL2

PBMCs were separated from heparinized peripheral blood of healthy individuals and breast cancer patients as described above. 25mm² tissue culture flasks were precoated with solid phase α CD3mAb (1 μ g/ml) for 2 hrs at 37°C or overnight at 4°C, thoroughly washed with normal saline. PBMCs (10x10⁶ cells) were suspended in 10ml cRPMI (10% heat inactivated human AB serum and antibiotics) supplemented with rhIL2 (100 IU/ml) and α CD28 (1 μ g/ml) and 5x10⁶ cells were seeded in pre-coated flask. For 4 days, the cells were fed with 1ml fresh cRPMI supplemented with rhIL2 (500 IU/ml), after replacement of 1 ml used medium. On 5th day, the cells were transferred to 75mm² culture flask, making final volume 10ml. The cells were expanded using rhIL2 (100 IU/ml) for 12 days with intermediate subculture after every 2-3 days.

3.6.2.2) Immunomagnetic separation of $\gamma\delta$ T cells from PBMCs

$\gamma\delta$ T cells were positively separated from freshly isolated PBMCs or α CD3-CD28/rhIL2 expanded PBMCs using TCR- $\gamma\delta$ Microbead Kit (Milteneq Biotech, Germany, Cat No.130-050-701). For which, expanded PBMCs (10×10^6 cells) were washed twice with normal saline and were suspended in 40 μ l MACS buffer [degassed PBS containing 0.5 % BSA (Sigma A7030) and 2mM EDTA]. The cells were incubated with 10 μ l TCR- $\gamma\delta$ hapten mAb for 10 min at 4°C, followed by addition of 30 μ l MACS buffer. The cells were subsequently incubated with 20 μ l anti hapten-FITC microbeads for 15 min at 4°C. Labeled cells were then washed with 5-8 ml MACS buffer at 400g for 10 min to remove excess/unbound antibody. Pelleted cells were resuspended in 500 μ l MACS buffer. MACS column [capacity of columns-MS: 10×10^6 cells (Milteneq Biotech, Germany), LS (Milteneq Biotech, Germany)] was placed in magnetic field of MACS separator and was pre-wet thrice with 1500 μ l MACS buffer (500 μ l each time). The labeled cells were then loaded on to pre-wet column (placed in magnetic field) and the column was repeatedly washed with MACS buffer to remove unlabeled cells (negative population). Further, the column was removed from the MACS separator (magnetic field) and labeled cells ($\gamma\delta$ -TCR positive population) were collected in separate tube by flushing them out of the column using MACS buffer. The purity of the sorted cells ($\gamma\delta$ TCR-FITC) was analyzed by flow cytometry and cells having >95% purity were used for experiments. Sorted cells were rested overnight before using them for any experiment.

3.6.2.4) Collection of cell free supernatant of $\gamma\delta$ T cells

Cytokine profile of $\gamma\delta$ T cells stimulated with rhIL2, BrHPP+rhIL2, α CD3/CD28+rhIL2 and Zoledronate+rhIL2 were analyzed by cytometric bead array (CBA). $\gamma\delta$ T cells (1×10^6) were stimulated with rhIL2 (2.5 IU), BrHPP (200nM) +rhIL2, α CD3/CD28 (1 μ g/ml) +rhIL2 (2.5 IU)

for 24 hrs at 37°C in 5% CO₂ incubator in 24 well plate. To stimulate $\gamma\delta$ T cells with Zoledronate, monocytes (antigen presenting cells) were separated from PBMCs by allowing them to adhere for to plate bottom 2 hrs. Adhered monocytes were treated with Zoledronate (100 μ M) for 16-18 hrs. After 16-18 hrs, monocytes were washed with pRPMI and $\gamma\delta$ T cells were incubated with Zoledronate treated monocytes for 24 hrs. As control, $\gamma\delta$ T cells were incubated with medium alone (unstimulated) for 24 hrs. After 24 hrs, cell free supernatants of unstimulated (control) and antigen stimulated $\gamma\delta$ T cells were collated and stored at -80°C till use.

3.6.2.5) Immunomagnetic separation of CD14⁺ cells from PBMCs

CD14⁺ cells were separated from PBMCs by positive selection method using CD14⁺ cell separation kit (Milteney Biotech, Germany). PBMCs (~100-200x10⁶) were suspended in 80 μ l MACS buffer and were labeled with bead conjugated anti-CD14⁺ antibody (20 μ l/test) for 15 min at 4°C. The cells were subsequently washed with MACS buffer and passed through magnetic column (as described above). CD14⁺ cells were later separated from column by plunging MACS buffer through the column. Purity of separated cells was analyzed using flow cytometry. Separated cells having >95% purity were further used for experiments.

3.7) Generation and characterization of mouse and human osteoclasts

3.7.1) Chemicals preparation

i) Reconstitution of rmMCSF, rmRANKL:

Recombinant mouse macrophage colony stimulating factor (10 μ g) and recombinant mouse receptor activator of nuclear factor kappa B (10 μ g) were stored at -20°C. rmMCSF and rmRANKL were reconstituted in sterile 1X PBS (pH 7.5) containing 0.1% BSA (bovine serum

albumin) at concentration of 10ng/ μ l. Similarly, reconstituted rmMCSF and rmRANKL (500ng/50 μ l) were stored at -80°C. As per the required concentration, the recombinant proteins were diluted with 1X PBS/ complete medium.

ii) Reconstitution of rhMCSF and rhRANKL/rhTRANCE:

RhMCSF (5 μ g) and rhRANKL/ rhTRANCE (TNF-related activation-induced cytokines, 10 μ g), stored at -20°C, were reconstituted in sterile 1X PBS (pH 7.5) containing 0.1% BSA at concentration of 10ng/ μ l. Similarly, reconstituted rhMCSF and rhRANKL (500ng/50 μ l) were stored at -80°C. As per the required concentration, the recombinant proteins were diluted in 1X PBS.

iii) Preparation of complete Modified Essential Medium with alpha modification medium (α MEM):

100ml α MEM was prepared by supplementing ρ MEM (Sigma, USA) with 10% inactivated fetal calf serum, antibiotics (penicillin, streptomycin, mycostatin, gentamycin), L-Glutamine and β -mercaptoethanol.

3.7.2) Neutral red pinocytosis assay using RAW 264.7 cell line:

RAW264.7, mouse macrophage cell line, is characterized by neutral red pinocytosis assay. RAW264.7 cells at different cell densities (3×10^3 , 5×10^3 , 1×10^4 , 5×10^4 per 200 μ l) were allowed to adhere in 96 well flat bottom plate for 2 hrs, followed by stimulation with (1 μ g/ml) bacterial lipopolysaccharide (Sigma, USA) for 48 hrs. Bacterial lipopolysaccharide induces transcription of several genes encoding proinflammatory mediators of immune responses. Further, these stimulated cells were incubated with 100 μ l neutral red (0.075% prepared in 1X PBS) for 2 hrs. After 2 hrs, supernatant was discarded, cells were washed with 1X PBS and were further incubated with 100 μ l cell lysis solution (ethanol: 0.01% acetic acid=1:1) for 2 hrs. Optical

density (OD) of neutral red upon cell lysis was analyzed at 570nm. ODs of medium alone, cells alone and medium+ neutral red were used as experimental control. The data is expressed as optical density observed at 570nm.

3.7.3) Generation of mouse osteoclasts from RAW264.7 cells

RAW264.7 cells (mouse macrophage cell line) were used to generate mouse osteoclasts [248]. RAW264.7 cells (3×10^3) were cultured in α MEM supplemented with rmRANKL (100ng/ml) for 7 days with intermediate feeding on every 3rd day. On 8th day, cultures were terminated and cells were stained for TRAP (tartarate resistant acid phosphatase) using Leukocyte Acid Phosphatase kit (Sigma-Aldrich, USA) as per the kit instructions. Multinucleated (>3 nuclei), TRAP positive cells were considered as mature osteoclasts.

3.7.4) Characterization of osteoclasts by tartarate resistant acid phosphatase (TRAP) staining

Mature osteoclasts were characterized by staining them for TRAP as per the kit instructions (Acid phosphatase, Leukocyte kit, Sigma). Osteoclasts were fixed in fixative solution (2.5ml citrate+6.5ml acetone+0.8ml 37% formaldehyde) for 30 sec. Fixed cells were repeatedly washed with pre-warmed deionized water (37°C) and were subsequently stained for acid phosphatase using sodium tartarate, fast Garnet GBC and naphthol AS-BI phosphate as a substrate for 1 hr in dark. After 1hr, cells were repeatedly washed with deionized water (37°C) to remove excess stain. Coverslips were air dried, mounted on glass slide and cells were imaged using upright microscope (Axioimager Z1.1, Zeiss). Images were analyzed using Axiovision software (version 4.6, Zeiss). Multinucleated (>3 nuclei) TRAP-positive cells were considered as mature osteoclasts.

3.7.5) Generation of mouse osteoclasts from bone marrow osteoclast precursor cells (BMOCPs)

6-8 week old Swiss CRL or C57BL6 mice were anesthetized using chloroform (Merck) and were sacrificed by cervical dislocation. Bone marrow cells were collected by flushing the femurs with α MEM using 26 gauge needle. Collected bone marrow cells were washed (400g, 10 min, RT) and were cultured in α MEM (30×10^6 cells/5ml) supplemented with rmMCSF (10ng/ml) for 24 hrs [to induce osteoclast precursor cells (OCPs) and to remove adherent stromal cells]. After 24 hrs, nonadherent OCPs were collected, washed and cultured for 7 days in α MEM (1×10^5 /200 μ l) supplemented with rmMCSF (30ng/ml) and rmRANKL (30ng/ml) on sterile thermanox coverslip (Nunc), which were placed in 96 well flat bottom plate). The cells were fed every 3rd day with rmMCSF and rmRANKL. On 8th day, presence of osteoclasts was confirmed by staining them for TRAP.

3.7.6) Generation and characterization of human Osteoclasts

Human osteoclasts were generated from CD14⁺ cells (monocytes). CD14⁺ cells (1×10^5) were cultured in complete α MEM medium supplemented with 30ng/ml rhMCSF and 40ng/ml rhRANKL on thermanox coverslips (Nunc, Denmark) in 96 well flat bottom plate. For 21 days, CD14⁺ cells were fed every 3rd day with rhMCSF and rhRANKL [249]. On day 21, mature multinucleated osteoclasts were characterized by staining them for expression of vitronectin receptor (α V β 3 integrin) using CD51/61-Alexafluor 488 mAb (IgG1, Biolegend) also known as 23c6 antibody along with nuclear stain DAPI (Sigma, D9542). Multinucleated cells (>3 nuclei) showing vitronectin receptor (23C6⁺) or TRAP positivity were considered as mature osteoclasts. Mature osteoclasts form a characteristic F-actin ring, which was analyzed by staining the

osteoclasts with Phalloidin-TRITC for 30 min at RT in dark. Images were acquired using Zeiss LCM 510 microscope and were analyzed using LSM Image analyzer software.

3.7.7) CD14⁺: $\gamma\delta$ T cell (1:10) coculture assay

CD14⁺ cells (1×10^5) were cocultured with unstimulated “activated $\gamma\delta$ T cells” (separated from α CD3/CD28+rhIL2 expanded PBMCs) or “non-activated/ freshly isolated $\gamma\delta$ T cells” (separated directly from PBMCs) were cocultured with $\gamma\delta$ T cells (1×10^4) in α MEM (200 μ l) containing rhMCSF (30ng/ml), rhRANKL (30ng/ml) and rhIL2 (0.5IU), in 96 well plate on day 1. The cells were incubated in 5% CO₂ incubator at 37°C. As a positive control, osteoclasts were generated from CD14⁺ cells in the presence of rhMCSF and rhRANKL only. To analyze the effect of phosphoantigen stimulated “non-activated $\gamma\delta$ T cells/ freshly isolated” on osteoclastogenesis; BrHPP (200nM) was added to cultures along with rhMCSF and rhRANKL on day 1. As experimental control, osteoclasts were also generated in the presence of rhIL2 or BrHPP+ rhIL2 along with rhMCSF and rhRANKL. For 21 days, CD14⁺: $\gamma\delta$ T cells (10:1) were fed every 3rd day with rhMCSF, rhRANKL and rhIL2. On 21st day, cultures were terminated and total number of osteoclasts generated per well were quantified by staining them for vitronectin receptor (CD51/61) using 23c6 mAb or TRAP.

3.7.8) Bone resorption assay

Cell free supernatants from “activated” or “non-activated/ freshly isolated” $\gamma\delta$ T cells stimulated with rhIL2 alone or BrHPP+rhIL2 were collected as described earlier. In brief, “activated” or “non-activated” $\gamma\delta$ T cells (5×10^4), suspended in cRPMI (200 μ l) were stimulated with rhIL2 (0.5IU) alone or BrHPP (200nM) + rhIL2 (0.5IU) in round bottom 96 well plate (Nunc) for 24 hrs at 37°C in 5% CO₂ incubator. After 24 hrs, cells free supernatants were collected and were stored at -80°C till use. Osteoclasts were generated from CD14⁺ cells (1×10^5) in the presence of

rhMCSF and rhRANKL for 12 days on Osteoclast Activity Assay Substrate (OAAS, BD Biosciences, USA). OAAS is a 16 well plate, with thin calcium-phosphate coated wells, resembling human bone and is used to evaluate functional activity of osteoclasts *in vitro*. 12th day onwards, every 3rd day, the cultures were fed with rhMCSF, rhRANKL and different volumes of cell free supernatant (50µl and 25µl) of rhIL2 or BrHPP+rhIL2 stimulated “activated” or “non-activated/freshly isolated” $\gamma\delta$ T cells. Osteoclasts generated in the presence of rhMCSF and rhRANKL only were kept as positive control. Baseline resorption observed on OAAS plates by macrophages (negative control, cultured in the presence of rhMCSF only) was also measured. On day 21, the cells were bleached out using bleaching solution (6% sodium hypochlorite and 5.2% sodium chloride). OAAS plates were air dried and resorption area/ pits generated by mature osteoclasts were imaged using light microscopy. The resorption area generated by mature osteoclast was calculated using ImageJ software.

3.7.9) IFN γ / IL6 neutralization Assay

Effect of IFN γ and IL6 on osteoclastogenesis was analyzed by neutralizing these cytokines in the cell free supernatants of $\gamma\delta$ T cells used for resorption assays. Osteoclasts were generated from CD14⁺ cells (1×10^5) in the presence of rhMCSF and rhRANKL for 12 days in OAAS module as described earlier. From 12th day onwards, every 3rd day, the cells were supplemented with rhMCSF, rhRANKL and cell free supernatant of unstimulated “activated” and “non-activated/freshly isolated” $\gamma\delta$ T cells (50µl), with or without monoclonal mouse antihuman α IFN γ or α IL6 neutralization antibody (10µg/ml) respectively. Osteoclasts generated in the presence of rhMCSF and rhRANKL were used as positive control. On day 21, the cultures were terminated and resorption area generated per OAAS well was calculated using ImageJ software.

3.8) Flow cytometry

3.8.1) Single color flow cytometry

3.8.1.1) Purity of immunomagnetically purified $\gamma\delta$ T cells

Single color flow cytometry was used to analyze the purity of MACS separated $\gamma\delta$ T cells using FACS Caliber flow cytometer (Becton Dickinson). Cells stained with IgG1-FITC conjugated antibody was kept as isotype control. Cells were selectively gated for lymphocyte population on the basis of forward scatter (FSC) and side scatter (SSC) plot. At least 10,000 events were acquired and data was analyzed using FlowJo software (Tree Star, USA).

3.8.1.2) Purity of immunomagnetically purified CD14⁺ cells

MACS purified CD14⁺ cells were analyzed for their purity using single color flow cytometry. CD14⁺ cells were stained with mouse anti human CD14-FITC mAb and acquired on a FACS Caliber flow cytometer (Becton Dickinson). CD14⁺ cells stained with IgG1-FITC conjugated antibody were used as isotype control. Cells were gated for monocyte population on the basis of forward scatter (FSC) and side scatter (SSC) plot and data was analyzed using FlowJo software (Tree Star, USA).

3.8.1.3) Analysis of cell cycle

To study the effect of Zoledronate on cell cycle, MCF7 cells were first arrested in G0 phase by serum starvation method. In brief, MCF7 cells were allowed to attain 60-70% confluency and then were serum starved for 72 hrs at 37°C in 5% CO₂ incubator. 50% used culture medium was replaced every 24 hr with fresh medium to remove dead cells and toxicity due to secreted metabolites. After 72 hrs, cells were incubated for next 4 hrs with 10% FCS containing cRPMI to drive the cells to log phase. These cells were then treated with Zoledronate (100 μ M) or left untreated for 16-18 hrs. After incubation, cells were washed thoroughly, trypsinized and fixed in

chilled 70% ethanol (1×10^6 cells/ml). Fixed cells were stored at 4°C for at least 24 hrs. Effect on cell cycle of tumor cells was analyzed by staining them with propidium iodide (PI, Sigma Aldrich,). Briefly, cells were washed twice with 1X PBS for complete removal of ethanol and were suspended in 500µl 1X PBS. Cells were incubated with RNase A (100µg/ml) and PI (40µM/ml) for 30 min in dark. Data was analyzed using ModfitLT software (version 2.0).

3.8.2) Multicolor flow cytometry

3.8.2.1. Detection of activation markers on stimulated $\gamma\delta$ T cells

Expression of early (CD69) and late activation markers (CD25 and RANKL) on $\gamma\delta$ T cells was analyzed by using multicolor flow. PBMCs were stimulated with rhIL2 (30IU) alone or in combination with BrHPP (200nM) or Zoledronate (100µM) for 12 days, with intermediate feedings on every 3rd day. For baseline expression (control) of activation markers on $\gamma\delta$ T cells was analyzed in untreated PBMCs (day 0). On day 12, the cultures were terminated; cells were collected, washed with cold 1X PBS and were suspended in FACS buffer [0.01M PBS (pH-7.5), 2% FCS, 0.01% sodium azide]. These cells (1×10^6 cells) were then stained for markers like anti-human $\gamma\delta$ -APC, anti-human CD69-FITC, anti-human CD25-PECy7 and anti-human RANKL-PE for 30 min at 4°C in dark. Anti-human CD3-FITC, anti-human CD3-PE, anti-human CD3-PECy7 and anti-human CD3-APC monoclonal antibodies were used for compensation. After 30 min, cells were washed with FACS buffer (to remove excess antibody) and were fixed in 1% cold paraformaldehyde at 4°C for 15 min in dark. At least 50000 events were acquired on FACS Aria (BD Biosciences, USA) and data was analyzed using FlowJo Software. Lymphocytes were gated on the basis of their FSC and SSC. Depending on the fluorescence intensity of $\gamma\delta$ -APC, $\gamma\delta$ T cells were gated. Further percentages of $\gamma\delta$ T cells expressing CD69, CD25 and RANKL (CD254) were analyzed on gated $\gamma\delta$ T cells. The gates were set according to only cell controls

for respective stimulation. Expression of activation markers (CD25, CD69 and CD254) were also analyzed on purified $\gamma\delta$ T cells (non-activated/ freshly isolated), for which $\gamma\delta$ T cells were directly purified from PBMCs ($\sim 100 \times 10^6$) on day 0 by MACS. These purified $\gamma\delta$ T cells (1×10^6 cells/ml) were left untreated or were stimulated with rhIL2 (2.5IU), α CD3/CD28 (1 μ g/ml), BrHPP (200nM), IPP (40 μ M), Picostim (20nM) or Zoledronate (100 μ M) for 24 hrs and then were stained for markers like $\gamma\delta$ -APC, CD69-FITC, CD25-PECy7 and CD254-PE). Expression of activation markers on them was then analyzed as describe above.

3.8.2.2. Immune profiling of healthy individuals and breast cancer patients

Immune profiles of healthy individuals and breast cancer patients (undergoing Zoledronate treatment and Zoledronate untreated) were generated by analyzing different immune cell subsets and their activation markers, memory markers and intracellular cytokines. PBMCs from healthy individuals and breast cancer patients were separated by ficoll-hypaque density gradient centrifugation as described earlier. Separated PBMCs were washed twice with cold 1X PBS (4°C) and were suspended in FACS buffer (1×10^6 cells/50 μ l). PBMCs (1×10^6 /50 μ l) were stained with fluorochrome labeled monoclonal antibodies for immune cell subset specific markers [CD3, CD4, CD8, NK (CD3⁻CD56⁺), NK-T (CD3⁺CD56⁺), B cells (CD19), regulatory T cells (CD4⁺CD25⁺CD127⁺FOXP3⁺), monocytes (CD14), $\gamma\delta$ T cells), activation markers [CD69, CD25, CD254], memory markers (CD45RA, CD27), intracellular cytokine [IFN γ , IL17] as per the recommended concentration, for 30 min at 4°C in dark. Cells were washed with 1X PBS and were then fixed in 1% paraformaldehyde for 15 min at 4°C in dark, followed by washing with FACS buffer. Cells were resuspended in 300 μ l FACS buffer and acquired on FACS Aria (BD Bioscience, San Jose, CA, USA). Atleast 50000 events were acquired and data was analyzed using FlowJo software (Version 7.5, Tree star, Germany). For intracellular staining (IL17, IFN γ ,

and FOXP3), PBMCs were permeabilized using 0.1% saponin buffer kept at 37°C for 5 min with gentle vortexing. The cells were then stained for intracellular makers, for 30 min at 4°C in dark. For intracellular staining the cells were washed with saponin buffer and were resuspended in FACS buffer for acquisition. **Antibodies used:** anti-human CD3-FITC (IgG1,B.D.Pharmingen), anti-human CD3-PE (IgG1, B.D.Pharmingen), anti-human CD3-PERCP (IgG1, B.D.Pharmingen), anti-human CD3-PECF594 (IgG1, B.D.Pharmingen), anti-human CD4-PECF594 (IgG1, B.D.Pharmingen), anti-human CD4-APC (IgG1, B.D.Pharmingen), anti-human CD8-PB (IgG1, B.D.Pharmingen), anti-human CD11b-AF488 (IgG1, B.D.Pharmingen), anti-human CD14-FITC (IgG1, B.D.Pharmingen), anti-human CD19-PE (IgG1, B.D.Pharmingen), anti-human CD25-PE (IgG1, B.D.Pharmingen), anti-human CD25-PECy5 (IgG1, B.D.Pharmingen), anti-human CD25-PECy7 (IgG1, B.D.Pharmingen), anti-human CD27-APC (IgG1, B.D.Pharmingen), anti-human CD45RA-PECy5 (IgG1, B.D.Pharmingen), anti-human CD69-FITC (IgG1, B.D.Pharmingen), anti-human CD127-APC(IL7R) (IgG1, B.D.Pharmingen), anti-human CD254-PE (IgG1, B.D.Pharmingen), anti-human FOXP3-AF488 (IgG1, B.D.Pharmingen), anti-human IL17-AF488 (IgG1, B.D.Pharmingen), anti-human IFN γ -PECy7 (IgG1, B.D.Pharmingen), anti-human HLADR-PE (IgG1,B.D.Pharmingen). **Antibodies used for compensation:** anti-human CD3-FITC (IgG1, B.D.Pharmingen), anti-human CD3-PE (IgG1, B.D.Pharmingen), anti-human CD3-PERCP (IgG1, B.D.Pharmingen), anti-human CD3-PECF594 (IgG1, B.D.Pharmingen), anti-human CD4-APC (IgG1, B.D.Pharmingen), anti-human CD3-PB (IgG1, B.D.Pharmingen), anti-human CD45RA-PECy5 (IgG1, B.D.Pharmingen), anti-human CD3-PECy7 (IgG1, B.D.Pharmingen).

3.8.2.3. Expression of HSP60 and HSP70 on MCF7 cells upon Zoledronate treatment

MCF7 (4×10^6) cells were treated with Zoledronate ($100 \mu\text{M}$) or left untreated for 24 hrs. After 24 hrs, cells were trypsinized, washed in 1X PBS and were suspended in saponin containing FACS buffer (1×10^6 cells/ $50 \mu\text{l}$) for permeabilization. Untreated and Zoledronate treated MCF7 cells were stained with anti-human HSP60-AF647 or anti-human HSP70-PE for 30 min at 4°C in dark. Cells were further washed with FACS buffer and were acquired on FACS Aria. The data was analyzed using FlowJo software.

3.9) Cytokine estimation in cell free supernatants of $\gamma\delta$ T cells

Detection of cytokine levels in cell free supernatants of $\gamma\delta$ T cells (healthy individuals and breast cancer patients) was carried out using cytometric bead array (CBA).

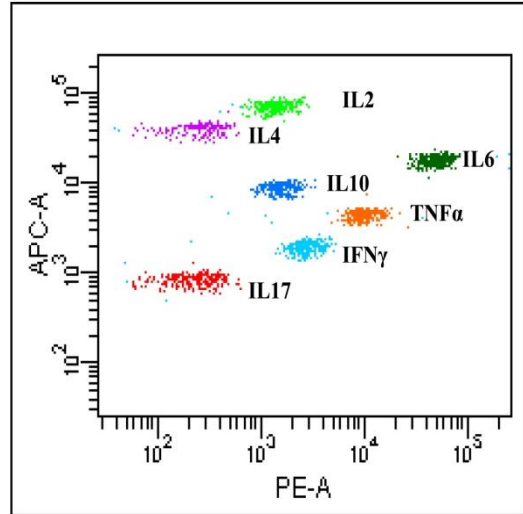
3.9.1) Collection of cell free supernatants for cytokine estimation

Cell free supernatants were obtained by stimulating immunomagnetically purified $\gamma\delta$ T cells (1×10^6) from healthy individuals and breast cancer patients with rhIL2 (2.5IU), BrHPP (200nM)+rhIL2, $\alpha\text{CD3/CD28}$ mAb ($1 \mu\text{g/ml}$)+rhIL2 or Zoledronate ($100 \mu\text{M}$)+rhIL2 for 24 hrs at 37°C in round bottomed 96 well plate. $\gamma\delta$ T cells cultured in medium only for 24 hrs was kept as control. After 24 hrs, supernatants were collected, centrifuged and were stored at -80°C . These supernatants were analyzed for their cytokine profiles.

3.9.2) Cytometric Bead Array (CBA)

Th1/Th2/Th17 cytokine profile of serum samples or cell free supernatants of $\gamma\delta$ T cells (unstimulated / stimulated) were analyzed by Cytometric Bead Array kit (BD Biosciences, USA)

as per the kit instructions. In brief, 50µl test samples and PE detection antibody were incubated with capture bead reagent for 3 hrs at RT in dark. Serum samples were treated with serum enhancing buffer before using them to estimate the cytokines. The beads were washed with 1 ml wash buffer and were suspended in 300µl wash buffer. Set-up beads were prepared (50µl of setup bead antibody + 450µl of wash



Standard graph for CBA

buffer). Samples were acquired on FACS Aria cytometer (BD Bioscience, San Jose, CA, USA), with gentle vortexing before acquisition. The data was analyzed using FCAP Array software (version 1.0, BD Biosciences, USA). Standard graph Th1/Th2/Th17 cytokines (IL2, IL4, IL6, IL10, TNFα, IFNγ and IL17A) was plotted and cytokines in test samples were quantified accordingly.

3.10) Confocal microscopy

3.10.1) Expression of HSPs on tumor cells

Breast tumor cells (MCF7 and MDAMB231, 500-1000 cells/500µl medium), were seeded on 22x22mm² sterile glass coverslip. The cells were allowed to adhere on glass coverslip for 5-6 hrs by incubating them at 37°C in 5% CO₂ incubator. Further, culture medium was removed and cells were fixed in 4% paraformaldehyde for 15 min at RT. Cells were washed thrice with 1X PBS and were permeabilized using chilled 90% methanol (-20°C) for 10 min at RT. Cells were washed with 1X PBS and blocking was done by incubating the cells in 1X PBS containing 3% FCS for 30 min at RT. Subsequently, cells were stained with anti-human HSP60-AF647 (IgG1,

B.D.Pharmingen) or anti-human HSP70-PE (IgG1, Biolegend) as per the recommended concentration, for 1 hr at RT in dark. The antibodies were diluted in 3% FCS containing 1X PBS. After 1 hr, excess antibody was removed by washing the cells with 1X PBS followed by staining with nuclear dye 4', 6-diamino-2-phenylindole (10ng/ml DAPI, Sigma Aldrich, USA) for 5 min at RT in dark. The images were acquired on Zeiss Laser-Scanning Microscope 510 (LSM510) META (Carl Zeiss, Jena, Germany) or Super resolution –Leica SP8/Sted 3X microscope and data was analyzed using LASAF software.

3.10.2) Effect of Zoledronate on reorganization of cytoskeletal elements in MCF-7

3.10.2.1) Actin microfilament reorganization

Effect of Zoledronate treatment on actin microfilament reorganization in MCF7 was analyzed by staining Zoledronate treated and untreated MCF7 cells with Phalloidin-TRITC. Phalloidin is a rigid bicyclic heptapeptide found in the death cap mushroom *Amanita phalloides*, binds tightly to filamentous actin (F-actin), stabilizing it and preventing it from depolymerization. Briefly, MCF7 cells were cultured on 22x22mm² glass coverslips (as described earlier) and were treated with Zoledronate or left untreated for 16-18 hrs. Further, cells were washed with 1X PBS and fixed in 4% paraformaldehyde for 15 min at 4°C. Further, cells were washed and stained with Phalloidin-TRITC for 30 min at RT in dark. Following incubation, the cells were washed and stained for nuclear dye DAPI (10ng/ml). Phalloidin stained cells were imaged by using LSM 510 microscope and images were analyzed using LSM Image analyzer.

3.10.2.2) Keratin 8 reorganization

Zoledronate treated or untreated MCF7 cells, cultured on coverslips and were washed twice with 1X PBS and were fixed in chilled methanol (-20°C) 1-1.5 ml chilled methanol was added

dropwise on the cells and kept at -20°C for 10 min. Further, cells were permeabilized using 1X PBS containing 0.3% Triton-X 100 for 10 min at RT and then were washed twice with 1X PBS. Cells were incubated with purified mouse anti human keratin 8 antibody (diluted as 1:150 in 1X PBS containing 3% BSA and 0.1% NP40) for 1hr at RT. Further, cells were alternatively washed 6 times with 1X PBS only or 1X PBS containing 0.1% NP40. Secondary antibody–GAM-AF488 was diluted (1:100) in same diluents and cells were incubated in dark for 30 min at RT. Subsequently cells were alternatively washed 10 times with 1X PBS only or 1X PBS containing 0.1% NP40. Nuclear dye DAPI was used to stain nuclei. Images were acquired on LSM 510 microscope and were analyzed using LSM Image analyzer software.

3.10.2.3) Tubulin reorganization

Zoledronate and untreated MCF7 cells were fixed in 4% paraformaldehyde for 20 min at RT and were then washed twice with 1X PBS. Cells were incubated in 1-1.5 ml 1X PBS containing 0.3% Triton-X 100 and 0.1% NP40 for 15 min at RT. Purified mouse anti human α -tubulin antibody was diluted as 1:400 in 1X PBS containing 3% BSA and 0.1% NP40 and cells were incubated for 2hr at RT or overnight at 4°C. Cells were alternatively washed 6 times with 1X PBS only or 1X PBS containing 0.1% NP40. Secondary antibody–GAM-AF488 was diluted (1:100) in same diluents and cells were incubated in dark for 1 hr at RT. Subsequently cells were alternatively washed 10 times with 1X PBS only or 1X PBS containing 0.1% NP40. DAPI (10ng/ml) was used to stain nuclei. Images were acquired on LSM 510 microscope and were analyzed using LSM Image analyzer software.

3.10.2.4) Characterization of mature human osteoclasts

Human osteoclasts were generated from CD14⁺ cells (monocytes) in the presence of rhMCSF and rhRANKL over the period of 21 days and were characterized by staining them for tartarate

resistant acid phosphatase (TRAP) or vitronectin receptor (CD51/61 or 23c6) as follows. Multinucleated (>3 nuclei) TRAP positive or 23c6+ cells were considered as mature osteoclasts.

3.10.2.5) Tartarate resistant acid phosphatase (TRAP) staining:

Osteoclasts were stained for tartarate resistant acid phosphatase (TRAP) using a leukocyte acid phosphatase kit (Sigma) as per the kit instructions. In brief, osteoclast culture were terminated on day 21 and cells were treated with fixative solution (2.5ml citrate + 6.5ml acetone + 0.8ml 37% formaldehyde) for 30 seconds, followed by washing with de-ionized water (37°C). The cells were then stained for acid phosphatase using sodium tartarate, fast garnet GBC and naphthol AS-BI phosphate as substrate for 1 hr in dark. Cells were repeatedly washed with de-ionized water (37°C) to remove excess stain. Slides were air dried and multinucleated TRAP-positive osteoclasts were imaged by light microscopy.

3.10.2.6) Staining human osteoclasts for vitronectin receptor (CD51/61 or 23c6)

The osteoclasts were generated as described above. Osteoclast cultures were terminated on day 21 and cells were fixed in 4% paraformaldehyde for 15 min at RT. Cells were then washed with 1X PBS and blocking was done in 0.5% BSA containing 1X PBS for 10 min at RT. Further, cells were incubated with recommended concentration (5µl/ 1x10⁶ cells/ test) of mouse anti-human CD51/61-AF488 monoclonal antibody (IgG1, Biolegend) for 1 hr at RT in dark. Excess antibody was removed by washing cell with 0.5% BSA containing 1X PBS. Cells were further stained for 5 min at RT in dark with nuclear dye DAPI (10ng/ml). Images were taken on Zeiss Laser-Scanning Microscope 510 (LSM510) META (Carl Zeiss, Jena, Germany) and were analyzed using LSM Image analyzer software.

3.11) MTT Assay

Effect of Zoledronate on survival of MCF7 cells was analyzed by conventional MTT (3-(4,5-Dimethylthiazol-2-yl)-2,5-Diphenyltetrazolium Bromide) assay. MTT assay is a colorimetric assay (Figure 7), which is based on the principle that yellow colored MTT is reduced by mitochondrial NAD (P)H-dependent cellular oxidoreductase enzymes of metabolically active cells to insoluble purple colored formazan (which can be dissolved in DMSO). Optical density of formazan is measured at 590nm.

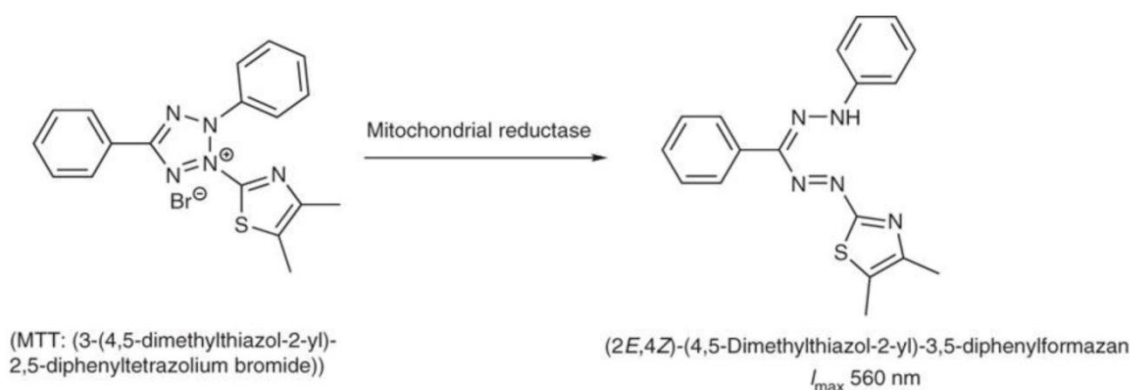


Figure 7: Principle of MTT assay

In brief, MCF7 cells (1×10^5 / well) were allowed to adhere in 96 well flat bottom plate and were then treated with different concentrations of Zoledronate [$0 \mu\text{M}$ (control), $50 \mu\text{M}$, $100 \mu\text{M}$, $200 \mu\text{M}$] for 16-18 hrs. After 18 hrs, used medium ($180 \mu\text{l}$) was replaced with $100 \mu\text{l}$ fresh cRPMI. MTT (5mg/ml) was freshly prepared in 1X PBS and stored in dark (light sensitive). The cells were incubated with $20 \mu\text{l}$ MTT (5mg/ml) for 4 hrs at 37°C in CO_2 incubator. Plate was centrifuged at $1000g$ for 15 min at RT and supernatant was removed. Cells were incubated with dimethyl sulphoxide ($100 \mu\text{l}$) for 15-30 min at 37°C on shaker to dissolve the formazan crystals. The optical density was measured at 540nm using reference wavelength 690nm . Test viability was calculated as [Test viability (%) = (Test O.D / Control O.D.) x 100].

3.12) Identification of differentially expressed protein in MCF7 cells upon

Zoledronate treatment by 2D PAGE-MALDI-TOF/TOF

3.12.1) Sodium Dodecyl Sulphate–Polyacrylamide gel electrophoresis (SDS-PAGE)

2D electrophoresis is a technique, which combines isoelectric focusing (IEF) with SDS-polyacrylamide gel electrophoresis (SDS-PAGE). Independently, IEF resolves proteins on its chemical property (isoelectric point, where charge on the proteins becomes neutral), while SDS-PAGE resolves proteins on the basis of their physical property (molecular weight). 2D-PAGE thus can resolve complex biological samples with a high degree of specificity and accuracy. These resolved proteins are then identified using MALDI-TOF.

3.12.1.1) Preparation of cell lysate

Urea based lysis buffer was used to prepare lysates for 2D-PAGE. The composition of the lysis buffer is described below. Lysis buffer (100µl) was added to cells (10×10^6) and cells were incubated overnight at 4°C. Further, cells were sonicated at 20hrzt for 30 duty cycles with intermittent cold shock on ice (5 seconds). The crude lysate was ultracentrifuged at 400000 g (55000rpm), 4°C for 1 hr and supernatant was collected. Protein estimation of the lysate was carried out by Lowry's method. Before protein estimation, proteins were acetone precipitated (as urea interferes with Lowry's reagent) using chilled acetone (-20°C) for 1 hr. After 1 hr, precipitated proteins were pelleted by centrifugation at 25900 g (14000 rpm), for 15 min at 4°C. Proteins were washed with chilled acetone by repeating the same procedure twice (for complete removal of detergents and other components).

Chemicals used:

- a) Urea (Sigma Aldrich,U6504)
- b) Thiourea (Sigma Aldrich, T7875)
- c) CHAPS (Sigma Aldrich, C3023)
- d) DTT (Sigma, D9779)
- e) 100X Biolyte 3/10 Ampholyte (1ml, Bio-Rad, Cat No. 1632094)
- f) 100X ReadyStrip 7-10 Buffer (1 ml, Bio-Rad, Cat No.163-2093)

Composition of the lysis buffer

Sr. No.	Component	Quantity/Volume
1	8M Urea	480 mg
2	2M Thiourea	152 mg
3	2% CHAPS	200ul from 10% stock
4	1% DTT	100ul from 10% stock
	Total Volume (with milliQ)	1000µl

3.12.1.2) Protein estimation by Folin- Lowry's method

Lowry's method is a colorimetric method developed by Oliver Lowry in 1951 (Figure 8). Under alkaline conditions the divalent copper ion forms a complex with peptide bonds in which it is reduced to a monovalent ion. Monovalent copper ion and the radical groups of tyrosine, tryptophan, and cysteine react with Folin reagent to produce an unstable product that becomes reduced to molybdenum/tungsten blue ($\text{Mo}^{6+} \rightarrow \text{Mo}^{2+}$). Lowry's method is pH sensitive method hence; pH has to be maintained at 10-10.5. Ammonium ions, zwitter ionic buffers, nonionic buffers, thiol compounds and detergents interfere with the Lowry reaction. It determines the proteins at low concentration (0.005 - 0.10 mg/ml). It also depends on with the composition of aromatic components of the proteins, especially cysteine.

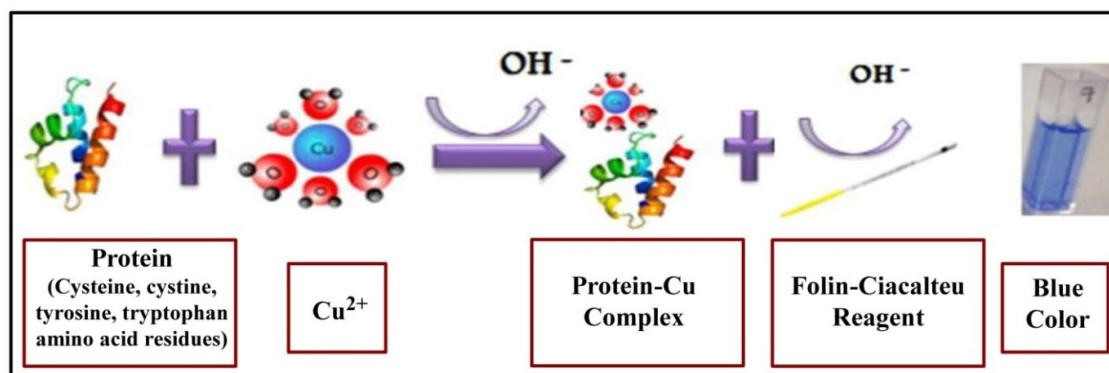


Figure 8: Principle of Folin-Lowry's method of protein estimation

BSA (1mg/ml) was dissolved in milliQ and was used as standard to determine protein concentration. BSA solution was further distributed as 20-100 μ g/ml. Test samples (untreated and Zoledronate treated MCF7 lysates) were also diluted as 1:5 or 1:10 or left undiluted (neat). Additions were carried out as described below. Folin-Lowry reagent was added to tubes and incubated for 30min in dark. Optical density (OD) was measured at 660nm and standard graph was drawn. Protein concentration of test samples was determined accordingly.

Chemical requirements:

1) CTC (Copper Tartarate Carbonate) solution:

Solution I - 20% Sodium carbonate (Na₂CO₃)

Solution II - 0.2% Copper sulphate (CuSO₄)

Solution III - 0.4% Sodium potassium tartarate (NaK-tartarate)

For 100ml of CTC, 0.05gram of Copper sulphate was dissolved in 20ml milliQ and 0.1gram Sodium potassium tartarate was dissolved in 20ml milliQ. Copper sulphate and sodium potassium tartarate were mixed and volume was adjusted to 50ml. To this equal volume (50ml) of 20% sodium carbonate was added by stirring continuously.

2) 10% Sodium dodecyl sulphate (SDS)

3) 0.8N NaOH

4) **Solution A:** CTC: 10% SDS: 0.8N NaOH: MilliQ=1:1:1:1 were mixed.

5) **Solution B:** Folin Lowry reagent was diluted 1:5 with milliQ

The BSA standards and test samples were added as described in the chart.

Component	Tube1	Tube2	Tube3	Tube4	Tube5	Tube6	Tube7
BSA (µl)	0	20	40	60	80	100	5 (Test)
MilliQ (µl)	100	80	60	40	20	0	95
MilliQ (µl)	100	100	100	100	100	100	100
Sol A (ml)	1	1	1	1	1	1	1
Sol B (µl)	500	500	500	500	500	500	500

Samples were incubated for 30 min in dark and absorbance was measured at 750nm.

3.12.1.3) Preparation of sample:

200 ug of sample protein was diluted in 330ul sample buffer (freshly prepared) for 17cm immobilized pH gradient (IPG) strips.

Composition of the sample buffer

Sr. No.	Component	Quantity/Volume
1	8M Urea	480 mg
2	2M Thiourea	152 mg
3	2% CHAPS	200ul from 10% stock
4	1% DTT	100ul from 10% stock
5	Ampholyte	
	Total Volume (using milliQ)	1000µl

3.12.1.4) Rehydration of the immobilized pH gradient (IPG) strip

2-DE of the proteins was done according to Laemmli [33]. Dry IPG 3-10 non-linear, 17cm dry strip (Bio-Rad, USA) was rehydrated using 330µl rehydration buffer containing 200µg protein

sample. Briefly, rehydration buffer containing the protein sample was dispensed along the length of the rehydration tray, the plastic cover of IPG strip was removed carefully and the strip was placed on the sample dispensed in rehydration tray (gel side facing down. IPG strips were allowed rehydrate for 30-45 min at RT. Subsequently, rehydrated strips were overlaid with 2-3ml mineral oil (Bio-Rad, USA) to prevent evaporation of sample during the process of rehydration and kept overnight at RT.

3.12.1.5) Isoelectric focusing

During IEF, proteins are separated on the basis of their isoelectric point, where charge on the protein becomes neutral on IPG strips. Next day, small paper wicks (4-5mm) were cut from Whatman filter paper and placed on both ends of electrodes in the Protean IEF focusing tray (Bio-Rad, USA). Paper wicks were pre--wet with 8-10µl of milliQ. IPG strips were carefully removed from the rehydration tray and excess mineral oil was drained out by placing the tip of the IPG strip on a tissue paper. The IPG strip was then placed in the IEF focusing tray (gel side facing down) and the strips were covered with 2ml of mineral oil. After removing air bubbles beneath the IPG strips, the IEF focusing tray was placed in the Protean IEF cell (Bio-Rad, USA) and the proteins were focused using the following program.

	Start Voltage	End Voltage	Time	Final Volt Hrs	
Step 1	0	250V	30 min	-	Linear
Step 2	250V	4000V	2.5 hrs	-	Linear
Step 3	4000	10000	3 hrs		Linear
Step 4	10000	40000 Vhrs		40000 Vhrs	

(Note: Temperature was maintained at - 20°C and maximum current was set at 50µA/strip.)

3.12.1.6) Equilibration of IPG strips

Once the proteins were separated on the basis of their isoelectric point, these proteins were further separated on the basis of their molecular weight. In order to neutralize the charges, proteins were treated with iodoacetamide (IAA, Sigma) and dithiothreitol (DTT, Sigma). After IEF, excess mineral oil was wiped out of the strips and strips were kept in equilibration buffer I for 20min at RT, followed by treatment with equilibration buffer –II for 20 min at RT.

Composition of Equilibration buffer I and II

S.No	Component	Equilibration Buffer I	Equilibration Buffer II
1	1MTris(pH8.8)	7.5 ml	7.5 ml
2	Urea	7.2 gram	7.2 gram
3	SDS	0.4 gram	0.4 gram
4	Glycerol	4 ml	4 ml
5	DTT	0.4 gram	-
6	IAA	-	0.5 gram
	Total Volume	20 ml	20 ml

3.12.1.7) Sodium dodecyl sulfate polyacrylamide gel electrophoresis (SDS-PAGE)

SDS-PAGE was carried out in PROTEAN® II xi Cell (BIO-RAD).

Chemicals required for SDS-PAGE:

a. Acrylamide:bisacrylamide (29:1) solution

29 grams of Acrylamide (Sigma USA) and 1gram of bisacrylamide (N,N Methylenebisacrylamide, Sigma USA) were dissolved in 70ml milliQ and volume was adjusted to 100ml. Solution was filtered using Whatmann filter paper and was stored in amber colored bottle at 4°C.

b. 1M Tris buffer (pH 6.8)

12.11grams of Tris base [Tris(hydroxymethyl)amino methane, Sigma USA] was dissolved in

60ml milliQ and pH was adjusted to 6.8 using concentrated HCl. Volume was adjusted to 100ml and solution was stored at 4°C.

c. 1.5 M Tris buffer (pH 8.8)

18.165 grams of Tris base was dissolved in 60 ml milliQ and pH was adjusted to 8.8 and volume was made to 100ml and stored at 4°C.

d. 10% Sodium dodecyl sulphate (SDS)

10 grams of SDS (Sigma, USA) was dissolved in 100 ml milliQ and solution was stored at RT.

e. 10% Ammonium persulphate (APC)

20 mg Ammonium Persulphate (MP Biochemicals, India) was dissolved in 200 µl milliQ (prepared fresh).

f. 1% Agarose

1 gram of agarose was dissolved in 100 ml milliQ and 1 ml Bromophenol blue solution (0.001%) was added to it.

g. TEMED

N,N,N,N-Tetramethyl-ethylene Diamine (Sigma USA)

h. Glycerol

Glycerol (MP Biochemicals, India) was used for stabilization.

i) Composition of stacking and resolving gel (20cm x 20cm gel)

S. No.	Component	Stacking Gel	Resolving Gel
1	MilliQ	8.4ml	14.4ml
2	30% Acrylamide- bisacrylamide	2ml	18ml
3	1.5M Tris (pH 6.8)	1.52ml	-
4	1.5 M Tris (pH 8.8)	-	11.7ml
5	10% SDS	120µl	450µl
6	10% APC	80µl	400µl
7	TEMED	10µl	20µl
	Final Volume	18ml	42ml

Preparation of 12% SDS-PAGE

To separate the proteins on the basis of molecular weight, 12% SDS-PAGE was prepared. Resolving and stacking gels (composition as described above) were casted in glass plates and glass plates were placed in electrophoresis apparatus. Upon equilibration, IPG strips were dipped in electrode buffer (to remove excess equilibration buffers) and placed on the 12% SDS-PAGE for the second-dimension separation in PROTEAN® II xi Cell. Strips were fixed in position using 1% agarose solution. For second dimension separation, 75V was kept constant. The reference dye, bromophenol phenol blue, was allowed to run till it touches the end of gel and then the instrument was switched off, gels were removed and protein profiles were detected by silver staining.

3.12.1.8) Detection of the proteins using silver staining:**Chemicals required for silver staining:****a) Fixing solution**

Fixing solution was prepared by mixing 45 ml of methanol (Merck), 10 ml of acetic acid (Qiagen) and 45 ml of milliQ.

b) 0.02% Sodium thiosulphate

0.02 gram of Sodium thiosulphate (SDFCL) was dissolved in 100 ml of milliQ.

c) 0.2% Silver nitrate Solution

0.2 gram of Silver Nitrate (Merck) was dissolved in 100 ml milliQ and 75 µl of formaldehyde was added at the time of staining.

d) Developer

6 grams of Sodium Carbonate (Merck) was dissolved in 98 ml of milliQ and 2 ml of 0.02% Sodium Thiosulphate solution and 50 µl of formaldehyde was added at the time of staining.

e) Destainer

Destainer was prepared by mixing 40 ml of methanol, 10 ml of acetic acid and 50 ml of milliQ.

Procedure: Upon electrophoresis, gels were removed and kept in fixing solution for 2 hrs, followed by wash twice using milliQ (20 sec each). Gels were then kept in 50% ethanol (prepared in milliQ) for 20 min and repeat wash with milliQ thrice (It was repeated thrice). Subsequently, gels were pre-incubated in 0.02% Sodium Thiosulphate for 1 min, washed with milliQ and stained in 0.2% silver nitrate for 30 min in dark. Excess Silver Nitrate was removed by washing with milliQ. Gels were developed using developer solution till the proteins get visible and reaction was stopped using destainer solution. Stained gels were stored in 10% acetic acid.

3.12.1.9) Analysis of differential protein expression in MCF7 cells upon Zoledronate treatment

Silver stained gel was scanned on the BIO-RAD GS-800 densitometer. Protein profiles of untreated and Zoledronate treated MCF7 cells were analyzed using PD Quest software (Version 7.2). Quantitative and qualitative differences in proteins between untreated and Zoledronate treated MCF7 gels were determined and proteins (silver stained gel plugs) were separated for identification by matrix assisted laser desorption/ionization-time of flight (MALDI-TOF).

3.12.1.10) Identification of differentially expressed proteins using PD Quest software

PDQuest software (BioRad, Version 2.0) was used to analyze qualitative (position on the gel) and quantitative (intensity of the spot) differences in protein profiles of untreated and Zoledronate treated MCF7 cells. Spot detection wizard from PDQuest software was used to determine the spots in the raw gel image. Once the spots were detected, original “raw” image was filtered and smoothed to clarify the spots, which was called as “filtered” image. From

“filtered” image, a synthetic image (Gaussian image) containing Gaussian spots were created. Gaussian spot is a 3D representation of an original scanned spot. “Gaussian image” helps to distinguish and quantify fuzzy, streaked or overlapping spots from dense clusters in a 2D gel. Different sets of gels (untreated and Zoledronate treated MCF7 cells) were matched, normalized and MasterSets were created from them (Untreated MasterSet and Zoledronate treated MasterSet). Normalization is necessary for accurate comparison between gels, where factors like inconsistency during sample preparation (due to changes in cell numbers or variations in reagents, protocols), handling errors, sample loss during preparation, inconsistent staining times between gels may be interfering. MasterSet is composed of the Raw2D, filtered and Gaussian image of the gels in an experiment. From both MatchSets, a synthetic “MatchSet Master” image was created, which included all the information from both untreated and Zoledronate treated MasterSets. Using, Spot review tool, Gaussian images of untreated MasterSets and Zoledronate treated MasterSets were compared for their quantitative and quantitative differences.

3.12.1.11) MALDI-TOF

Chemicals required for Mass-spectrometry:

a) **50 mM Ammonium bicarbonate** (NH_4HCO_3 , Sigma Aldrich)

40 mg of NH_4HCO_3 was dissolved in 10 ml milliQ in T15 tube.

b) **Potassium ferricyanide** ($\text{K}_3[\text{Fe}(\text{CN})_6]$, Merck)

100 mg of $\text{K}_3[\text{Fe}(\text{CN})_6]$ was dissolved in 10 ml milliQ in a T15 tube.

c) **Sodium thiosulphate** ($\text{Na}_2\text{S}_2\text{O}_3$, Merck)

0.24 gram of $\text{Na}_2\text{S}_2\text{O}_3$ dissolved in 10 ml milliQ in a T15 tube.

d) Trypsin for *in-gel* digestion

20µg trypsin (proteomics grade, Sigma,USA) powder was dissolved in 2ml of 25mM ammonium bicarbonate to make a 10 ng/µl solution of trypsin. 100 µl aliquots were stored at -20 °C for further use.

e) Extraction buffer for extraction of peptides

500µl of acetonitrile (Sigma, USA) and 50µl of trifluoroacetic acid (TFA, Applied Biosystems) were added in 450µl of milliQ.

f) Reconstitution buffer

500µl of acetonitrile and 1µl of TFA were mixed in 499µl of milliQ.

g) Matrix for loading of peptides on to the MALDI plate

Saturated solution of α -Cyano Hydroxy Cinnamic acid (CHCA, Bruker, prepared in 50 % acetonitrile and 0.1 % TFA as 20 mg/ml.

Procedure:

Protein in the silver stained gel plugs were identified by mass spectrometry upon trypsin digestion of these proteins according to Shevchenko et al [250]. Silver stained gel plugs were repeatedly washed with milliQ and then destained using 100µl destaining solution (100mM Sodium thiosulphate: 30mM, Potassium Ferricyanide mixed 1:1 v/v) for 30 min at RT. Destained gel plugs were washed thrice with milliQ for 5 min each. These gel plugs were incubated in 100µl of 50mM of Ammonium bicarbonate: acetonitrile (1:1, v/v) for 15 min with vortexing. Gel plugs were then dried in 100% of acetonitrile for 5 min, followed by drying in speed-vac. Silver stained gel plugs obtained from 1D gel were reduced using 10mM DTT (prepared in 50mM ammonium bicarbonate) for 45 min at 56°C, chilled at RT and further alkylated using 55mM of iodoacetamide (prepared in 50mM ammonium bicarbonate) for 30 min in dark. For 2D gel

proteins, reduction and alkylation is done during equilibration of the gels. To the dried protein plugs, 10ng/ μ l Trypsin in 25mM ammonium bicarbonate (10 μ l/plug) was added and trypsinization was carried out overnight at 37°C. Peptides were recovered using 35-50 μ l of 50% acetonitrile and 5% trifluoroacetic acid (TFA) and dried in speed-vac. Tryptic peptides were reconstituted in 10% acetonitrile with 0.1% TFA before using them for mass spectrometric analysis. The MS data was acquired in an automated manner using a solid state NdYAG laser at 337nm on MALDI-TOF TOF, Ultraflex model (Bruker Daltonics, Germany). Reconstituted samples were mixed with suitable matrix (sinapinic acid, alpha-cyano/CHCA, 2,5 dihydroxybenzoic acid, mostly acidic in nature, therefore act as a proton source to encourage ionization of the analyte), loaded onto metal plate on MALDI-TOF and allowed to air dry. The sample was irradiated with a pulsed laser (UV lasers e.g. nitrogen lasers (337 nm) and frequency-tripled and quadrupled Nd:YAG lasers (355 nm and 266 nm respectively) which triggered ablation and desorption of the sample and matrix material. Finally, the analyte molecules were ionized by being protonated or deprotonated in the hot plume of ablated gases and time of flight is calculated. MALDI TOF/TOF mass spectrometers were used to reveal amino acid sequence of peptides using post-source decay or high energy collision-induced dissociation. The MS data was acquired in an automated manner using Biotoools software (Bruker Daltonics, Germany) and was analyzed using Flex analysis 3.0 (Bruker Daltonics, Germany) software. Intense peaks of peptides were subjected to MS/MS. The MS peaklist and MS/MS ions of the chosen peptides were searched against SwissProt database version 2012_08 onwards using MASCOT search engine for protein ID with precursor tolerance of 100 ppm for MS and fragment tolerance of 0.7 to 1Da for MS/MS analysis. Selected proteins were validated by western blotting or flow cytometry.

3.13) *Liquid chromatography-Mass spectrometry*

Change in expression of proteins in MCF7 upon Zoledronate treatment in MCF7 was analyzed by more advanced, sensitive and robust method, iTRAQ (isobaric tags for relative and absolute quantification) followed by liquid chromatography-mass spectrometry (LC-MS).

Principle: The iTRAQ tags are isobaric labels that react with primary amines of peptides including the N-terminus and ϵ -amino group of the lysine side-chain. Each label has a unique charged reporter group, a peptide reactive group, and a neutral balance group to maintain an overall mass of 145 for each reagent and the same peptide reactive group. When a peptide is fragmented by MS/MS fragmentation, the iTRAQ reporter groups break off and produce distinct ions at m/z 114, 115, 116, 117, 118, 119, 121 and 122. The relative intensities of the reporter ions are directly proportional to the relative abundances of each peptide in the samples that being compared. In addition to producing strong reporter ion signals for quantification, MS/MS fragmentation of iTRAQ tagged peptides also produces strong y- and b-ion signals for more confident identification. Thus, it is a much more sensitive method.

3.13.1) **Chemical requirements:**

a) 1M (4-(2-hydroxyethyl)-1-piperazineethanesulfonic acid (HEPES)

23.83 grams of HEPES sodium salt (Sigma) was dissolved in milliQ, pH was adjusted to 7.6 and volume was finalized to 100 ml. It is a zwitterionic organic chemical buffering agent

b) 1M Sodium Chloride (NaCl)

5.844 grams of NaCl (Qualigens) was dissolved in milliQ and volume was adjusted to 100 ml. It is added to maintain ionic strength of medium.

c) 1% Triton X

1ml of Triton-X 100 (Qualigen) was dissolved in 100 ml of milliQ. Detergents were used to solublize of poorly soluble proteins.

d) 1M Magnesium Chloride

20.33 grams of MgCl₂ (SRL) was dissolved in milliQ and volume was adjusted to 100ml. It is used as a stabilizing agent for proteins.

e) 1M [Ethylene glycol-bis(β-aminoethyl ether)-N,N,N',N'-tetraacetic acid tetrasodium salt]

37.22 grams of EGTA (Sigma Aldrich, USA) was dissolved in milliQ, pH was adjusted to 8 and volume was finalized to 100 ml. It is used to reduce oxidation damage, chelate metal ions. It is also a metalloproteases inhibitor. Metalloproteases (protease family members) contain a metal ion at their active site which acts as a catalyst in the hydrolysis peptide binds.

f) 1M Ethylene diamine tetraacetic acid (EDTA, pH=8)

37.22 grams of EDTA (Sigma, USA) was dissolved in 50ml milliQ, pH was adjusted to 8 and volume was finalized to 100 ml. It acts as a metalloproteases inhibitor.

g) 1M Sodium fluoride (NaF)

41.9 mg of NaF (Sigma, USA) was dissolved in 400 µl milliQ and volume was adjusted to 1 ml. NaF is used to inactivate endogenous phosphatases and protect protein phosphorylation.

h) 1M sodium orthovanadate (Na₃VO₄)

1.839 gram of Na₃VO₄ (Sigma, USA) was dissolved in milliQ and volume was adjusted to 1 ml. It is a phosphatase inhibitor for protein phosphoseryl and phosphothreonyl phosphatases (PSPs).

i) 2mg/ml Leupeptin

2mg Leupeptin (Sigma, USA) was dissolved in 1 ml milliQ. It is a cysteine and serine protease inhibitor.

j) 2mg/ml phenylmethylsulfonyl fluoride (PMSF)

2mg of PMSF (Sigma, USA) was dissolved in 1ml DMSO. PMSF is a serine protease inhibitor.

k) 1mg/ml Pepstatin-A

1mg of pepstatin-A (Sigma, USA) was dissolved in 1ml DMSO. Pepstatin-A is an aspartic protease inhibitor.

l) 1mg/ml Aprotinin

1mg aprotinin (Sigma, USA) was dissolved in 1ml milliQ. Aprotinin is a basic pancreatic serine protease.

m) 50mM Tris (pH 8)

6.055 gram tris base was dissolved in milliQ, pH was adjusted to 8 and volume was finalized to 100 ml.

n) 50mM Tris (pH 7.5)

6.055 grams of tris base was dissolved in milliQ, pH was adjusted to 7.5 and volume was finalized to 100 ml.

o) 6M urea

3.603 grams of urea was dissolved in 50mM tris buffer (pH=8) and volume was adjusted to 10ml.

p) 200mM Dithiothretol

0.3085 gram DTT was dissolved in 50mM tris buffer (pH 8) and volume was adjusted to 10 ml.

It reduces oxidation damage and also assists protein denaturant

q) 200mM Iodoacetamide (IAA)

0.3699 gram IAA was dissolved in 50mM tris buffer (pH 8) and volume was adjusted to 10 ml.

r) 1mM Calcium chloride

1.1098 mg CaCl₂ (HiMedia, India) was dissolved in 50mM tris buffer (pH 7.5) and volume was adjusted to 10 ml.

s) Trypsin

20µg trypsin (Proteomics grade, Sigma Aldrich promega, USA) was dissolved in 1ml of 25mM ammonium bicarbonate, mixed properly and aliquots were stored at -20°C.

t) Composition of lysis Buffer:

S. No.	Component	Stock	Volume added
1	50mM HEPES pH 7.6	1M	50 µl
2	150mM NaCl	1M	150 µl
3	1% Triton X100	-	10 µl
4	5mMgCl ₂	1M	1.5 µl
5	5Mm EGTA	0.5 M	10 µl
6	5Mm EDTA	0.5M	10 µl
7	1.5mM NaF	1M	1.5 µl
8	1mM Leupeptin	2mg/ml	10 µl
9	2mM PMSF	2mg/ml	175 µl
10	10ug/ml Pepstatin	1mg/ml	10 µl
11	10ug/ml Aprotinin	1ng/ml	10 µl
12	1mM Na ₃ VO ₄	1M	1 µl
13	MilliQ	-	461 µl
	Total Volume		1000 µl

3.13.2) Preparation of cell lysate

1ml lysis buffer was added to 1x10⁶ MCF7 cells (untreated or Zoledronate treated) and cells were kept on ice for 20 minutes. Subsequently, lysate was centrifuged at 400000g for 20 min at 4°C; supernatant was collected and stored at -20°C.

3.13.3) Delipidation

1ml lysate was passed through delipidation column (capacity 250 μ l, where lipids will bind) and filtrate was collected. The filtrate (~200 μ l at a time) was further passed through buffer exchange columns to remove salts and other contaminants. 100 μ l TEAB buffer was aspirated in the column without damaging the membrane and content was spinned down to remove the contaminants. It was repeated thrice. 50 μ l TEAB buffer was again added to the column, mixed properly and content was aspirated. Concentrated protein lysate/sample was stored at -20°C. Protein estimation was carried out by Lowry's method.

3.13.4) *In-solution* trypsin digestion and labeling of samples

0.1-1mg of protein sample was reconstituted in 100 μ l of 6M urea. To this 5 μ l of 200mM DTT was added and incubated at RT for 1 hr. To this mixture, 20 μ l of 200mM IAA (prepared in 50mM Tris-HCl, pH-8) was added, gently vortexed and incubated at RT for 1 hr in dark. Further, 855 μ l 1mM CaCl₂ was added to reduce the urea concentration to ~0.6M. Trypsin solution was added to a final ratio of 1:50 (w/w, trypsin:protein), gently vortexed and incubated at 37°C for 16-18 hrs. The reaction (trypsinization) was stopped by adding 1 μ l formic acid (which decreases the pH to 3-4). Samples were dried using speed vac and stored at -20C. Samples were reconstituted in 0.1% formic acid prepared in milliQ. Salt and detergent contaminants from samples were further removed using Zip-Tip (Millipore, 0.6 μ L, c-18 RESIN, with 5 μ g analyte binding capacity). In brief, Zip-tip was pre-wet by carefully aspirating 20 μ l of 100% acetonitrile (ACN) 8-10 times. Equilibration of the tip was carried out by slowly passing 20 μ l of 0.1% formic acid (prepared in milliQ) through the tip. 20 μ l of sample, reconstituted in 0.1% formic acid, was aspirated in tip 8-10 times, allowing binding of the proteins/peptides in the zip-tip column. Further, 0.1% formic acid was used to wash the column of zip-tip. Proteins/peptides

were eluted using 20µl of elution buffer (60% ACN prepared in 0.1% formic acid) 2-3 times. Sample was dried by speed-vac and stored at -20°C or -80°C. The digested samples were labeled as per kit instruction (iTRAQ® Reagents - 4plex Applications Kit – Protein, AB SCIEX). Samples were acquired on Nano LC-ESI-Q TOF (Model: Triple TOF 5600⁺, AB SCIEX, USA). The data was analyzed using Protein Pilot™ Software (version 3.0).

3.14) Validation of differentially expressed proteins by western blotting

3.14.1) Chemicals used for western blotting:

a) Composition of NP-40 based lysis buffer

S.No.	Component	Quantity
1	50mM Tris-Cl (pH 8)	50µl (1M Tris-Cl)
2	150mM NaCl	50µl (3M NaCl)
3	5mM EDTA	100µl (50mM EDTA)
4	1.5mM MgCl ₂	30µl (50mM MgCl ₂)
5	10% glycerol	100µl
6	1 % NP-40	10µl
7	10X (PIC)	100µl
8	MilliQ	560µl
	Total volume	1000µl

b) 2X Loading Buffer

S. No.	Components	Quantity
1	1M Tris HCL (pH 6.8)	1.6 ml
2	10% SDS	4 ml
3	Glycerol	2 ml
4	β-mercaptoethanol (2ME)	1 ml
5	Bromophenol blue	4 mg
6	MilliQ water	1.4 ml
	Total Volume	10ml

c) Buffers

S. No.	Components	Electrode buffer	Transfer buffer
1	Tris (0.025M)	3.0275 gram	3.0275 gm
2	Glycine	14.413 gram	14.413 gm
3	SDS	1gram	-
4	Methanol	-	200ml
5	MilliQ	1000ml	800ml
	Total Volume	1000ml	1000ml

d) Ponceau stain

0.1 gram ponceau dye was added to 5ml glacial acetic acid, volume was adjusted to 100 ml with milliQ and solution was stored at RT.

e) 10X TBS (Tris Buffered Saline)

43.8 grams of NaCl (1.5M) was dissolved properly in 1M tris, pH was adjusted to 7 and volume was adjusted to 100 ml. It was stored at 4°C.

f) 1X TBS

10ml of 1X TBS was mixed properly with 90 ml milliQ and stored at 4°C.

g) 1X TBST/wash buffer

0.1 ml Tween20 (Thermo fisher Scientific, USA) was added to 100 ml 1X TBST, mixed properly and stored at RT.

h) 5% blocking solution

5 grams of non-fat dry milk powder was dissolved in 100ml 1X TBST and always prepared fresh just before the experiment.

i) 1% BSA

1 gram of BSA was dissolved in 1X TBS buffer

j) 90% chilled methanol

90ml methanol was mixed properly with 10 ml of milli-Q and stored at 0°C.

3.14.2) Preparation of cell lysate

100µl of NP-40 based lysis buffer was added to untreated or Zoledronate treated MCF7 cells (10×10^6) and samples were boiled for 10 min. Samples were stored at 4°C (long term -20°C) and were boiled for 5 min before loading. These lysates were used to analyze effect of Zoledronate on expression of cytoskeletal elements (β -actin, α -tubulin and keratin 8), HSPs (HSP60 and HSP70) and expression of epidermal growth factor receptor (EGFR).

3.14.3) Electroblothing and Immunoblotting

Protein estimation was carried out by Lowry's method. 20ug protein was loaded onto SDS-PAGE and electrophoresis was carried out at 100 volts. After electrophoresis under reducing conditions, separated proteins were electrophoretically transferred onto mdi nitrocellulose membrane (Advanced microdevices Pvt. Ltd., India) in transfer buffer at RT for 1hr at a voltage of 100V using the vertical transfer apparatus (Biorad). The membrane containing standard molecular weight marker along with protein lysates was stained with Ponceau S. The membranes containing the lysates were completely destained in wash buffer and blocked with 5% skimmed milk or 1% BSA, prepared in wash buffer for 1 hr-2 hr respectively at RT. The membranes were then incubated with the appropriate concentration of the primary antibody (diluted in 5% skimmed milk/ 1% BSA) overnight at 4°C. After washings (3 washings with TBS buffer containing 0.1% Tween-20 for 15 min each), the membranes were incubated with the appropriate secondary antibody conjugated to horseradish peroxidase (HRPO) diluted in 5% skimmed milk/ 1% BSA for 1 hr at RT. After washing off the excess of the secondary antibody, the protein bands were detected by enhanced chemiluminescence (ECL; Amersham, U.K.) detection kit.

Antibody Dilutions used for validation:

S. No	Protein	Blocking	1° Antibody dilution	2° Antibody dilution
1	HSP60	5% Skimmed Milk	1:5000	GAM-HRPO, 1:3000
2	HSP70	5% Skimmed Milk	1:1000	GAM-HRPO, 1:5000
3	α -Tubulin	5% Skimmed Milk	1:2500	GAR-HRPO, 1:2500
4	Keratin 8	3% BSA	1:5000	GAM-HRPO, 1:10000
5	EGFR	5% Skimmed Milk/ 1% BSA	1:1000	GAR-HRPO, 1:1000
6	β -Actin	5% Skimmed Milk/ 1% BSA	1:5000	GAR-HRPO, 1:5000

Chapter 4

*To investigate the effect of $\gamma\delta$ T cells on
osteoclastogenesis*

Bone appears to be static in nature, but it is a dynamic structure which undergoes continuous remodeling and is under the tight control of osteoblasts and osteoclasts. Under normal conditions, osteoclasts and osteoblasts work in coordinated manner to maintain normal bone physiology, while their imbalance results in pathological conditions, such as osteoporosis, rheumatoid arthritis (RA), Paget's disease and osteopetrosis. Skeletal system shares a number of cytokines, chemokines, signaling molecules and transcription factors with immune cells and tumor cells [44,251,252]. Metastasized tumor cells also interrupt the normal bone metabolism by releasing factors which induce differentiation and activation of osteoclasts [43]. It has also been reported that cytokines secreted by lymphocytes present in the bone microenvironment affect bone metabolism [253]. Investigations are focused on understanding how conventional T lymphocytes interact with osteoclasts and influence their function.

Aminobisphosphonates and anti-RANKL therapies are used to treat patients with bone metastasis to reduce the skeletal complications and tumor burden [54,55,56,57]. Aminobisphosphonates (Zoledronate) inhibit farnesyl pyrophosphate synthase (FPPS), a key enzyme in mevalonate pathway, which results in upregulation of isopentenyl pyrophosphate (IPP). IPP is consecutively condensed to dimethylallyl diphosphate (DMAPP) for synthesis of isoprenoids. In eukaryotes, these precursors are generated by mevalonate pathway, while in eubacteria they are generated by nonmevalonate/ rohmer pathway [254,255]. IPP acts as a potent activator of $\gamma\delta$ T cells and also behaves like a chemoattractant for $\gamma\delta$ T cells [256]. Bromohydrin pyrophosphate (BrHPP) or phosphostim (synthetic analogs of IPP) and picostim (synthetic analog of (E)-4-Hydroxy-3-methyl-but-2-enyl pyrophosphate, an intermediate molecule in bacterial non-mevalonate or rohmar pathway) acts as potent activators of $\gamma\delta$ T cells.

The objective of the present study was to have a comparative analysis of “activated” and “freshly isolated” $\gamma\delta$ T cells with respect to their phenotype, activation markers and effect on generation and function of osteoclasts.

4.1) Analysis of activation markers on $\gamma\delta$ T cells

4.1.1) $\gamma\delta$ T cell separation

Peripheral blood mononuclear cells (PBMCs) were separated from 20ml heparinized blood by ficoll hypaque density gradient centrifugation method. $\gamma\delta$ T cells were immunomagnetically separated from PBMCs using TCR γ/δ^+ T Cell isolation kit (Milteney Biotech) as per the kit instructions (Materials and method, section 3.6.2.2). Figure 9 gives a schematic representation of isolation of $\gamma\delta$ T cells directly from freshly isolated PBMCs and from α CD3/CD28+rhIL2 expanded PBMCs. Hereafter, $\gamma\delta$ T cells, directly separated from PBMCs would be termed as “freshly isolated” $\gamma\delta$ T cells, while those separated from α CD3/CD28+rhIL2 expanded PBMCs (materials and methods section 3.6.2.1) would be termed as “activated” $\gamma\delta$ T cells.

As shown in Table 3, recovery of “freshly isolated” $\gamma\delta$ T cells ranged from 0.3×10^6 to 8.9×10^6 cells (mean \pm SEM, $3.5 \pm 1.5 \times 10^6$) with starting population of PBMCs ranging from 40.1×10^6 to 180.6×10^6 cells (mean \pm SEM, $100.8 \pm 27.6 \times 10^6$). The mean percent recovery of “freshly isolated” $\gamma\delta$ T cells was $3.2 \pm 0.4\%$. Similarly, expansion of “activated” $\gamma\delta$ T cells ranged from 2.1×10^6 to 13.2×10^6 (mean \pm SEM, $5.7 \pm 2.9 \times 10^6$) from starting population of 10×10^6 PBMCs (Table 4). Over the period of 12 days, expansion of PBMCs ranged from 79.2×10^6 to 217.5×10^6 cells with mean \pm SEM of $131.5 \pm 39.4 \times 10^6$ cells. The percent yield of “activated” $\gamma\delta$ T cells was $4.1 \pm 0.4\%$. The purity of the separated $\gamma\delta$ T cells (freshly isolated and activated $\gamma\delta$ T

cells) was evaluated by flow cytometry and populations showing more than 95% purity were used for further experiments (Figure 9).

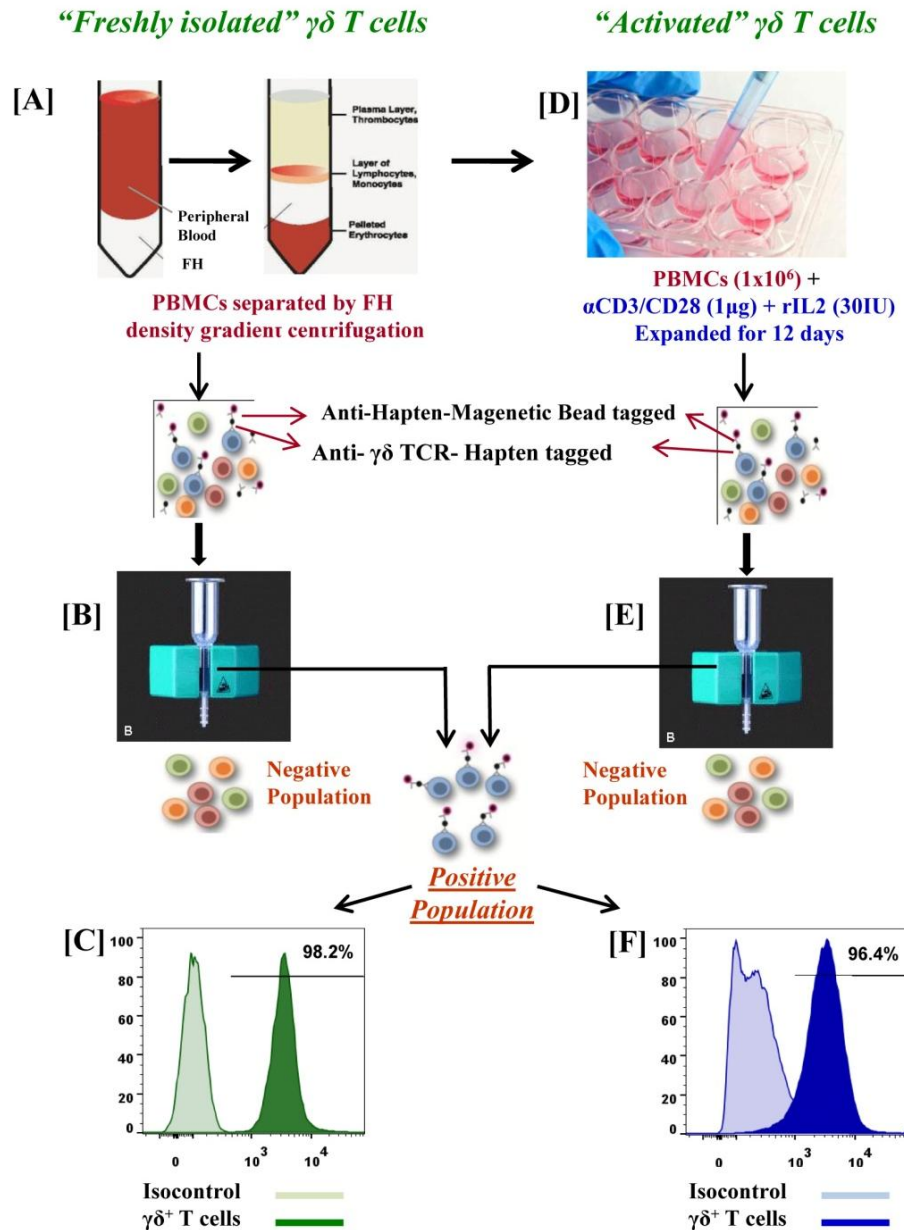


Figure 9: Immunomagnetic separation of “freshly isolated” and “activated” $\gamma\delta$ T cells

A prototype experiment of isolation of $\gamma\delta$ T cells from peripheral blood is described. PBMCs were separated on Ficoll Hypaque density gradient [A] or were expanded using α CD3/CD28 ($1 \mu\text{g}$) + rIL2 (30IU) for 12 days [D]. $\gamma\delta$ T cells were immunomagnetically purified from PBMCs directly using anti $\gamma\delta$ TCR hapten tagged antibody were termed as “freshly isolated” $\gamma\delta$ T cells [B] and those which were purified from expanded PBMCs were termed as “activated $\gamma\delta$ T cells” [E]. Purity of freshly isolated $\gamma\delta$ T cells (98.2%) [C] and “activated $\gamma\delta$ T cells” (96.4%) [F] was assessed by flow cytometry.

Table 3: Percent yield of “freshly isolated” $\gamma\delta$ T cells from healthy individuals (HI)

Healthy Individual (HI)	Amount of blood	Total number of PBMCs used for MACS	MACS purified $\gamma\delta$ T cells	Percent yield of $\gamma\delta$ T cells (%)
HI 1	30 ml	106.33 X 10 ⁶	6 X 10 ⁶	5.6
HI 2	20 ml	67 X 10 ⁶	0.32 X 10 ⁶	1.97
HI 3	25 ml	93 X 10 ⁶	3.48 X 10 ⁶	3.74
HI 4	35ml	136.5 X 10 ⁶	1.5 X 10 ⁶	1.09
HI 5	20 ml	90.1 X 10 ⁶	2.27 X 10 ⁶	2.5
HI 6	20 ml	40.125 X 10 ⁶	5.8 X 10 ⁶	4.13
HI 7	25 ml	74.5 X 10 ⁶	5.3 X 10 ⁶	7.11
HI 8	25 ml	84.8 X 10 ⁶	0.675 X 10 ⁶	0.79
HI 9	35 ml	132 X 10 ⁶	3.03 X 10 ⁶	2.29
HI 10	25 ml	86.7 X 10 ⁶	0.99 X 10 ⁶	1.14
HI 11	30 ml	122.4 X 10 ⁶	1.45 X 10 ⁶	1.88
HI 12	35 ml	180.6 X 10 ⁶	8.99 X 10 ⁶	4.98
HI 13	25 ml	78.5 X 10 ⁶	2.5 X 10 ⁶	3.19
HI 14	25 ml	87.4 X 10 ⁶	1.87 X 10 ⁶	2.14
HI 15	20 ml	56.1 X 10 ⁶	2.14 X 10 ⁶	3.83
HI 16	25 ml	98.5 X 10 ⁶	6.5 X 10 ⁶	6.69
HI 17	25 ml	77.4 X 10 ⁶	1.04 X 10 ⁶	1.35
HI 18	35 ml	135.9 X 10 ⁶	6.11 X 10 ⁶	4.25
HI 19	35 ml	160.0 X 10 ⁶	8.16 X 10 ⁶	5.1
HI 20	25 ml	81.6 X 10 ⁶	1.22 X 10 ⁶	1.15
HI 21	30 ml	128.2 X 10 ⁶	4.48 X 10 ⁶	3.35

Mean cell count of PBMCs: 100.8±27.6 X10⁶

Mean cell count of “freshly isolated” $\gamma\delta$ T cells: 3.5±1.5 x10⁶

Mean % recovery of “freshly isolated” $\gamma\delta$ T cells: 3.2 ± 0.4 %

A representative table for yields of $\gamma\delta$ T cells from 21 healthy individuals. $\gamma\delta$ T cells were immunomagnetically purified by MACS from freshly separated PBMCs.

Table 4: Percent yield of “activated” $\gamma\delta$ T cells from healthy individuals (HI)

Healthy Individual (HI)	PBMCs seeded on Day 1	Total <i>ex vivo</i> expanded PBMCs on Day 12	MACS purified $\gamma\delta$ T cells	Percent yield of $\gamma\delta$ T cells (%)
HI 22	10 X 10 ⁶	122.1 X 10 ⁶	4.2 X 10 ⁶	3.5
HI 23	10 X 10 ⁶	217.5 X 10 ⁶	13.2 X 10 ⁶	6.1
HI 24	10 X 10 ⁶	101.5 X 10 ⁶	3.104 X 10 ⁶	3.06
HI 25	10 X 10 ⁶	130.3 X 10 ⁶	5.5 X 10 ⁶	4.28
HI 26	10 X 10 ⁶	165 X 10 ⁶	8.5 X 10 ⁶	5.16
HI 27	10 X 10 ⁶	99.5 X 10 ⁶	2.25 X 10 ⁶	2.28
HI 28	10 X 10 ⁶	132.0 X 10 ⁶	4.7 X 10 ⁶	3.32
HI 29	10 X 10 ⁶	125 X 10 ⁶	5.4 X 10 ⁶	4.32
HI 30	10 X 10 ⁶	175 X 10 ⁶	6.3 X 10 ⁶	3.6
HI 31	10 X 10 ⁶	79.2 X 10 ⁶	3.2 X 10 ⁶	4.16
HI 32	10 X 10 ⁶	115.1 X 10 ⁶	2.4 X 10 ⁶	2.12
HI 33	10 X 10 ⁶	147.3 X 10 ⁶	7.79 X 10 ⁶	5.3
HI 34	10 X 10 ⁶	123.0 X 10 ⁶	4.4 X 10 ⁶	3.58
HI 35	10 X 10 ⁶	157.3 X 10 ⁶	13 X 10 ⁶	8.32
HI 36	10 X 10 ⁶	83.1 X 10 ⁶	2.1 X 10 ⁶	2.5

Mean cell count of PBMCs: 131.5 ± 39.4 x10⁶

Mean cell count of “activated” $\gamma\delta$ T cells: 5.7±2.9 x10⁶

Mean % recovery of “activated” $\gamma\delta$ T cells: 4.1 ± 0.4%

A representative table for yields of “activated” $\gamma\delta$ T cells of healthy individuals from 15 $\gamma\delta$ T cell lines established as shown. PBMCs were stimulated with solid phase α CD3/CD28 for 12 days and $\gamma\delta$ T cells were immunomagnetically purified by MACS after 12 days of coculture.

4.1.2) Expression of activation markers (CD69, CD25 and RANKL) on $\gamma\delta$ T cells

Expression of activation markers [CD69, CD25 and RANKL/CD254] on $\gamma\delta$ T cells were analyzed by stimulating these cells with α CD3/CD28, phosphoantigens [IPP, BrHPP and Picostim] or aminobisphosphonate (Zoledronate) in the presence of rhIL2. IPP (synthetic analog is BrHPP) is an intermediate molecule in eukaryotic mevalonate pathway, while HMBPP (synthetic analog is picostim) is an intermediate molecule in bacterial rohmer pathway/non-mevalonate pathway.

Purified (“freshly isolated”) $\gamma\delta$ T cells were either left unstimulated (control) or were stimulated with rhIL2 alone or a combination of α CD3/CD28+rhIL2, IPP+rhIL2, BrHPP+rhIL2, Picostim+rhIL2 and Zoledronate+rhIL2 for 24 hrs. As shown in Figure 10, in an unstimulated state “freshly isolated” $\gamma\delta$ T cells showed lower levels of CD69 (5.04%, MFI=126), CD25 (2.48%, MFI=103) and RANKL (1.72%, MFI=41.4). Upon stimulation with rhIL2 for 24 hrs, increase in the expression of CD69 (29.2%, MFI=295), CD25 (9.10% MFI=354) and RANKL (3.79%, MFI=81.3) was observed. “Freshly isolated” $\gamma\delta$ T cells stimulated with α CD3/CD28+rhIL2 showed markedly higher levels of CD69 (39.8%, MFI = 344), CD25 (13.2%, MFI = 512) and RANKL (7.38%, MFI=106) as compared to unstimulated and rhIL2 stimulated $\gamma\delta$ T cells. Stimulation of “freshly isolated” $\gamma\delta$ T cells with IPP+rhIL2 or BrHPP+rhIL2 showed markedly higher levels of CD69 (44.1%, MFI=392 and 52.4%, MFI=335 respectively), CD25 (20.9%, MFI=834 and 18.3%, MFI=677 respectively) and RANKL (7.79%, MFI=114 and 9.49%, MFI=77.6 respectively) as compared to unstimulated and rhIL2 stimulated $\gamma\delta$ T cells. Further stimulation of “freshly isolated” $\gamma\delta$ T cells with picostim+rhIL2 showed significant increase in expression of early activation marker CD69 (86.2%, MFI=624) along with late activation marker CD25 (52.7%, MFI=1916) and RANKL (22.7%, MFI=300). Zoledronate

+rhIL2 stimulation of “freshly isolated” $\gamma\delta$ T cells showed remarkable increase in expression of CD69 (92.7%, MFI=1092), CD25 (19.5%, MFI=736) and RANKL (23%, MFI=260).

Expression of these markers was also analyzed on “ $\gamma\delta$ T cells” in PBMCs which were stimulated with α CD3/CD28 + rhIL2, BrHPP + rhIL2 and Zoledronate+rhIL2 for 12 days. As shown in Figure 11, unstimulated PBMCs (Day 0) showed lower expression levels of CD69 (3.62% [percent positive], MFI=72.5[mean fluorescent intensity]), CD25 (16.2%, MFI=405) and RANKL (4.06%, MFI=115) on gated $\gamma\delta$ T cells. However, a marked increase in expression of CD25 and RANKL was observed on $\gamma\delta$ T cells upon stimulation of PBMCs with α CD3/CD28+rhIL2 (100%, MFI=134,379 and 53.5%, MFI=641 respectively) or BrHPP+rhIL2 (99.1%, MFI=17,740 and 36.4%, MFI = 654 respectively) for 12 days. Almost all $\gamma\delta$ T cells were positive for CD25 expression after stimulation, indicating that these cells were in highly activated state. Expression of CD69 (early activation marker) on $\gamma\delta$ T cells was found marginal changed upon stimulation of PBMCs with α CD3/CD28 + rhIL2 (0.9%, MFI=-714) and BrHPP + rhIL2 (2.82%, MFI=211) for 12 days compared to unstimulated PBMCs (3.62%, MFI=72.5). Upon stimulation of PBMCs with Zoledronate+rhIL2, a remarkable increase in expression of CD25 (99.6%, MFI=43425) and RANKL (15.7%, MFI=273) was observed along with reduced expression of CD69 (0.36%, MFI=51.4) expression.

Figure 12 shows comparative analysis of percentage of “freshly isolated” and “activated” $\gamma\delta$ T cells expressing CD69, CD25 and RANKL, among PBMCs stimulated with rhIL2 alone or in combination of rhIL2 with α CD3/CD28, BrHPP and Zoledronate. It was observed that, “freshly isolated” $\gamma\delta$ T cells showed upregulation of early activation marker CD69 upon stimulation with rhIL2 alone or in combination with α CD3/CD28, BrHPP and Zoledronate. Similarly, “activated” $\gamma\delta$ T cells upon stimulation with rhIL2 alone or in combination with

α CD3/CD28 and BrHPP showed increased expression of CD25 and RANKL compared to “freshly isolated” $\gamma\delta$ T cells.

Thus on the basis of expression of activation markers (CD69, CD25 and RANKL) $\gamma\delta$ T cells were considered as “non-activated” (freshly isolated) and “activated” (isolated from α CD3/CD28 + rhIL2 stimulated PBMCs) $\gamma\delta$ T cells.

24 hrs
Stimulation with
Unstimulated

rhIL2

α CD3/CD28+
rhIL2

IPP+rhIL2

BrHPP+rhIL2

Picostim+rhIL2

Zoledronate
+ rhIL2

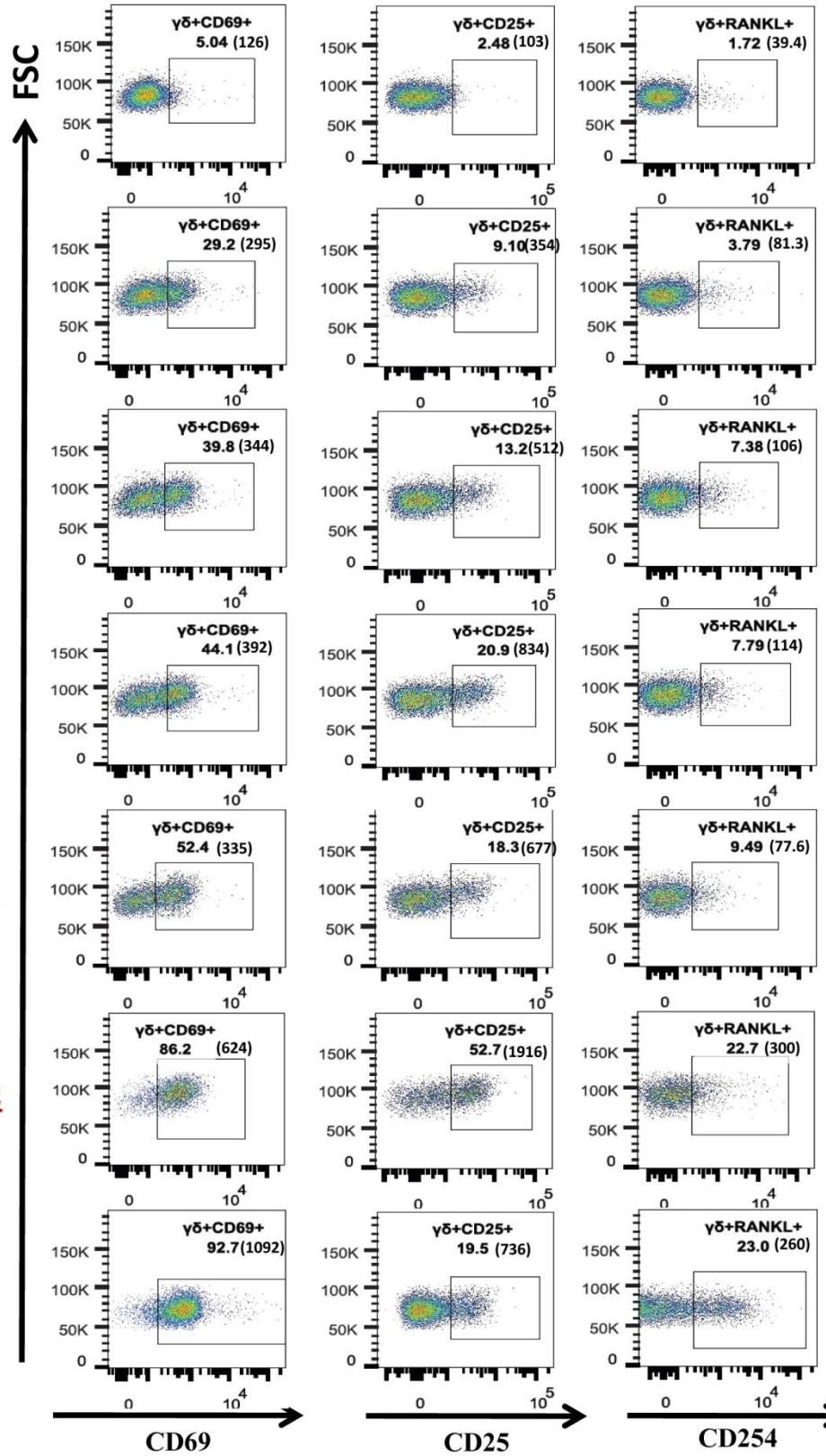


Figure 10: Analysis of activation markers (CD69, CD25, and RANKL) on “freshly isolated (FI)” $\gamma\delta$ T cells

Expression of activation markers (CD69, CD25, and RANKL) was analyzed on “freshly isolated/purified” $\gamma\delta$ T cells, which were stimulated with rhIL2 alone, α CD3/CD28+rhIL2, IPP+rhIL2, BrHPP+rhIL2, picostim+rhIL2, Zoledronate+rhIL2 or left unstimulated (medium alone) for 24hrs. After 24hrs, “freshly isolated” $\gamma\delta$ T cells were stained using $\gamma\delta$ -APC, CD69-FITC, CD25-PeCy7, and RANKL-PE. The gating strategy used was as follows: Lymphocytes were gated based on their forward and side scatter. Depending on the fluorescence intensity of $\gamma\delta$ -APC, $\gamma\delta$ T cells were gated. Further percentages of $\gamma\delta$ T cells expressing CD69, CD25 and RANKL were analyzed on gated $\gamma\delta$ T cells. The gates have been set according to only cell controls for respective stimulation. (Representative figure of three independent experiments.)

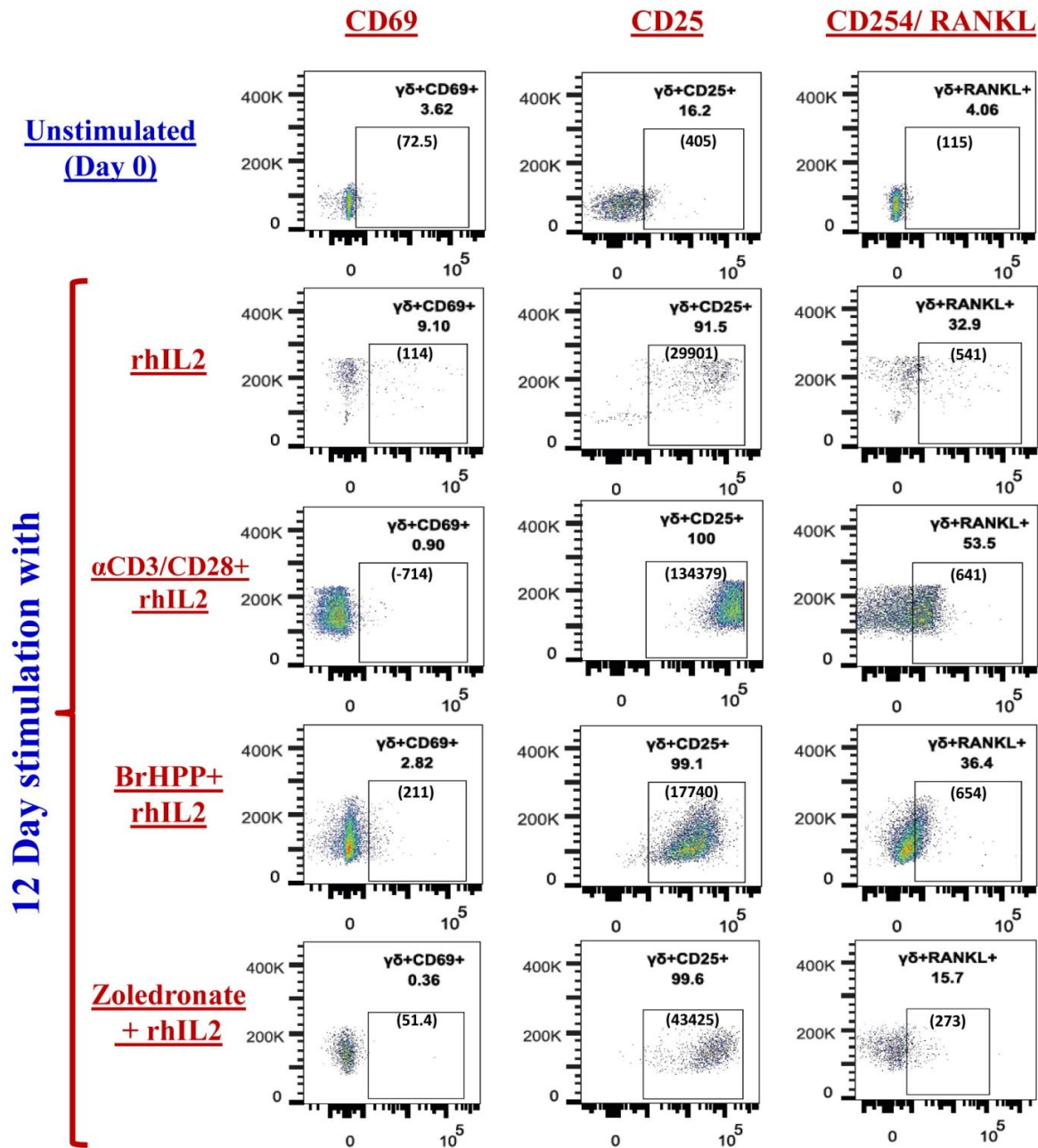


Figure 11: Analysis of activation markers (CD69, CD25, and RANKL) on “activated (ACT)” $\gamma\delta$ T cells

Expression of activation markers (CD69, CD25, and RANKL) was analyzed on $\gamma\delta$ T cells in unstimulated PBMCs (1×10^6 /ml/well) or PBMCs expanded with rhIL2 (30IU/ml) alone, α CD3/CD28 (1 μ g) + rhIL2 or BrHPP (200 nM) + rhIL2 for 12 days. After the 12th day, PBMCs were stained using $\gamma\delta$ -APC, CD69-FITC, CD25-PeCy7, and RANKL-PE. Baseline expression of these markers on $\gamma\delta$ T cells was analyzed by staining unstimulated PBMCs (Day 0, control). The gating strategy used was as follows: Lymphocytes were gated based on their forward and side scatter. Depending on the fluorescence intensity of $\gamma\delta$ -APC, $\gamma\delta$ T cells were gated. Further

percentages of $\gamma\delta$ T cells expressing CD69, CD25 and RANKL were analyzed on gated $\gamma\delta$ T cells. The gates have been set according to only cell controls for respective stimulation. (Representative figure of three independent experiments.)

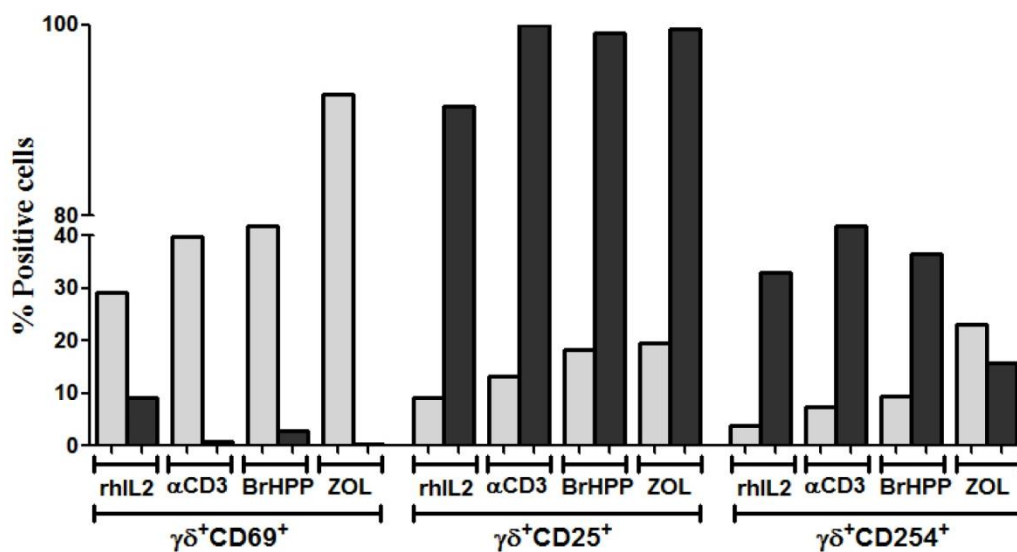


Figure 12: Comparative analysis of activation markers on antigen activated “freshly isolated” and “activated” $\gamma\delta$ T cells

“Activated” $\gamma\delta$ T cells (■) showed increased expression of activation markers (CD25, CD69 and CD254) as compared to “freshly isolated” (□) $\gamma\delta$ T cells. Stimulation of both “activated” and “freshly isolated” $\gamma\delta$ T cells showed increase in CD25 and RANKL expression upon stimulation with α CD3/CD28, BrHPP and Zoledronate as compared to rhIL2 stimulation control. [b] Mean fluorescent intensity of CD25 and CD254 was found to be higher on “activated” $\gamma\delta$ T cells as compared to “freshly isolated” $\gamma\delta$ T cells. (Representative figure of three independent experiments).

4.2) Effect of $\gamma\delta$ T cells on human osteoclastogenesis

4.2.1) Generation and characterization of mouse osteoclasts

For standardization of osteoclast generation and functional assays, mouse osteoclasts were generated from [a] mouse macrophage cell line (RAW 264.7) and [b] osteoclast precursor cells isolated from bone marrow of Swiss CRL or C57BL6 mice. Osteoclasts are multinucleated cells, formed by fusion of monocyte/ macrophage cells. Osteoclast precursor cells (monocytes/ macrophages) are cultured in the presence of macrophage colony stimulating factor (MCSF) and receptor activator of nuclear factor kappa B ligand (RANKL). MCSF is essential for survival and fusion of the precursor cells and RANKL plays a pivotal role in osteoclast differentiation. MCSF binds to cFms or MCSF receptor on osteoclast precursor cell and activates Akt signaling pathway [257]. RANKL upon binding to RANK activates NF κ B [258], which further transcribes osteoclast specific genes like cathepsin K, tartarate resistant acid phosphatase (TRAP), vitronectin receptor (α V β 3) and mature osteoclast are generated.

4.2.2.1) From mouse macrophage cell line RAW 264.7

RAW 264.7 is a mouse macrophage cell line that was established from a tumor induced by albeson murine leukemia virus in adult BALB/c mice and is adherent in nature. RAW 264.7 cells are characterized by neutral red pinocytosis assay, where lipopolysaccharide (LPS) stimulated cells pinocytose neutral red. As shown in Figure 13, LPS stimulated RAW 264.7 cells showed active uptake of neutral red dye. This was quantitated by lysing the cells in ethanol: acetic acid (1:1, v/v). The optical density (OD) of the lysate was measured at 570nm. Increase in OD indicated the uptake of neutral red by RAW 264.7 cells, which is the characteristic of macrophage cell line.

RAW 264.7 cells were then used to generate mouse osteoclasts. RAW 264.7 cells (3×10^5) were cultured in α MEM containing rmRANKL (100ng/ml) for 7 days with intermediate feeding after every 3rd day. After 7 days, mature osteoclasts were characterized by staining them for TRAP (tartarate resistant acid phosphatase) using Leukocyte Acid Phosphatase kit (material and method section 3.7.4). In brief, TRAP catalyses conversion of naphthol AS-BI phosphoric acid to naphthol AS-BI in presence of tartarate. This naphthol AS-BI forms complex with fast garnet-GBC generating maroon colored deposits. Thus, osteoclasts can be visualized due to generation of stained with characteristic maroon color. Multinucleated (>3 nuclei), TRAP-positive cells were considered as mature osteoclasts (Figure 13).

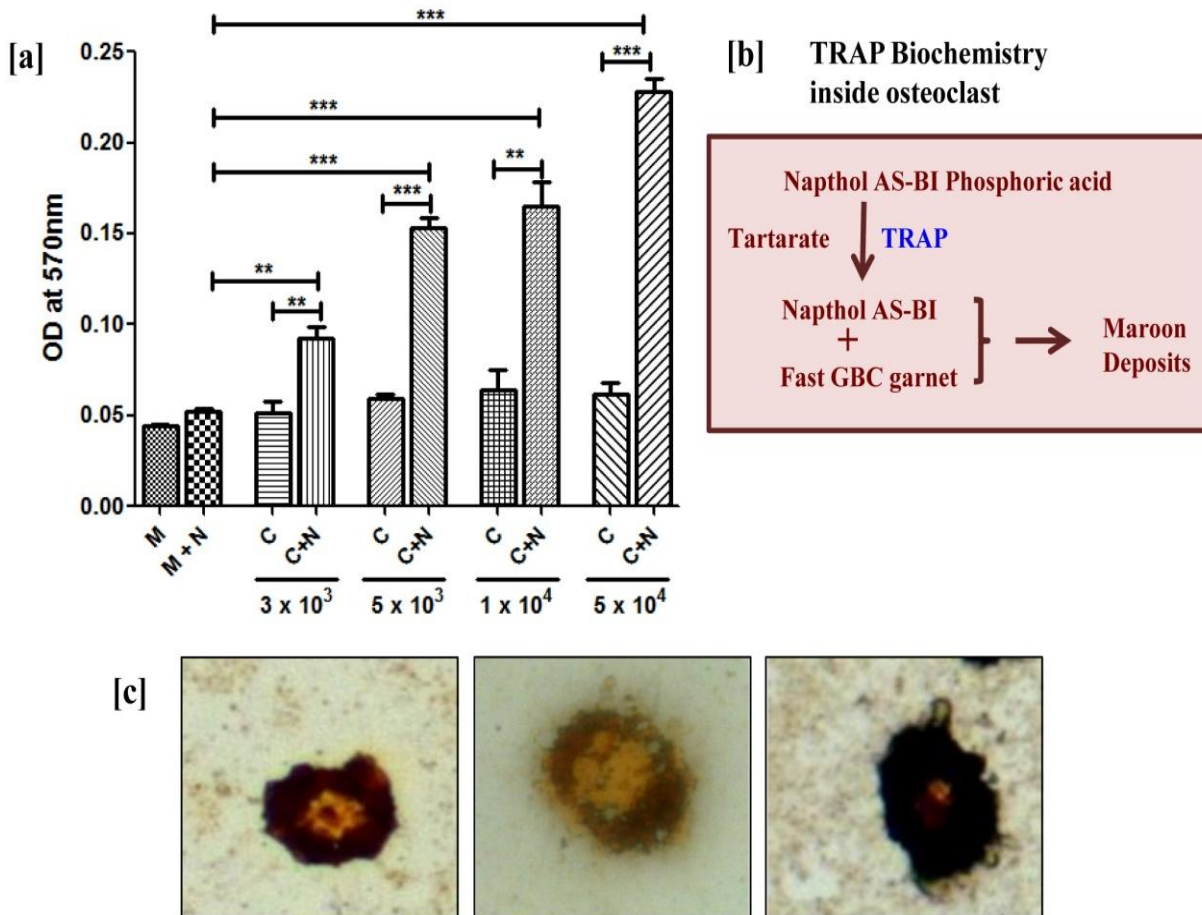


Figure 13: Generation of osteoclasts from mouse macrophage cell line (RAW264.7)

[a] Raw264.7 cell line was characterized by standard neutral red pinocytosis assay using different cell numbers (3×10^3 - 5×10^4). Active pinocytosis of neutral red by macrophages was confirmed by calculating the optical density (OD) of neutral red at 570nm. OD of medium only (M), medium+ neutral red (M+N) and cells only (C) were used as experimental controls. [b] Osteoclasts were generated from RAW264.7 cells cultured in α MEM supplemented with rmRANKL (100ng/ml). Cells were cultured for 7 days with intermediate feedings after every 3rd day. On 8th day, presence of osteoclasts was confirmed by staining them for tartarate resistant acid phosphatase (TRAP) using Leukocyte Acid Phosphatase kit. [c] Multinucleated (≥ 3), TRAP positive cells were considered as mature osteoclasts.

4.2.2.2) From bone marrow osteoclast precursor cells

Generation of mouse osteoclast culture was standardized using bone marrow cells from two mice models: Swiss CRL and C57BL6. 6-8 week old Swiss CRL or C57BL6 mouse was sacrificed and femurs were collected. Bone marrow cells (BMCs) were aspirated from femurs and were cultured in α MEM (30×10^6 cells/5ml) supplemented with rmMCSF (10ng/ml) for 24 hrs. This aided separation of adherent stromal cells from non-adherent osteoclast precursor cells (OPCs) and induction of OPCs from monocytes/macrophages. After 24 hrs, OPCs were collected and cultured in α MEM (1×10^5 cells/200 μ l) containing rmMCSF (30ng/ml) and rmRANKL (30ng/ml) for 7 days on sterile thermanox coverslips in 96 well flat bottom plate. Every 3rd day, the cells were fed with rmMCSF and rmRANKL. On 8th day, the cultures were terminated and osteoclasts were characterized by staining them for TRAP. As shown in Figure 14, multinucleated (>3 nuclei) TRAP-positive osteoclasts were considered as mature osteoclasts. It was observed that osteoclasts generated from C57BL6 mice showed more multinucleation as compared to osteoclasts generated from Swiss CRL mice. These experiments helped us to standardize protocols for generation and characterization of human osteoclasts.

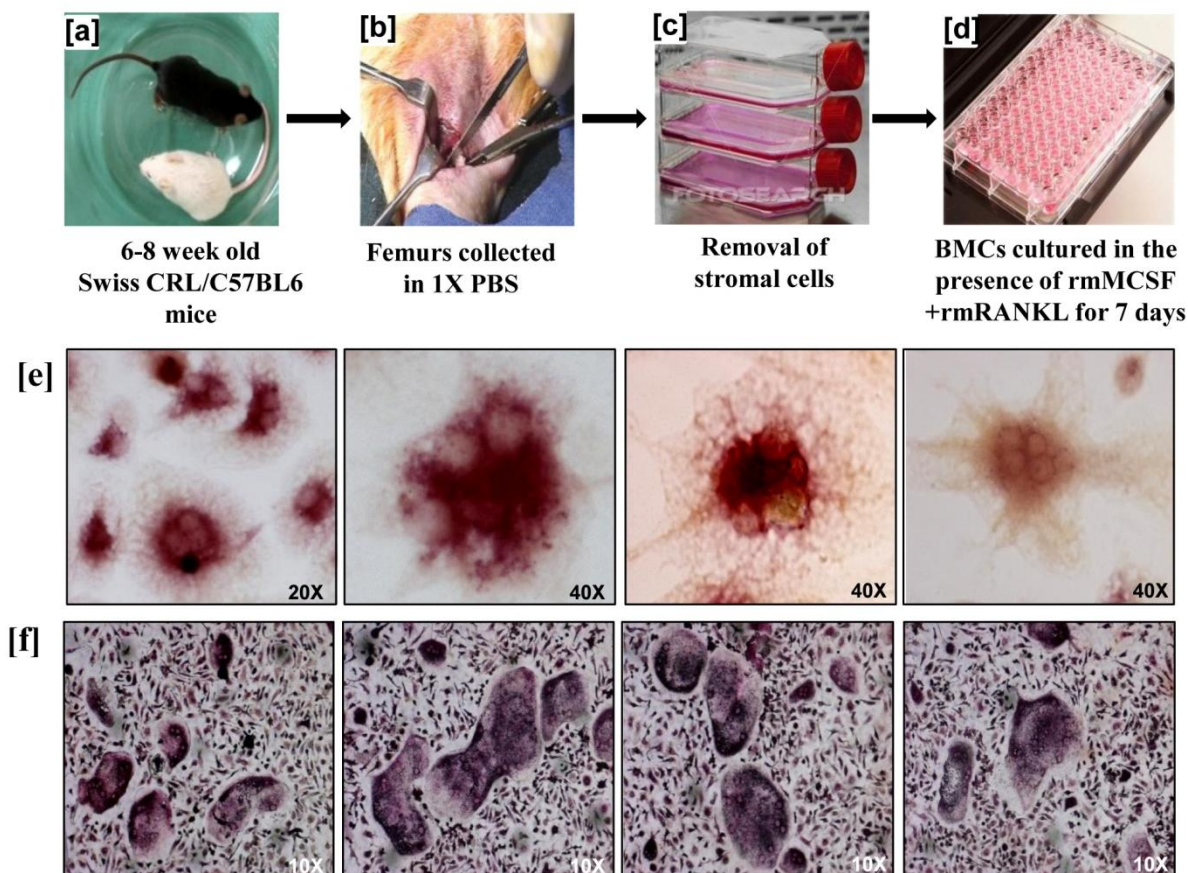


Figure 14: Generation of mouse osteoclasts from bone marrow precursor cells

6-8 week old Swiss CRL or C57BL6 mouse [a] was sacrificed and bone marrow cells (BMCs) were aspirated from femurs [b]. BMCs were cultured in α MEM (30×10^6 cells/5ml) supplemented with 10ng/ml rmMCSF for 24 hrs [c]. After 24 hrs, nonadherent osteoclast precursor cells (OCPs) were collected, washed and cultured in rmRANKL (30ng/ml) and rmMCSF (30ng/ml) containing α MEM (1×10^5 cells/200 μ l) on sterile thermanox coverslips placed in 96 well flat bottom plate. The cells were cultured for 7 days with intermediate feeding after every 3rd day [d]. On 8th day, generation of osteoclasts was confirmed by staining them for TRAP. Multinucleated (≥ 3) TRAP positive cells were considered as mature osteoclasts. Osteoclasts were generated from BMCs of Swiss CRL mice [e] and C57BL6 mice [f].

Henceforth, all the experiments were carried out using human osteoclasts generated from CD14⁺ precursor cells

4.2.3) Generation and characterization of human osteoclasts

CD14⁺ cells were immunomagnetically separated from PBMCs using CD14⁺ cell separation kit (Milteney Biotech, Germany) as per the kit instructions and separated population showing >95% purity were used for experiments (Figure 15). As discussed in Table 5, average yield of CD14⁺ cells from PBMCs ranged from 1.31×10^6 to 11.3×10^6 (mean \pm SEM, $5.8 \pm 0.6 \times 10^6$) with starting population of PBMCs ranging from 35.6×10^6 to 168.1×10^6 (mean \pm SEM, $97.5 \pm 8.4 \times 10^6$). Human osteoclasts were generated from CD14⁺ cells (monocytes) in the presence of rhMCSF (30ng/ml) and rhRANKL (40ng/ml) on thermanox coverslips in 96 well plate over the period of 21 days, with intermediate feedings on every 3rd day. On 21st day, mature osteoclasts were characterized by staining them for expression of vitronectin receptor (α V β 3 integrin) using monoclonal antibody for CD51/61(23c6) and TRAP staining. Multinucleated (>3 nuclei) TRAP positive cells were considered as mature osteoclasts (Figure 16a). Human osteoclasts form characteristic F-actin ring, which was analyzed by staining the osteoclasts with Phalloidin-TRITC (Figure 16b). Mature human osteoclasts were also characterized for their function i.e. bones resorption on Osteoclast Activity Assay Substrate (OAAS), which is a synthetic calcium phosphate coated substrate (Figure 16c). Like human osteoclasts, activated macrophages also express TRAP [259]. As macrophages differentiate into osteoclasts, α V β 5 integrins expressed by macrophages gets replaced with α V β 3. Hence α V β 3 (vitronectin receptor) positivity was used to differentiate osteoclasts from multinucleated macrophages (Figure 17a and 17b).

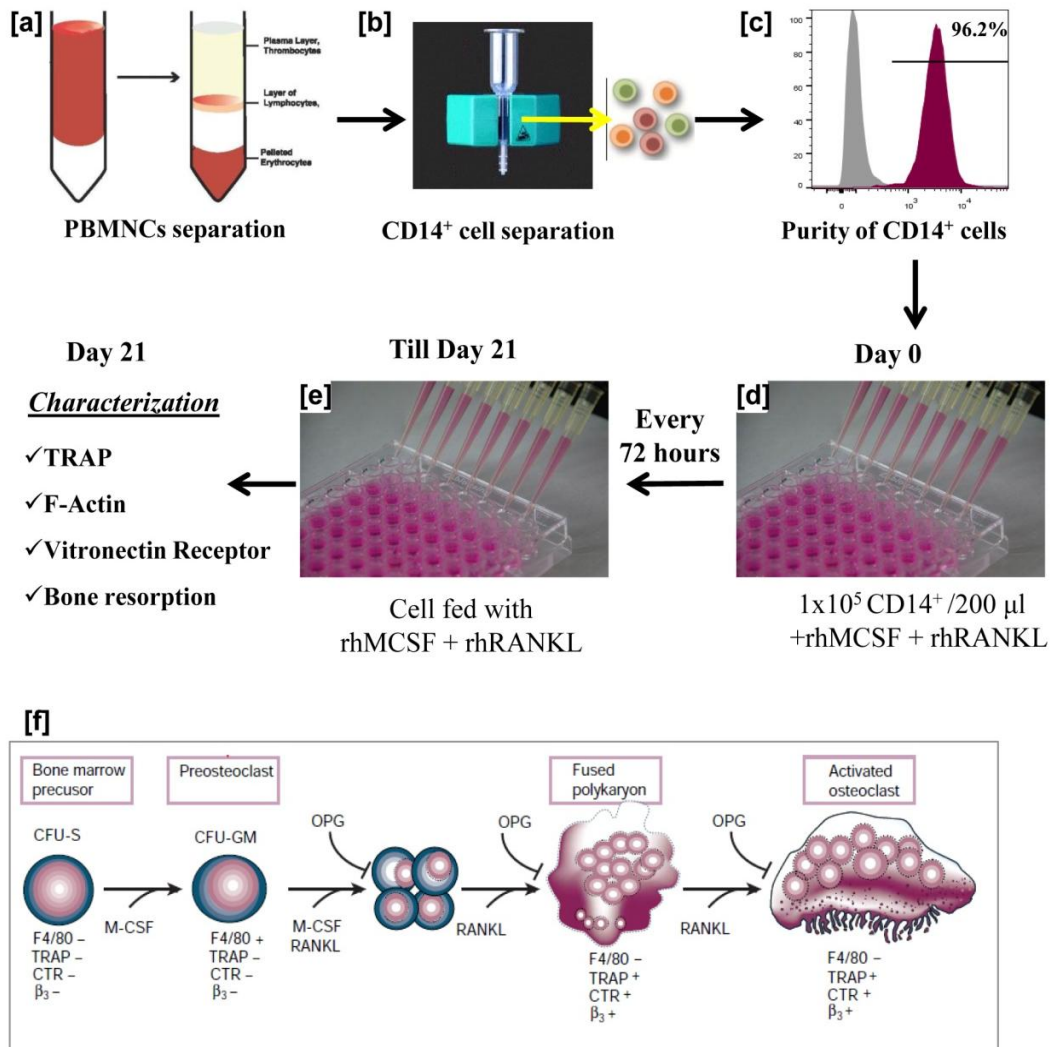


Figure 15: Generation of human osteoclasts from CD14⁺ precursor cells

CD14⁺ cells were immunomagnetically separated from PBMNCs [a] by positive selection method using CD14⁺ cell separation kit [b]. Purified population was analyzed for purity and populations having $\geq 95\%$ were used for osteoclast generation [c]. CD14⁺ cells (1×10^5) were cultured in α MEM (200 μ l) supplemented with rhMCSF (30 ng/ml) and rhRANKL (40 ng/ml) on sterile thermanox coverslips placed in flat bottom 96 well plate at 37°C [d]. The cells were fed every 3rd day with rhMCSF and rhRANKL for 21 days [e]. On 21st day, cultures were terminated and osteoclasts were characterized by staining them for TRAP, vitronectin receptor (α V β 3), F-actin ring formation along with multinucleation and bone resorption. [f] Schematic representation of process of human osteoclastogenesis [Boyle et al. (2003); Nature; 423: 337-342].

Table 5: Percent yield of CD14⁺ cells from healthy individuals (HI)

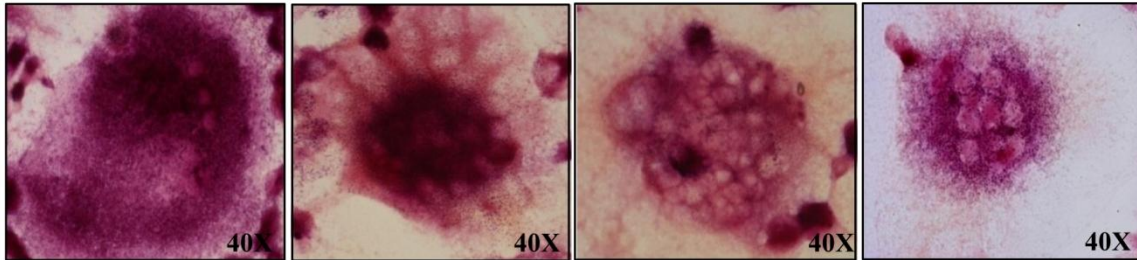
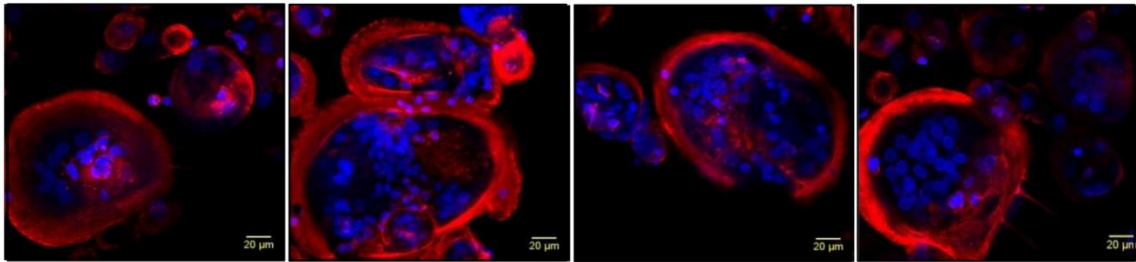
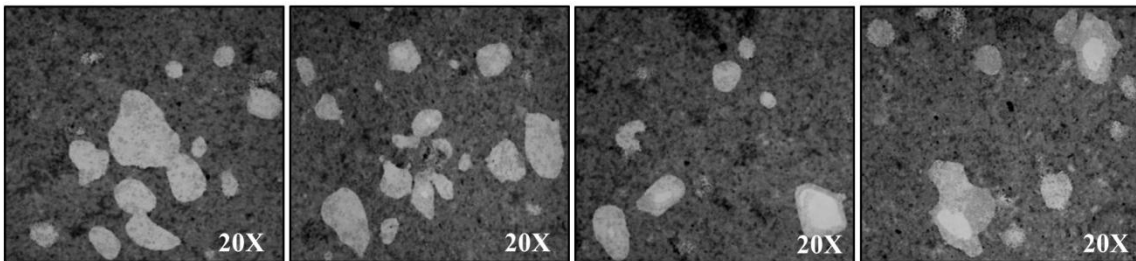
Healthy Individual (HI)	Amount of blood	Total number of PBMCs used for MACS	MACS purified CD14 ⁺ cells	Percent yield of CD14 ⁺ cells (%)
HI 1	20 ml	67 X 10 ⁶	3.99 X 10 ⁶	5.9
HI 2	25 ml	93 X 10 ⁶	3.51 X 10 ⁶	3.77
HI 3	35 ml	132.2 X 10 ⁶	8.37 X 10 ⁶	6.33
HI 4	30 ml	98.4 X 10 ⁶	2.8 X 10 ⁶	2.84
HI 5	25 ml	97.5 X 10 ⁶	4.1 X 10 ⁶	4.2
HI 6	30 ml	125.7 X 10 ⁶	9.0 X 10 ⁶	7.15
HI 7	25 ml	89.2 X 10 ⁶	8.11X 10 ⁶	9.1
HI 8	20 ml	35.6 X 10 ⁶	1.31 X 10 ⁶	3.68
HI 9	25 ml	76.3 X 10 ⁶	4.7 X 10 ⁶	6.25
HI 10	35 ml	168.1 X 10 ⁶	8.9 X 10 ⁶	5.3
HI 11	35 ml	134.1 X 10 ⁶	11.3 X 10 ⁶	8.44
HI 12	35 ml	163.0 X 10 ⁶	10.4 X 10 ⁶	6.41
HI 13	25 ml	80.2 X 10 ⁶	5.8 X 10 ⁶	7.25
HI 14	20 ml	45.1 X 10 ⁶	1.96 X 10 ⁶	4.35
HI 15	35 ml	138 X 10 ⁶	7.64 X 10 ⁶	5.54
HI 16	25 ml	70.6 X 10 ⁶	6.0 X 10 ⁶	8.5
HI 17	20 ml	65.1 X 10 ⁶	3.1 X 10 ⁶	4.61
HI 18	25 ml	84.3 X 10 ⁶	5.3 X 10 ⁶	6.3
HI 19	25 ml	127.5 X 10 ⁶	5.41 X 10 ⁶	4.25
HI 20	20 ml	58.8 X 10 ⁶	4.77 X 10 ⁶	8.12

Mean cell count of PBMCs: $97.5 \pm 8.4 \times 10^6$

Mean cell count of CD14⁺ cells: $5.8 \pm 0.6 \times 10^6$

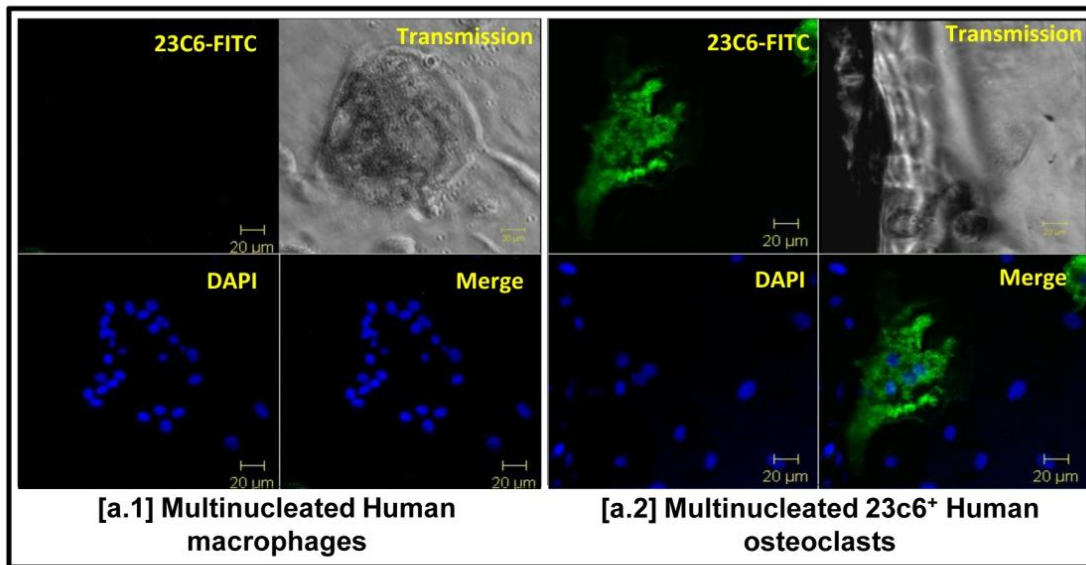
Mean % recovery of CD14⁺ cells: $5.9 \pm 0.4 \%$

A representative table for yields of CD14⁺ cells which were immunomagnetically purified by MACS from PBMCs of healthy individuals (n=20).

[a] Tartarate resistant acid phosphatase (TRAP) staining**[b] F-Actin ring formation****[c] Bone resorption on osteoclast activity assay substrate (OAAS)****Figure 16: Characterization of human osteoclasts**

Osteoclasts generated from CD14⁺ cells were characterized by staining them for multinucleation, TRAP, F-actin ring/ bundle formation or functional assays like bone resorption. [a] Enzymatic reactions catalyzed by TRAP enzyme present in osteoclasts generate characteristic maroon colored deposits in the presence of tartarate, staining osteoclasts pink/maroon. Multinucleated (>3 nuclei) TRAP positive cells were considered as mature osteoclasts. [b] Human osteoclasts also show characteristic F-actin ring formation, which was analyzed by staining them with phalloidin-TRITC (red), along with nuclear dye DAPI (blue). [c] Resorption pits (clear zones) were analyzed by generating osteoclasts on Osteoclast Assay Activity Substrate (OAAS).

[a] CD51/61 (α V β 3) staining of human macrophages and osteoclast



[b] α V β 3 stained human osteoclasts

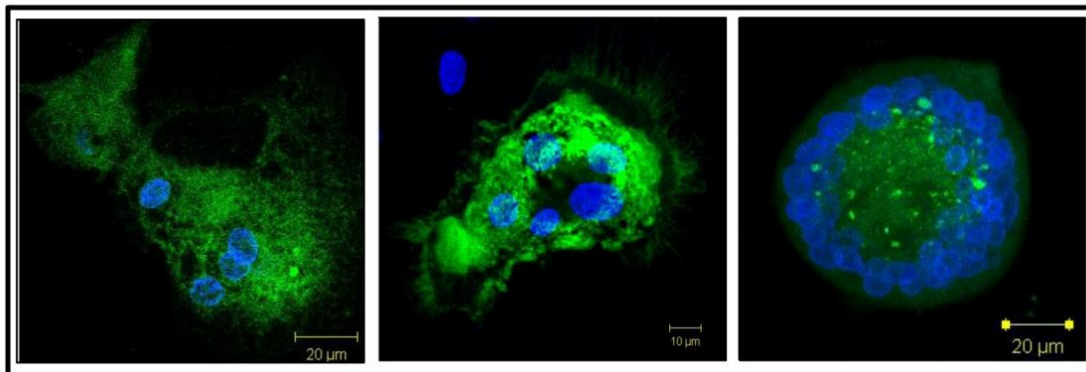


Figure 17: Differentiation of human osteoclasts from macrophages

CD14⁺ cells (monocyte/macrophage precursor cells) fuse under the influence of rhMCSF to form a multinucleated cell, which differentiate in the presence of rhRANKL to mature osteoclast. Vitronectin receptor positivity was used as a criterion to differentiate human osteoclasts from human macrophages. [a1] Human macrophages show multinucleation (DAPI, blue) but no vitronectin receptor (α V β 3 or CD51/61 or 23c6) expression. [a.2] Human osteoclasts express high levels of vitronectin receptors (CD51/61-AF647, green) along with multinucleation (DAPI, blue). [b] Representative images of multinucleated osteoclasts showing vitronectin receptor positivity.

4.2.4 Direct effect of $\gamma\delta$ T cells on generation of human osteoclasts

CD14⁺ cells (1×10^5 /well, osteoclast precursor cells) were cocultured with “activated” or “freshly isolated” $\gamma\delta$ T cells (1×10^4 /well, 10:1) in the presence of rhMCSF, rhRANKL and rhIL2 for 21 days (described in material and methods Section 3.7.7), with intermediate feedings on every 3rd day. Osteoclasts generated in the presence of rhMCSF and rhRANKL served as a positive control, while osteoclasts generated in the presence of rhMCSF alone were considered as negative control. Osteoclasts showing multinucleation (≥ 3 nuclei) and 23c6 positivity (vitronectin receptor) were considered as mature osteoclasts. Number of osteoclasts generated (25 ± 4 osteoclasts/well) in the presence of rhMCSF and rhRANKL (positive control) were normalized to 100% and data has been represented as relative increase or decrease in number of osteoclasts generated per well compared to positive control. Coculture of “activated” $\gamma\delta$ T cells with CD14⁺ cells in the presence of rhMCSF and rhRANKL showed significant reduction (1.5 ± 0.5 osteoclasts/well, 93.6% reduction, $p=0.0012$) in 23c6⁺ multinucleated osteoclasts compared to positive control (Figure 18). In contrast, generation of osteoclasts in the presence of “freshly isolated” $\gamma\delta$ T cells showed marked increase in the number of 23c6⁺ multinucleated osteoclasts (53.5 ± 14.5 osteoclasts/well, 110% increase, $p=0.0458$). These results indicated that “activated” $\gamma\delta$ T cells inhibit osteoclastogenesis, while “freshly isolated” $\gamma\delta$ T cells tend to increase the number of osteoclasts upon coculture. In order to confirm this observation “freshly isolated” $\gamma\delta$ T cells were cocultured with CD14⁺ cells in the presence of phosphoantigen BrHPP along with rhMCSF, rhRANKL and rhIL2. It was interesting to observe that generation of osteoclasts in the presence of “freshly isolated” $\gamma\delta$ T cells that were stimulated with BrHPP showed significant reduction (2.5 ± 1.5 osteoclasts/well, 88.8% reduction, $p = 0.0078$) in the total number of 23c6⁺ osteoclasts, confirming that “activation status” of $\gamma\delta$ T cells govern their

function to regulate osteoclastogenesis. CD14⁺ cells cultured in the presence of rhMCSF and rhRANKL in the presence of rhIL2 (26.5±3.5 osteoclasts/well) or BrHPP+ rhIL2 (28±3 osteoclasts/well) showed osteoclast numbers that were comparable to that observed in positive control (25±4 osteoclasts/well), indicating that rhIL2 or BrHPP + rhIL2 had no effect on osteoclast generation.

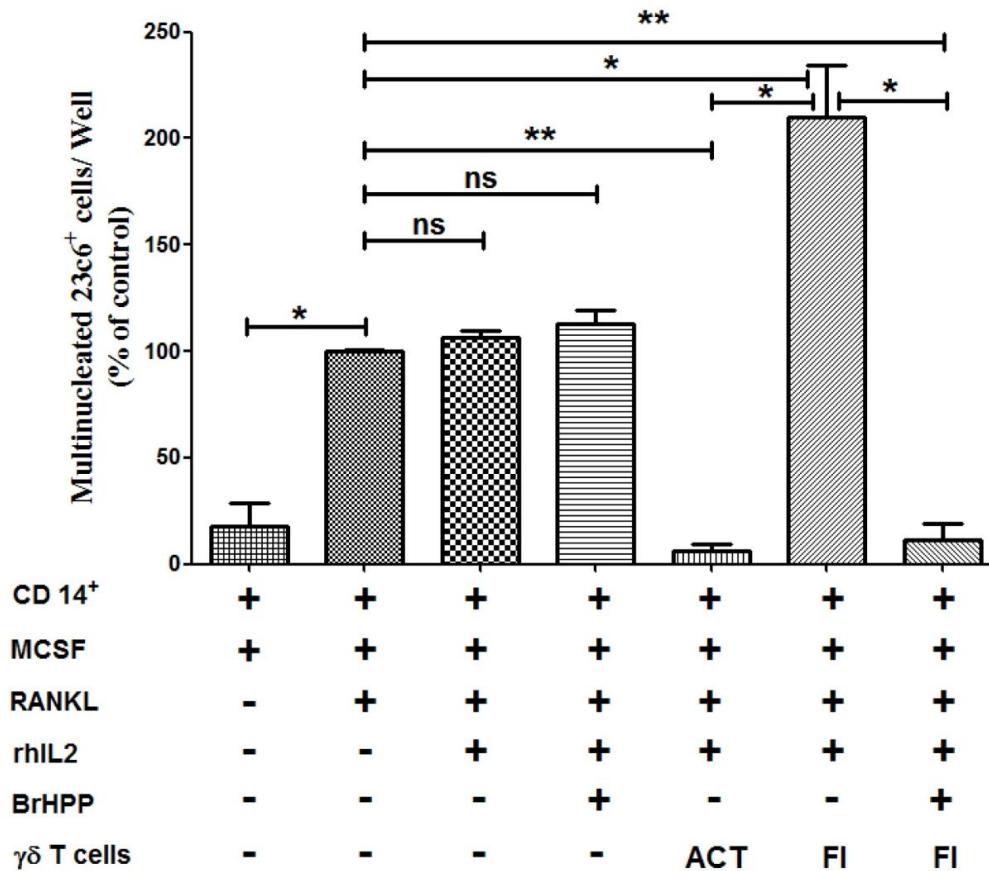


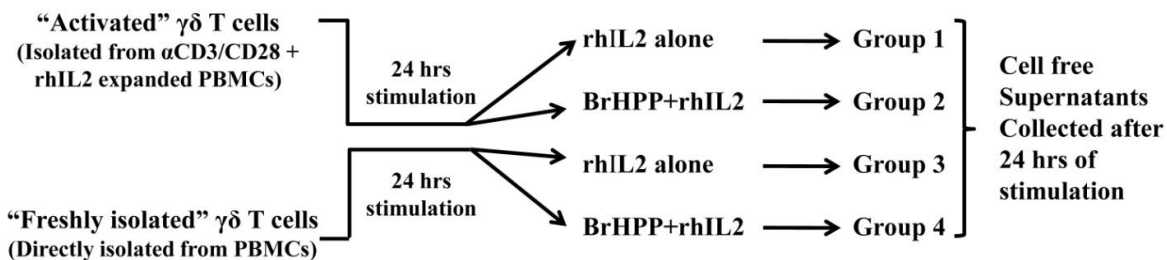
Figure 18: Direct effect of “activated” and “freshly isolated” $\gamma\delta$ T cells on generation of human osteoclasts

CD14⁺ cells (1×10^5 /well) were co-cultured with “activated” (ACT) or “freshly isolated” (FI) $\gamma\delta$ T cells (1×10^4) in α MEM supplemented with rhMCSF (30 ng/ml), rhRANKL (40 ng/ml) and rhIL2 (0.5 IU/well) on thermanox coverslips (Nunc) in flat bottom 96 well plate. Osteoclasts generated in the presence of rhMCSF and rhRANKL were kept as positive control. CD14⁺ cells cultured in the presence of MCSF were considered as negative control. “Freshly isolated” $\gamma\delta$ T cells were stimulated with phosphoantigen by supplementing the cultures with BrHPP (200nM) along with rhMCSF, rhRANKL and rhIL2 on Day 0. The CD14⁺: $\gamma\delta$ T cell cocultures were fed with rhMCSF, rhRANKL, rhIL2 every 3rd day for 21 days. On the 21st day, osteoclasts were characterized by staining them for vitronectin receptor (anti-human-CD51/CD61-AF488) and total number of osteoclasts (multinucleated 23c6⁺ cells) generated per well were quantitated. Number of osteoclasts generated in the presence of rhMCSF and rhRANKL (positive control)

were normalized to 100% and data has been represented as relative increase or decrease in number of osteoclasts generated per well compared to positive control. Three independent experiments were carried out and the data is represented as mean \pm SEM. [$p < 0.05$ (*), $p < 0.005$ (**), $p < 0.0005$ (***)].

4.2.5) *In vitro* bone resorption assay using Osteoclast Activity Assay Substrate (OAAS)

To analyze the effect of soluble factors secreted by $\gamma\delta$ T cells on function of osteoclasts (bone resorption), osteoclasts were cultured in the presence of cell free supernatant of antigen stimulated $\gamma\delta$ T cells. Cell free supernatants were acquired by stimulating “activated” or “freshly isolated” $\gamma\delta$ T cells (5×10^4) with rhIL2 (0.5IU) alone or in combination with BrHPP (200nM) for 24 hrs (described below).



OPCs were generated from $CD14^+$ cells (1×10^5) in the presence of rhMCSF and rhRANKL for 12 days on OAAS. From 12th day onwards, every 3rd day, the cultures were fed with cell free supernatants of “activated” or “freshly isolated” $\gamma\delta$ T cells, along with rhMCSF and rhRANKL. Cell free supernatants of rhIL2 or BrHPP+rhIL2 stimulated “activated” (Group 1, 2 respectively) or “freshly isolated” (Group 3, 4 respectively) $\gamma\delta$ T cells were added in different volumes (50 μ l and 25 μ l). Baseline resorption observed on OAAS plates by osteoclasts generated in the presence of rhMCSF and rhRANKL (positive control) and activated macrophages (negative control, cultured in the presence of rhMCSF only) was also analyzed. On 21st day, cultures were terminated and functional ability of these osteoclasts was tested on

OAAS by calculating the total resorbed area (μm^2) generated in a well. Resorption areas generated by osteoclasts cultured in the presence of rhMCSF and rhRANKL was normalized to 100% and data has been represented as relative increase or decrease in resorption area compared to positive control (100%). As shown in Figure 19, addition of cell free supernatants from rhIL2 stimulated “activated” $\gamma\delta$ T cells (50 μl and 25 μl) showed significant reduction in total resorption area (68%, $p < 0.0001$ and 55.1%, $p = 0.01$ respectively) compared to positive control (100%). The baseline resorption by monocytes / macrophages (negative control) was also calculated and was found negligible. Osteoclasts generated in the presence of cell free supernatants of BrHPP+rhIL2 stimulated “activated” $\gamma\delta$ T cells (50 μl and 25 μl) also showed significant reduction in resorption area (67.5%, $p < 0.0001$ and 32.5%, $p < 0.0001$ respectively) as compared to positive control. Simultaneously, the effect of soluble factors secreted by phosphoantigen stimulated “freshly isolated” $\gamma\delta$ T cells were also analyzed on osteoclast function. As shown in Figure 20, osteoclasts generated in the presence of cell free supernatants of rhIL2 stimulated “freshly isolated” $\gamma\delta$ T cells (50 μl and 25 μl) showed increase in total resorption area (307.6%, $p = 0.02$ and 204.7%, $p = 0.01$ respectively) compared to positive control, indicating their pro-osteoclastogenic effect. Cell free supernatants of BrHPP+rhIL2 stimulated “freshly isolated” $\gamma\delta$ T cells also showed increase in resorption area compared to positive control, although the increase was not statistically significant but it was lesser when compared to rhIL2 stimulated “freshly isolated” $\gamma\delta$ T cells. This clearly indicated that, short term stimulation of $\gamma\delta$ T cells has pro-osteoclastogenic effect, while “activated” $\gamma\delta$ T cells have a better potential to suppress osteoclast generation and function.

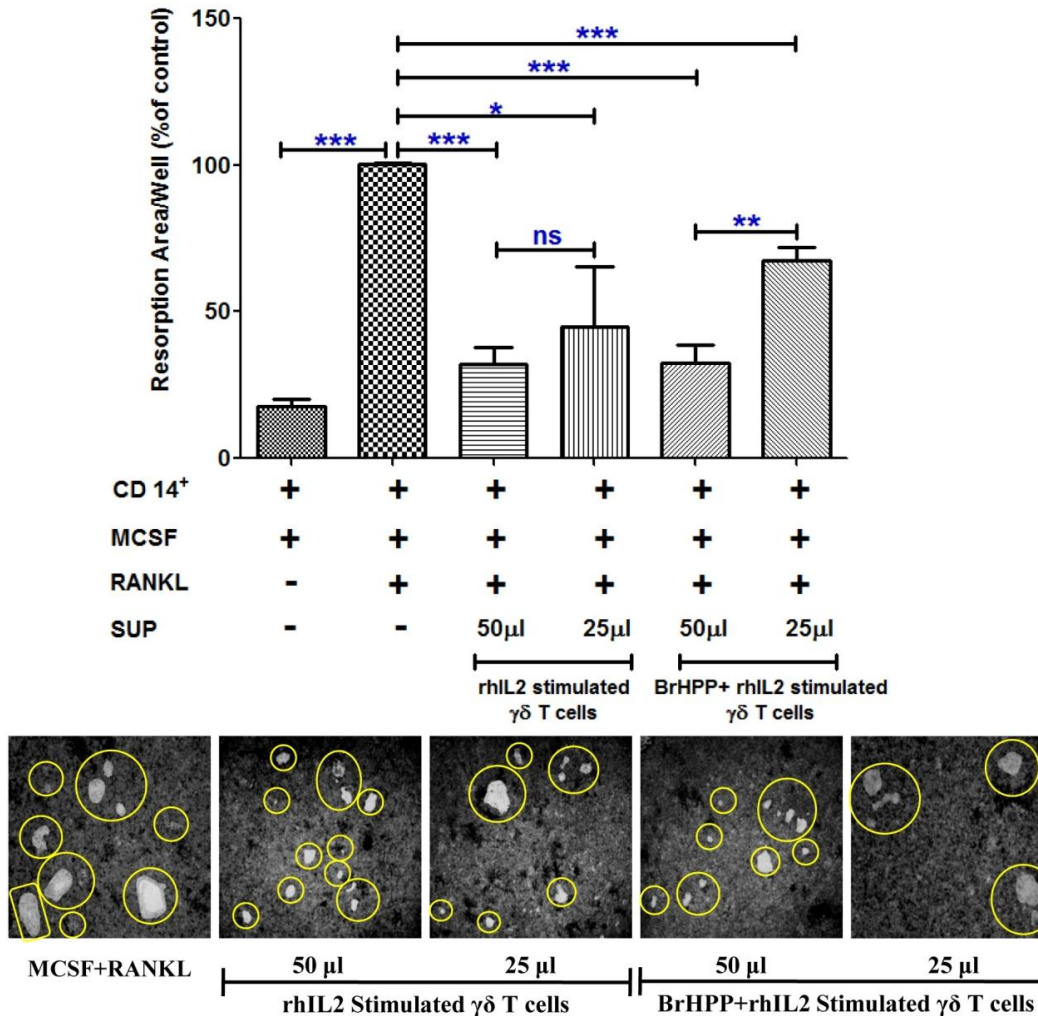


Figure 19: Effect of soluble factors secreted by “activated” $\gamma\delta$ T cells on function of human osteoclasts

Osteoclasts were generated from CD14⁺ cells (1×10^5 / well) in the presence of rhMCSF (30ng/ml) and rhRANKL (40ng/ml) for 12 days on osteoclast activity assay substrate (OAAS). From 12th day onwards, along with rhMCSF and rhRANKL, the cultures were fed on every 3rd day with different volumes (50 μl and 25 μl) of cell free supernatants of “activated” $\gamma\delta$ T cells, which were stimulated with of rhIL2 or BrHPP+rhIL2 for 24 hrs. Osteoclasts generated in the presence of rhMCSF and rhRANKL were kept as positive control. The cultures were terminated on 21st day and the area resorbed by mature osteoclasts was calculated using ImageJ software. Total resorption area generated per well by osteoclasts cultured in the presence of rhMCSF and rhRANKL (positive control) was normalised to 100% and data has been represented as relative increase or decrease in resorption area compared to positive control. The data shown is mean \pm SEM of three independent experiments. [$p < 0.05$ (*), $p < 0.005$ (**), $p < 0.0005$ (***)].

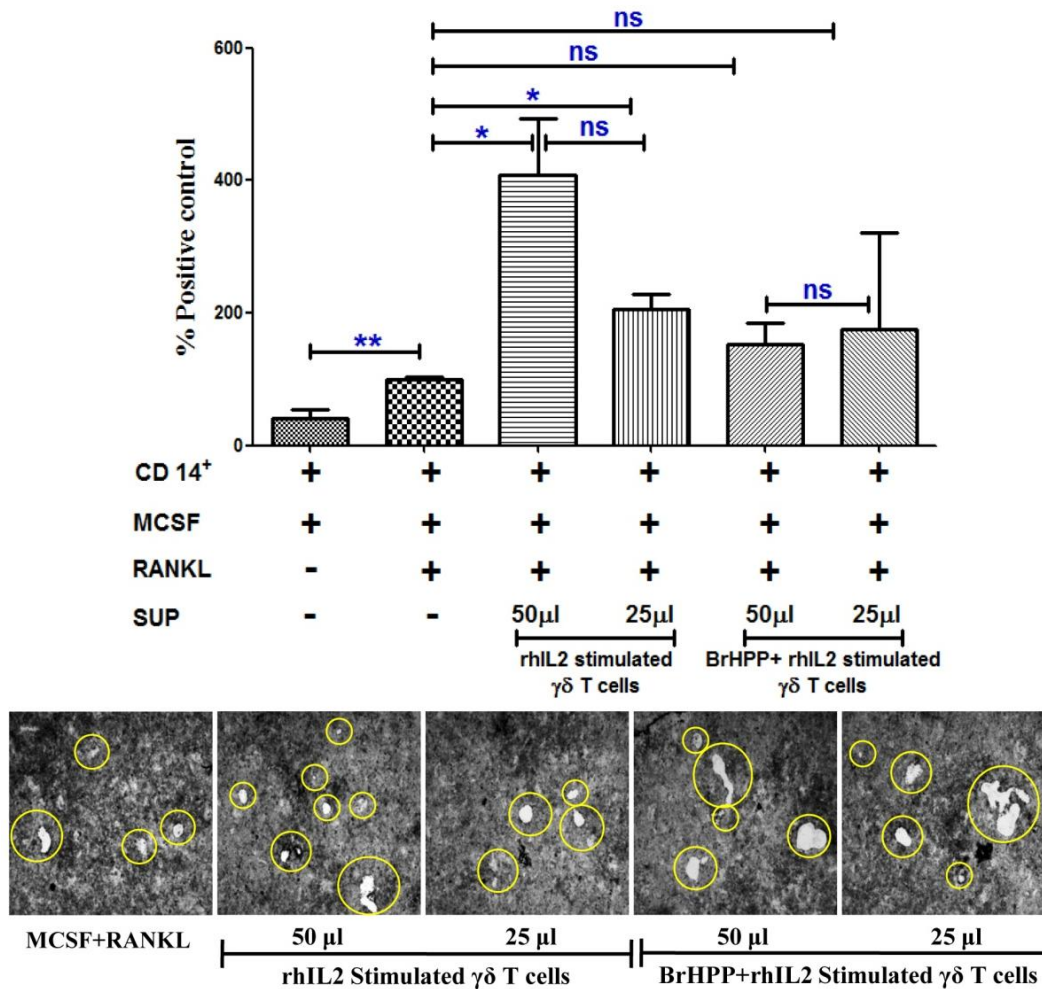
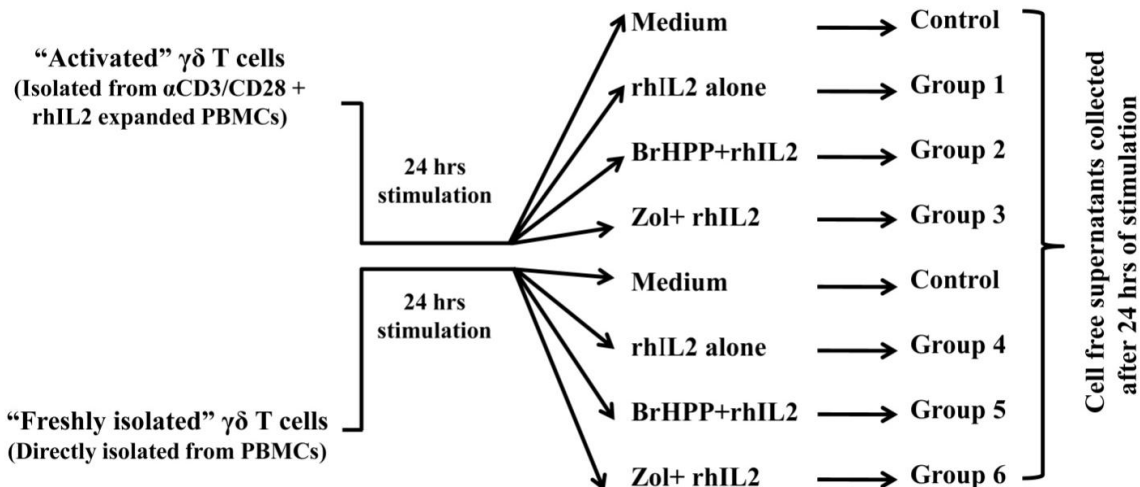


Figure 20: Effect of soluble factors secreted by “freshly isolated” $\gamma\delta$ T cells on function of human osteoclasts

Osteoclasts were generated from CD14⁺ cells (1×10^5 / well) in the presence of rhMCSF and rhRANKL for 12 days on OAAS. From 12th day onwards, along with rhMCSF and rhRANKL, the cultures were fed on every 3rd day with different volumes (50 μl and 25 μl) of cell free supernatants of rhIL2 or BrHPP+rhIL2 stimulated “freshly isolated” $\gamma\delta$ T cells. Osteoclasts generated in the presence of rhMCSF and rhRANKL were kept as positive control. The cultures were terminated on 21st day and the area resorbed by mature osteoclasts was calculated using ImageJ software. Total resorption area generated per well by osteoclasts cultured in the presence of rhMCSF and rhRANKL (positive control) was normalised to 100% and data has been represented as relative increase or decrease in resorption area compared to positive control. The data shown is mean \pm SEM of three independent experiments. [p<0.05(*), p<0.005(**), p<0.0005(***)].

4.3) Cytokine profiling of cell free supernatants of antigen activated $\gamma\delta$ T cells

Cell free supernatants were collected from “activated” (ACT) and “freshly isolated” (FI) $\gamma\delta$ T cells. The various groups are described below. “Activated” and “freshly isolated” $\gamma\delta$ T cells were either left unstimulated (medium only, control 1 and control 2 respectively) or were stimulated with rhIL2 alone (Group 1 and Group 4 respectively), BrHPP + rhIL2 (Group 2 and Group 5 respectively) and Zoledronate (Group 3 and Group 6 respectively). Cell free supernatants of these cells were collected and analyzed for Th1/Th2/Th17 cytokines by CBA, as described in Materials and methods section 3.9.

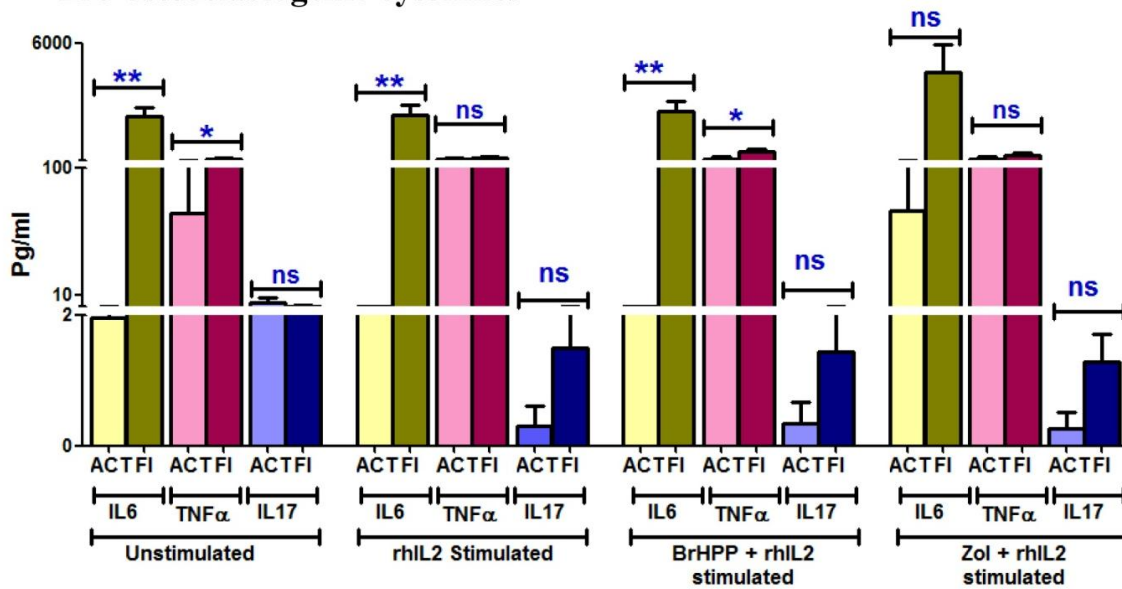


Analysis of cell free supernatants of “activated” and “freshly isolated” $\gamma\delta$ T cells in the unstimulated control group interestingly showed significant differences in levels of two cytokines- IL6 (pro-osteoclastogenic) and IFN γ (anti-osteoclastogenic) compared to other cytokines (Table 6). As shown in Figure 21, in an unstimulated state, “freshly isolated” $\gamma\delta$ T cells showed higher levels of IL6 (Mean \pm SEM 2318 \pm 471 pg/ml), while “activated” $\gamma\delta$ T cells showed significantly ($P=0.005$) lower levels of IL6 (1.9 \pm 0.3 pg/ml). Comparison of IFN γ levels showed that, “freshly isolated” $\gamma\delta$ T cells secreted very low (3.2 \pm 0.27 pg/ml) levels of IFN γ , while “activated” $\gamma\delta$ T cells showed significantly ($p=0.008$) higher levels of IFN γ (274.1 \pm 111.2

pg/ml). Upon stimulation with rhIL2, supernatant of “activated” $\gamma\delta$ T cells (Group 1) showed significantly higher levels of IFN γ (706.5 \pm 211.8 pg/ml, p=0.0044) compared to “freshly isolated” $\gamma\delta$ T cells (33.5 \pm 29.1 pg/ml, Group 4). Similarly, upon stimulation with BrHPP+rhIL2, “activated” $\gamma\delta$ T cells (Group 2) showed significantly higher levels of IFN γ (879.7 \pm 240 pg/ml, p=0.0264) compared to “freshly isolated” $\gamma\delta$ T cells (260.7 \pm 101.2 pg/ml Group 5). After stimulation with Zoledronate+rhIL2, levels of IFN γ secretion were found increased by both “activated” $\gamma\delta$ T cells (Group 3, 1066 \pm 395.6 pg/ml) and “freshly isolated” $\gamma\delta$ T cells (Group 6, 640.9 \pm 372.4 pg/ml). Levels of IL6 remained higher in case of “freshly isolated” $\gamma\delta$ T cells (4574 \pm 1349 pg/ml) levels as compared to “activated” $\gamma\delta$ T cells (69.1 \pm 47.2 pg/ml). “Freshly isolated” $\gamma\delta$ T cells upon stimulation with rhIL2 showed a progressive increase in IFN γ production that further enhanced with BrHPP+rhIL2 (p=0.01) and Zoledronate+rhIL2 stimulation compared to unstimulated $\gamma\delta$ T cells. Other Th1/Th2/ Th17 cytokines analyzed by CBA are given in Table 6.

The levels of IL6 secreted by “activated” (Group 1 and Group 3) and “freshly isolated” (Group 2 and Group 4) $\gamma\delta$ T cells were not significantly different compared to supernatants of unstimulated $\gamma\delta$ T cells (control). Upon Zoledronate stimulation, levels of IL6 were found increased as compared to unstimulated and rhIL2 control, but IFN γ secretion was remarkably increased. Results indicate that “freshly isolated” $\gamma\delta$ T cells secrete higher levels of IL6, thus have pro-osteoclastogenic effect, while “activated” $\gamma\delta$ T cells maintain higher levels of IFN γ playing an anti-osteoclastogenic role.

[a] Pro-osteoclastogenic cytokines



[b] Anti-osteoclastogenic cytokines

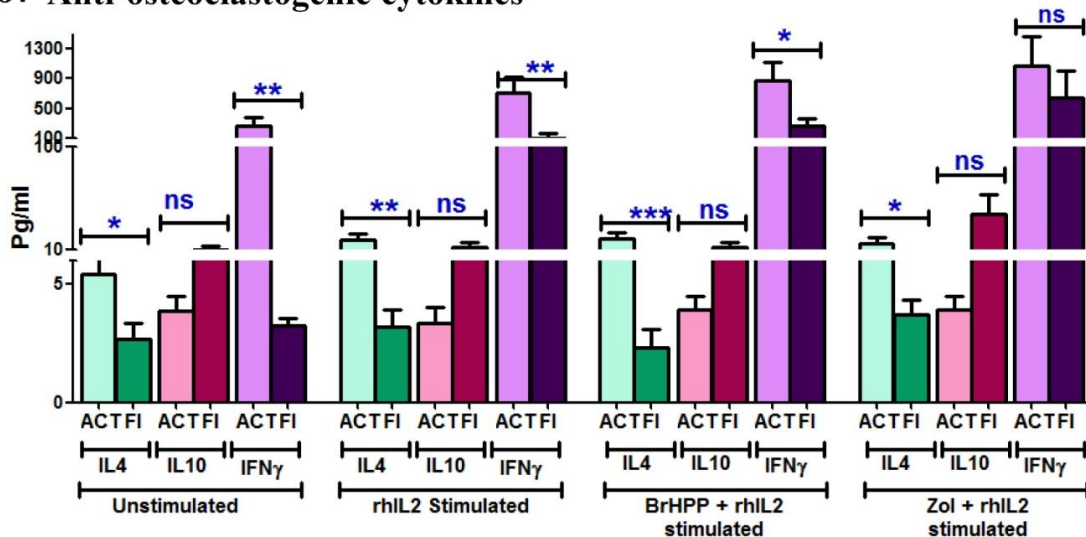


Figure 21: Estimation of Th1/Th2/Th17 cytokines in cell free supernatants of “activated” (ACT) and “freshly isolated” (FI) $\gamma\delta$ T cells

“Activated” (purified from α CD3/CD28+rhIL2 expanded PBMCs) or “freshly isolated” (directly purified from PBMCs on Day 0) $\gamma\delta$ T cells (5×10^4 /well) were stimulated with rhIL2 (0.5 IU/well), BrHPP (200nM)+rhIL2 or Zoledronate+rhIL2 for 24 hrs at 37°C in CO₂ incubator. Both “activated” and “freshly isolated” $\gamma\delta$ T cells, which were unstimulated (incubated in culture medium alone), were kept as control. After 24 hrs, the cell free supernatants were collected. Th1/Th2/Th17 cytokines of these cell free supernatants were quantified by cytometric bead array

(CBA). Based on their effect on osteoclastogenesis, cytokines are distributed as pro-osteoclastogenic [a] and anti-osteoclastogenic cytokines [b]. “Freshly isolated” $\gamma\delta$ T cells T cells showed significantly higher levels of pro-osteoclastogenic cytokines (IL6, TNF α), while [b] “activated $\gamma\delta$ T cells” showed increased levels of anti-osteoclastogenic cytokines (IFN γ and IL4). (“Activated” $\gamma\delta$ T cells (n=5), “freshly isolated” $\gamma\delta$ T cells (n= 7)). [p < 0.05 (*), p <0.005 (**), p< 0.0005 (***)].

Table 6: Cytokine profiling of cell free supernatants of antigen activated $\gamma\delta$ T cells

	<u>Unstimulated $\gamma\delta$ T cells</u>			<u>IL2 stimulated $\gamma\delta$ T cells</u>			<u>BrHPP stimulated $\gamma\delta$ T cells</u>			<u>Zol stimulated $\gamma\delta$ T cells</u>		
	Cytokine Concentration (pg/ml)		P value	Cytokine Concentration (pg/ml)		P value	Cytokine Concentration (pg/ml)		P value	Cytokine Concentration (pg/ml)		P value
	ACT (n=5)	FI (n=7)		ACT (n=5)	FI (n=7)		ACT (n=5)	FI (n=7)		ACT (n=5)	FI (n=7)	
IL2	2.7 ± 0.9	17.2 ± 9.4	ns	13.7 ± 3.4	680.2 ± 412	ns	14.1 ± 5.0	366.9 ± 330.4	ns	15.9 ± 7.5	30.6 ± 12.8	ns
IL4	5.4 ± 0.8	2.6 ± 0.6	*	18.3 ± 5.4	3.1 ± 0.6	**	20.2 ± 4.6	2.3 ± 0.7	***	15.74 ± 5.4	3.7 ± 0.6	*
IL6	1.9 ± 0.3	2318 ± 471	**	2.4 ± 0.09	2375 ± 537.8	**	2.24 ± 0.07	2563 ± 498.7	**	69.1 ± 47.2	4574 ± 1349	ns
IL10	3.8 ± 0.6	10.6 ± 3.2	ns	3.3 ± 0.6	12.2 ± 4.5	ns	3.9 ± 0.5	12.3 ± 3.8	ns	3.9 ± 0.6	41.7 ± 16.5	*
TNFα	67.5 ± 37	205.7 ± 38.3	*	165.5 ± 82	254.9 ± 48.9	ns	188.1 ± 90.9	547.1 ± 104.9	*	201.1 ± 88.5	394.1 ± 102.1	ns
IFNγ	274.1 ± 111	3.2 ± 0.2	**	706.5 ± 211	33.5 ± 29.21	**	879.7 ± 240	260.7 ± 101.2	*	1066 ± 395.6	640.9 ± 372.4	ns
IL17	4.5 ± 4.1	2.0 ± 0.9	ns	0.3 ± 0.3	1.4 ± 0.5	ns	0.3 ± 0.3	1.4 ± 0.6	ns	0.3 ± 0.3	1.280 ± 0.4	ns

TH1/Th2/Th17 cytokines in cell free supernatants obtained from “activated” and “freshly isolated” $\gamma\delta$ T cell were analysed using cytometric bead array. “Freshly isolated” $\gamma\delta$ T cells showed higher baseline levels (control) of IL6, while higher level of IFN γ was detected in supernatants of “activated” $\gamma\delta$ T cells. Stimulation of “activated” and “freshly isolated” $\gamma\delta$ with rhIL2 (0.5IU), BrHPP (200nM), Zoledronate (100 μ M) enhanced IFN γ secretion. Levels of IL4 and TNF α were also found increased upon stimulation of “freshly isolated” $\gamma\delta$ T cells.

4.4) Effect of IL6 and IFN γ neutralization in cell free supernatants of “unstimulated” $\gamma\delta$ T cells on osteoclast function

To validate that the effect of $\gamma\delta$ T cells on osteoclastogenesis is mediated through cytokines (IFN γ and IL6), functional assays were carried out using neutralizing antibodies to these cytokines. Osteoclasts were generated in the presence of cell free supernatants of unstimulated “activated” and “freshly isolated” $\gamma\delta$ T cells in the presence or absence of α IFN γ or α IL6 antibody. As shown in Figure 22, osteoclasts generated in the presence of cell free supernatants of “activated” $\gamma\delta$ T cells showed significant (57.4%) reduction in resorption area ($10.78 \pm 1 \mu\text{m}^2$) compared to positive control ($25.4 \pm 0.5 \mu\text{m}^2$, 100%), After addition of α IFN γ antibody to these cultures the inhibition was reversed and brought to 89.7% ($22.7 \pm 0.3 \mu\text{m}^2$), which was comparable to that observed in positive control, confirming our observation that IFN γ is a major cytokine generated by “activated” $\gamma\delta$ T cells that inhibits osteoclastogenesis. Similarly, osteoclasts generated in the presence of cell free supernatants of “freshly isolated” $\gamma\delta$ T cells showed increase in resorption area by 191.9% ($74.1 \pm 1.6 \mu\text{m}^2$) over positive control (100%). Upon addition of α IL6 antibody to the cultures, there was a marked reduction in the resorption area ($34.5 \pm 0.2 \mu\text{m}^2$, $p=0.0068$) reducing from 191.9% to 36.1% over positive control (100%). Our results suggests that the dynamics of IFN γ and IL6 play a major role in mediating the pro and antiosteoclastogenic effects of “activated” $\gamma\delta$ T cells and “freshly isolated” $\gamma\delta$ T cells respectively.

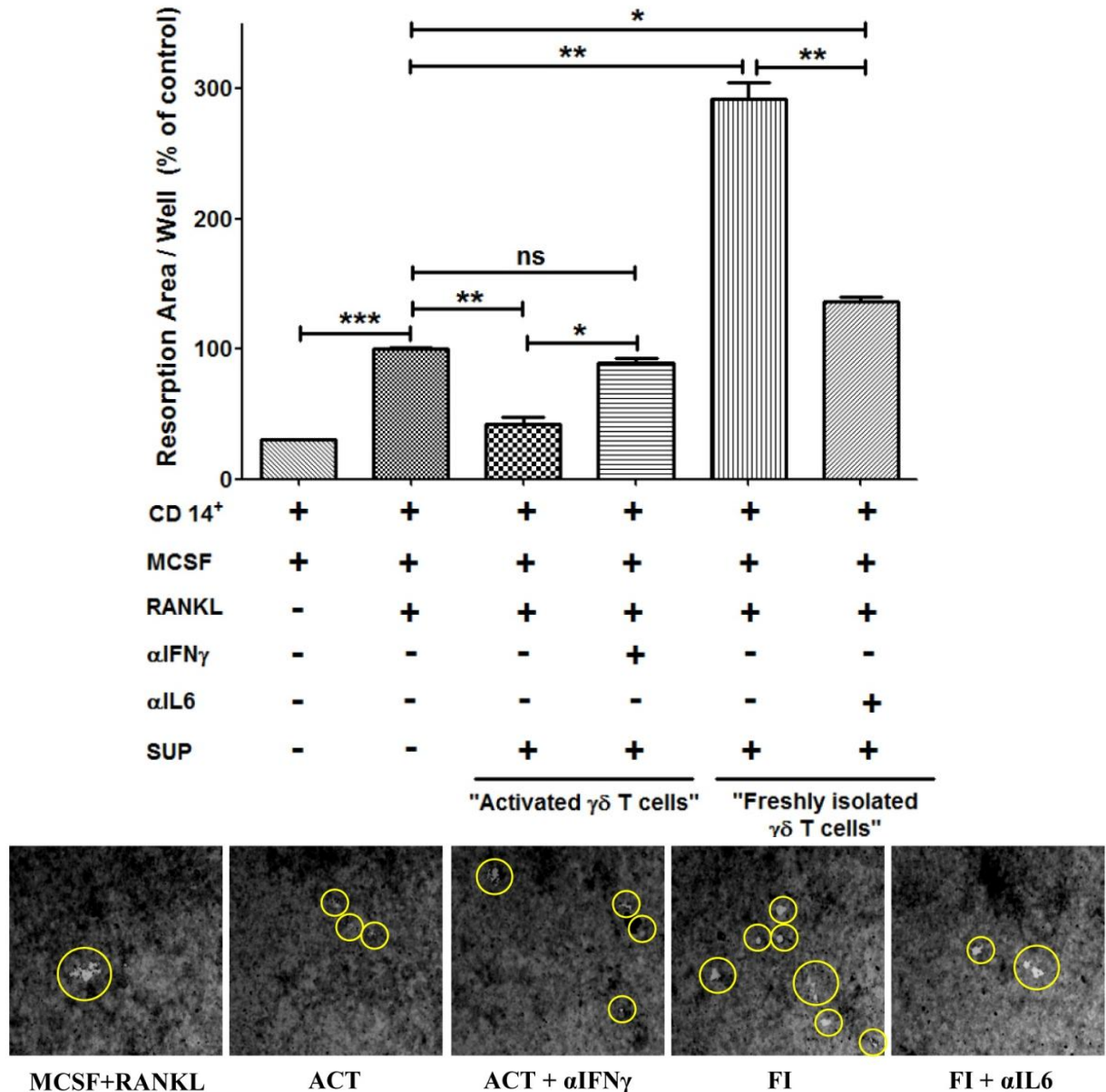


Figure 22: Effect of IFN γ and IL6 neutralization in cell free supernatants of “activated” (ACT) and “freshly isolated” (FI) $\gamma\delta$ T cells on osteoclast function.

CD14⁺ cells (1×10^5) were cultured in the presence of rhMCSF and rhRANKL for 12 days in OAAS module to generate OPCs. After which, every 3rd day, the cultures were supplemented with 50 μ l supernatants of unstimulated “activated” and “freshly isolated” $\gamma\delta$ T cells, rhMCSF, and rhRANKL with or without monoclonal mouse α IFN γ or α IL6 neutralization antibody (10 μ g/ml/well). Osteoclasts generated in the presence of rhMCSF and rhRANKL were kept as positive control. CD14⁺ cells cultured in the presence of MCSF only was considered as negative

control. On the 21st day, the cultures were terminated and resorption area was calculated. Resorption area generated in positive control was normalized to 100% and data has been represented as relative increase or decrease in resorption area compared to positive control. The data shown is mean \pm SEM of two independent experiments. [$p < 0.05$ (*), $p < 0.005$ (**), $p < 0.0005$ (***)].

The present chapter investigated the role of $\gamma\delta$ T cells in osteoclastogenesis. Our data indicated that, “activated” $\gamma\delta$ T cells secrete higher levels of IFN γ and have inhibitory effect on generation and function of osteoclasts. “Freshly isolated” $\gamma\delta$ T cells showed pro-osteoclastogenic effect through higher levels of IL6, IL17 and TNF α . Neutralization of only IL6 and IFN γ showed significant differences explaining their decisive role in controlling osteoclastogenesis.

Chapter 5

To understand the effect of aminobisphosphonate (Zoledronate) on protein profiles of breast tumor cells

Zoledronic acid is a third generation aminobisphosphonate (Chemical formula: $C_5H_{10}N_2O_7P_2$, molecular weight: 272.08 g/mol) with potent antiresorptive and antitumor activity, thus is used in the treatment of skeletal disorders and metastasis associated skeletal malignancies [58,59,60]. Zoledronate is known to inhibit farnesyl pyrophosphate synthase (FPPS) enzyme in mevalonate pathway, thus inhibits synthesis of farnesyl pyrophosphate and geranyl geranyl pyrophosphate, ultimately inhibiting essential cellular processes. *In vitro* studies on inhibition of tumor cell growth and induction of apoptosis by Zoledronate have been reported [77,78]. Earlier studies from our lab demonstrated that, tumor cells (MCF7, PC3 and SaOS2) when treated with aminobisphosphonates (Pamidronate and Zoledronate) are recognized and aggressively killed by $\gamma\delta$ T cells [26]. $\gamma\delta$ T cells were found to form a strong conjugate with aminobisphosphonate pretreated tumor cells. This process was NKG2D and $\gamma\delta$ TCR dependent, as blocking of these molecules inhibited cytotoxic effect by $\gamma\delta$ T cells. The study further investigated the role of conventional molecules like MICA, ICAM1 and FasL present on the tumor cells which are known to be involved in conjugate formation between tumor cells and $\gamma\delta$ T cells [26]. Zoledronate treatment did not alter expression of MICA, ICAM1 and FasL, indicating involvement of other molecules. The present study was an attempt to investigate the protein profiles of breast tumor cells (MCF7) after Zoledronate treatment to identify molecules that may play key role in conjugate formation with $\gamma\delta$ T cells. Comparative analysis of protein profiles of Zoledronate treated and untreated MCF7 were analyzed using two proteomic approaches- [1] 2D-gel electrophoresis-Matrix assisted laser desorption ionization – time of flight (MALDI-TOF/TOF) and [2] Liquid chromatography- Mass spectrometry.

5.1) Determination of sublethal concentration of Zoledronate for treatment of MCF7 cells

MCF7 cells (at different cell densities- 1×10^3 , 3×10^3 and 5×10^3) were treated with varying concentrations of Zoledronate (50 μ M, 100 μ M, 200 μ M) or left untreated (control) for 16-18 hrs and viability of the cells was determined by MTT assay. Optical density was measured at 540nm with reference wavelength 690nm. The results are represented as percent viability of control [Test viability (%) = (Test O.D / Control O.D.) x 100]. As shown in Figure 23, Zoledronate concentration upto 100 μ M did not affect viability of MCF7 cells, while Zoledronate concentration at 200 μ M reduced the viability by 50%. Thus, for further experiments, 100 μ M Zoledronate concentration was used for treatment of MCF7 cells.

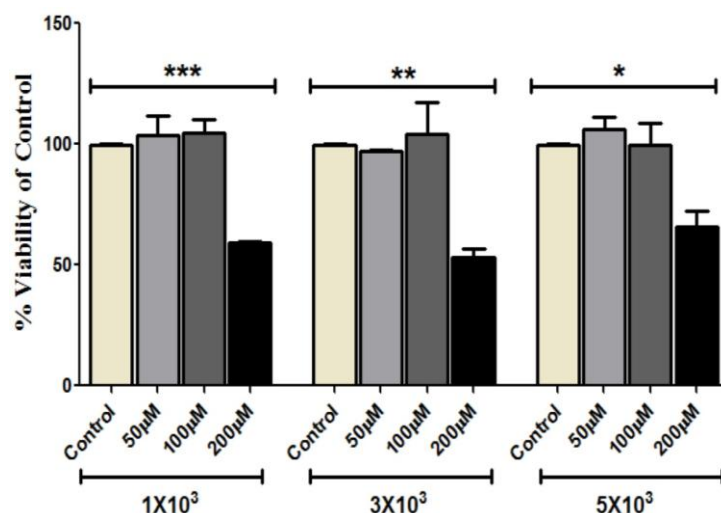


Figure 23: Determination of sublethal concentration of Zoledronate for *in vitro* assays using MTT Assay

Sublethal concentration of Zoledronate for the treatment of tumor cells was assessed by MTT assay. MCF7 cells (at different cell densities- 1×10^3 , 3×10^3 , 5×10^3) were treated with Zoledronate (50 μ M, 100 μ M, 200 μ M) or left untreated (control) for 16-18 hrs and viability of the cell was assessed by measuring optical density at 540nm. The data is represented as percent viability of control cells [viability of the test cells = (OD of treated cells / OD of control) x 100]. Three independent experiments were carried out. Significance obtained is indicated by p value as $p < 0.05$ (*) and $p < 0.005$ (**), $p < 0.0005$ (***).

5.2) Separation of differentially expressed proteins in MCF7 cells upon Zoledronate treatment by 2-dimensional (2D) polyacrylamide gel electrophoresis

In 2D electrophoresis, proteins are separated on the basis of their isoelectric point (IEF) and molecular weight (SDS-PAGE). These resolved proteins are then identified using a mass spectrometer. To analyze the effect of Zoledronate treatment on MCF7 cells, comparative analysis of protein profiles of Zoledronate treated and untreated MCF7 cells was carried out by 2DGE-MS. Involvement of these proteins in various cellular processes and protein-protein interactions was analyzed by PANTHER analysis tool and interactome software STRING respectively.

5.2.1) Generation of protein profiles for Zoledronate treated and untreated MCF7 cells using 2D-PAGE

IEF was standardized for pH 3-10 nonlinear (NL), 17cm immobilized pH gradient (IPG) strip. Figure 24 shows representative silver stained 2D gel pictures of untreated (A) and Zoledronate treated (B) MCF7 cells. Images of silver stained gels were scanned on Bio-Rad GS-800 densitometer (raw images). Comparative analysis of the scanned gel images of untreated and Zoledronate treated MCF7 cells generated by software PDQuest (Version 7.2).

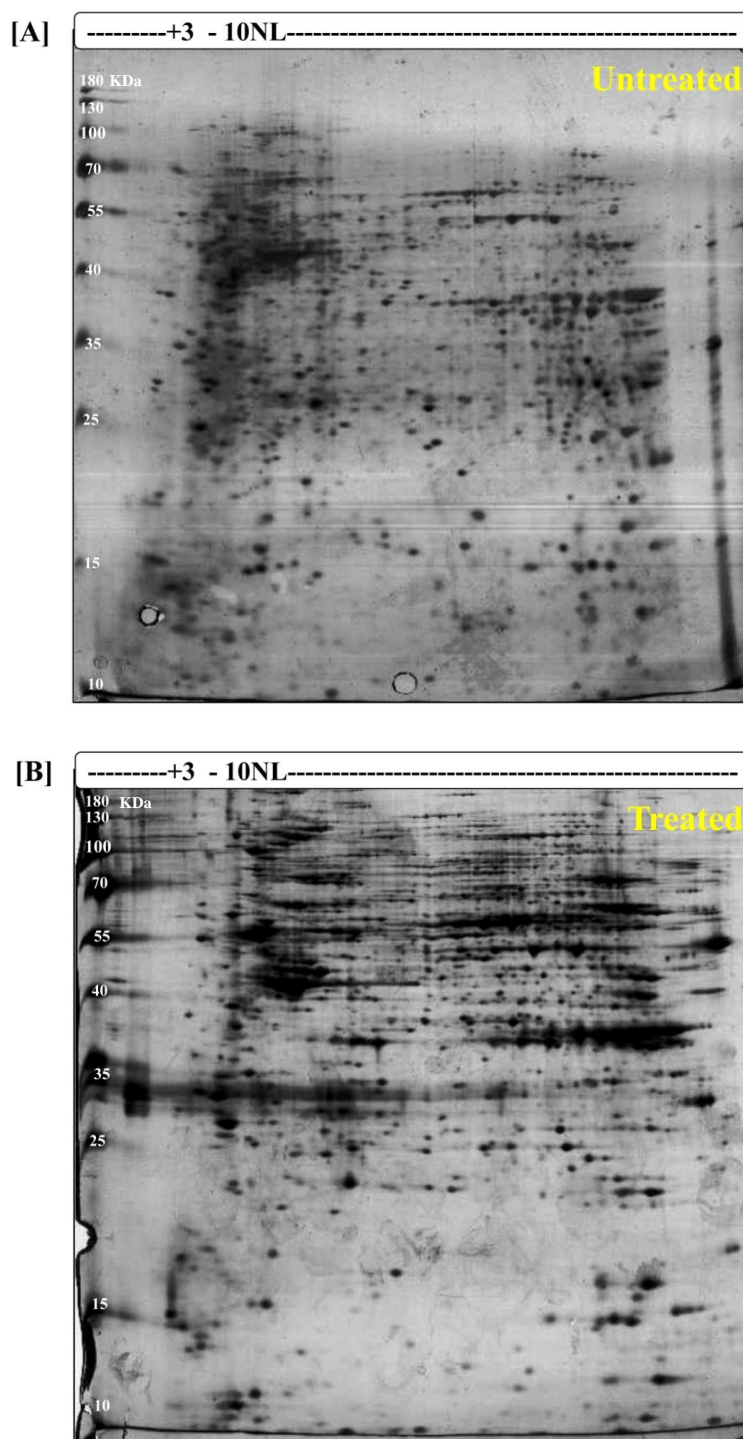


Figure 24: Images of silver stained 2D-Gels generated using pH 3-10NL, 17cm IPG strip

A representative image of silver stained 2-dimensional protein profiles of untreated [A] and Zoledronate treated [B] MCF7 cells, generated using pH 3-10NL, 17 cm IPG strip.

5.2.2) Analysis of differential protein expression in MCF7 cells upon Zoledronate treatment

PDQuest software (BioRad, Version 7.2) was used to analyze qualitative (position on the gel) and quantitative (intensity of the position matched spot) differences in protein profiles of untreated and Zoledronate treated MCF7 cells (Materials and methods 3.12.1.9). Protein profiles of untreated and Zoledronate treated MCF7 were generated and then analyzed by PDQuest software for differential protein expression (Figure 25). Zoledronate treatment of MCF7 cells showed expression of 79 new proteins, while untreated MCF7 cells had 51 unique proteins. Upon Zoledronate treatment, 96 proteins showed 2 fold change in their expression and 75 proteins showed 3 fold change. Gel plugs containing proteins were separated from silver stained 2D gels and proteins were identified using MALDI-TOF/TOF.

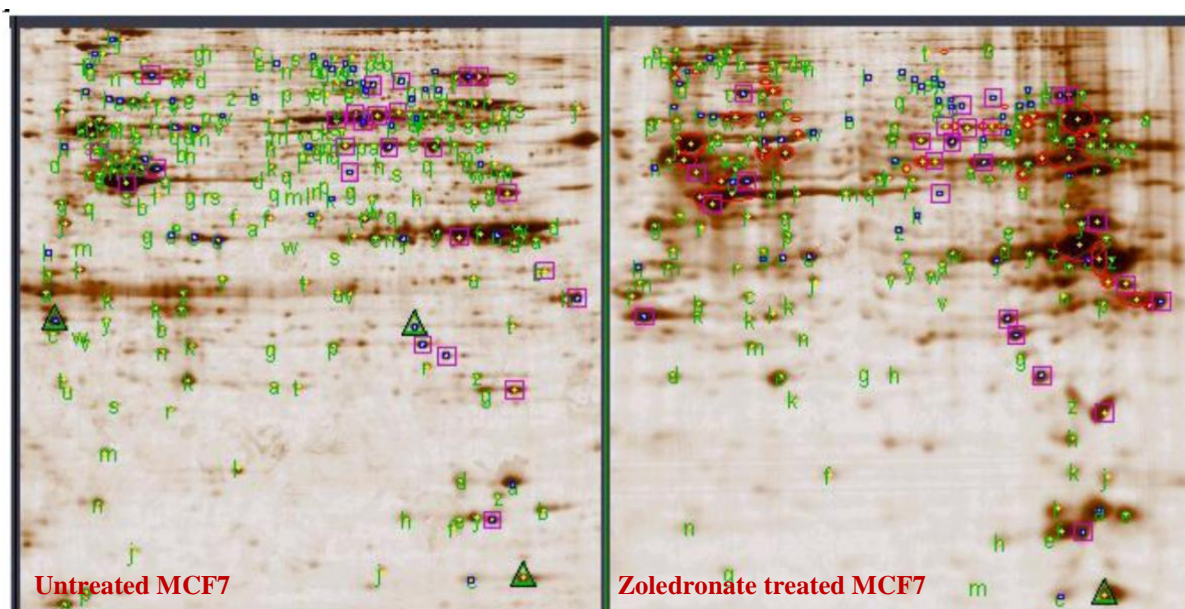


Figure 25: Comparative analysis of 2D profiles of untreated and Zoledronate treated MCF7 cells using PDQuest software

Protein profiles of untreated and Zoledronate treated MCF7 cells were compared using PDQuest software to analyze differential protein expression. Based on densitometry and position of the spot, quantitative and quantitative differences in protein expression of Zoledronate treated and untreated MCF7 cells were detected. Zoledronate treatment showed changes in expression of proteins (blue squares- 2 fold change, red open circles- more than 2 fold change). Yellow filled circles show total number of proteins in a gel, while pink squares show manually added proteins spots during generation of MasterSets.

5.2.3) In-solution digestion of proteins

In-solution digestion of proteins separated from silver stained 2D-gels generated using untreated MCF7 cells was carried out using trypsin (Materials and methods, section 3.12.3.8). Figure 26 shows schematic representation of in solution digestion of proteins. Detailed information of identified proteins is given in Table 7. Figure 27 is a representation of total 34 identified proteins form gel.

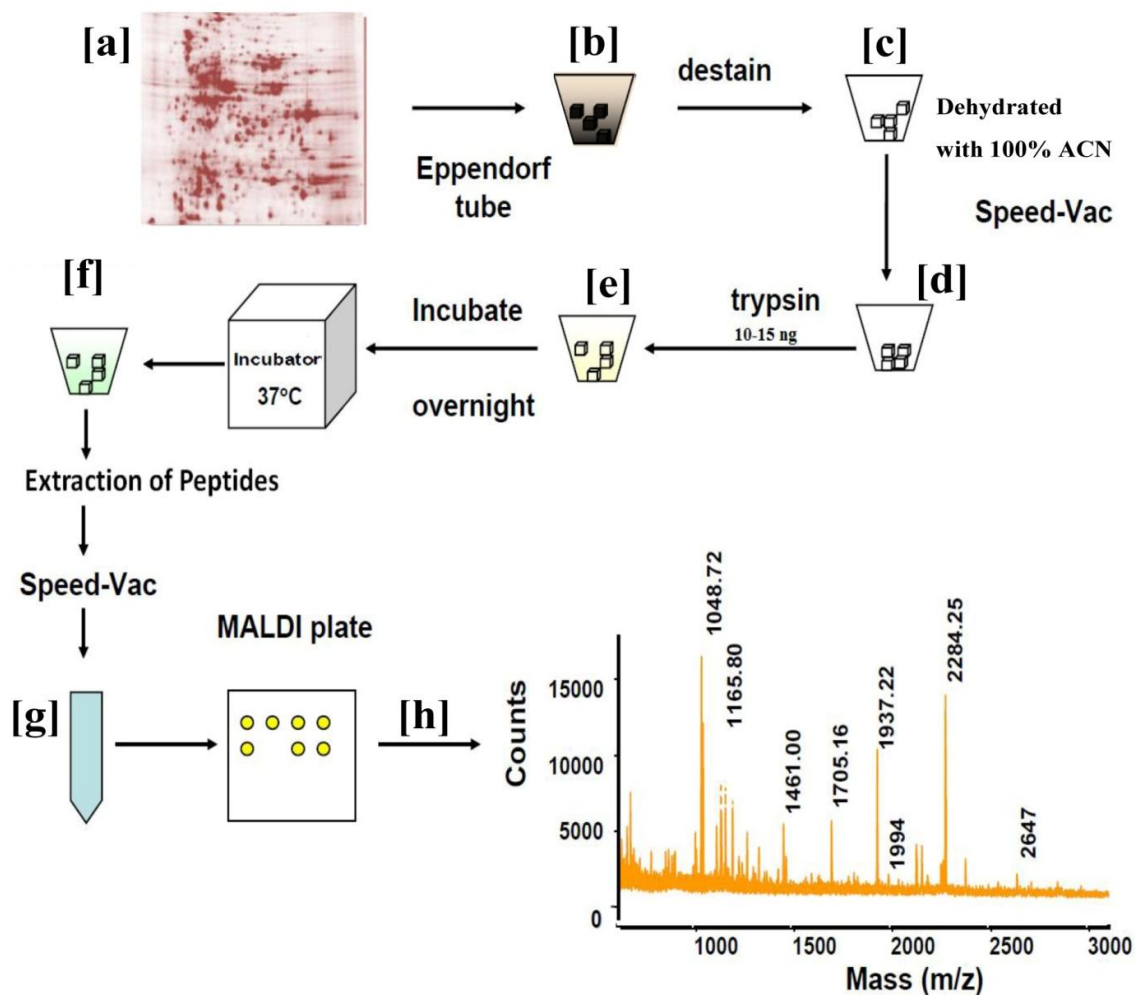


Figure 26: Schematic presentation of *in gel* digestion of proteins

The cartoon explaining the processing of mass spectrometry sample from silver stained 2D-PAGE. [a] Gel plug containing protein was separated from silver stained gel and [b] were repeatedly washed in milliQ. [c] The gel plug was destained using destaining solution (30nM $C_6N_6FeK_3+100mM Na_2S_2O_3$ in 1:1 volume), [d] dehydrated using 100%ACN and [e] incubated with 10ng trypsin overnight. [f] Digested peptides were extracted using extraction buffer (5%TFA+50%ACN) and [g] were dried in speed-vac. Dried peptides were reconstituted in reconstitution buffer (0.1%TFA+50%ACN) and mixed with 2 μ l matrix. [h] Samples were loaded on MALDI plate, allowed to dry and then acquired.

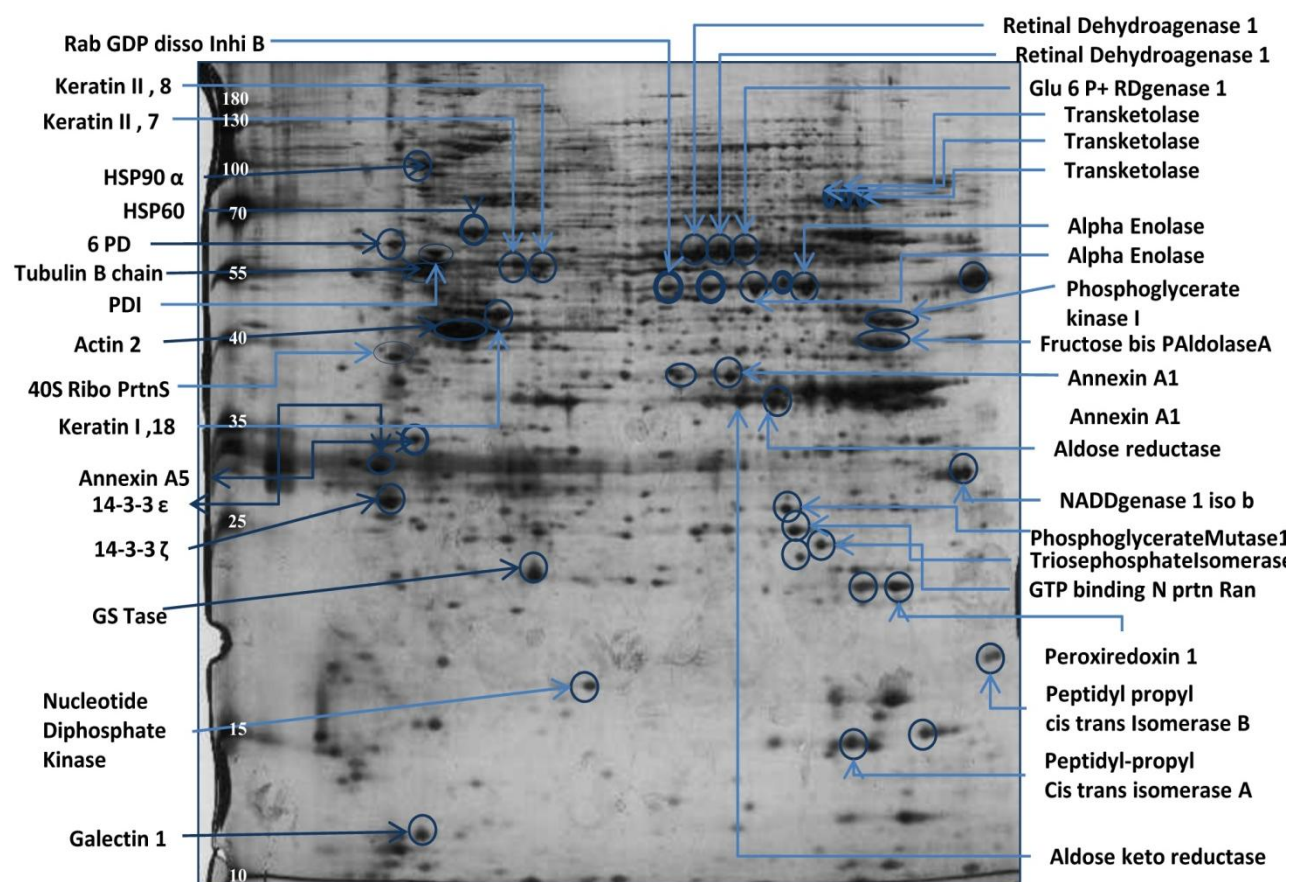


Figure 27: Diagrammatic representation of identified proteins in untreated MCF7 cell lysate using MALDI-TOF/ TOF

Gel plugs containing protein samples were separated from silver stained gels and proteins were digested in-gel using trypsin. Separated proteins were dried, reconstituted and analyzed identified using MALDI-TOF/TOF. Acquired mass spectras were analyzed on Biotools software and proteins were searched against SwissProt database.

Table 7: Identification of *in gel* digested proteins separated from 2D silver stained gel by MALDI-TOF/TOF

S.No	Protein Name	MW	PI	MS Score	MS-MS Score	Cellular function
1	14-3-3 protein ζ/δ	27899	4.7	71	93.9	Adapter protein implicated in regulation of a large spectrum of signaling pathways
2	Glutathione S transferase P	23569	5.4	87	350	Enzymes involved in detoxification
3	Phosphoglycerate Mutase 1	28900	6.6	192	301	Glycolytic enzyme
4	Triosephosphate isomerase	26938	6.4	144	276	Glycolytic enzyme
5	NAD DH Dehydrogenase 1 isoform b	27335	8.7	165	257	Accessory subunit of the mitochondrial membrane respiratory chain NADH dehydrogenase
6	Peroxiredoxin 1	18964	6.4	114	209	Involved in redox regulation of the cell
7	Peptidyl-propyl Cis trans isomerase A	18229	7.6	73	161	Interconverts <i>cis</i> & <i>trans</i> isomers of peptide bonds with amino acid proline
8	Heat shock protein HSP90 a	85006	4.9	165	64.3	Proper proteins folding, stabilizing proteins against heat stress & aids in protein degradation
9	Protein Disulphide isomerase	57480	4.7	89	56.6	Catalyzes the formation & breakage of disulfide bonds between cysteine residues within proteins during folding fold
10	60 KDa HSP, Mitochondrial	61187	5.7	65	55.6	Mitochondrial protein import & macromolecular assembly. Facilitate correct folding of imported proteins. Prevent misfolding & promote refolding & proper assembly of unfolded polypeptides generated under stress conditions in mito. matrix
11	Transketolase	68519	7.5	86	66.4	Connects PPP pathway to glycolysis
12	Retinal Dehydrogenase 1	55454	6.3	78	126	Catalyzes conversion of retinal to retinoic acid
13	Rab GDP dissociation Inhibitor β	51087	6.1	62	51.3	Regulates the GDP/GTP exchange reaction of most Rab proteins by inhibiting the dissociation of GDP from them, and the subsequent binding of GTP to them
14	α Enalase	47481	7.0	154	166	Glycolytic enzyme
15	6 Phosphoglucanal Dehydrogenase	53619	6.8	62	35	Enzyme in PPP pathway
16	Actin, cytoplasmic 2	42052	5.2	109	95.1	Cytoskeletal element

Table 7 (continued...)

S.No	Protein Name	MW	PI	MS Score	MS-MS Score	Cellular function
17	Keratin type 1, cytoskeletal 18	48029	5.3	179	182	Filament reorganization
18	40S Ribosomal Protein SA	32947	4.7	56	57	Required for the assembly and/or stability of the 40S ribosomal subunit, Cell surface receptor for laminin, Cell adhesion to basement membrane & in consequent activation of signaling transduction pathways
19	Tubulin β chain	50095	4.7	178	164	Main constituent of microtubules
20	Aldose reductase	36230	6.5	80	130	Cytosolic NADPH-dependent oxidoreductase, catalyzes reduction of a variety of aldehydes and carbonyls & monosaccharides
21	Annexin A1	38918	6.5	125	81.4	Protect against DNA damage, inhibits NF- κ B signal transduction pathway
22	Aldo keto reductase	36230	6.5	130	139	Detoxification of lipid aldehydes, Nuclear receptor signaling
23	Keratin type II, cytoskeletal 7	24579	7.0	98	158	Structural component of cytoskeleton
24	Keratin type II, cytoskeletal 8	35971	4.9	96	90	Structural component of cytoskeleton
25	Phosphoglycerate kinase I	29326	4.6	84	74.01	Glycolytic enzyme
26	Fructose-Bisphosphate aldolase A	16238	9.6	94	96.3	Enzyme in glycolysis & gluconeogenesis pathway
27	GTP binding nuclear protein Ran	17309	5.8	110	107	Nucleocytoplasmic transport, Chromatin condensation & control of cell cycle
28	Ropporin 1A	15048	5.3	57	57.7	Unknown
29	Annexin A5	35971	4.9	82	69.5	Unknown
30	14-3-3 Protein epsilon	29326	4.6	64	92.2	Adapter protein implicated in regulation of a large spectrum of both general & specialized signaling pathways
31	28 Ribosome protein S18C	16238	9.6	58	61.8	Structural component of ribosome
32	Nucleoside diphosphate kinase A	17308	5.8	75	68	Catalyzes exchange of terminal phosphate between different NDP & NTP in a reversible manner to produce NTPs
33	Peptidyl-propyl cis-trans isomerase B	23784	5.7	91	127	Catalyzes cis-trans isomerization of proline imidic peptide bonds, allowing it to regulate protein folding of type I collagen
34	Galectin 1	15048	5.3	61	93.4	Modulating cell-cell and cell-matrix interactions

5.3) Identification of differentially expressed proteins in MCF7 upon Zoledronate treatment by 2DPAGE/MALDI-TOD TOF

Gel plugs of differentially expressed proteins detected on 2D gel using PDQuest software were excised from the gel, peptides were extracted and proteins were identified using MALDI-TOF/TOF as described earlier. Using MASCOT search engine, MS peaklist and MS/MS ions of the chosen peptides were searched in SwissProt database. The parameters used for search were mass tolerance of 100 ppm for MS and fragment tolerance of 1 Da for MS/MS analysis. Detailed information of identified proteins (name of the identified protein, combined MS and MS-MS score, upregulated/downregulated, molecular weight, isoelectric point, cellular localization and cellular function) are represented in Table 8. Total 12 differentially expressed proteins were identified in Zoledronate treated MCF7 cells, which included cytoskeletal elements, heat shock proteins and cellular enzymes. Among the cytoskeletal elements, expression of keratins was found downregulated while β -tubulin showed increase in its expression. HSP60 and HSP90 expression was also found to be upregulated upon Zoledronate treatment of MCF7 cells. Expression of glycolytic enzymes α -enolase, phosphoglycerate mutase-1, triosephosphate isomerase was found upregulated, while expression of an anti-oxidative enzyme peroxiredoxin-1 was downregulated. Also, expression of 14-3-3 ζ was found to be downregulated in MCF7 cells upon Zoledronate treatment. Comparative analysis of Zoledronate treated and untreated MCF7 cells using 2D-PAGE/ MALDI-TOF approach showed changes in protein profiles upon Zoledronate treatment, which needed to be confirmed by a more robust approach.

Table 8: Differentially expressed proteins in 2D-PAGE identified by MS/MS

S.No	Protein Name	Combined MS-MS Score	Up/Down	MW	PI	Cellular Localization	Cellular Function
1	Keratin 7	98	Down	54	6.5	Cytoplasm	Maintaining cellular structural integrity
2	Keratin 8	96	Down	36	4.9	Cytoplasm	Maintaining cellular structural integrity, signal transduction & cellular diff.
3	Keratin 18	179	Down	48	5.3	Cytoplasm	Maintaining cellular structural integrity
4	Tubulin β Chain	178	Up	45	4.7	Cytoplasm	Structural support, intra-cellular transport, DNA segregation
5	HSP60	65	Up	60	5.7	Mito. Cyto., ER Golgi, PM	Transportation & refolding of proteins from cytoplasm into mitochondrial matrix
6	HSP90 α	165	Up	90	4.9	Cytosolic	Protein folding, protein degradation, anti-apoptotic as stabilizes PI3K/AKT, signaling molecules & growth factors receptors
7	α -Enolase	166	Up	47	7.1	Cytoplasm	Glycolytic enzyme (converts 2-phospho-glycerate to phosphoenolpyruvate)
8	Phosphoglycerate mutase 1	301	UP	28.9	6.6	Cytoplasm	Glycolytic enzyme (conversion of 3-phosphoglycerate to 2-phosphoglycerate)
9	Triosephosphate isomerase	276	Up	26.9	6.4	Cytoplasm	Glycolytic enzyme (interconversion of triosephosphate isomers dihydroxy-acetone phosphate and D- glyceraldehyde 3-phosphate)
10	Peroxiredoxin 1	114	Up	18	6.4	Cytoplasm	Anti-oxidant enzyme, reduction of ROS. Protects the cells from oxidative stress & promotes cell survival
11	14-3-3 ζ	71	Down	27.8	4.7	Ubiquitous	Regulates multiple oncogenes Over expression: anchorage independent growth & anti-apoptosis. Acts as heat shock related molecular chaperon. Co-operates with Her 2 to increase cancer invasion
12	GTP binding nuclear protein Ran	110	Down	17.3	5.8	Nucleus, Cytoplasm, Nuclear envelope	Nucleocytoplasmic transport, RNA export, chromatin condensation, cell cycle

Table 8: 2D profiles of Zoledronate treated and untreated MCF7 were compared using PDQuest software for differential protein expression. These proteins were separated from gels, extracted by *in gel* digestion method and were identified using MS/MS.

5.4) Identification of differentially expressed proteins in Zoledronate treated MCF7 cells by liquid chromatography-mass spectrometry (LC-MS)

Quantitative estimation of differentially expressed proteins in MCF7 cells upon Zoledronate treatment was analyzed labeling of samples using iTRAQ (isobaric tags for relative and absolute quantification) reagents and further separation and detection of peptides by LC-MS. Details of iTRAQ/LC-MS are provided in detail in Materials and methods section 3.12.2. Digested proteins (peptides) from untreated and Zoledronate treated MCF7 cells were labeled with different isotopes, mixed together and analyzed on LC/MS. Differentially expressed proteins are identified based on relative changes in test sample compared to control sample. Proteins in Zoledronate treated MCF7 cells were analyzed for relative changes in expression to untreated MCF7 cells. Proteins showing ≥ 1.5 fold increase in their expression upon Zoledronate treatment were considered as “upregulated proteins”, while proteins with ≤ 0.5 fold decrease in their expression upon Zoledronate treatment were considered as “downregulated proteins”. Total 31 proteins were found to be significantly upregulated (Table 9), while 64 proteins showed significant downregulation (Table 10) in MCF7 cells. The data was analyzed using PANTHER analysis tool, where upregulated and downregulated proteins were classified on the basis of molecular function, their involvement in biological processes and protein class. Figure 28 and Figure 29 shows detailed PANTHER analysis of upregulated and downregulated proteins respectively.

Among both upregulated and downregulated proteins, most of the proteins were associated with metabolic (39.6% and 35.3% respectively) and cellular processes (28.6% and 20.6% respectively), as classified by PANTHER. Classification of upregulated and downregulated proteins on the basis of their biological processes showed changes in proteins with binding activity (41.3% upregulated and 36.4% downregulated) and with catalytic activity (36.5% upregulated and 27.3% downregulated). Zoledronate treatment upregulated expression of

signaling molecules (8.1 %), while expression of cytoskeletal elements (10.5%), ligases (10.5%), membrane trafficking proteins (10.5%) and nucleic acid binding proteins (26.3%) were found to be downregulated.

Table 9: List of upregulated proteins in MCF7 upon Zoledronate treatment

S.No	Protein ID	Gene ID	Name	Pep (95%)	114:117 (T:C)	Cellular Function
1	Q5H909	Q5H909	Melanoma- associated antigen D2	1	3.1	Tumor antigen
2	P62745	RHOB	Rho-related GTP-binding protein RhoB	5	2.8	Mediates apoptosis
3	Q58FF4	Q58FF4	HSP90Bf	4	2.8	Member of HSP90
4	P05109	S10A8	Protein S100-A8	2	2.6	Acts as DAMPs, chemotaxis of innate immune cells, induction of apoptosis & autophagy
5	G8JLD5	G8JLD5	Dynamin-1-like protein	11	2.1	Producing microtubule bundles, vesicular trafficking , Receptor-mediated endocytosis
6	Q59H39	Q59H39	STAT 5B variant (frag)	1	2.1	TCR signaling, apoptosis,
7	P08582	TRFM	Melanotransferrin	1	2.0	Iron uptake, melanoma tumor antigen p97
8	Q59G80	Q59G80	Diphosphomevalonate decarboxylase variant (Frag.)	1	2.0	Involved in the pathway cholesterol biosynthesis, which is part of Steroid biosynthesis. ATP + (R)-5-diphosphomevalonate = ADP + phosphate + isopentenyl diphosphate + CO ₂
9	O60220	TIM8A	Mito. Inner membrane translocase subunit Tim8 A	1	1.9	Insertion of multi-pass transmembrane proteins into the mitochondrial inner membrane
10	P35754	GLRX1	Glutaredoxin-1	4	1.9	GNT-binding proteins, downstream of G protein-coupled receptors
11	Q9Y3A3	PHOCN	Phocin	1	1.9	Membrane trafficking,
12	K7EPV0	K7EPV0	Cytochrome c oxidase assembly protein 3	1	1.9	Essential for cytochrome c oxidase function
13	J3KQ73	J3KQ73	Peptidyl-prolyl cis-trans isomerase FKBP8	3	1.8	Chaperone for BCL2, phosphorylates it & interfering with binding of BCL2 to its targets
14	Q6IB91	Q6IB91	PCK2 protein	5	1.8	Rate-limiting step: Producing glucose from lactate & other precursors from TCA cycle
15	E9PMQ6	E9PMQ6	HSF1	1	1.8	Transcribe HSP genes
16	Q03167	TGBR3	Transforming growth factor beta receptor type 3	0	1.8	Capturing and retaining TGF-beta for presentation to the signaling receptors
17	K7ELW3	K7ELW3	EGFR substrate 8-like protein 1	0	1.7	Membrane ruffling & remodeling of actin cytoskeleton
18	Q53FV3	Q53FV3	COP9 signalosome subunit 4	2	1.7	Promoting & protection of p53/TP53, c-Jun/JUN from degradation by phosphorylation
19	Q0VAM0	Q0VAM0	Catenin, beta like 1	1	1.7	Component of PRP19-CDC5L complex (spliceosome). May induce apoptosis.
20	L0R849	L0R849	Enolase	47	1.6	Glycolytic enzyme, growth control, hypoxia tolerance & allergic responses, receptor & activator of plasminogen on cell surface of cells. May be a tumor suppressor

Table 9 (continued...)

S.No	Protein ID	Gene ID	Name	Pep (95%)	114:117 (T:C)	Cellular Function
21	Q7Z426	Q7Z426	Putative MAPK activating protein	4	1.6	Proliferation, gene expression, differentiation, mitosis, cell survival, and apoptosis
22	Q6NTG0	Q6NTG0	SLC9A3R2 protein (Frag.)	7	1.6	Scaffolding proteins. Binding to & regulating membrane expression & protein-protein interaction of membrane receptors & transport proteins
23	Q9Y320	TMX2	Thioredoxin-related transmembrane protein 2	4	1.6	Cell proliferation-inducing gene 26 protein, stress sensors
24	Q7Z6K5	CO038	UPF0552 protein C15orf38	2	1.6	Inhibitor of actin polymerization
25	Q59GU6	Q59GU6	Sorting nexin 1 isoform a variant (Frag.)	2	1.6	Targeting ligand-activated EGFR to the lysosomes for degradation after endocytosis from cell surface & release from Golgi
26	P61586	RHOA	Transforming protein RhoA	19	1.6	Regulates a signal transduction pathway linking plasma membrane receptors to assembly of focal adhesions and actin stress fibers
27	Q9Y5K6	CD2AP	CD2-associated protein	1	1.5	Receptor clustering & cytoskeletal polarity in the junction between T-cell & APCs
28	Q9NYJ1	COA4	Cytochrome c oxidase assembly factor 4	1	1.5	Putative COX assembly factor
29	P17858	K6PL	6-phosphofructokinase, liver type	4	1.5	Catalyzes phosphorylation of D-fructose 6-phosphate to fructose 1,6-bisphosphate by ATP (committing step of glycolysis)
30	P10909	CLUS	Clusterin	3	1.5	Facilitates folding of secreted proteins in ATP-independent way. Lipid transport, membrane recycling, cell adhesion, programmed cell death & complement-mediated cell lysis
31	O60888	CUTA	Protein CutA	1	1.5	Copper binding protein

Table 9: Protein profiles of Zoledronate treated and untreated MCF7 were analyzed on LC-MS followed by iTRAQ labeling. Proteins showing ≥ 1.5 fold increase upon Zoledronate treatment were considered as upregulated proteins.

Table 10: List of downregulated proteins in MCF7 upon Zoledronate treatment

S. No	Protein ID	Gene ID	Name	Pep (95%)	114:117 (T:C)	Cellular Function
1	B2RA72	B2RA72	cDNA, FLJ94734, CHMP1.5 protein	1	0.2	Vacuolar transport
2	P62312	LSM6	U6 snRNA-associated Sm-like protein LSm6	2	0.2	RNA processing
3	P17900	SAP3	Ganglioside GM2 activator	1	0.2	Phospholipids & FA metabolism
4	A8K180	A8K180	cDNA FLJ76749, highly similar to Homo sapiens Wiskott-Aldrich syndrome-like (WASL), mRNA	2	0.3	Actin filament reorganization
5	P40855	PEX19	Peroxisomal biogenesis factor 19	2	0.3	Early peroxisomal biogenesis
6	R4GMT0	R4GMT0	Alpha-centractin	2	0.3	Microtubule based vesicle motility
7	Q59G16	Q59G16	SWI/SNF-related matrix-associated actin-dependent regulator of chromatin c2 isoform b variant (Frag.)	1	0.3	Chromatin remodeling
8	E5RFF9	E5RFF9	DNA replication complex GINS protein SLD5	1	0.4	Essential role in the initiation of DNA replication
9	Q9H7H1	RUIT1	Putative uncharacterized protein encoded by RUNX1-IT1	1	0.4	Chromatin remodeling
10	Q9NTM9	CUTC	Copper homeostasis protein cutC homolog	1	0.4	Copper export
11	B3KPR5	B3KPR5	cDNA FLJ32094 fis, clone	0	0.4	Translation elongation factor activity
12	Q7Z727	Q7Z727	PRKCA protein (Frag.)	1	0.4	Phosphorylates variety of proteins in diverse cellular signaling pathways
13	O95864	FADS2	Fatty acid desaturase 2	1	0.4	Fatty acid metabolism
14	Q8N1X3	Q8N1X3	cDNA FLJ37317 fis, clone BRAMY2017455, highly similar to Homo sapiens ATP-binding cassette protein M-ABC1 mRNA	1	0.4	Transport various substrates across cellular membranes
15	Q8NDH3	PEPL1	Probable aminopeptidase NPEPL1	2	0.4	Removal of unsubstituted N-terminal amino acids from various peptides
16	E9PQN3	E9PQN3	Lysosomal Pro-X carboxypeptidase (Frag.)	1	0.4	Serine-type peptidase activity
17	B0UX83	B0UX83	HLA-B associated transcript 3, isoform CRA a	4	0.4	Not known
18	Q8NBL9	Q8NBL9	cDNA PSEC0119 fis, clone PLACE1002376, highly similar to GPI transamidase component PIG-S	1	0.4	Attachment of GPI anchor to protein

Table 10 (continued...)

S. No	Protein ID	Gene ID	Name	Pep (95%)	114:117 (T:C)	Cellular Function
19	F8VZN8	F8VZN8	Protein phosphatase 1 regulatory subunit 12A (Frag.)	2	0.4	phosphatase regulator activity and signal transduction
20	F8W1Z8	F8W1Z8	ADP-ribosylation factor-like protein 1	1	0.4	phosphatase regulator activity and
21	K7ERU7	K7ERU7	Uncharacterized protein C19orf43	1	0.4	Not known
22	Q53GF4	Q53GF4	Syntaxin binding protein 2 variant (Frag.)	2	0.4	Intracellular vesicle trafficking and vesicle fusion with membranes
23	Q96FJ2	DYL2	Dynein light chain 2, cytoplasmic	2	0.5	Non-catalytic accessory components of cytoplasmic dynein 1 complex
24	Q9NX47	MARH5	E3 ubiquitin-protein ligase MARCH5	2	0.5	Control of mitochondrial morphology by acting as a positive regulator of mitochondrial fission
25	B4DZF1	B4DZF1	cDNA FLJ56541, highly similar to Ubiquilin-2	8	0.5	Increases half-life of proteins destined to be degraded by proteasomes, Modulates proteasome-mediated protein degradation
26	H7BXQ8	H7BXQ8	Armadillo repeat-containing protein 10	1	0.5	Cell survival and cell growth, Suppress the transcriptional activity of p53/TP53
27	Q8N8I9	Q8N8I9	cDNA FLJ39408 fis, clone PLACE6013672	1	0.5	Phosphotransferase activity
28	Q8TBX8	PI42C	Phosphatidylinositol 5-phosphate 4-kinase type-2 gamma	2	0.5	production of Phosphatidylinositol bisphosphate (PIP2), in the endoplasmic reticulum
29	P62249	RS16	40S ribosomal protein S16	2	0.5	RNA binding protein
30	Q32Q10	Q32Q10	RSU1 protein (Frag.)	3	0.5	Ras suppressor protein
31	J3KN55	J3KN55	Cob(Dyrinic acid a,c-diamide adenosyl-transferase, mitochondrial	1	0.5	Cobalamin biosynthetic process
32	Q6NZX3	Q6NZX3	5'-nucleotidase,ecto (CD73)	9	0.5	Hydrolase activity
33	Q5RLJ0	Q5RLJ0	CLE	1	0.5	Not known
34	P11441	UBL4A	Ubiquitin-like protein 4A	1	0.5	Post-translational delivery of tail-anchored (TA) membrane proteins to ER mem
35	Q96I60	Q96I60	6-phosphofructokinase	9	0.5	Glycolytic Enzyme
36	F5H4Q5	F5H4Q5	Vacuolar protein sorting-associated protein 37C Frag	1	0.5	Vacuolar protein sorting
37	H0YFI1	H0YFI1	Regulator complex protein LAMT	1	0.5	Interacts with the Rag GTPases, recruits them to lysosomes & is essential for mTORC1 activation
38	B0ZTD4	B0ZTD4	Forkhead box A2	0	0.5	DNA-binding proteins, interacts with chromatin
39	Q10567	AP1B1	AP-1 complex subunit β -1	1	0.5	Protein sorting in the late-Golgi/trans-Golgi network

Table10 (continued...)

S. No	Protein ID	Gene ID	Name	Pep (95%)	114:117 (T:C)	Cellular Function
40	B3KNU0	B3KNU0	cDNA FLJ30470 fis, clone BRAWH1000040, highly similar to Rap1 GTPase-GDP dissociation stimulator 1	1	0.5	Stimulates GDP/GTP exchange reaction of a group of G proteins (Rap1a/Rap1b, RhoA, RhoB and kRas)
41	Q96CT7	CC124	Coiled-coil domain-containing protein 124	2	0.5	Essential for proper progression of late cytokinetic stages
42	D6W4Z6	D6W4Z6	HCG23833, isoform CRAb	2	0.5	Oxidoreductase activity
42	B4E245	B4E245	cDNA FLJ61538, highly similar to Switch-associated protein 70	3	0.5	Mediates signaling of membrane ruffling, Regulates the actin cytoskeleton
43	Q5H9T5	Q5H9T5	Putative uncharacterized protein DKFZp686A2068	2	0.5	Signal transduction
44	F8W022	F8W022	CD63 antigen (Frag.)	1	0.5	Promotes cell survival, reorganization of actin cytoskeleton, cell adhesion, spreading and migration, role in intracellular vesicular transport processes, VEGFA signaling via its role in regulating the internalization of KDR/VEGFR2
45	J3KNJ2	J3KNJ2	Eukaryotic translation initiation factor 3 subunit M (Frag)	1	0.5	Component of eukaryotic translation initiation factor 3 (eIF-3) complex, which is required for several steps in the initiation of protein synthesis
46	Q9H3H3	CK068	UPF0696 protein C11orf68	2	0.5	Poly(A) RNA binding protein
47	J3QRJ1	J3QRJ1	Secernin-2	1	0.5	Have dipeptidase activity, Function in exocytosis
48	H7BZ18	H7BZ18	Multiple coagulation factor deficiency protein 2 (Frag.)	1	0.5	The MCFD2-LMAN1 complex forms a specific cargo receptor for ER-to-Golgi transport of selected proteins
49	Q5H9M0	MUML1	PWWP domain-containing protein MUM1L1	1	0.5	Mutated melanoma-associated antigen 1-like protein 1
50	B4DDM6	B4DDM6	Mitotic checkpoint protein BUB3	1	0.5	BUB1/BUB3 complex plays role in inhibition of APC/C
51	Q9UQ98	Q9UQ98	Multidrug resistance protein (Frag.)	1	0.5	Extrusion of drugs from cell
52	Q5T0G8	Q5T0G8	Annexin	14	0.5	Vesicular transport, Membrane scaffolding, apoptosis
53	Q96T76	MMS19	MMS19 nucleotide excision repair protein homolog	2	0.5	Key component of cytosolic Fe-S protein assembly complex, involved in DNA meta. & genomic integrity
54	L0R6Q1	L0R6Q1	Alternative protein SLC35A4	1	0.5	Probable UDP-sugar transporter protein SLC35A4
55	H7C426	H7C426	E3 ubiquitin-protein ligase RNF181 (Frag.)	1	0.5	Protein ubiquitination

Table 10 (continued...)

S. No	Protein ID	Gene ID	Name	Pep (95%)	114:117 (T:C)	Cellular Function
56	Q13619	CUL4A	Cullin-4A	0	0.5	Protein ubiquitination
57	P52701	MSH6	DNA mismatch repair protein Msh6	1	0.5	Post-replicative DNA mismatch repair system
58	Q05BU7	Q05BU7	WASF2 protein (Frag.)	2	0.5	Regulates actin filament reorganization via its interaction with Arp2/3 complex
59	F8W6G1	F8W6G1	Nuclear receptor-binding protein	1	0.5	Subcellular trafficking between ER & Golgi apparatus through interactions with Rho-type GTPases
60	Q6IAH1	Q6IAH1	DnaJ (Hsp40) homolog, subfamily C, member 12, isoform CRA_a	1	0.5	DnaJ (HSP40) homolog
61	C9JKQ2	C9JKQ2	NADH dehydrogenase [ubiquinone] 1 beta subcomplex subunit 3 Frag	1	0.5	Accessory subunit of mitochondrial membrane respiratory chain NADH dehydrogenase

Table 10: Protein profiles of Zoledronate treated and untreated MCF7 were analyzed on LC-MS followed by iTRAQ labeling. Proteins showing ≤ 0.5 fold increase upon Zoledronate treatment were considered as downregulated proteins.

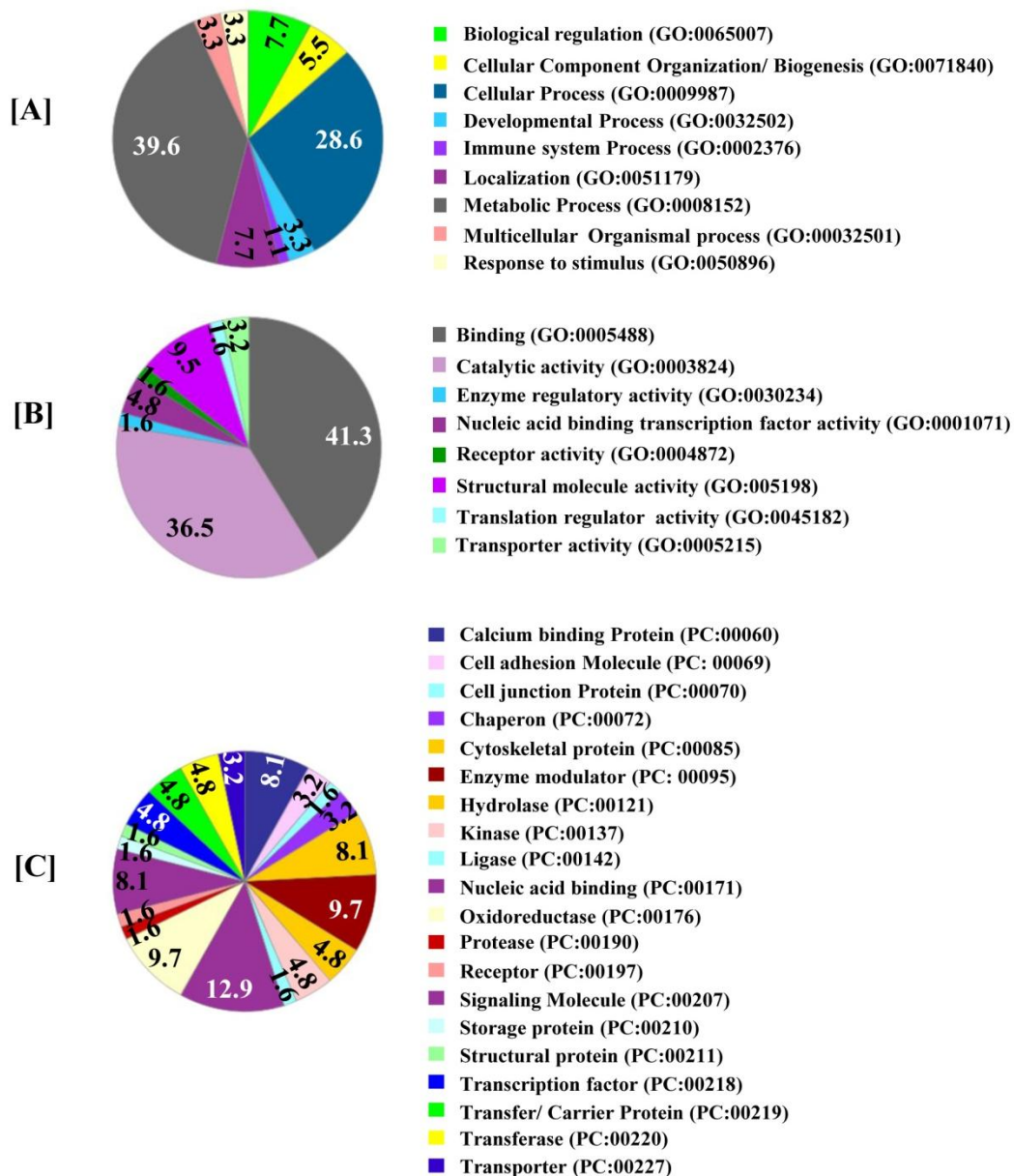


Figure 28: Classification of upregulated proteins by gene ontology based on their biological processes, molecular function and protein class in MCF7 cells upon Zoledronate treatment

A) Distribution of proteins based on their molecular function using PANTHER analysis tool

B) Distribution of proteins based on their biological processes using PANTHER analysis tool

C) Distribution of proteins based on their protein class using PANTHER analysis tool

(Note: Only genes with well defined gene ontologies (GO) has been considered for analysis)

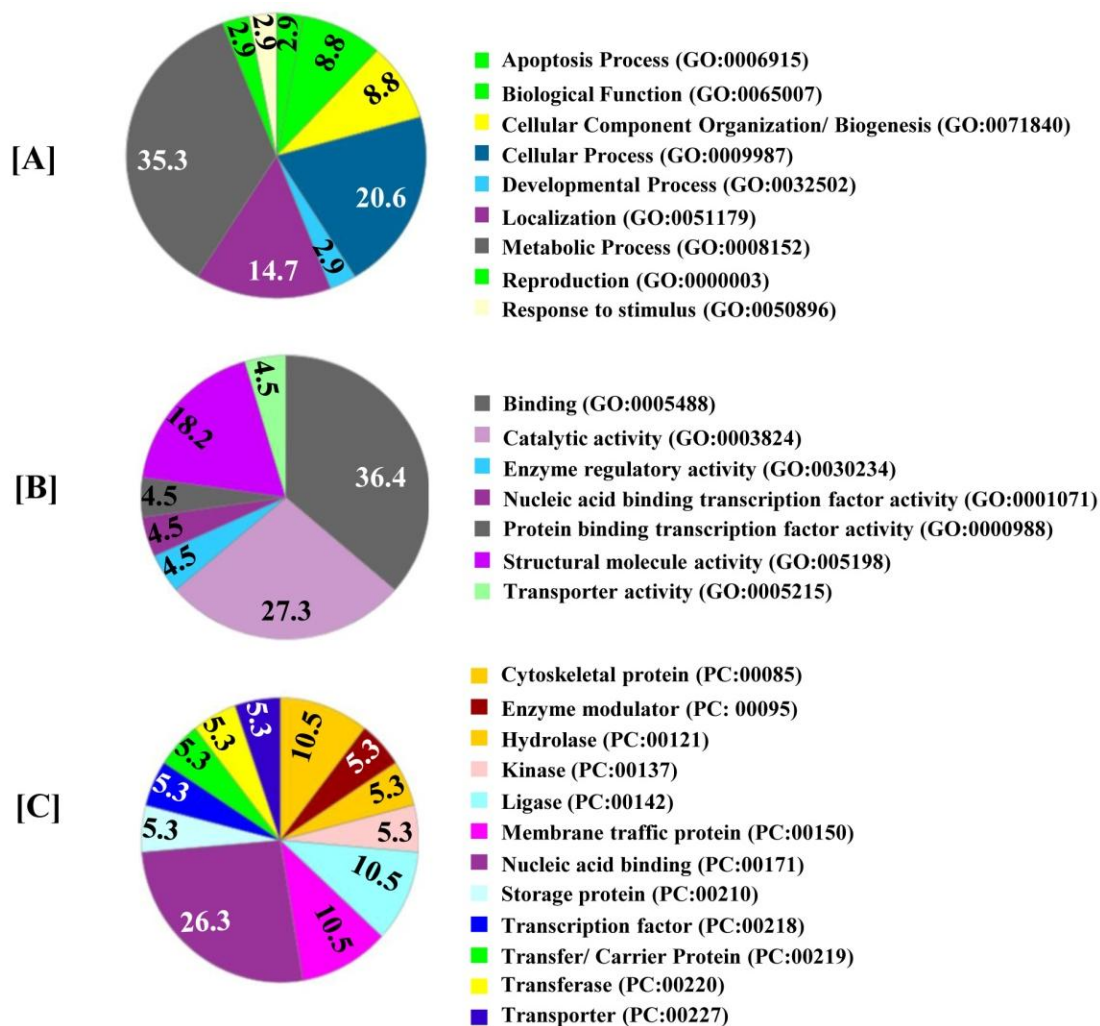


Figure 29: Classification of downregulated proteins by gene ontology based on their biological processes, molecular function and protein class in MCF7 cells upon Zoledronate treatment

A) Distribution of proteins based on their molecular function using PANTHER analysis tool

B) Distribution of proteins based on their biological processes using PANTHER analysis tool

C) Distribution of proteins based on their protein class using PANTHER analysis tool

(Note: Only genes with well defined gene ontologies (GO) has been considered for analysis)

5.4.2) Proteins associated with recruitment, activation and interaction with immune cell

Earlier studies from our laboratory have shown that, aminobisphosphonate (Pamidronate and Zoledronate) treated tumor cells (MCF7) did not show any changes in expression of molecules like MICA, FasL, ICAM-I, which are involved in conjugate formation, suggesting role of other molecules. Therefore, protein profiles of untreated and Zoledronate treated MCF7 were analyzed by proteomics approach. Comparative analysis of protein profiles of Zoledronate treated and untreated MCF7 cells showed increase in expression of proteins involved in recruitment and activation of $\gamma\delta$ T cells along with increase in proteins involved in immune synapse formation between T cells and target cells (Table 11). We observed, a significant increase in IPP synthesizing enzyme “diphosphomevalonate decarboxylase” and calcium binding family protein S100A8, in Zoledronate treated MCF7 cells. Increase in expression of heat shock factor 1 (HSF1) and HSP90bf was also noted in Zoledronate treated MCF7 cells. Our lab has earlier reported that, HSPs are potent activators of $\gamma\delta$ T cells and can specifically expands $\gamma\delta$ T cells from PBMCs [71]. Zoledronate treated MCF7 cells showed increased expression of α -enolase, which acts as a receptor and activator of plasminogen on the cell surface leukocytes [260]. Expression of melanoma associated antigen D2 (acts as tumor associated antigen [261]) were also found upregulated in Zoledronate treated MCF7 cells. Zoledronate treated MCF7 cells also showed a significant increase in melanoma-associated antigen D2. Zoledronate treated MCF7 cells also showed a significant increase in molecules involved in synapse formation between T cells and target cells which included dynamin-1-like protein, CD2-associated protein, transforming protein RhoA, phocein, SLC9A3R2 protein, clusterins and laminin. Role of dynamin-1-like protein has been proposed to regulate synaptic vesicle membrane dynamics,

while CD2-associated proteins are implicated in dynamic actin remodeling and membrane trafficking that occurs during receptor endocytosis and cytokinesis.

Table 11: List of differentially expressed proteins in MCF7 involved in immune cell activation

S. No	Protein ID	Gene ID	Name	Pep (95%)	114:117 (T:C)	Cellular Function
1	Q59G80	Q59G80	Diphosphomevalonate decarboxylase Variant (Frag.)	1	2.0	Involved in the pathway cholesterol biosynthesis, which is part of Steroid biosynthesis. ATP + (R)-5-diphosphomevalonate = ADP + phosphate + isopentenyl diphosphate + CO ₂
2	P05109	S10A8	Protein S100-A8	2	2.6	Acts as DAMPs, chemotaxis of innate immune cells, induction of apoptosis & autophagy
3	E9PMQ6	E9PMQ6	Heat shock factor protein 1	1	1.8	Transcription of HSP genes
4	L0R849	L0R849	Enolase	47	1.6	Serves as a receptor & activator of plasminogen on cell surface of cells such as leukocytes.
5	Q5H909	Q5H909	Melanoma-associated antigen D2	1	3.1	Tumor antigen
6	G8JLD5	G8JLD5	Dynamin-1-like protein	11	2.1	Producing microtubule bundles, Vesicular trafficking , Receptor-mediated endocytosis
7	Q9Y5K6	CD2AP	CD2-associated protein	1	1.5	Receptor clustering & cytoskeletal polarity in junction between T-cell & APCs
8	P61586	RHOA	Transforming protein RhoA	19	1.6	Regulates a signal transduction pathway linking plasma membrane receptors to assembly of focal adhesions and actin stress fibers
9	Q9Y3A3	PHOCN	Phocin	1	1.9	Membrane trafficking, specifically in membrane budding reactions
10	K7ELW3	K7ELW3	EGFR substrate 8-like protein 1	0	1.7	Membrane ruffling & remodeling of actin cytoskeleton
11	Q6NTG0	Q6NTG0	SLC9A3R2 protein (Frag.)	7	1.6	Scaffolding proteins. Binding to & regulating membrane expression & protein-protein interaction of membrane receptors & transport proteins
12	P10909	CLUS	Clusterin	3	1.5	Facilitates folding of secreted proteins in ATP-independent way. Lipid transport, membrane recycling, cell adhesion, programmed cell death & complement-mediated cell lysis

Table 11: Comparative analysis of iTRAQ labeled proteins of untreated and Zoledronate treated MCF7 cells was carried out using LC-MS. Proteins showing ≥ 1.5 fold increased expression upon Zoledronate treatment were considered as upregulated proteins, while proteins with ≤ 0.5 fold decrease in their expression upon Zoledronate treatment were considered as downregulated proteins.

5.4.3) Protein associated with cell metabolism and apoptosis

Zoledronate affected the cell metabolism through multiple cellular processes, mostly by perturbing essential cellular processes or by upregulating expression of apoptosis inducers or tumor suppressors (Table 12). Zoledronate treated MCF7 cells showed significant downregulation in proteins involved in vacuolar transport or vesicle trafficking. Expression of protein involved in sorting and transport of proteins from endoplasmic reticulum to Golgi or early/late Golgi compartments were found downregulated (Table 12A) in Zoledronate treated MCF7 cells. As shown in Table 12B, proteins involved in fatty acid metabolism such as gangliosides GM2 activator and fatty acid desaturase 2 were found downregulated upon Zoledronate treatment in MCF7. Zoledronate treatment showed a significant reduction in expression of PEX19 proteins, which is essential in early peroxisomal biogenesis pathway. Pex19 binds to hydrophobic residues of newly synthesized peroxisomal membrane proteins in cytoplasm, stabilizes them and targets them to peroxisomal membranes. Zoledronate treatment of MCF7 was also found to affect copper homeostasis by changing expression of copper transport protein. Expression of CutA (binds to copper and retains it inside the cell) was upregulated, whereas and expression of CutC (plays key role in export of excessive copper outside the cell) was downregulated. A significant upregulation in FKBP8 protein, which belongs to peptidyl-prolyl cis-trans isomerase enzyme, was observed in Zoledronate treated MCF7 cells. This protein acts as a chaperone, which phosphorylates BCL2 & interferes binding of BCL2 to its targets. Significant increase in expression of cytochrome C assembly factor 3 and 4, which are essential for cytochrome c oxidase function was found in Zoledronate treated MCF7 cells. Zoledronate treated MCF7 cells also induced expression of apoptosis inducers as mentioned in Table 12C. It

clearly indicates that, Zoledronate puts the breast tumor cells in metabolic crisis and induces apoptosis.

Table 12: List of differentially expressed proteins in MCF7 involved in important cellular processes

A) Protein Synthesis, Trafficking and degradation						
S.No	Protein ID	Gene ID	Name	Pep (95%)	114:117 (T:C)	Cellular Function
1	B2RA72	B2RA72	cDNA, FLJ94734, CHMP1.5	1	0.2	Vacuolar transport
2	Q8N1X3	Q8N1X3	cDNA FLJ37317 fis, clone BRAMY2017455, highly similar to Homo sapiens ATP-binding cassette protein M-ABC1 mRNA	1	0.4	Transport various substrates across cellular membranes
3	Q53GF4	Q53GF4	Syntaxin binding protein 2 variant (Frag.)	2	0.4	Intracellular vesicle trafficking and vesicle fusion with membranes
4	Q96FJ2	DYL2	Dynein light chain 2, cytoplasmic	2	0.5	Non-catalytic accessory components of cytoplasmic dynein 1 complex
5	F5H4Q5	F5H4Q5	Vacuolar protein sorting-associated protein 37C Fra	1	0.5	Vacuolar protein sorting
6	Q10567	AP1B1	AP-1 complex subunit β 1	1	0.5	Protein sorting in the late-Golgi/trans-Golgi network
7	Q5T0G8	Q5T0G8	Annexin	14	0.5	Vesicular transport, Membrane scaffolding, apoptosis
8	H7C426	H7C426	E3 ubiquitin-protein ligase RNF181 (Frag.)	1	0.5	Protein ubiquitination
9	J3KNJ2	J3KNJ2	Eukaryotic translation initiation factor 3 subunit M (Frag)	1	0.5	Component of eukaryotic translation initiation factor 3 (eIF-3) complex, which is required for several steps in the initiation of protein synthesis
10	H7BZ18	H7BZ18	Multiple coagulation factor deficiency protein 2 (Frag.)	1	0.5	The MCFD2-LMAN1 complex forms a specific cargo receptor for ER-to-Golgi transport of selected proteins
11	F8W6G1	F8W6G1	Nuclear receptor-binding protein	1	0.5	Subcellular trafficking between ER & Golgi apparatus through interactions with Rho-type GTPases
12	Q59GU6	Q59GU6	Sorting nexin 1 isoform a variant (Frag.)	2	1.6	Targets ligand-activated EGFR to lysosome for degradation after endocytosis from cell surface & release from golgi

Table 12 (continued...)

B) Important cellular processes						
S.No	Protein ID	Gene ID	Name	Pep (95%)	114:117 (T:C)	Cellular Function
1	P17900	SAP3	Ganglioside GM2 activator	1	0.2	Phospholipids & FA metabolism
2	P40855	PEX19	Peroxisomal biogenesis factor 19	2	0.3	Early peroxisomal biogenesis
3	O95864	FADS2	Fatty acid desaturase 2	1	0.4	Fatty acid metabolism
4	Q32Q10	Q32Q10	RSU1 protein (Frag.)	3	0.5	Ras suppressor protein
5	F8W022	F8W022	CD63 antigen (Frag.)	1	0.5	Promotes cell survival, migration, intracellular vesicular transport processes
6	Q9NTM9	CUTC	Copper homeostasis protein cutC homolog	1	0.4	Copper export
7	Q7Z727	Q7Z727	PRKCA protein (Frag.)	1	0.4	Phosphorylates proteins in diverse signaling pathways
8	Q9UQ98	Q9UQ98	Multidrug resistance protein (Frag.)	1	0.5	Extrusion of drugs from cell
9	C9JKQ2	C9JKQ2	NADH dehydrogenase [ubiquinone] 1 β subcomplex subunit 3 Frag	1	0.5	Accessory subunit of mito. membrane respiratory chain NADH dehydrogenase
10	H7BXQ8	H7BXQ8	Armadillo repeat-containing protein 10	1	0.5	Cell survival and cell growth, Suppress the transcriptional activity of p53/TP53
11	L0R6Q1	L0R6Q1	Alternative protein SLC35A4	1	0.5	Probable UDP-sugar transporter protein SLC35A4
12	B4E245	B4E245	cDNA FLJ61538, highly similar to Switch-associated protein 70	3	0.5	Mediates signaling of membrane ruffling, Regulates the actin cytoskeleton
13	O60888	CUTA	Protein CutA	1	1.5	Copper binding protein
14	Q9NYJ1	COA4	Cytochrome c oxidase assembly factor 4	1	1.5	Putative COX assembly factor
15	Q9Y320	TMX2	Thioredoxin-related transmem protein 2	4	1.6	Stress sensors
16	J3KQ73	J3KQ73	Peptidyl-prolyl cis-trans isomerase FKBP8	3	1.8	Phosphorylate BCL2 & interferes with binding of BCL2 to targets
17	P35754	GLRX1	Glutaredoxin-1	4	1.9	GNT-binding proteins, downstream of G protein-coupled receptors
18	Q9Y3A3	PHOCN	MOB-like protein phocein	1	1.9	Involved in hippo pathways (plays pivotal role in organ size control & tumor, suppression by restricting proliferation & promoting apoptosis)
19	K7EPV0	K7EPV0	Cytochrome c oxidase assembly protein 3	1	1.9	Essential for cytochrome c oxidase function

Table 12 (continued...)

C) Apoptosis Inducers and tumor suppressor						
S.No	Protein ID	Gene ID	Name	Pep (95%)	114:117 (T:C)	Cellular Function
1	P14923	PLAK	Junction plakoglobin	3	1.5	Pivotal role in regulation of cell-cell adhesion, regulates gene expression, cell proliferation, apoptosis, invasion & migration, acts as a tumor/ metastasis suppressor
2	Q7Z426	Q7Z426	Putative MAPK activating protein	4	1.6	Proliferation, gene expression, differentiation, mitosis, cell survival, and apoptosis
3	Q0VAM0	Q0VAM0	Catenin, beta like 1	1	1.7	Component of PRP19-CDC5L complex (spliceosome). May induce apoptosis.
4	Q53FV3	Q53FV3	COP9 signalosome subunit 4	2	1.7	Promoting & protection of p53/TP53, c-jun/JUN from degradation by phosphorylation
5	J3KQ73	J3KQ73	Peptidyl-prolyl cis-trans isomerase FKBP8	3	1.8	Chaperone for BCL2, phosphorylates it & interfering with binding of BCL2 to its targets
6	Q9Y3A3	PHOCN	Phocein	1	1.9	Membrane trafficking, specifically in membrane budding reactions
7	P35754	GLRX1	Glutaredoxin-1	4	1.9	GNT-binding proteins, downstream of G protein-coupled receptors
8	P62745	RHOB	Rho-related GTP-binding protein RhoB	5	2.8	Mediates apoptosis

Table 12: Expression of number proteins involved in cellular processes like A) protein synthesis, trafficking and degradation, B) Important cellular processes, C) apoptosis inducers and tumor suppressors, were found changed in Zoledronate treated MCF7 cells. Comparative analysis of iTRAQ labeled proteins of untreated and Zoledronate treated MCF7 cells was carried out using LC-MS. Proteins showing ≥ 1.5 fold increased expression upon Zoledronate treatment were considered as upregulated proteins, while proteins with ≤ 0.5 fold decrease in their expression upon Zoledronate treatment were considered as downregulated proteins.

5.5) *Interactome analysis*

The data was also analyzed using an interactome software- STRING (Search Tool for the Retrieval of Interacting Genes/Proteins) database (version 9.6). STRING database contains information from numerous sources, including experimental data, computational prediction methods and public text collections and is used to predict protein-protein interactions. The proteins were selected through textmining, experiments and databases at medium confidence (0.4) interaction score. STRING analysis showed effect of Zoledronate treatment on cellular metabolism like cytoskeletal elements, DNA-RNA processing and degradation, protein synthesis, protein degradation, vesicular trafficking (Figure 30). Interestingly, some proteins showed functional link to epidermal growth factor receptor (EGFR).

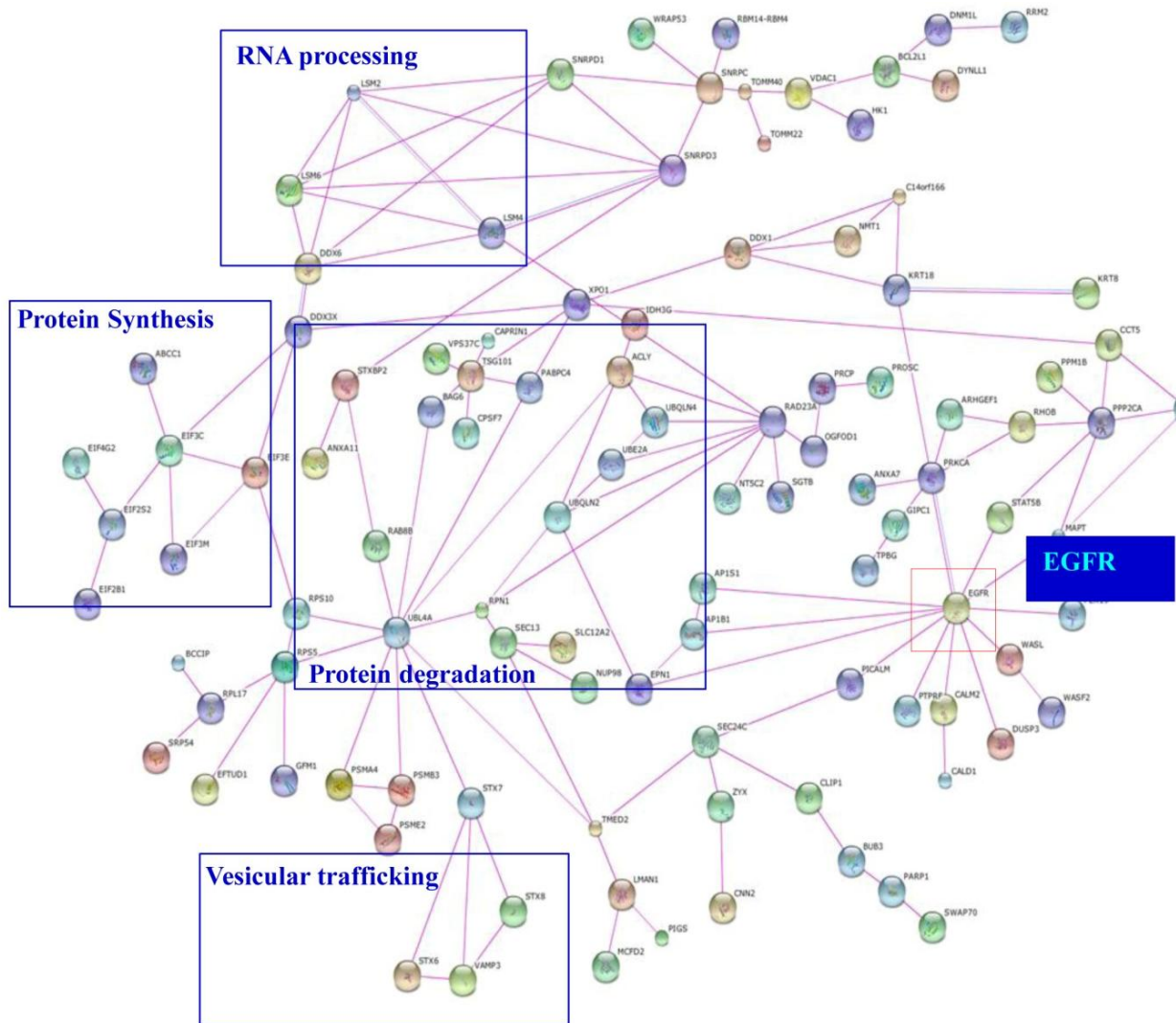


Figure 30: Interactome analysis of differentially expressed proteins in MCF7 upon Zoledronate treatment

Analysis of differentially expressed proteins in MCF7 cells using interactome software STRING showed important cellular processes like RNA processing, protein synthesis, protein degradation and vesicular trafficking. Some of the differentially expressed proteins were showing link to epidermal growth factor receptor.

5.6) Validation of differentially expressed proteins

5.6.1) Effect of Zoledronate on cytoskeletal elements

5.6.1.1) Effect of Zoledronate on actin rearrangement in MCF7 cells

Actin microfilaments are major component of the cytoskeletal elements which controls shape and movement of the cell. Actin structures are controlled by the Rho family of small GTP-binding proteins such as Rho. Actin is a globular protein (42KDa) which reversibly polymerizes to form filamentous structure known as F-actin [262]. Expression of multiple components of the actin related protein 2/3 (ARP 2/3) was found to be downregulated in Zoledronate treated MCF7 cells (Table 13A). ARP2/3 is known as actin nucleation core as it is involved in initial process of actin polymerization. It binds to the existing/mother filaments and initiates growth of a new/daughter filament. Expression of another protein arpin protein (UPF0552 protein C15orf3), which inhibits actin-nucleating activity of Arp2/3 complex was found upregulated upon Zoledronate treatment in MCF7 cells. Overall, proteins involved in the process of actin polymerization were found to be majorly affected upon Zoledronate treatment of MCF7 cells. This effect was verified by confocal imaging, where untreated and Zoledronate treated MCF7 cells were stained with phalloidin-TRITC. As shown in Figure 31A, Zoledronate treated MCF7 cells showed disorganization of actin cytoskeleton. A marked derangement in actin filaments was observed in Zoledronate treated MCF7 cells. It was observed that, Zoledronate disrupted the focal adhesions and actin bundles/ fibers in MCF7 cells. However at the protein level, there was no change observed in the expression of β -actin upon Zoledronate treatment, as validated by western blotting (Figure 31A and D).

5.6.1.2) Effect of Zoledronate on keratins in MCF7 cells

Keratins provide scaffold for epithelial cells, sustain mechanical stress, maintain structural integrity, ensure mechanical resilience, protect against variations hydrostatic pressure and establish cell polarity. Expressions of both acidic and basic keratins were found downregulated upon zoledronate treatment in MCF7 cells, when analyzed by 2D-PAGE/MALDI-TOF (Table 8) and iTRAQ/LC-MS (Table 13B). Expression of keratin 8, when validated by western blotting, did not show significant changes upon Zoledronate treatment at protein level, (Figure 31B and D). However, confocal imaging of keratin 8 showed thinning of keratin filaments in Zoledronate treated MCF7 cells.

5.6.1.3) Effect of Zoledronate on tubulin in MCF7 cells

Microtubules are the largest filamentous structures of the cytoskeleton with a diameter of about 20 nm. α - and β -tubulin molecules form heterodimers to form microtubules. Protofilaments are formed from these heterodimers using GTPases, which further combines to form a hollow microtubule. Microtubules are polarized and, thus, can act as conveyor belts for micro-motor molecules (e.g. dynein, kinesin) similar to microfilaments. Microtubules have the ability to shift through various formations which enables the cell to undergo mitosis or to regulate intracellular transport. Upregulation of tubulin was observed in both 2D-PAGE/MALDI-TOF (Table 8) and iTRAQ/LC-MS (Table 13C). Thus the effects of Zoledronate treatment on re-organization and expression of microtubules was analyzed by staining Zoledronate treated and untreated MCF7 cells with anti α -tubulin antibody. Since tubulin forms heterodimer of α and β tubulin subunits, which share >50% homology, we used α tubulin antibody for confocal imaging and western blotting experiments. Zoledronate treatment of MCF7 cells did not affect reorganization, which

was analyzed by confocal imaging. However, when analyzed by western blotting, Zoledronate treated MCF7 cells showed upregulation in expression of α -tubulin (Figure 31C and D).

Table 13: List of differentially expressed proteins in MCF7 related to cytoskeletal elements

[A] Microfilaments

S. No	Protein ID	Gene ID	Name	Pep (95%)	114:117 (T:C)	Cellular Function
1	A8K180	A8K180	cDNA FLJ76749, highly similar to Homo sapiens Wiskott-Aldrich syndrome-like (WASL), mRNA	2	0.3	Actin filament reorganization
2	Q05BU7	Q05BU7	WASF2 protein (Frag.)	2	0.5	Regulates actin filament reorganization via its interaction with Arp2/3 complex
3	Q9H7Z5	Q9H7Z5	ARP2/3 complex 20KD subunit	2	0.6	Major role in the regulation of actin cytoskeleton,
4	B1ALC0	B1ALC0	ARP2/3 complex subunit 5	2	0.7	Involved in initial process of actin polymerization, hence called as “actin nucleation core”, Binds to the existing / mother filaments and initiates growth of a new/daughter filament
5	P61158	ARP3	Actin related protein 3	20	0.8	
6	Q7Z6K5	CO038	UPF0552 protein C15orf38 (Arpin)	2	1.6	Inhibits actin-nucleating activity of Arp2/3 complex

[B] Intermediate filaments

S. No	Protein ID	Gene ID	Name	Pep (95%)	114:117 (T:C)	Cellular Function
1	P02533	K1C14	Keratin, type I cytoskeletal 14	5	0.6	Components of the intermediate filaments
2	P05787	K2C8	Keratin, type I cytoskeletal 8	35	0.7	Forms scaffolds for the cytoskeleton, Sustain mechanical stress, maintain structural integrity, ensure mechanical resilience, protects against variations in hydrostatic pressure and maintain cell polarity
3	Q14533	KRT81	Keratin, type II cuticular Hb1	21	0.7	Can rapidly disassemble and reassemble providing flexibility to cytoskeleton
4	P08729	K2C7	Keratin, type II cytoskeletal 7	15	0.7	Categorized d mainly as
5	B2RA03	B2RA03	Keratin 18	21	0.7	I) Acidic keratins or Type I: K9-K23, 40 - 56.5 KDa
6	P35908	K22E	Keratin, type II cytoskeletal 2	13	0.8	II) Basic keratins or Type II: K1-K8, 52-61 KDa

Table 13 (continued...)

[C] Microtubules

S. No	Protein ID	Gene ID	Name	Pep (95%)	114:117 (T:C)	Cellular Function
1	R4GMT0	R4GMT0	α -Centractin	2	0.3	Microtubule based vesicle motility
2	A2BDK6	A2BDK6	Microtubule-associated protein 1B	3	0.6	Binds to at least two tubulin subunits in the polymer & this bridging of subunits might be involved in nucleating microtubule polymerization and in stabilizing microtubules. Acts as a positive cofactor in DAPK1-mediated autophagic vesicle formation and membrane blebbing
3	B7U472	B7U472	Microtubule-associated protein tau	1	0.7	Promotes microtubule assembly and stability
4	Q5SU16	Q5SU16	Tubulin β -5 chain	107	1.2	Belongs to microtubule family Assembled from α and β tubulin heterodimers Microtubules are largest filamentous structures of cytoskeleton (20nm)
5	Q13509	TBB3	Tubulin β -3 chain	51	1.2	
6	Q9BUF	TBB6	Tubulin β -6 chain	36	1.2	

Table 13: Changes in expression of cytoskeletal elements and proteins involved in reorganization of [A] microfilament, [B] Intermediate filament and [C] microtubules were found in MCF7 upon Zoledronate treatment. Proteins showing ≥ 1.5 fold increased expression upon Zoledronate treatment were considered as upregulated proteins, while proteins with ≤ 0.5 fold decrease in their expression upon Zoledronate treatment were considered as downregulated proteins

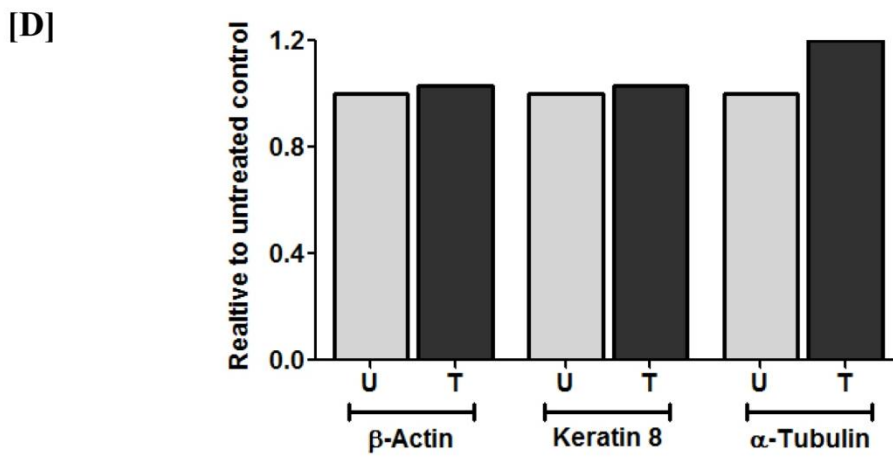
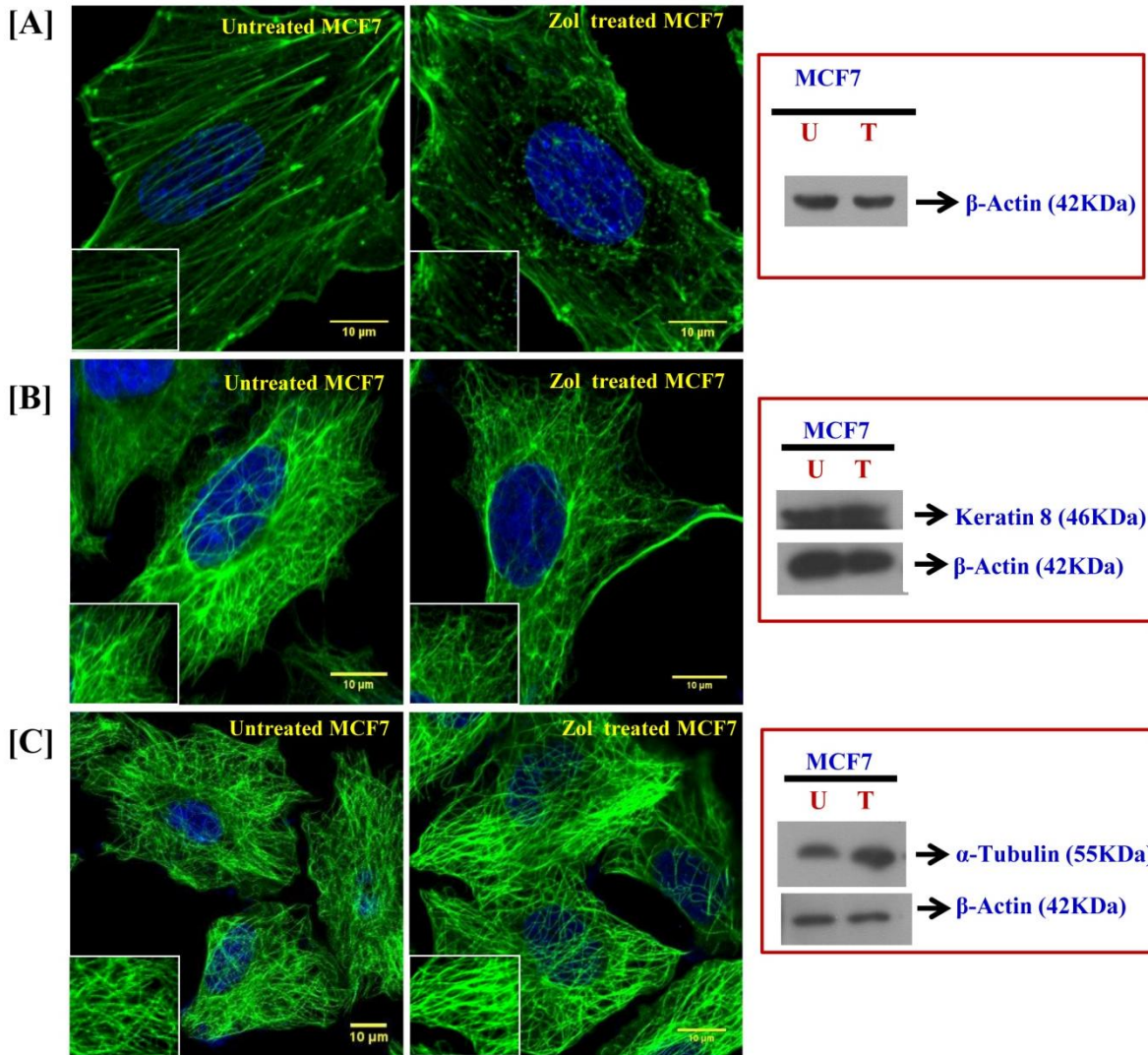


Figure 31: Effect of Zoledronate treatment on reorganization and expression of cytoskeletal elements in MCF7

Re-organization and expression of actin, keratin 8 and tubulin in MCF7 cells upon Zoledronate treatment was analyzed by confocal microscopy and western blotting respectively. [A] To analyze changes in expression of actin, Zoledronate treated and untreated MCF7 cells were stained with Phalloidin-TRITC. Change in expression of β -actin was analyzed by western blotting. [B] Untreated and Zoledronate treated MCF7 cells were stained with anti-human Keratin-8-AF488. [C] To study changes in reorganization of α -tubulin, untreated and Zoledronate treated MCF7 cells were stained with α -Tubulin-AF488 antibody, [D] Densitometry analysis of fold changes in expression of β -actin, keratin 8 and α -Tubulin in Zoledronate treated MCF7 cells relative to untreated MCF7 cells (control). The figure is representative of three independent experiments.

5.6.2) *Effect of Zoledronate on expression of heat shock proteins in MCF7 cells*

Role of HSP 60 expressed on tumor cells in activation of $\gamma\delta$ T cells has earlier been discussed [71]. HSP60 is a eukaryotic mitochondrial chaperone, which also localizes in the cytosol, on cell surface, extracellular space and in the peripheral blood under normal physiological conditions [263,264]. HSP60 plays an important role in prevention of apoptosis by forming complexes with the proteins involved in apoptosis. HSP activates “danger signal cascade” of immune response, generated as a response to prevent any infection or disease. HSPs act as potent antigens of $\gamma\delta$ T cells [71,265,266, 267]. In our studies, Zoledronate treated MCF7 cells showed increased expression of heat shock factor 1 and HSP90 α when analyzed by iTRAQ/LCMS (Table 9). Heat shock factor 1 is a transcription factor transcribes expression of HSP70 and HSP90. Therefore, effect of Zoledronate on expression of heat shock proteins (HSP60 and HSP70) was analyzed by western blotting. Expression of HSP60 was not significantly altered, as analyzed both by western blotting (Figure 32A) or confocal microscopy (Figure 32B). Further, flow cytometry was used to study time kinetics of HSP60 and HSP70 expression (surface and intracellular) upon zoledronate treatment in MCF7 cells. Expression of HSP60 and HSP70 on Zoledronate treated (100 μ M) and untreated MCF7 cells were monitored after every 2 hrs for 24 hrs at 37°C with baseline expression at 0th hr. As shown in Figure 32C, changes in expression of HSP60 were observed with transient increase after 18 hrs in Zoledronate treated MCF7 cells compared to untreated MCF7 cells. In case of HSP70, the expression was found to be reduced upon Zoledronate treatment (Figure 32D).

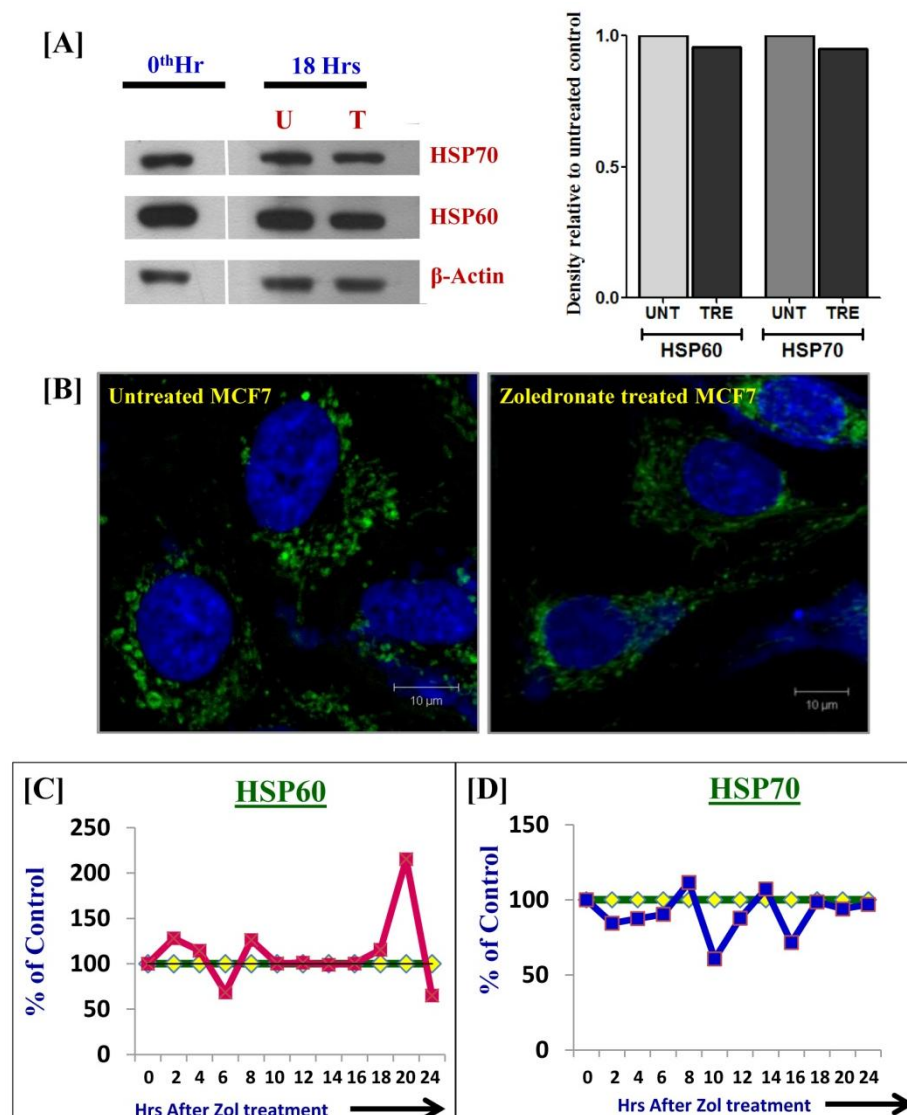


Figure 32: Effect of Zoledronate treatment on expression of heat shock proteins in MCF7 cells

Effect of Zoledronate treatment on expression of HSPs in MCF7 cells was analyzed by [A] western blotting, [B] confocal microscopy and [C] flow cytometry. No difference in expression of HSP60 was found upon Zoledronate treatment in MCF7 after 18 hrs by both western blotting and confocal microscopy. Time kinetics of HSP60 revealed increase in expression of HSP60 after 18 hrs of Zoledronate treatment. HSP70 expression also did not show any changes upon Zoledronate treatment, which was validated by both western blotting and time kinetics study. Densitometry analysis shows changes in expression of HSP60 and HSP70 in Zoledronate treated MCF7 cells relative to untreated MCF7 cells (control). The figure is representative of three independent experiments.

5.6.3) Effect of Zoledronate treatment on expression of epidermal growth factor receptor (EGFR/ErbB1) in MCF7 cells

Interactome analysis of upregulated and downregulated proteins using STRING showed link to EGFR. Zoledronate treated cells MCF7 showed increased expression of RhoB and sortin nexin1 protein (Table 14). RhoB, a small GTPase from Rho family, is the only protein known to exist as both farnesylated and geranylgeranylated forms within the cell [268]. Farnesyl transferase inhibitors cause increase in geranylgeranylated form of RhoB, which causes EGFR degradation [269]. As shown in Figure 33A, EGFR dimers are internalized and are transferred to microvesicular bodies (MVBs), where it is degraded by lysosomal enzymes. RhoB has been shown to be associated with both early endosomal vesicles and MVBs (a prelysosomal compartment which is involved in the sorting of internalized receptors for degradation [268,270]. Mammalian sortin nexin family proteins have been implicated in endocytic trafficking of cell surface receptors. Sortin nexin 1 (SNX1) was identified particularly by its interaction with EGFR [271]. SNX1 recognizes EGFR lysosome targeting signals and targets EGFR to lysosome [271]. Expression of EGFR was found to be reduced upon Zoledronate treatment in MCF7 cells when analyzed by western blotting (Figure 33B).

Table 14: List of differentially expressed proteins in MCF7 involved in EGFR signaling

S. No	Protein ID	Gene ID	Name	Pep (95%)	114:117 (T:C)	Cellular Function
1	P62745	RHOB	Rho-related GTP-binding protein RhoB	5	2.8	Involved in trafficking of the EGFR from late endosomes to lysosomes
2	Q59GU6	Q59GU6	Sorting nexin 1 isoform a variant (Frag.)	2	1.6	Targets ligand-activated EGFR to lysosome for degradation after endocytosis from cell surface & release from Golgi

Table 14: Proteins involved in EGFR degradation in ErbB/ HER signaling pathway showed increase in their expression. Comparative analysis of iTRAQ labeled proteins of untreated and Zoledronate treated MCF7 cells was carried out using LC-MS. Proteins showing ≥ 1.5 fold increased expression upon Zoledronate treatment were considered as upregulated proteins, while proteins with ≤ 0.5 fold decrease in their expression upon Zoledronate treatment were considered as downregulated proteins.

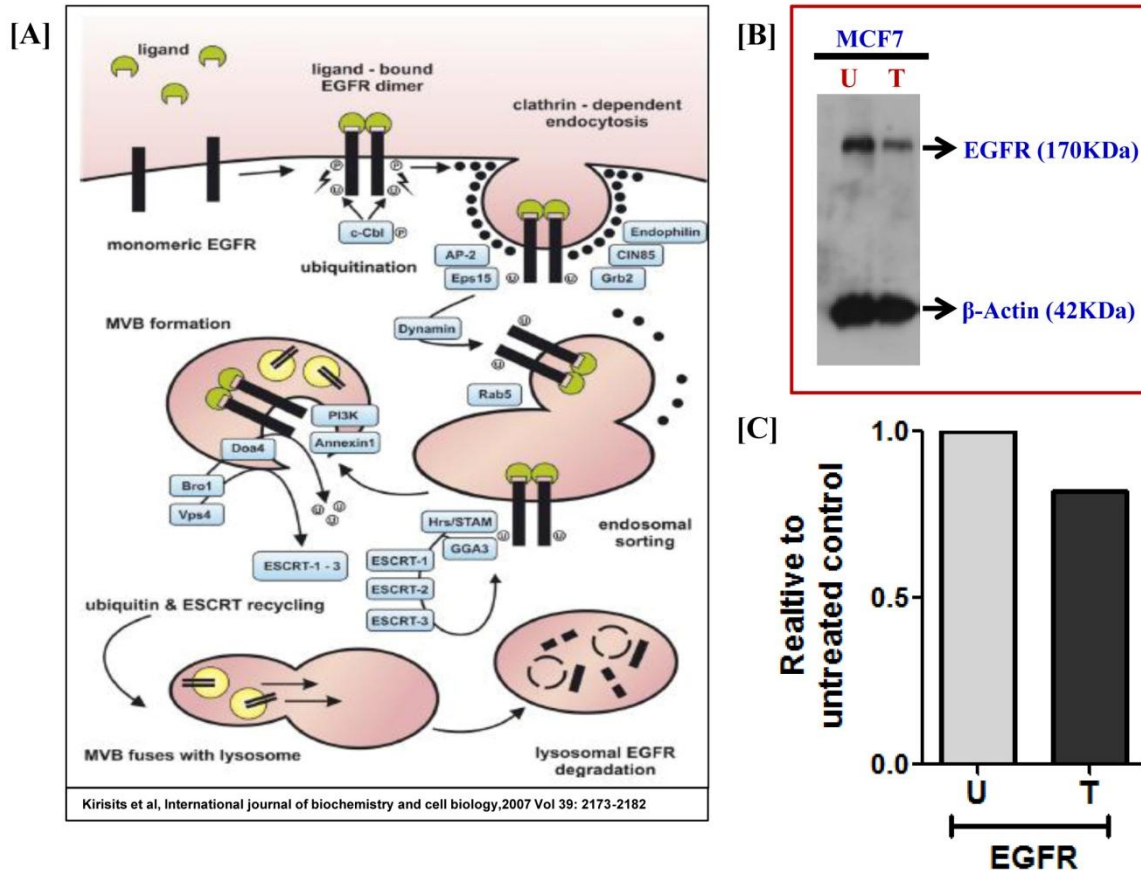


Figure 33: Effect of Zoledronate treatment on expression of epidermal growth factor receptor (EGFR) in MCF7 cells

MCF7 Cells were treated with Zoledronate showed upregulation of proteins involved in EGFR degradation pathway. [A] Schematic representation of EGFR degradation pathway, [B] Expression of EGFR was analyzed in Zoledronate treated and untreated MCF7 cells using anti-EGFR antibody. Zoledronate treated MCF7 cells showed reduced expression of EGFR compared to untreated MCF7 cells, as analyzed by western blotting. Densitometry analysis shows changes in expression of EGFR in Zoledronate treated MCF7 cells relative to untreated MCF7 cells (control). The figure is representative of three independent experiments.

5.6.4 Effect of Zoledronate on cell cycle on breast tumor cell line

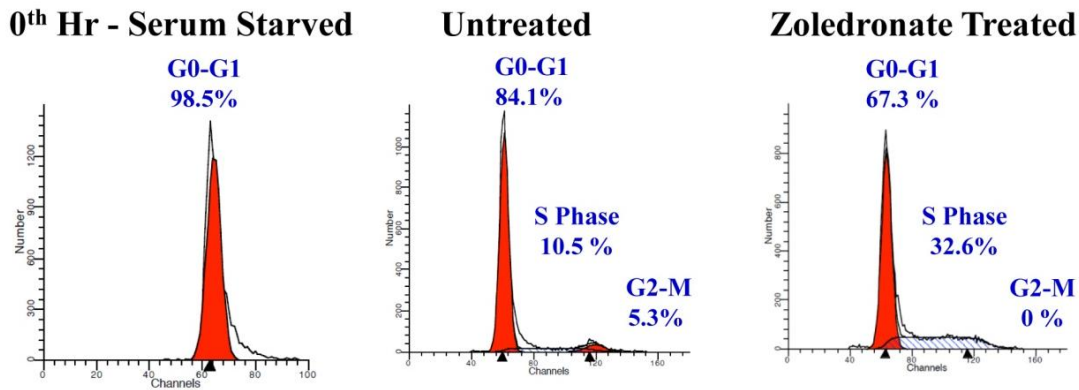
Upon Zoledronate treatment MCF7 cells showed changes in expression of proteins required for initiation of DNA replication, chromatin remodeling, cells cycle progression and DNA repair (Table 15). Thus effect of Zoledronate treatment on cell cycle of breast tumor cells lines (MCF7 and MDAMB-231) was analyzed by flow cytometry by detection of nucleic acid stained with propidium iodide (PI). Breast tumor cells lines (MCF7 and MDAMB-231) were serum starved and then were treated with Zoledronate or left untreated for 16-18 hrs. Control (0th hr cells, before addition of Zoledronate) and test (cells incubated with Zoledronate or in medium alone for 16-18 hrs) breast tumor cells (MCF7 cells and MDAMB-231) were fixed in chilled 70% ethanol and were then stained with PI. With Modfit software, cells were gated on singlets using width and area signals and cells in G0-G1, S and G2-M phase were calculated. Percentage of cells in a particular phase of cell cycle were analyzed by calculating the differences in their DNA content (PI) depicted as deconvolutions of histogram. As shown in Figure 34A and B, after serum starvation more that ~98% MCF7 cells, while 90% MDAMB-231 cells were found arrested in G0 phase. As shown in Figure 34A, Zoledronate treatment arrested MCF7 cells in S-phase. As shown in Figure 34C, after 16-18 hrs, untreated MCF7 cells showed 85% (mean \pm SEM) cells in G0 phase with 8% cells in S-phase and 7% cells in G2-M phase, while Zoledronate treatment significantly arrested MCF7 cells in S- phase (30%) with 68 % cells in G0-G1 phase and nearly absent in G2-M phase. In case of MDAMB-231 cells, Zoledronate treatment arrested the cells in G0-G1 phase (Figure 34B). As shown in Figure 34D, Zoledronate treatment in MDAMB-231 cells showed G0-G1 arrest (73%) with 20% cells in S-phase and 6% cells in G2-M phase. Among untreated MDAMB-231 cells, 45% cells were G0-G1, 45% cells were in S-phase and 10% cells in G2-M phase.

Table 15: List of differentially expressed proteins in MCF7 involved in cell cycle

S.No	Protein ID	Gene ID	Name	Pep (95%)	114:117 (T:C)	Cellular Function
1	P62312	LSM6	U6 snRNA-associated Sm-like protein LSm6	2	0.2	RNA processing
2	Q59G16	Q59 G16	SWI/SNF-related matrix-associated actin-dependent regulator of chromatin c2 isoform	1	0.3	Chromatin remodeling
3	R4GMT0	R4GMT0	α -Centractin	2	0.3	G2-M transition of cell cycle
4	E5RFF9	E5RFF9	DNA replication complex GINS protein SLD5	1	0.4	Initiation of DNA replication & progression of DNA replication forks
5	Q9H7H1	RUIT1	Putative uncharacterized protein encoded by RUNX1-IT1	1	0.4	Chromatin remodeling
6	E5RFF9	E5RFF9	DNA replication complex GINS protein SLD5	1	0.4	Essential role in the initiation of DNA replication
7	Q96T76	MMS19	MMS19- NER protein	2	0.5	Key role in nucleotide excision repair (NER) & RNA polymerase II (POL II) transcription, involved in DNA metabolism & genomic integrity
8	Q9H3H3	CK068	UPF0696 protein C11orf68	2	0.5	Poly(A) RNA binding protein
9	B4DDM6	B4DDM6	Mitotic checkpoint protein BUB3	1	0.5	BUB1/BUB3 complex plays role in inhibition of APC/C
10	Q96CT7	CC124	Coiled-coil domain-containing protein 124	2	0.5	Essential for proper progression of late cytokinetic stages
11	P52701	MSH6	DNA mismatch repair protein Msh6	1	0.5	Post-replicative DNA mismatch repair system, repairs dsDNA
12	Q13042	CDC16	Cell division cycle protein 16 homolog	0	1.6	Anaphase promoting complex / cyclosome component, controls progression through mitosis and the G1 phase of cell cycle

Table 15: Comparative analysis of iTRAQ labeled proteins of untreated and Zoledronate treated MCF7 cells was carried out using LC-MS. Proteins showing ≥ 1.5 fold increased expression upon Zoledronate treatment were considered as upregulated proteins, while proteins with ≤ 0.5 fold decrease in their expression upon Zoledronate treatment were considered as downregulated proteins.

[A] MCF7



[B] MDAMB-231

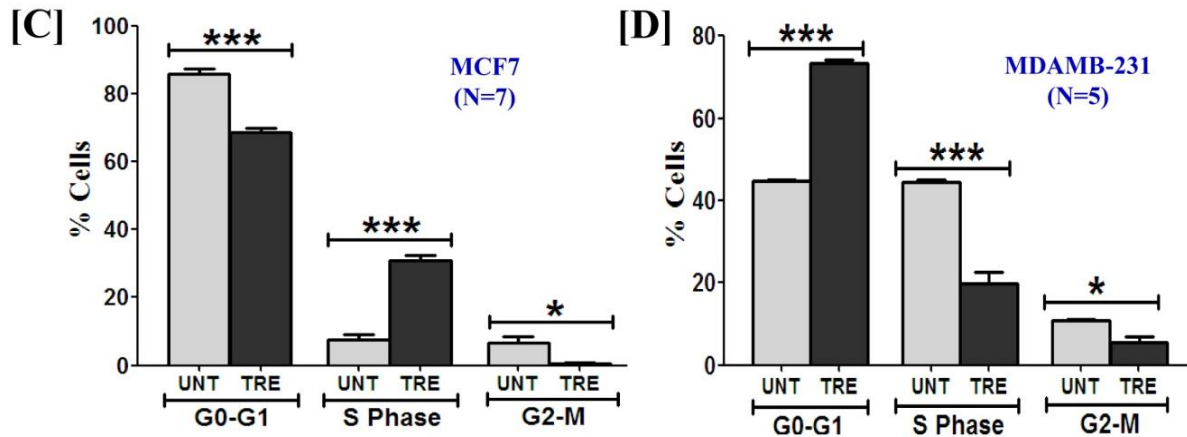
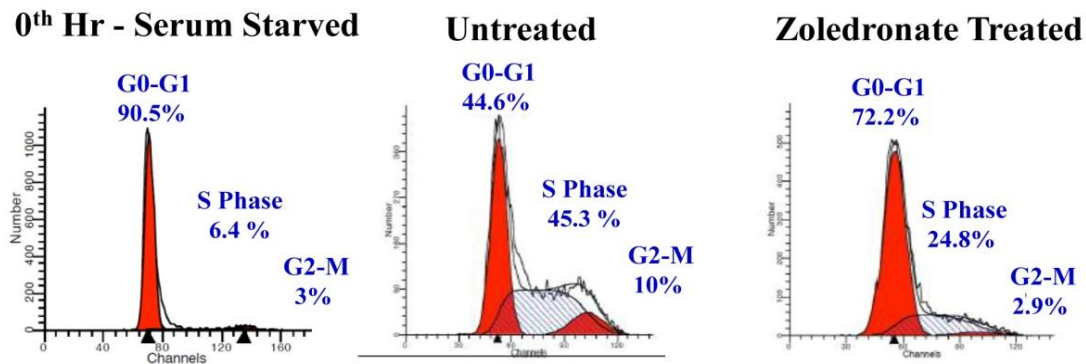


Figure 34: Effect of Zoledronate treatment on cell cycle of breast tumor cells

Breast tumor cell lines (MCF7 and MDAMB-231) were serum starved for 72 hrs and then treated with Zoledronate or left untreated for 16-18 hrs. Further cells were stained for propidium iodide. At least 10000 events were acquired on FACS Caliber and data was analyzed using

Modfit software. [A,C] Upon Zoledronate treatment MCF7 cells got arrested in S-phase, with no cells in G2-M phase. [B, D] In case of MDAMB-231 cells, Zoledronate treated cells were arrested in G0-G1 phase showing reduced percentages of cells in S-phase and G2-M phase. Data shown as mean \pm SEM of atleast 5 independent experiments. Significance is given by p value as $p < 0.05$ (*), $p < 0.005$ (**) and $p < 0.0005$ (***)

In conclusion, Zoledronate treatment mediates its antitumor effect by two mechanisms- by destabilizing cellular metabolism and through activation of $\gamma\delta$ T cells. Zoledronate treated breast tumor cells exhibited increased expression of proteins which could potentially recruit and activate $\gamma\delta$ T cells, which are known to have antitumor functions against broad range of tumors.

Chapter 6

*Immune profiling of breast cancer patients on
Zoledronate treatment*

Zoledronate is used for prevention of skeletal-related events in patients with bone metastases and other skeletal malignancies such as osteoporosis [58,214,272,273,274]. During the last few years, evidence has accumulated that in addition to reducing osteolysis and preserving bone, Zoledronate has shown anti cancer activity during adjuvant therapy of breast cancer. Adjuvant Zoledronic Acid to Reduce Recurrence (AZURE) trial did not support the use of Zoledronate as adjuvant therapy in breast cancer [275,276]. However further analysis indicated that Zoledronate adjuvant therapy improve disease free survival in postmenopausal breast cancer patients but not in premenopausal women. These findings were in contrast to another study- the ABCSG-12 trial, showing improved disease free survival in premenopausal early- stage breast cancer patients receiving Zoledronate adjuvant therapy [277,278]. Thus there may be other cells or factors modulating the Zoledronate antitumor effects in addition to the role of Zoledronate in targeting osteoclasts. Emerging evidence suggest that immune cells play a critical role in controlling local tumor growth within the bone microenvironment. Zoledronate was reported to increase the number of $\gamma\delta$ T cells, however these studies were not in breast cancer and not done *in vivo*. As mentioned earlier, Zoledronate inhibits FPPS enzyme of the mevalonate pathway and this results in the upregulation of intracellular levels of IPP, which is a potent activator of $\gamma\delta$ T cells.

The purpose of the present study was to characterize the immunomodulatory effects of Zoledronate in breast cancer patients who had bone metastasis and were on Zoledronate treatment versus untreated breast cancer patients.

6.1) Demographic analysis of breast cancer patients

Peripheral blood samples were collected from two groups of breast cancer patients (stage I-IV, n=36) - (a) patients who were on Zoledronate treatment (Rx^+ , n= 21) for at least 3 months and (b) patients who had not received Zoledronate treatment i.e untreated (Rx^- , n=15). Zoledronate (4 mg) was intravenously (15 min) administered to the breast cancer patients at the interval of every 4 weeks. As control, peripheral blood samples were collected from age matched healthy female volunteers (n=38). Diagnosis for breast cancer was histologically confirmed in both the groups of patients and was majorly found to be invasive ductal carcinoma (IDC). Demographic analysis carried out showed equal distribution of patients among the two groups of breast cancer patients (Rx^- and Rx^+) on the basis of their age, menopausal status and site of metastasis. Table 16 shows detailed inclusion- exclusion criteria used for the breast cancer patients.

Due to limited sample size, we did not stratify patients based on ER, PR and Her2 status. The data was analyzed in the two groups of breast cancer patients a) who did not receive Zoledronate treatment (Rx^-), b) who received Zoledronate treatment (Rx^+). In the thesis, patients who did not receive Zoledronate treatment (Rx^-) are referred to as “untreated” breast cancer patients.

Age distribution of healthy individuals ranged from 23-48 years (38 ± 1 , mean+ SEM). In case of untreated breast cancer patients, age distribution ranged from 32-77 years (45 ± 3), while in case of Zoledronate treated breast cancer patients, it ranged from 28-64 years (49 ± 2).

Premenopausal [48%, (10/21)] and postmenopausal [52%, (11/21)] women were almost equally distributed in Zoledronate treated breast cancer patients (Rx^+). Among the

untreated breast cancer patients (Rx-), 73% (11/15) were premenopausal, whereas 27% (4/15) were postmenopausal.

All the breast cancer patients on Zoledronate treatment (Rx⁺) showed bone metastasis, while patients from untreated group (Rx⁻) did not show bone metastasis, but 6/15 showed metastasis to liver/ lung/ brain/ lymph nodes.

Table 16: Inclusion- exclusion criteria for breast cancer patients

Criteria	Untreated Group (Rx-)	Zoledronate Treated Group (Rx+)
Inclusion	<ul style="list-style-type: none"> • Females • Age >18 years • Patients who have confirmed diagnosis for invasive breast cancer • Patients with any receptor pattern (ER, PR, Her2) • Patients who have been planned for definitive treatment but are treatment naïve at the time of inclusion 	<ul style="list-style-type: none"> • Females • Age >18 years • Patients who have confirmed diagnosis for invasive breast cancer • Patients who have confirmed diagnosis for metastasis • Patients who have confirmed diagnosis for bone metastasis • Patients with bone metastasis who have received treatment for Zoledronate injection for at least 3 months • Patients with any receptor pattern (ER, PR, Her2)
Exclusion	<ul style="list-style-type: none"> • Males • Patients who refused to give consent • Patients who were receiving any treatment at the time of inclusion 	<ul style="list-style-type: none"> • Males • Patients who refused to give consent • Patients who were not receiving Zoledronate treatment

Table 16: Breast cancer patients were categorized into untreated (Rx-) and Zoledronate treated (Rx+) groups based on these inclusion exclusion criteria.

6.2) Immune profile of metastatic (Zoledronate treated) and non-metastatic (untreated) breast cancer patients

Comparative immune profiling of healthy individuals (HI) and breast cancer patients on Zoledronate treatment (Rx^+) or without Zoledronate treatment (Rx^-) was carried out using multicolor flow cytometry. As shown in Figure 35, percentages of $CD3^+$ T cells, $CD4^+$ T cells, $CD8^+$ T cells and B cells ($CD19^+$) in PBMCs were evaluated in HI, breast cancer patients on Zoledronate treatment (Rx^+) and untreated breast cancer patients (Rx^-). It was observed that, $CD3^+$ T cells population from Zoledronate treated breast cancer patients (Rx^+) did not differ from untreated breast cancer patients (Rx^-). Total $CD3^+$ T cell population from peripheral blood of breast cancer patients (both Rx^+ and Rx^-) was found to be lower as compared to HI. In case of $CD4^+$ T cell population, Zoledronate treated (Rx^+) and untreated (Rx^-) breast cancer patients did not show any differences, though the percentages were significantly lower as compared to HI. Interestingly, $CD8^+$ T cell population was significantly elevated in Zoledronate treated breast cancer patients (Rx^+) as compared to untreated (Rx^-) breast cancer patients ($p=0.03$) and HI ($p<0.0001$). Untreated breast cancer patients showed reduced percentages of B cells as compared to HI ($p=0.03$). However, a significant increase in percentages of B cells was observed in Zoledronate treated breast cancer patients as compared to untreated breast cancer patients ($p=0.02$).

Amongst the other immune cells, a marked increase was observed in percentages of NK cells ($CD3^-CD56^+$) in Zoledronate treated breast cancer patients (Rx^+) as compared to HI ($p=0.003$). However, a marginal increase in NK cells were observed in Zoledronate treated breast cancer patients (Rx^+) as compared to untreated breast cancer patients (Rx^-), but the increase was not significant. No significant changes were observed in NK-T cells ($CD3^+CD56^+$) in Zoledronate treated breast cancer patients (Rx^+) as compared to untreated breast cancer patients

(Rx^-) and HI. Interestingly, a sharp decline was observed in $\gamma\delta$ T cells in patients who were on Zoledronate treatment as compared to untreated breast cancer patients ($p=0.03$) and HI ($p=0.0006$). This was surprising, as Zoledronate is known to activate $\gamma\delta$ T cells. Further we analyzed the percentages of regulatory T cells ($CD4^+CD25^+CD127^-$) in HI and breast cancer patients (Rx^- and Rx^+). A significantly increased percentages of regulatory T cells were observed in untreated breast cancer patients (Rx^-) and Zoledronate treated breast cancer patients (Rx^+) as compared to HI ($p=0.003$ and $p=0.008$ respectively). However, Zoledronate treated breast cancer patients showed a marginal reduction in percentages of regulatory T cells as compared to untreated breast cancer patients. Median fluorescent intensity (MFI) of FoxP3, a transcription factor associated with regulatory T cells, showed an increasing trend in expression in untreated and Zoledronate treated breast cancer patients compared to HI, but the differences were not statistically significant. Untreated breast cancer patients (Rx^-) showed increased percentages of monocytes ($CD14^+$ cells) as compared to HI ($p=0.01$). However, Zoledronate treated breast cancer patients (Rx^+) showed a remarkable reduction in percentages of monocytes as compared to untreated breast cancer patients ($p=0.0009$) and HI ($p=0.0037$).

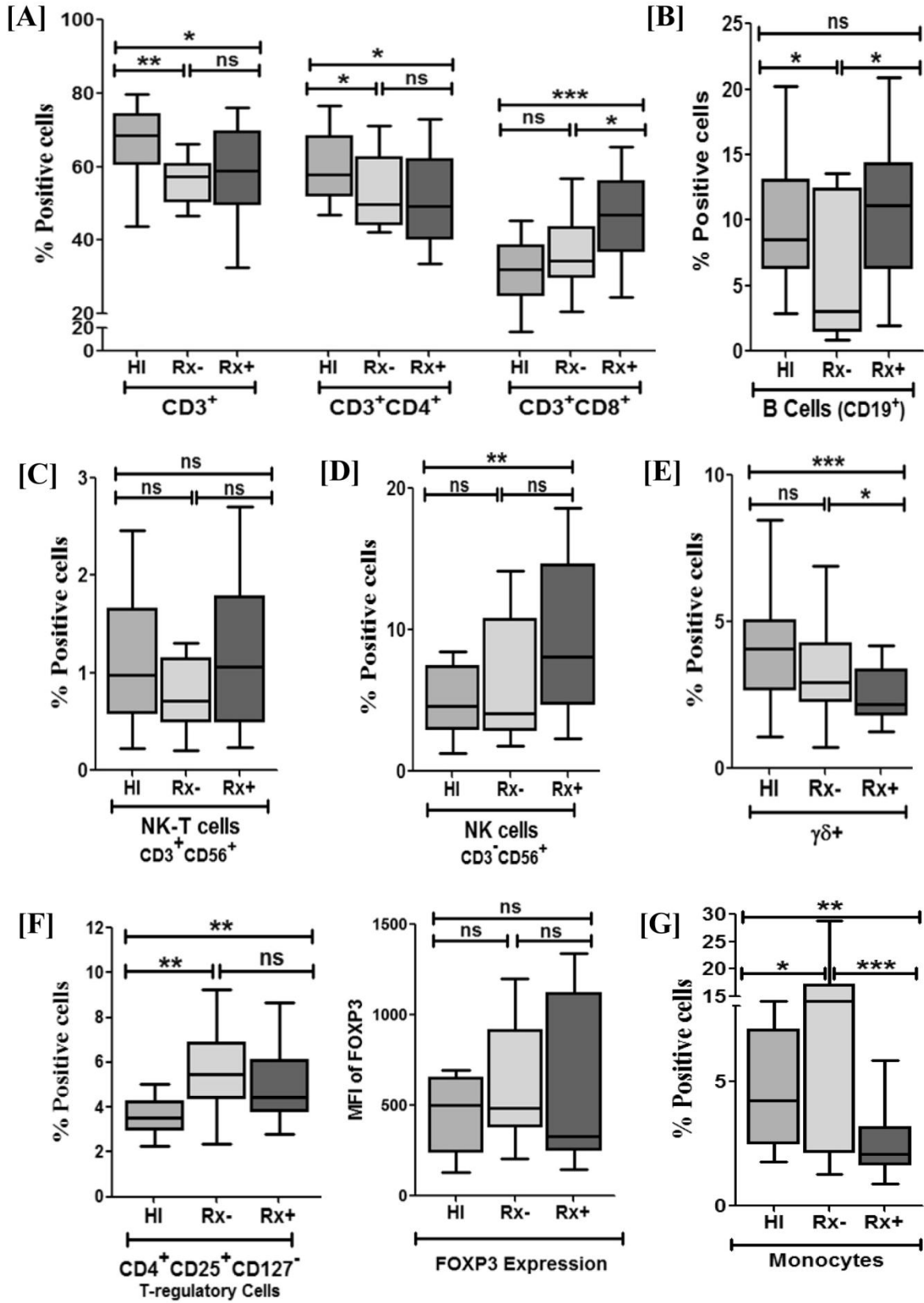


Figure 35: Immune profile of breast cancer patients on Zoledronate treatment and untreated breast cancer patients

PBMCs separated from healthy individuals (HI, n=38), untreated breast cancer (Rx⁻, n=15) and Zoledronate treated breast cancer patients (Rx⁺, n=21) were analyzed for different immune cell subtypes, which included [A] CD3⁺, CD4⁺, CD8⁺, [B] B cells, [C] NK-T cells, [D] NK cells, [E] $\gamma\delta$ T cells monocytes, [F] regulatory T cells and [G] monocytes. Zoledronate treated breast cancer patients showed increase percentages of CD3⁺CD8⁺, B cells, NK cells, while percentages of monocytes and $\gamma\delta$ T cells were found to be reduced in peripheral blood. Significance is given by p value as p<0.05(*), p<0.005(**), p<0.0005(***) and p \geq 0.05 (not significant/ns).

6.3) Zoledronate treatment activated both $\alpha\beta$ and $\gamma\delta$ T cells in breast cancer patients

Activated T cells are known to exhibit cytotoxic properties [279]. Thus, activation status of $\alpha\beta$ and $\gamma\delta$ T cells from HI and breast cancer patients (on Zoledronate treatment and untreated) was investigated by analyzing expression of early (CD69) and late (CD25 and CD254/RANKL) activation markers on them using multicolor flow cytometry (Figure 36). CD69 is a human transmembrane C-Type lectin protein which is the earliest inducible glycoprotein upon lymphocyte activation, while CD25 alpha chain of the IL2 receptor which associates with beta chain of IL2 receptor creating high affinity receptor for IL2. It was observed that, there were no changes in $\alpha\beta$ ⁺CD69⁺ and $\gamma\delta$ ⁺CD69⁺T cells among HI, Zoledronate treated and untreated breast cancer patients. A remarkable increase in percentages of $\alpha\beta$ T cells expressing late activation marker CD25 was observed in Zoledronate treated breast cancer patients as compared to HI (p=< 0.0001) and untreated breast cancer patients (p=<0.0001) (Figure 36A). Percentages of $\gamma\delta$ T cells expressing CD25 were considerably higher in Zoledronate treated breast cancer patients (p=< 0.0001) and untreated breast cancer patients (p=< 0.0001) as compared to HI.

Similarly, expression of another late activation marker, RANKL (CD254), which plays important role in osteoclastogenesis and immune responses, was also analyzed on $\alpha\beta$ and $\gamma\delta$ T cells. Untreated breast cancer patients showed increased percentages of RANKL expressing $\alpha\beta$ T cells as compared to HI ($p=0.0004$). However, Zoledronate treated breast cancer patients and HI showed comparable levels of $\alpha\beta^+RANKL^+$ T cells, while percentages of $\alpha\beta^+RANKL^+$ T cells were found reduced in Zoledronate treated breast cancer patient ($p=<0.0001$). Compared to HI, percentages of $\gamma\delta^+RANKL^+$ T cells were higher in untreated breast cancer patients ($p= 0.0001$) and Zoledronate treated breast cancer patients ($p= 0.0033$). Comparative analysis between $\alpha\beta$ and $\gamma\delta$ T cells showed that, percentage of $\gamma\delta^+CD25^+$ and $\gamma\delta^+RANKL^+$ T cells were higher in HI and breast cancer patients (both Zoledronate treated and untreated) compared to $\alpha\beta$ T cells (Figure 36C).

Median fluorescent intensity (MFI) of CD25 and RANKL was analyzed on $\alpha\beta$ and $\gamma\delta$ T cells (Figure 36D-E). It was observed that, expression of CD25 on $\alpha\beta$ and $\gamma\delta$ T cells was comparable between HI and untreated breast cancer patients but was found remarkably increased upon Zoledronate treatment ($p=0.02$). As shown in Figure 36E, expression of RANKL on $\alpha\beta$ T cells was found to be upregulated in untreated breast cancer patients as compared to HI ($p= 0.009$). RANKL expression on $\alpha\beta$ T cells was found significantly reduced upon Zoledronate treatment as compared to untreated breast cancer patients ($p= 0.007$) and was comparable to HI. In case of $\gamma\delta$ T cells, no significant changes were observed in expression of RANKL among HI and untreated breast cancer patients. Expression of RANKL on $\gamma\delta$ T cells was found significantly reduced in Zoledronate treated breast cancer patients as compared to untreated breast cancer patients ($p=0.02$). Details of MFI expressed by $\alpha\beta$ and $\gamma\delta$ T cells from HI and breast cancer patients (both Zoledronate treated and untreated) are given in Table 17.

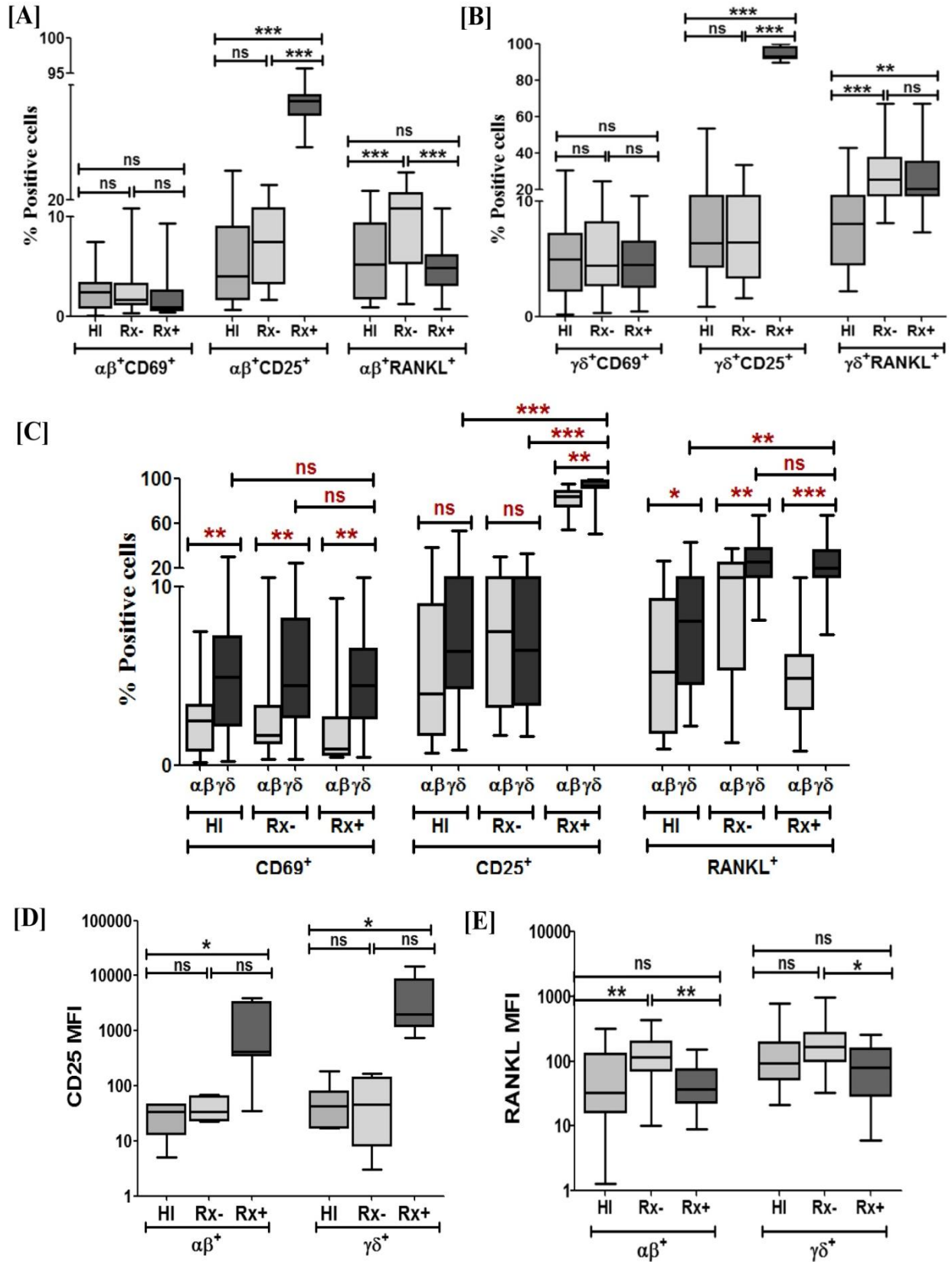


Figure 36: Effect of Zoledronate treatment on activation status of $\alpha\beta$ and $\gamma\delta$ T cells

PBMCs from HI (n=38), untreated breast cancer patients (Rx⁻, n=15) and Zoledronate treated breast cancer patients (Rx⁺, n=21) were stained for $\alpha\beta$ TCR-FITC/ $\gamma\delta$ TCR-FITC, CD69-FITC, CD25-PECy7 and RANKL-PE. Expression of activation markers were analyzed on [A] $\alpha\beta$ and [B] $\gamma\delta$ T cells. [C] Comparative analysis $\alpha\beta$ and $\gamma\delta$ T cells with respect to their activation makers was carried out. Median fluorescent intensity of [D] CD25 and [E] RANKL expressed on $\alpha\beta$ and $\gamma\delta$ T cells from HI, Rx⁻ and Rx⁺ patients was compared. Significance is given by p value as p<0.05(*), p<0.005(**), p<0.0005(***) and p \geq 0.05 (not significant/ns).

Table 17: Median fluorescent intensity of activation markers (CD69, CD25 and RANKL) on $\alpha\beta$ and $\gamma\delta$ T cells

		HI	Rx-	P value	HI	Rx+	P value	Rx-	Rx+	P value
CD69	$\alpha\beta$ +	21.6 ± 8.5	53. ± 13.7	ns	21.6 ± 8.5	25.9 ± 10.3	ns	53 ± 13.7	25.9 ± 10.3	ns
	$\gamma\delta$	27.2 ± 6.8	63.8 ± 14	*	27.2 ± 6.8	76 ± 21.2	ns	63.8 ± 14	76 ± 21.2	ns
CD25	$\alpha\beta$	30 ± 5.5	41.9 ± 9.5	ns	30 ± 5.5	1322 ± 466.5	*	41.9 ± 9.5	1322 ± 466.5	ns
	$\gamma\delta$	61 ± 22	65.33 ± 36.4	ns	61 ± 22	4743 ± 1658	*	65.33 ± 36.4	4743 ± 1658	ns
RANKL	$\alpha\beta$	70.6 ± 17.3	147.5 ± 21.7	**	70.6 ± 17.3	53.4 ± 13.1	ns	147.5 ± 21.7	53.4 ± 13.1	**
	$\gamma\delta$	164.6 ± 37.9	220.1 ± 39.3	ns	164.6 ± 37.9	97.69 ± 18.9	*	220.1 ± 39.3	97.69 ± 18.9	ns

Table 17: Median fluorescent intensity of activation markers CD69, CD25 and RANKL expressed by $\alpha\beta$ and $\gamma\delta$ T cells from healthy individuals (HI, n=38) and breast cancer patients who were on Zoledronate treatment (Rx⁺, n=21) and those who were not on Zoledronate treatment (Rx⁻, n=15) was analyzed. Significance is given by p value as p<0.05(*), p<0.005(**), p<0.0005(***) and p \geq 0.05 (not significant/ns).

6.4) Zoledronate treatment activated central memory $\gamma\delta$ T cells

We further analyzed the memory status of $\gamma\delta$ T cells in breast cancer patients and HI by staining them for CD45RA and CD27. *CD45RA* is a protein tyrosine phosphatase, receptor type C enzyme and is located on naive T cells while memory T cells express different isoform (CD45RO). CD27 is a tumor necrosis factor receptor family member, acts as a co-stimulatory molecule and is required for generation and long term maintenance of T cells [280]. Naïve or unprimed cells (CD45RA⁺CD27⁺) are less cytotoxic, need stronger signals for proliferation but have migratory capacity to lymph nodes and other secondary lymphoid organs, while central memory cells (CD45RA⁻CD27⁺, CM) are more sensitive to antigenic stimuli, but are less proliferative. On the other hand, effector memory cells (CD45RA⁻CD27⁻, EM) are rapidly proliferating cells with rapid effector functions and secrete higher amounts of cytokine such as IFN γ , IL4, perforin and granzyme. CD45RA expressing effector memory cells (CD45RA⁺CD27⁻, TEMRA) are terminally differentiated cells with low proliferative capacity but highest cytotoxic activity by exerted secretion of cytolytic granules and IFN γ [281,282,283,284,285,286]. As shown in Figure 37, Zoledronate treated breast cancer patients showed a significant increase in effector memory RA⁺ subtype of $\gamma\delta$ T cells as compared to untreated breast cancer patients (p=0.0009) and HI (p=<0.0001). A significant reduction in percentages of central memory cells was observed in Zoledronate treated breast cancer patients as compared to untreated breast cancer patients (p= 0.0014) and HI (p= 0.0002). Zoledronate treated breast cancer patients also showed reduced percentages of naive $\gamma\delta$ T cells as compared to HI (p= 0.04). The data clearly showed conversion of central memory cells to effector memory cells after Zoledronate treatment. No significant changes in other subcellular populations of $\gamma\delta$ T cells were observed. .

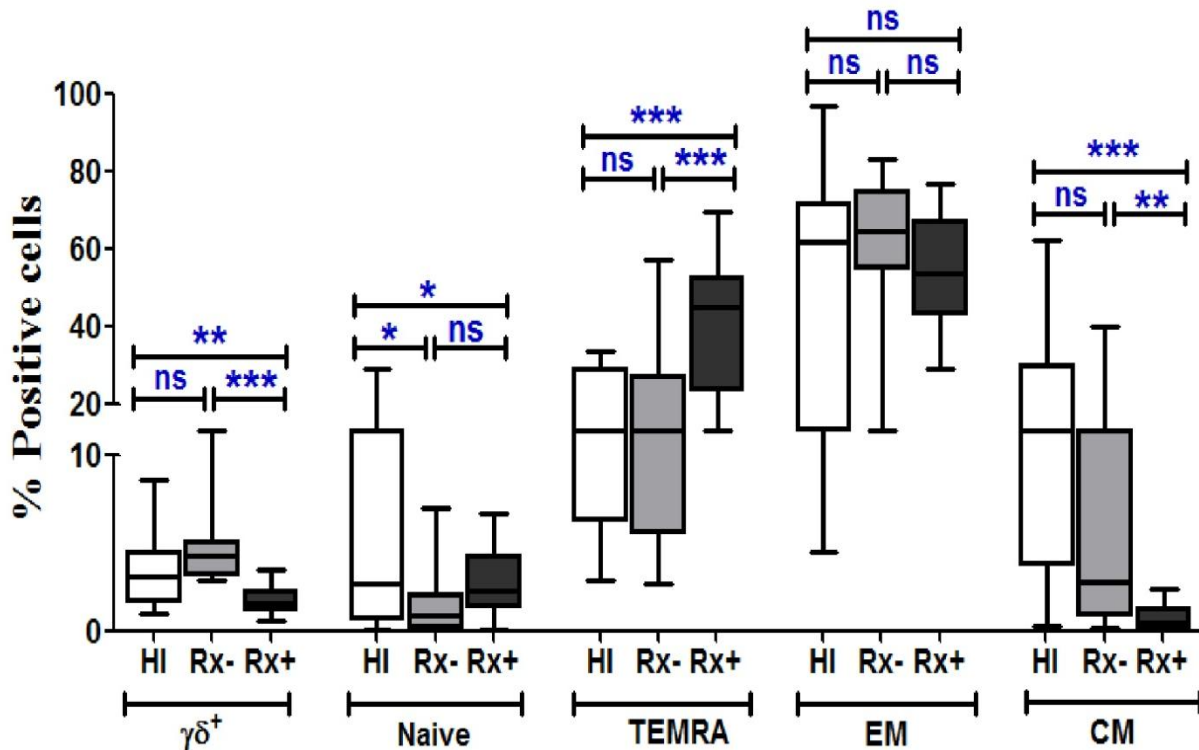


Figure 37: Effect of Zoledronate treatment on memory status of $\gamma\delta$ T cells

Memory status of $\gamma\delta$ T cells was analyzed by staining the PBMCs from HI (n=38), untreated breast cancer patients (Rx⁻, n=15) and Zoledronate treated breast cancer patients (Rx⁺, n=21) for $\gamma\delta$ TCR-FITC, CD45RA-PECy5 and CD27APC. $\gamma\delta$ T cells were gated and memory subsets were analyzed as central memory (CM, CD45RA⁻CD27⁺), naive (Naive, CD45RA⁺CD27⁺), terminally differentiated effector memory (TEMRA, CD45RA⁺CD27⁻) and effector memory (EM, CD45RA⁻CD27⁻) in gated population. Significance is given by p value as p<0.05(*), p<0.005(**), p<0.0005(***) and p \geq 0.05 (not significant/ns).

6.5) Effect of Zoledronate treatment on intracellular cytokine profile of $\gamma\delta$ T cells

To understand the effect of Zoledronate on effector function of $\gamma\delta$ T cells, expression of intracellular cytokines IFN γ and IL17 were measured in $\gamma\delta$ T cells at baseline and after *in vitro* stimulation with phorbol myristate acetate (PMA) and ionomycin using multicolor flow cytometry. PBMCs from HI (n= 38) and breast cancer patients who were on Zoledronate treatment (n= 21) and those who were not on Zoledronate treatment (n= 15) were stimulated with PMA+ Ionomycin or left untreated (in medium alone) for 6 hrs in the presence of Golgi-stop brefeldin-A. The PBMCs were further stained for $\gamma\delta$ TCR-FITC, IL17-PE and IFN γ -PECy7. Ca²⁺ ionophores induce increase in Ca²⁺ in treated cells by virtue of their ability to transport Ca²⁺ across biologic membranes. Calcium ionophores are mitogenic for PBMC and when synergize with direct PKC activators, such as phorbol esters activate in inducing T and B cell activation and proliferation [287,288]. As shown in Figure 38, it was observed that Zoledronate treated breast cancer patients showed notably increased percentages of $\gamma\delta^+$ IFN γ^+ T cells at baseline level as compared to Zoledronate untreated breast cancer patients (p=< 0.0001) or HI (p=< 0.0001). The percentages of $\gamma\delta^+$ IL17⁺ cells were not significantly different in the three groups i.e. HI, untreated and Zoledronate treated breast cancer patients when measured at baseline.

Upon stimulation of PBMCs from HI with PMA+Ionomycin, we found significant increase in $\gamma\delta^+$ IFN γ^+ T cells as compared to unstimulated $\gamma\delta$ T cells (p=< 0.0001), however, no significant changes were observed in $\gamma\delta^+$ IL17⁺ cell percentages upon stimulation. In case of Zoledronate untreated breast cancer patients, upon PMA+Ionomycin stimulation, percentages of $\gamma\delta^+$ IL17⁺ and $\gamma\delta^+$ IFN γ^+ T cells were found increased as compare to unstimulated $\gamma\delta$ T cells (p=0.008 and p=0.005, respectively). It was notable that, though there was increase in $\gamma\delta^+$ IFN γ^+ T cells upon antigenic stimulation, $\gamma\delta$ T from untreated breast cancer patients gave

moderate response as compared to HI and Zoledronate breast cancer patients. In case of Zoledronate treated breast cancer patients, a significant increase in $\gamma\delta^+IFN\gamma^+$ T cells was observed upon PMA+Ionomycin stimulation ($p=0.03$). Percentages of $\gamma\delta^+IL17^+$ cells were also found increased upon stimulation with PMA+Ionomycin in Zoledronate treated breast cancer patients, but the percentage of $\gamma\delta^+IFN\gamma^+$ T cells were remarkably higher (Figure 38). It clearly indicated that, $\gamma\delta$ T cells from Zoledronate treated breast cancer patients were functionally active and responded well upon receiving antigenic stimuli.

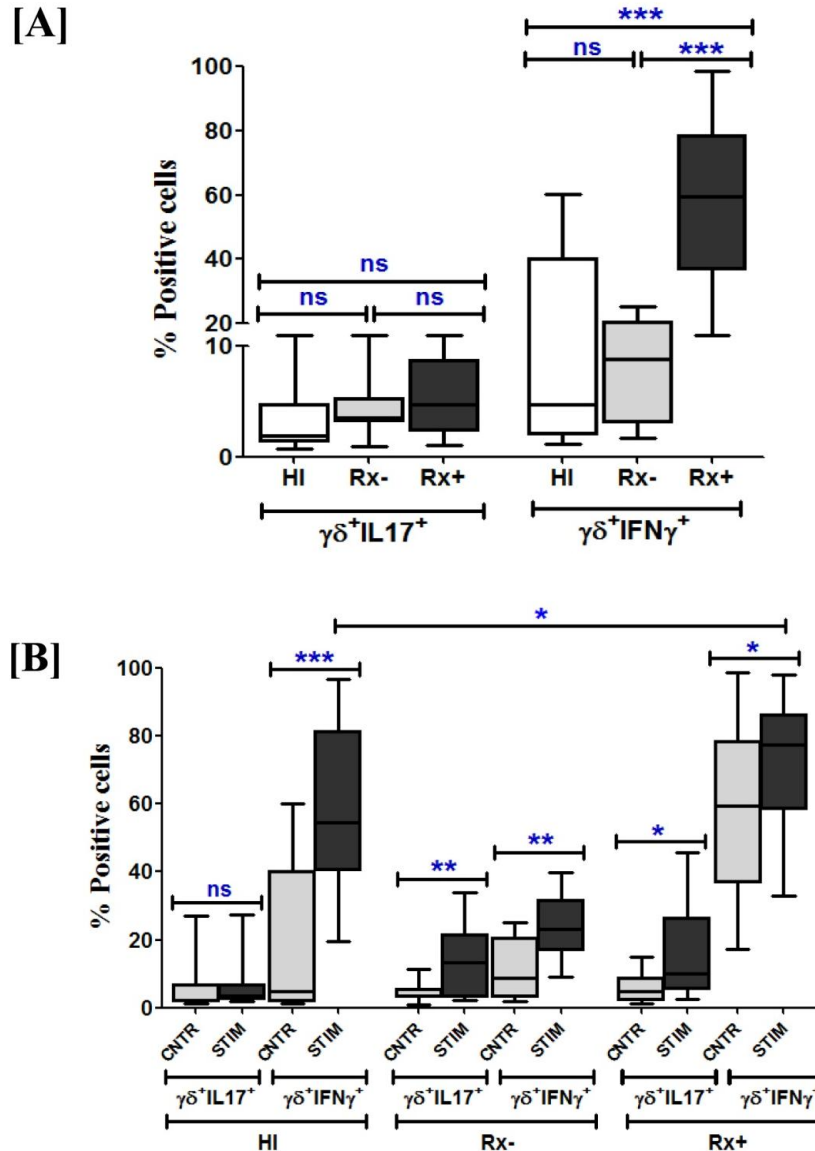


Figure 38: Intracellular cytokine profiling of Zoledronate treated breast cancer patients

PBMCs from HI (n= 38), untreated breast cancer patients (Rx⁻, n=15) and Zoledronate treated breast cancer patients (Rx⁺, n=21) were stimulated with PMA+Ionomycin for 6 hrs (STIM) or left in medium alone/control (CNTR) for 6 hrs in the presence of Golgistop brefeldin-A (5μg/ml). Percentages of γδ T cells showing expression of intracellular cytokines IFNγ and IL17 were analyzed by staining PBMCs for γδTCR-FITC, IL17-PE and IFNγ-PECy7. [A] Percentages of γδ T cells expressing intracellular cytokines IFNγ and IL17 were measured in control (CNTR) group. [B] Comparative analysis of experimental group medium alone (CNTR) and PMA+ Ionomycin (STIM) showing percentages of γδ T cells producing IFNγ and IL17. Significance is given by p value as p<0.05(*), p<0.005(**), p<0.0005(***) and p ≥0.05 (not significant/ns).

6.6) Cytokine profiling of cell free supernatants of $\gamma\delta$ T cells isolated from HI and breast cancer patients (Rx^- and Rx^+)

Besides measuring intracellular cytokines in $\gamma\delta$ T cells, we also analyzed cytokines in the cell free supernatants of purified $\gamma\delta$ T cells isolated from HI (n=5) and breast cancer patients who were on Zoledronate treatment (Rx^+ , n=5) or without Zoledronate treatment (Rx^- , n=5). PBMCs from HI, untreated breast cancer patients (Rx^-) and Zoledronate treated breast cancer patients (Rx^+) were expanded using $\alpha CD3/CD28+rhIL2$ for 12 days and $\gamma\delta$ T cells were immunomagnetically separated (materials and methods section 3.6.2). Purified $\gamma\delta$ T cells were rested overnight and then cultured in medium alone for 24 hrs and cell free supernatants were collected. These cell free supernatants were analyzed for Th1/Th2/Th17 cytokines (IL2, IL4, IL6, IL10, TNF α , IFN γ and IL17) by cytometric bead array. As shown in Figure 39, cell free supernatants of $\gamma\delta$ T cells from untreated breast cancer patients (Rx^-) showed significantly higher levels of IL6 (pro-tumorigenic and pro-osteoclastogenic) as compared to HI. However a remarkable reduction in IL6 levels (p=0.0002) was noted in cell free supernatants of $\gamma\delta$ T cells from Zoledronate treated breast cancer patients (Rx^+) as compared untreated breast cancer patients and HI. Cell free supernatants of $\gamma\delta$ T cells from HI and untreated breast cancer patients did not show any significant differences in the levels of IFN γ . However, levels of IFN γ were found significantly reduced in Zoledronate treated breast cancer patients compared to Zoledronate untreated breast cancer patients (p=0.009). We also found significant reduction in levels of IL10 (immunosuppressive anti-inflammatory cytokine) in cell free supernatants of Zoledronate treated breast cancer patients as compared to untreated breast cancer patients (p<0.0001). Concentrations of other cytokines detected in cell free supernatants of $\gamma\delta$ T cells isolated from HI, Rx^- and Rx^+ are provided in Table 18.

Significant changes in cytokine IL6 was observed when comparisons were made between $\gamma\delta$ T cells HI and Rx-, Rx- and Rx+. Similarly, IL10 was reduced in Rx+ as compared to Rx- group.

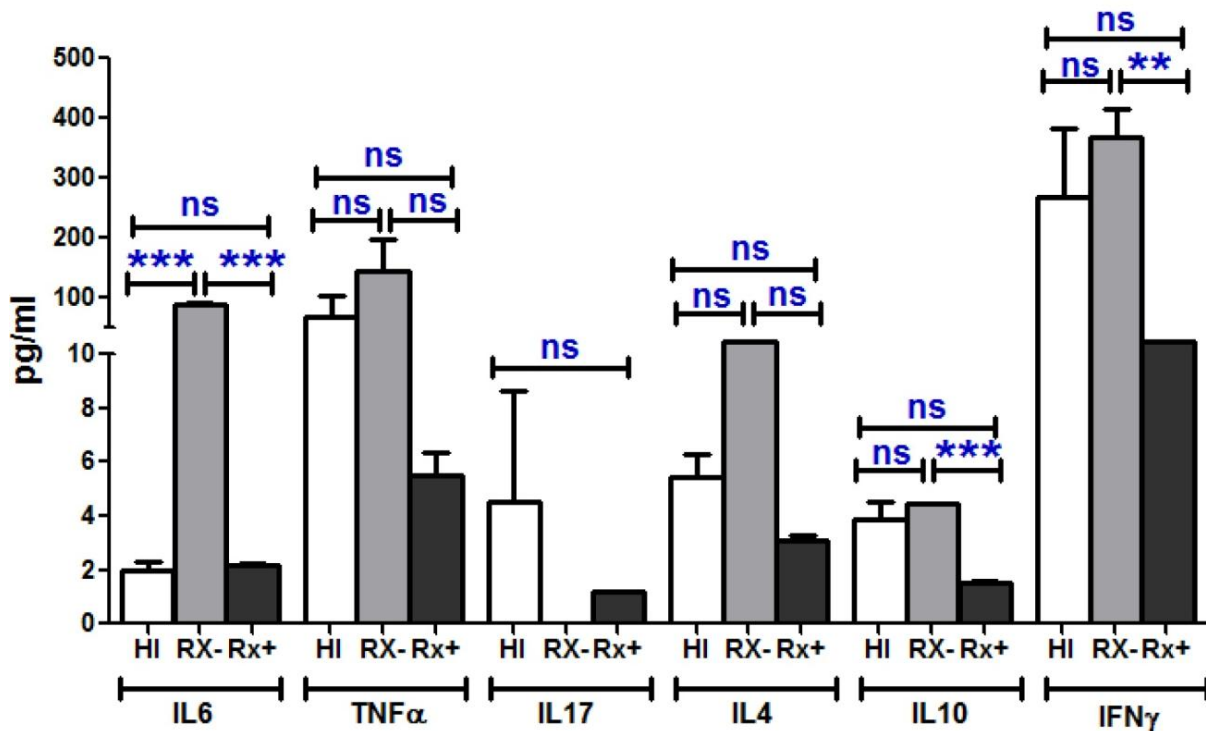


Figure 39: Estimation of Th1/Th2/Th17 cytokines in cell free supernatants of HI and breast cancer patients

PBMCs separated from healthy individuals (n= 5), breast cancer patients who were not on Zoledronate treatment (RX⁻, n=5) and those who were Zoledronate treatment (Rx⁺, n=5). These PBMCs were expanded using α CD3/CD28+rhIL2 for 12 days and $\gamma\delta$ T cells were immunomagnetically separated. Purified $\gamma\delta$ T cells were rested overnight and then cultured in medium alone for 24 hrs. After 24 hrs, cell free supernatants were collected and were analyzed for Th1/Th2/Th17 cytokines (IL2, IL4, IL6, IL10, TNF α , IFN γ and IL17) by cytometric bead array. Significance is given by p value as p<0.05(*), p<0.005(**), p<0.0005(***) and p \geq 0.05 (not significant/ns).

Table 18: Cytokine profiling of cell free supernatants of antigen activated $\gamma\delta$ T cells

Cytokine levels secreted by α CD3/CD28+rhIL2 expanded $\gamma\delta$ T cells									
	HI (n=5)	Rx ⁻ (n=5)	P value	HI (n=5)	Rx ⁺ (n=5)	P value	Rx ⁻ (n=5)	Rx ⁺ (n=5)	P value
IL2	2.7 ± 0.9	3.7 ± 1.3	ns	2.7 ± 0.9	3.1 ± 0.1	ns	3.7 ± 1.3	3.1 ± 0.1	ns
IL4	5.4 ± 0.8	11.2 ± 9.0	ns	5.4 ± 0.8	3.1 ± 0.2	ns	11.2 ± 9.0	3.1 ± 0.2	ns
IL6	1.9 ± 0.3	89.6 ± 3.2	***	1.9 ± 0.3	2.2 ± 0.06	ns	89.6 ± 3.2	2.2 ± 0.1	***
IL10	3.8 ± 0.6	4.4 ± 0.04	ns	3.8 ± 0.6	1.5 ± 0.03	ns	4.4 ± 0.04	1.5 ± 0.03	***
TNFα	67.5 ± 37.04	143.9 ± 55.5	ns	67.5 ± 37.04	5.5 ± 0.9	ns	143.9 ± 55.5	5.5 ± 0.9	ns
IFNγ	274.1 ± 111.2	369.0 ± 45.4	ns	274.1 ± 111.2	20.1 ± 6.5	ns	369.0 ± 45.4	20.1 ± 6.5	**
IL17	4.5 ± 4.1	0	-	4.5 ± 4.1	1.2 ± 0.03	ns	0	1.2 ± 0.03	-

Table 18: PBMCs separated from healthy individuals (HI, n=5) and breast cancer patients who were on Zoledronate treatment (Rx+, n=5) and those who were not on Zoledronate treatment (Rx-, n=5) were expanded for 12 days using α CD3/CD28+rhIL2. Further, $\gamma\delta$ T cells were immunomagnetically purified, rested overnight and cultured in medium alone for 24 hrs. Cell free supernatants were collected and TH1/Th2/Th17 cytokines were analysed using cytometric bead array. Significance is given by p value as p<0.05(*), p<0.005(**), p<0.0005(***) and p \geq 0.05 (not significant/ns).

In conclusion, it was observed that, Zoledronate improves antitumor immune responses by increasing the pool of CD8⁺ T cells and effector memory $\gamma\delta$ T cells. Activated $\gamma\delta$ T cells (CD25⁺) showed a marked increase in the intracellular levels of IFN γ which explains their ability to mediate antitumor responses. Interestingly, Zoledronate treatment was also found to reduce IL6 secretion by $\gamma\delta$ T cells, a potent pro-osteoclastogenic cytokine (chapter 4). The study highlights a new role of Zoledronate in breast cancer patients that can be explored further.

Chapter 7

Discussion

Bone is the preferential site of metastasis in breast cancer, prostate cancer and multiple myeloma [38,289]. Metastasized tumor release factors which induce differentiation and activation of osteoclasts [43]. Cytokines secreted by lymphocytes present in the bone microenvironment affect bone and disturbs the normal bone metabolism, which is otherwise a very ordinate process [253,290]. The process of bone remodeling is majorly influenced by soluble factors (cytokine, chemokines and soluble proteins) secreted by osteoblasts, stromal cells, tumor cells and immune cells present in bone microenvironment [44]. Aminobisphosphonates are used for the treatment skeletal related events associated with bone metastasis such as breast cancer [52]. Effect of these aminobisphosphonates on tumor cells and immune cells is not well understood. Activated CD4⁺ T cells are known to play pro-osteoclastogenic role through expression of RANKL and cytokines such as IL1 β , IL6, IL17, TNF α and RANKL [29,30,45,47]. Interestingly, it has also been reported that activated T lymphocytes secrete cytokines such as IFN γ , IL4, IL10 and GM-CSF that inhibit osteoclastogenesis [31,32]. It is still not understood what dictates the pro and anti-osteoclastogenic behavior of the lymphocytes. Although the role of CD4⁺ $\alpha\beta$ T cells in osteoclastogenesis has been investigated, the role of $\gamma\delta$ T cells is not well understood. The objective of the present thesis is to investigate how $\gamma\delta$ T cells interact with osteoclasts and influence their function and further investigate how aminobisphosphonate influence $\gamma\delta$ T cells and cytokine dynamics in breast cancer patients.

$\gamma\delta$ T cells are a unique subset of T cells, which harbor properties of both innate and adaptive immune cells [233]. They represent <10% of the total T cell population, where >90% population resides in peripheral blood and expresses V γ 9V δ 2 TCR. $\gamma\delta$ T cells possess unique properties with respect to antigen recognition, tissue tropism, MHC-independent antigen

recognition and antitumor response [74]. $\gamma\delta$ T cells recognize unique antigens, different from conventional $\alpha\beta$ T cells, which include small phosphoantigens such as isopentenyl pyrophosphate (IPP) and (E)-4-Hydroxy-3-methyl-but-2-enyl pyrophosphate (HMBPP), phospholipids, heat shock proteins, alkylamines and aminobisphosphonates [72]. IPP is an intermediate molecule in eukaryotic mevalonate/ cholesterol pathway, while HMBPP is an intermediate molecule in bacterial non-mevalonate/ Rohrer pathway. Aminobisphosphonate (Zoledronate), a class of potent antiresorptive drug, is used as a standard treatment modality to treat postmenopausal osteoporosis and cancer patients with bone metastasis. $\gamma\delta$ T cells are Th1 type cells but are extensively plastic and differentiate into different subsets like Th2, Th17, T-follicular helper and T-regulatory cells under different pathological conditions, producing different sets of cytokines [13]. $\gamma\delta$ T cells have been appreciated for their role in antitumor cytotoxicity [15,16], wound healing and tissue repair [17,18,19] and thus have generated much interest in recent years. These cells produce several cytokines like IL17, IL6, IL10, TNF α , IFN γ and RANKL depending on their activation status. Many of these factors are known to influence bone metabolism. Most of the $\gamma\delta$ T cell based studies, in context of osteoimmunology, have been done in patients of rheumatoid arthritis (RA) and multiple myeloma [28,291]. Their presence has been demonstrated in bone microenvironment, in synovial fluids of rheumatoid arthritis patients and at bone fracture sites [28,292]. Various groups have also shown presence of chemokine receptors like CCL5 and CCR1 on $\gamma\delta$ T cells, which indicate their propensity to migrate to bone. It has been reported that, Th17⁺ cells, and not IL17⁺ $\gamma\delta$ T cells drive arthritic bone destruction in RA patients [28]. In contrast, another report shows that, IL17⁺ producing $\gamma\delta$ T cells are increased in synovial fluids and peripheral blood of RA patients [292]. Also, RA patients have shown changes in $\gamma\delta$ T cell subpopulations and their phenotypes [293,294]. Recently, IL17 producing $\gamma\delta$

T cells were shown to promote bone formation and facilitate bone fracture healing [295]. However, role of $\gamma\delta$ T cells in fracture healing has remained controversial as $\gamma\delta$ T cell deficient mice had shown stable fracture repair and better biochemical strength of bone [296]. Therefore, the role of $\gamma\delta$ T cells is not well understood in bone metabolism. The present study was therefore an attempt to analyze the effect of “activated” and “freshly isolated” $\gamma\delta$ T cells on osteoclast generation and function.

We used $\gamma\delta$ T cells from two sources; those that were isolated directly from PBMCs (“freshly isolated” $\gamma\delta$ T cells) and those that were isolated from PBMCs stimulated with α CD3/CD28+rhIL2 (“activated” $\gamma\delta$ T cells). Coculture of “freshly isolated” $\gamma\delta$ T cells with CD14⁺ cells enhanced the generation of osteoclasts and stimulated their resorptive ability. On the contrary, “activated” $\gamma\delta$ T cells showed inhibitory effect on generation and function of osteoclasts. The process of osteoclastogenesis is majorly influenced by cytokine milieu in the microenvironment, where IL6, IL17, TNF α , TGF β , IFN γ and RANKL play indispensable role. Analysis of cell free supernatants of “freshly isolated” $\gamma\delta$ T cells at baseline levels (unstimulated) showed marked difference in their IL6 and IFN γ levels. In an unstimulated state, “freshly isolated” $\gamma\delta$ T cells were major producers of IL6, with negligible levels of IFN γ . IL6 is a potent pro-osteoclastogenic cytokine, with the capacity to induce osteoclastogenesis in RANKL independent manner [176] and it also acts in synergistic manner with TNF α to induce osteoclastogenesis [297]. IL6 has been reported to stimulate formation of osteoclast like multinucleated cells in long term cultures of human bone marrow through induction of IL1 β [48]. T lymphocytes from IL6^{-/-} mice have shown lesser production of IL17 (pro-osteoclastogenic) and also affected RANKL/OPG production by T lymphocytes [298]. Cultures of osteoclasts from bone marrow cells of IL6^{-/-} mice in the presence of MCSF and RANKL

produced ~50% lesser osteoclasts as compared to wild type mice [298]. On the contrary, IFN γ has been appreciated for its protective role in osteoclastogenesis by inhibiting osteoclast formation and bone resorption in vitro [51,299]. Mice lacking one of the components of IFN γ receptor (IFN γ R1) showed enhanced osteoclastogenesis from bone marrow derived monocyte/macrophage precursor cells (BMMs) and bone loss[51]. Also, IFN γ producing activated T cells showed osteoclast generation from BMMs in the absence of RANKL in IFN γ R^{-/-} mice[51]. IFN γ either downregulates TRAF6 (TNF receptor associated factor 6) expression or activates/ enhances ubiquitin dependent proteosomal systems whose direct target is TRAF6 [51,300], which results in disruption of RANK-RANKL signaling. We observed that “activated” $\gamma\delta$ T cells secreted significantly higher levels of IFN γ and negligible levels of IL6. In order to confirm that IL6 and IFN γ are the key cytokines involved in the pro and anti-osteoclastogenic effects mediated by “freshly isolated” and “activated” $\gamma\delta$ T cells respectively, neutralization experiment was carried out using α IL6 and α IFN γ antibodies. Addition of α IL6 antibody to the supernatants of “freshly isolated” $\gamma\delta$ T cells showed a marked reduction in the resorption area. However, the resorption area remained marginally above that was observed with positive control (rhMCSF+rhRANKL). The data indicates that other cytokines like TNF α and IL17 may also contribute to the pro-osteoclastogenic effect, which may be present in the supernatants after blocking IL6. Similarly blocking of IFN γ significantly reversed (90%) the anti-osteoclastogenic effect, indicating that IFN γ is the dominant cytokine inhibiting osteoclastogenesis.

Human $\gamma\delta$ T cells are Th1 type cells which produce copious amounts of IFN γ upon stimulation [301,302,303]. BrHPP (analog of IPP) and Zoledronate (aminobisphosphonate), potent antigen of $\gamma\delta$ T cells, were used to stimulate “freshly isolated” $\gamma\delta$

T cells in the presence of rhIL2. Upon stimulation with BrHPP+rhIL2 and Zoledronate +rhIL2 the activation markers (CD69, CD25 and RANKL) on these cells were found to be increased compared to unstimulated $\gamma\delta$ T cells. CD69, an early activation marker, is expressed on T cells upon triggering through TCR complex [304]. T cell activation through CD69 results in upregulation of CD25 and induction of Th1 cytokine (IL2 and IFN γ), ultimately triggering proliferation of the lymphocytes [305]. As expected, higher levels of IFN γ along with increased expression of activation markers (CD25 and RANKL) were observed on “activated” $\gamma\delta$ T cells (which were expanded using α CD3/CD28+rhIL2 or Zoledronate+rhIL2), while no significant change was observed in early activation marker CD69. “Freshly isolated” $\gamma\delta$ T cells upon stimulation with BrHPP+rhIL2 showed increase in IFN γ production, along with significant increase in early activation markers like CD69 and RANKL. Zoledronate treated “freshly isolated” $\gamma\delta$ T cells” showed remarkable higher levels of CD69 expression along with increased IFN γ secretion. As Zoledronate induces apoptosis in osteoclasts [10], activation of $\gamma\delta$ T cells in coculture assays was carried out by addition of BrHPP. “Freshly isolated” $\gamma\delta$ T cells stimulated with BrHPP+rhIL2, irrespective of short or long term activation, showed inhibitory effect on generation (vitronectin receptor expression) and resorptive ability (resorption area on OAAS plates) of osteoclasts. Thus, “freshly isolated” $\gamma\delta$ T cells stimulated with phosphoantigen (BrHPP+rhIL2) exhibited the characteristics of “activated” $\gamma\delta$ T cells to suppress osteoclast generation and function.

Our study has shown that activation status and the cytokines released by $\gamma\delta$ T cells dictates their effect on osteoclastogenesis. Zoledronate activate $\gamma\delta$ T cells which function as anti-osteoclastogenic cells. Thus apart from exhibiting anti-osteoclastogenic activity [52], Zoledronate also prevents osteoclastogenesis through activated $\gamma\delta$ T cells. This data adds a new

dimension towards understanding the crosstalk of $\gamma\delta$ T cells and osteoclasts mediated by Zoledronate.

Besides its anti-resorptive ability, Zoledronate also has antitumor activity. It is well reported that, Zoledronate induces apoptosis in breast tumor cells [10,59,60,78,214,306]. Studies from our laboratory have shown that breast tumor cells treated with Zoledronate *in vitro* are aggressively lysed by $\gamma\delta$ T cells [26] compared to untreated cells. These results prompted us to look at the changes in protein profiles of breast tumor cells after Zoledronate treatment. We therefore used two proteomic approaches- MALDI/TOF-TOF and LC-MS, to compare the protein profiles of MCF7 breast cancer cells before and after treatment with Zoledronate.

A normal cell metabolism involves nonspontaneous, energy-consuming processes such as generation of concentration gradients, cytoskeletal dynamics, DNA repair, basal transcription and translation, protein turnover and vesicle trafficking [307]. These cellular requirements are fulfilled through multiple pathways. In the present study we observed that, Zoledronate treated MCF7 cells showed changes in expression of proteins associated with crucial metabolic pathways including glucose and fatty acid metabolism, cytoskeletal reorganization, cell cycle progression, protein synthesis, trafficking and degradation, copper homeostasis, apoptosis induction, epidermal growth factor receptor (EGFR) trafficking. We observed a significant increase in 6-phosphofructokinase (PFK) and α -enolase (enzymes involved in glycolytic pathway) in Zoledronate treated MCF7 cells. PFK catalyzes the first committing step of glycolysis (phosphorylation of D-fructose 6-phosphate to fructose 1,6-bisphosphate by ATP), while α -enolase catalyses the penultimate step of glycolysis (conversion of 2-phosphoglycerate to phosphoenolpyruvate). Interestingly, we also found increase in expression of cytochrome c oxidase assembly factor 3 and 4, with significant decrease in expression of

NADH dehydrogenase 1 beta subunit complex. NADH: ubiquinone reductase is the first enzyme of the mitochondrial electron transport chain. It is located in inner mitochondrial membrane and also known to largest of five complexes. Downregulation of protein or mutation in NADH dehydrogenase 1 gene leads to mitochondrial dysfunction [308]. While expression of assembly subunits of cytochrome c oxidase (COX) enzyme, involved in mitochondrial phosphorylation, were found to be upregulated. Eukaryotic COX is a multimeric enzyme of dual genetic origin (13 subunits, 3 coded by mitochondrial genes and 10 by nuclear genes), whose assembly is a complicated and highly regulated process. More than 20 assembly proteins are required for the assembly of this protein. It is the last enzyme in mitochondrial respiratory chain [309]. Cytochrome c oxidase shuttles electrons from cytochrome c to molecular oxygen to capture energy in the membrane potential by asymmetric proton uptake and proton pumping [310]. Cytochrome c oxidase assembly factor 3 and 4 plays a critical role in the biogenesis and activity of cytochrome c oxidase. Overall it indicated that, Zoledronate treated tumor cells showed increase in glycolytic enzymes and reduced the key enzyme in mitochondrial phosphorylation chain. To the best of our knowledge, this is the first study showing the differentially expressed proteins in MCF7 cells after Zoledronate treatment that regulate key pathways related to glycolysis and mitochondrial phosphorylation.

Zoledronate treatment significantly downregulated expression of two crucial proteins involved in lipid metabolism. Zoledronate treated MCF7 cells showed a significant downregulation of fatty acid desaturase 2 enzyme, which catalyses first and rate limiting step in biosynthesis of polyunsaturated fatty acid from its precursors. These highly unsaturated fatty acids play pivotal roles in many biological functions. Expression of GM2 activator protein (GM2AP) and PEX19 was found downregulated in Zoledronate treated MCF7 cells. For cellular

membrane homeostasis, lysosomal digestion of membranes is essential. Glycosphingolipids are present in cell membrane and functions as antigens, mediators of cell adhesion, and modulators of signal transduction [311]. Breakdown-products of glycosphingolipids are continuously recycled and re-utilized in salvage processes [312]. After endocytosis, glycosphingolipids are degraded on the surface of intralysosomal membranes in a sequential pathway in a stepwise manner, with the assistance of small glycoprotein cofactors like GM2A protein [313]. GM2A is a small glycolipid transport protein which acts as a substrate specific co-factor for β -hexosaminidase A enzyme present in the lysosome. GM2 ganglioside activator and β -hexosaminidase A enzyme together catalyzes degradation of ganglioside GM2, and other terminal N-acetyl hexosamines containing molecules. It binds to ganglioside GM2, extracts them from membranes and presents them to β -hexosaminidase A for cleavage. It is proposed that, GM2-activator contains a hydrophobic cavity for binding of the ceramide portion of GM2 or other lipids. In an open conformation, the empty activator binds to the membrane with the aid of hydrophobic loops and penetrates into the hydrophobic region of the bilayer. The lipid recognition site of the activator can interact with the substrate, and its ceramide moiety moves inside the hydrophobic cavity. The lipid loaded activator can change to the closed conformation, becomes more water soluble and might leave the membrane. In solution or at the membrane surface, it present gangliosides GM2 or GM1 to water-soluble hydrolases such as β -hexosaminidase A [313]. Apart from ganglioside GM2, GM2AP can also extract other lipids, in a pH-dependent fashion from membranes. GM2-activator acts as a lipid transfer protein that can carry lipids from donor to acceptor liposomes *in vitro* [314]. The enzymatic, lysosomal degradation of the ganglioside GM2 is catalyzed by β -hexosaminidase A (HexA) and requires the GM2A protein as cofactor [313,315]. Defects or mutations in the genes of the subunits α and

β or the gene encoding the GM2AP lead to the various forms of GM2 gangliosidosis [316]. GM2A protein can also activate T cells through lipid presentation.

Expression of Pex19 protein, which plays indispensable role in peroxisome biogenesis, was found significantly reduced in Zoledronate treated MCF7 cells. Pex19 acts as chaperone keeping newly synthesized membrane proteins in import-competent conformations and is required for the import and/or membrane assembly of numerous peroxisomal membrane proteins. Pex19 are required for proper localization and stability of peroxisomal membrane proteins. Peroxisomes function as sites for biosynthesis of ether phospholipids (plasmalogens), cholesterol and bile acids, polyunsaturated fatty acids and degradation of amino acids, purines, α -oxidation of fatty acids, β -oxidation of fatty acids, decomposition of hydrogen peroxide. Pex19 is farnesylated form and is found predominantly in the cytosol but also on peroxisomal membranes [317,318,319]. Pex19 interacts with many integral membrane proteins and also with some peripheral membrane proteins [317,319,320,321]. Farnesylation of Pex19 protein is necessary for its structural integrity and to recognize membrane proteins during peroxisome biogenesis [322]. Cells lacking Pex19 are either rapidly degraded in the cytosol or mislocalized to mitochondria [317,319,320]. Thus in the absence of Pex19, cells lack functional peroxisomes [317,318,323].

Zoledronate inhibits farnesyl pyrophosphate synthase enzyme in mevalonate pathway, an exclusive route of isoprenoid production in eukaryotes, involved in cholesterol biosynthesis and synthesis of intermediates important for intracellular signaling and growth control [324]. Inhibition of FPPS enzyme causes a reduction in farnesyl pyrophosphate (FPP) and geranylgeranylpyrophosphate (GGPP), which leads to impaired prenylation and defective intracellular localization of GTPase signaling proteins such as Ras, Rho and Rac [325]. We

observed a significant upregulation in expression of RhoB in Zoledronate treated MCF7 cells. RhoB is small GDP/GTP binding GTPase, which belongs to Rho family and shares 86% sequence similarity with RhoA, but their functions are completely different. Other GTPases (RhoA, Ras, Rac1 and cdc42) promotes oncogenesis, invasion and metastasis [326,327,328,329,330,331,332,333]. RhoB have tumor suppressive role and has been reported to inhibit cell proliferation, induce apoptosis and inhibit tumor growth in a nude mouse xenograft model [334,335,336, 337]. Farnesyltransferase inhibitors (FTIs) like aminobisphosphonates and geranylgeranyltransferase I inhibitors (GGTIs) have been shown to upregulate RhoB protein expression by increasing transcription of RhoB through increase in histone deacetylase 1 (HDAC1) dissociation, histone acetyltransferase (HAT) association and histone acetylation of the RhoB promoter in number of human cancer cells (breast, pancreatic, lung, colon, bladder and brain cancers) [338]. Treatment of cells with FTIs reduces farnesylated form of RhoB, with concomitant increase in geranylgeranylated form (RhoB-GG), which is associated with loss of growth-promoting activity [335]. Geranylgeranylated form of RhoB supports the FTI associated inhibition of cell growth by inducing phenotypic reversion, cell growth inhibition, and activation of the cell cycle kinase inhibitor p21WAF1 [335,336]. In tumors, expression of RhoB was found to be reduced with increase in aggressiveness of the tumors [339,340,341]. RhoB has been noted to be an essential factor for the apoptotic response of neoplastic cells to DNA damage [334]. RhoB has been shown to block ability of Ras/PI3K/Akt pathway to activate NF κ B inhibit [342]. These pathways are involved in uncontrolled proliferation and tumor survival. Oncogenes EGFR, ErbB2 and Ras oncogenes suppress RhoB expression through PI3K/Akt pathway which leads to malignant transformation [342,343].

Our interactome analysis using STRING software showed some proteins associated with EGFR trafficking. EGFR is a transmembrane tyrosine kinase receptor and functions in proliferation, survival and migration of both normal and cancerous cells [344]. EGFR ligands (EGF, transforming growth factor- α (TGFA), heparin-binding EGF-like growth factor, amphiregulin, betacellulin, epiregulin and epigen) binding to the inactive monomeric EGFR leads to homodimerisation or heterodimerisation (with any of the other ErbB family members like ERBB2/Her2, ERBB3/ Her3, and ERBB4/ Her4) [345]. EGFR and HER2 is the most common heterodimers, while HER2:3 plus neuregulin is the most potent combination [344]. Binding of ligand to EGFR triggers internalization and subsequent degradation of ligand-EGFR complex, desensitizing the cells from mitotic signals. Ligand binding causes recruitment of active ligand-receptor complexes to clathrin coated vesicles/pits (CCPs) and dynamins carries out vesicle fission from the plasma membrane [346]. These CCPs further gets fused to early endosomes. From there, free EGFR is either recycled back to cell surface or ligand bound EGFR gets sorted into internal vesicles of multivesicular bodies (MVBs) [347]. Early endosomes mature into late endosomes, where EGF-EGFR complexes accumulate in internal vesicles of MVBs [348], preventing interaction of EGFR with its cytoplasmic targets. Subsequently late endosomes fuses with pre-existing lysosomes causing lysosomal protease mediated degradation of ligand-EGFR complexes. EGFR signaling pathway is attenuated by internalization of the ligand-EGFR complex. Internalization is not necessarily an attenuation process itself [349], but EGFR needs to be degraded. An impaired or ineffective EGFR degradation pathway plays a major role in increased ErbB-signaling leading to cancer development. In various cancers dysregulated EGFR pathway has been shown due to constitutive overexpression, overstimulation or mutational activation of EGFR [350]. EGFR overexpression in breast cancer has been

reported and anti-EGFR targeted therapies are also used in such cancers [351]. Control of EGFR signaling is either by neutralizing monoclonal antibodies (cituximab, panitumumab) and small-molecule tyrosine kinase inhibitors targeted as therapeutic strategy [344]. Potential of EGFR degradation for therapeutic purpose have been considered as promising approach for treatment of cancer [352]. We observed that, Zoledronate treatment increased expression of protein involved in EGFR internalization, endosomal and multivesicular body (MVB) sorting and lysosomal degradation. Zoledronate treated MCF7 showed upregulated expression of RhoB and SNX1, whose involvement in degradation is very well reported [271,348,352]. Thus, reduction in EGFR expression upon Zoledronate treatment in MCF7 cells has unraveled a novel therapeutic target and added a new dimension to the mechanism of action of Zoledronate.

Zoledronate treatment also affected cell cycle progression in breast tumor cells (MCF7 and MDAMB231). Cell cycle is vital and tightly controlled event by which cells divides to produce two daughter cells. It is crucial for the cell to detect and repair genetic damages, which otherwise may leads to cell death, apoptosis or uncontrolled cell division. DNA repair processes and cell cycle checkpoints regulate genome stability and cell cycle progression respectively [353]. Deregulation of the cell cycle components may lead to uncontrolled cells division and tumor formation [354]. Expression of proteins associated with initiation of DNA replication, chromatin remodeling and DNA repair were found significantly downregulated upon Zoledronate treatment in MCF7 cells. Zoledronate treated MCF7 cells showed significant downregulation in expression of α -centractin, which is involved in G2-M transition of cell cycle. In the present study we observed that, MCF7 cells upon Zoledronate treatment showed S-phase arrest, while MDAMB231 largely arrested the G0-G1 phase.

Cytoskeleton essentially provides a structural framework/scaffold to the cell, organizes cell cytoplasm and is important for cell movement. Using confocal microscopy and immunoblotting we demonstrated that, Zoledronate treated MCF7 cells showed thinning of cytokeratin 8 filaments, while total protein expression (western blotting) remained unaltered. Expression of tubulin was also found increased upon Zoledronate treatment in MCF7 cells. Zoledronate preferentially affected actin reorganization compared to other two cytoskeletal elements. Actin cytoskeleton is an essential in multiple biological functions which include cell contraction, cell motility, vesicular trafficking, intracellular organization, cytokinesis and apoptosis [262]. Zoledronate restricted polymerization of actin by increasing level of arpin and inhibiting expression of proteins involved in actin polymerization process such as ARP3/2, WASF2 and WASL. WASF2 and WASL are Wiskott-Aldrich syndrome (WAS) family proteins which associate with a variety of signaling molecules to alter the actin cytoskeleton. WASP family proteins bind to ARP2/3 proteins and activate them [355]. ARP2/3 protein acts as actin nucleation core protein and organizes actin filaments into a branching network with filament ends attached to the sides of other filaments at a fixed angle (70°) [356]. Binding of arpin to Arp2/3 complex inhibits actin filament nucleation [356]. Role of actin as initiator and mediator of apoptosis is very well discussed [262,357]. Sudden actin derangement has been shown to induce cellular apoptosis [262,358,359,360]. Actin disruption also leads to aberrant mitochondrial morphology and distribution [361,362]. In tumor cell, inhibition of actin polymerization by cytochalasin D induced the apoptosis by receptor clustering of CD95 (FasL) with aggregated nonfilamentous actin [357]. Treatment of mammalian cells with actin polymerization inhibitors induced caspase mediated cytochrome C releases indicating that actin also regulates mitochondrial membrane permeability [262]. It was reported that actin

cytoskeleton regulates the subcellular compartmentalization of death effector molecules, while disruption actin cytoskeleton leads to up-regulation of caspase-3 protease activity and increased accessibility of active caspase-3 to its substrate, ultimately leading to apoptotic cell death [363]. In an another report, cytoskeleton disruption in the apoptotic cells promoted damage to mitochondrial membrane and resulted in the enhanced release of cytochrome c necessary for the activation of caspase-9, which initiates the pro-apoptotic caspase cascade [364]. It was observed that, Zoledronate also induced expression of other apoptosis inducing proteins, which involved mainly the cytochrome C oxidase assembly protein subunits, catenin- β , MAPK activating protein and RhoB.

Essential cellular enzymes require microelements like copper as a cofactor. Copper is an essential micronutrient and is required for important cellular processes like mitochondrial respiration, iron metabolism, biosynthesis of neurotransmitter, and free radical detoxification, indicating its vital function [365]. Cut family proteins (cutA, cutB, cutC, cutD, cutE, and cutF) are associated with copper homeostasis and involved in uptake, storage, delivery, and efflux of copper [366]. Zoledronate treated MCF7 cells showed significant upregulation in expression of CutA protein while expression of CutC protein was found reduced. CutA is a copper binding protein, while CutC protein plays an important role in the intracellular trafficking of Cu(I) [366,367,368]. Overexpression of CutA isoforms sensitized HeLa cells to copper-induced apoptosis [369]. CutC protein is conserved from bacteria to mammals and is expressed ubiquitously in all the tissues [366]. CutC protein is involved in intracellular trafficking of Cu (I). Biologically human CutC protein behaves as an enzyme involved in copper homeostasis using Cu(I) as a cofactor rather than a copper transporter [366]. Knockdown of CutC gene has been shown to cause copper sensitivity in cells and induced apoptosis [370]. Upregulation of

copper binding protein CutA and downregulation of copper export protein CutC would create an imbalance in intracellular copper distribution or metabolism. Excessive copper damages lipids and proteins [371,372]. Zoledronate induced changes in expression of CutA and CutC protein would make the cells susceptible to copper-mediated metal stress, eventually causing cells to undergo apoptosis. Increase in copper inside the cells causes apoptosis in cell due to copper toxicity [373]. This adds a new aspect to our understanding of the mechanism of action of Zoledronate not reported earlier.

Apart from these effects, Zoledronate also exposed the breast tumor cells to the lytic action of $\gamma\delta$ T cells and other immune cells. Zoledronate inhibits farnesyl pyrophosphate synthase enzyme of eukaryotic mevalonate pathway, thus intracellular levels of isopentenyl pyrophosphate (IPP) increases [374,375]. IPP is a known activator of $\gamma\delta$ T cells [75] and also acts as chemotactic molecule for $\gamma\delta$ T cells [256]. Interestingly, Zoledronate treated MCF7 cells showed significant upregulation (2 fold) of “diphosphomevalonate decarboxylase” enzyme. This enzyme catalyses the last step of IPP synthesis in mevalonate pathway [(ATP + (R)-5-diphosphomevalonate = ADP + phosphate + isopentenyl diphosphate + CO₂]. Thus apart from inhibition of FPPS enzyme by Zoledronate, expression of IPP was found to be increased by upregulation of IPP synthesizing enzyme.

Another protein, S100A8 was also found significantly upregulated (2.6 fold) in MCF7 cells upon Zoledronate treatment. S100A8 belongs to S100 subfamily of calcium binding proteins and conduct intracellular and extracellular processes [376,377,378]. Among their many function, these proteins also acts like cytokines by binding to cell surface receptors like toll like receptors (TLRs) or receptor for advanced glycation end products (RAGE) of the same cell. $\gamma\delta$ T cells have been shown to express TLRs [379] and are known to mediate antitumor responses by

activation of TLRs [380]. S100A8 acts as a “danger associated molecular pattern (DAMP)” and recruits innate immune cells by chemotaxis. Binding of S100A8 to RAGE induces apoptosis and autophagy [376].

Zoledronate treated breast tumor cells (MCF7) also enhanced expression of heat shock factor 1 (HSF1), which is transcription factor for HSPs. HSPs are molecular chaperons, which functions as molecular chaperons which facilitating the folding of unfolded or nascent polypeptides under stressed conditions [381]. Heat shock proteins (HSPs), play important roles in antigen presentation and cross-presentation, activation of macrophages and lymphocytes, and activation and maturation of dendritic cells [261]. Earlier reports from our lab showed that $\gamma\delta$ T cells recognized HSP60/70 expressed on tumor cells (oral and esophageal) and mediate the lysis of tumor cells through recognition of HSP60/70 [27,71]. Upon validation by flow cytometry, upregulation in HSP60 expression was observed in MCF7 cells upon Zoledronate treatment, while HSP70 expression was reduced. HSP60 and HSP70 are also released by the tumor cells [382,383,384,385] and therefore their expression on tumor cells may vary. α -enolase, apart from being a glycolytic enzyme also serves as a receptor & activator of plasminogen on cell surface of cells such as leukocytes and neoplastic cells [386]. Binding of plasminogen to enolase recruits monocytes [387]. Molecules involved in synapse formation between T cells and target cells (tumor) like dynamin-1-like protein, CD2-associated protein, transforming protein RhoA, phosphoinositide 3-kinase, SLC9A3R2 protein, clusterins and laminin were found significantly upregulated in Zoledronate treated MCF7 cells. Expression of NKG2D, perforin and granzyme increases upon activation of the $\gamma\delta$ T cells, through which $\gamma\delta$ T cells are known to conduct their cytotoxic functions [26]. It correlated with the early observation that, $\gamma\delta$ T cells get recruited to Zoledronate treated MCF7 cells, interact with them and kill them. Simultaneously, expression of

melanoma antigen D2 (MAGE-D2) was also found upregulated in Zoledronate treated MCF7 cells. MAGE-D2 serves as a tumor-associated antigen that elicits immune responses [261]. To conclude, our proteomics data on Zoledronate treated breast tumor cells have discovered novel therapeutic targets that can be investigated further.

Further, the *in vivo* effect of Zoledronate was analyzed by comparing immune profiles of breast cancer patients on Zoledronate treatment (Rx⁺) and untreated breast cancer patients (Rx⁻) using multicolor flow cytometry. As control, immune profiles of healthy individuals were analyzed. Peripheral blood samples of breast cancer patients (untreated and Zoledronate treated) and healthy individuals were analyzed for different adaptive [CD3⁺, CD4⁺ T cells (T helper cells), CD8⁺ T cells (cytotoxic T cells), B cells], innate [NK cells, NK-T cells, $\gamma\delta$ T cells] and suppressive [regulatory T cells and monocytes] immune cells subsets. Activation and memory markers and intracellular cytokines profiles were also analyzed to determine functional status of the immune cells.

Zoledronate is known to activate $\gamma\delta$ T cells [74,75,388]. It was observed that, Zoledronate treated breast cancer patients showed reduced percentages of $\gamma\delta$ T cells in peripheral blood as compared to Zoledronate untreated breast cancer patients and healthy individuals. Reduction in percentages of $\gamma\delta$ T cells in peripheral blood of Zoledronate treated patients has also been noted earlier [389]. This could be due to persistent activation of T cells, which induces apoptosis (known as activation induced cell death/AICD) [390]. Despite the fact that, $\gamma\delta$ T cells from Zoledronate treated breast cancer patients were reduced in number, they were in highly activated state (increased expression of CD25). Further, memory status of the $\gamma\delta$ T cells was analyzed as, immune cells at different memory status are known to behave differently [281]. TEMRA cells (CD45RA⁺CD27⁻) are poorly proliferating cells, but produce copious amounts of

IFN γ and mediate antitumor cytotoxicity [391]. We observed that, $\gamma\delta$ T cells in Zoledronate treated breast cancer patients showed increased percentages of terminally differentiated effector memory $\gamma\delta$ T cells (TEMRA, CD45RA⁺CD27⁻), with concomitant reduction in central memory cells (CD45RA⁻CD27⁺), indicating conversion of central memory cells to effector memory cells, as reported by others [392]. Zoledronate has been shown to induce immune responses through increase in effector memory $\gamma\delta$ T cells in early and metastatic breast cancer patients [393].

We also found a significant increase in percentages of NK cells in peripheral blood of Zoledronate treated breast cancer patients. NK cells are known to contribute to innate immune responses against neoplastic cells because NK cells usually recognize and attack tumor cells that lack MHC class I molecules [394,395,396]. They are also one of the major producers of IFN γ . NK cell based therapies are considered as potential therapies against cancer [395,397,398]. Activated $\gamma\delta$ T lymphocytes are also known to costimulate activation of NK cells [399].

A significant increase in percentages of CD8⁺ T cells (T cytotoxic) cells was observed in Zoledronate treated breast cancer patients. Activated $\gamma\delta$ T cells behave as antigen presenting cells [400,401]. Activated $\gamma\delta$ T cells take up and crosspresent microbial and tumor antigens to CD8⁺ T cells and induce proliferation, target cell killing and cytokine production responses in antigen-experienced and naïve CD8 T cells [402]. Upon activation, $\gamma\delta$ T cells also activate CD4⁺ cells [402]. A significant increase in percentages of B cells in peripheral blood was found unregulated in Zoledronate treated breast cancer patients. B cells represent humoral arm of the immune system, which get activated when MHC-II bound peptides are presented by CD4⁺ cells. Humoral immunity plays a vital role in metastasis-free survival of breast cancer patients [403].

We found a significant reduction in percentages of monocytes in Zoledronate treated breast cancer patients as compared to untreated breast cancer patients and healthy individuals. It is well reported that Zoledronate induces apoptosis in monocytes [404]. Monocytes are the osteoclast precursor cells and thus reduction in their percentages might reduce osteoclastogenesis in metastatic breast cancer patients. Regulatory T cells ($CD4^+CD25^+CD127^-FoxP3^+$) are immune suppressor cells and are considered as bad prognostic marker in breast cancer [405]. In concordance to the earlier reports [406,407,408], we observed a significant increase in regulatory T cells in untreated breast cancer patients. Zoledronate activated $\gamma\delta$ T cells are have been shown to reduce regulatory T cells in multiple myeloma patients [409]. We found marginal decrease in percentages of regulatory T cells in Zoledronate treated breast cancer patients as compared to untreated breast cancer patients.

$\alpha\beta$ and $\gamma\delta$ T cells from Zoledronate treated breast cancer patients showed increased percentages of CD25 expressing cells as compared to untreated breast cancer patients and healthy individuals. High CD25 expressing cells are sensitive to antigenic signals and are highly active [410]. A transient increase in expression of CD25 correlated with production of IFN- γ [411]. RANKL is also considered as an activation marker. It is expressed by stromal cells, osteoblasts and activated T cells and plays indispensable role in osteoclastogenesis and immune system [412]. Through RANKL signaling, T cells significantly enhances immunity by promoting the survival and function of DCs, the most potent professional antigen-presenting cells, in the context of an immune response [31]. Activated CD4 T cells enhance osteoclastogenesis through increased expression of RANKL and pro-osteoclastogenic cytokines [51,413]. We observed that, percentages of $RANKL^+$ $\gamma\delta$ T cells were higher in breast cancer patients (irrespective of Zoledronate treatment) as compared to healthy individuals. It is well reported that, activated T

cells release soluble RANKL [47,414,415]. RANKL MFI on $\alpha\beta$ and $\gamma\delta$ T cells was found to be reduced upon Zoledronate treatment, but still remained higher on $\gamma\delta$ T cells as compared to $\alpha\beta$ T cells.

Though, stimulation of $\gamma\delta$ T cells with phosphoantigens (bromohydrin pyrophosphate and Zoledronate) increased the expression of RANKL, IFN γ secretion was also found to be increased. We observed, baseline percentages of IFN γ^+ $\gamma\delta$ T cells to be higher in Zoledronate treated breast cancer patients as compared to untreated breast cancer patients. Activated $\gamma\delta$ T cells are known to inhibit osteoclast generation and function through secretion of increased levels of IFN γ [416]. IFN γ inhibits generation (degradation of TRAF6 adaptor protein in RANKL signaling) and function (downregulated expression of cathepsin-k) of osteoclasts [299]. Increased RANKL expression on activated $\gamma\delta$ T cells assists their interaction with osteoclasts; while increased IFN γ disrupts RANK-RANKL signaling thus inhibiting osteoclast survival. IFN γ , which plays critical role in conducting innate and adaptive immunity and has antiviral, immunoregulatory, and anti-tumor properties [417]. IFN γ is majorly produced by NK cells, CD8 T cells and $\gamma\delta$ T cells and has multiple functions which include activation of macrophages and NK cells, activating T-helper and T cytotoxic cells by increasing expression of MHC-I and MHC-II expression on antigen presenting cells, induces production of IgG2a and IgG3 from activated plasma B cells. IFN γ induces type I immune response and directly acts on cancer cells [395]. Stimulation of $\gamma\delta$ T cells with PMA+ionomycin further enhanced percentages of IFN γ^+ $\gamma\delta$ T cells in healthy individuals and breast cancer patients (both Zoledronate treated and not treated with Zoledronate). Cell free supernatants of Zoledronate treated breast cancer patients showed reduced levels of IFN γ . This could be due to exhaustion of the cells because of activation induced cell death [418].

Interestingly, cell free supernatants of antigen activated $\gamma\delta$ T cells from Zoledronate treated and untreated breast cancer patients showed major differences in their IL6 levels. $\gamma\delta$ T cells from breast cancer patients who were on Zoledronate treatment showed reduced secretion of IL6 as compared to breast cancer patients who were not on Zoledronate treatment. These results also corroborated with our in vitro data (Results-I), where “activated $\gamma\delta$ T cells” showed reduced IL6 levels as compared to freshly isolated or non-activated $\gamma\delta$ T cells”. IL6 is an inflammatory cytokine with potent pro-osteoclastogenic and pro-tumorigenic activity [48,419]. IL6 has been associated with tumor progression through inhibition of cancer cell apoptosis, stimulation of angiogenesis, and drug resistance, thus anti-IL6 therapies have been in use for treatment of cancer [419].

To conclude, the data demonstrated that Zoledronate can activate several immune cell types in breast cancer patients. A marked increase was observed in the activated levels of $\gamma\delta$ T cells that belong to the effector memory phenotype clearly explaining that besides the antitumor effect of Zoledronate, the mechanism of action of Zoledronate could also be mediated through the activation of $\gamma\delta$ T cells. The decrease in levels of IL6 and IL10 secreted by $\gamma\delta$ T cells in breast cancer patients treated with Zoledronate, clearly indicates how the action of pro-osteoclastogenic /immunosuppressive cytokines are reversed.

The present study has contributed towards understanding the crosstalk between skeletal system, immune system and tumor cells mediated through aminobisphosphonate Zoledronate. In detail proteomic analysis of Zoledronate treated breast cancer cells has deciphered the mechanism of action of Zoledronate on tumor cells and has unraveled molecules that may be viewed as potential therapeutic targets. The lacunae in the field has been the unavailability of a good metastatic bone tumor model in immunocompetent mice and therefore

the role of the immune system remains largely unexplored. Additional studies are needed to further elucidate the key immunosuppressive cell types and identify biomarkers that can predict responses to therapy in breast/ prostate cancer patients with bone metastasis.

Chapter 8

Summary and Conclusion

Human $\gamma\delta$ T cells represent a small population of total T cells (~1-10%), but play an indispensable role in host defense against exogenous pathogens, immune surveillance of endogenous pathogens and immune system homeostasis. $\gamma\delta$ T cells bridge the gap between innate and adaptive immunity. Various *in vitro* and *in vivo* studies have reported antitumor activity of $\gamma\delta$ T cells against solid tumors and hematologic malignancies. $\gamma\delta$ T cells recognize unique set of antigens, which include small phosphoantigens, heat shock proteins, alkylamines and aminobisphosphonates. Unlike $\alpha\beta$ T cells, $\gamma\delta$ T cells do not need antigen processing. They recognize antigen in MHC unrestricted manner and exert cytotoxic function, which make them ideal candidates for cancer immunotherapy.

Aminobisphosphonates constitutes an important treatment modality for osteolytic metastasis, observed in breast cancer patients. Aminobisphosphonates have high affinity for calcium and thus locate to bone, where they are released by resorbing osteoclasts in bone microenvironment. Zoledronate, a third generation aminobisphosphonate, is currently approved for the prevention and treatment of skeletal complications in patients with bone metastases. Zoledronate inhibits farnesyl pyrophosphate synthase (FPPS), a key enzyme in the mevalonate pathway of cholesterol metabolism, which induces osteoclast and tumor cell apoptosis. However, the process of osteoclastogenesis is influenced by number of cytokines released by immune cells present in the bone microenvironment. Activated $CD4^+$ T cells have been shown to enhance osteoclast generation and activity through RANKL and pro-osteoclastogenic cytokines like IL17 and IL6. However, the role of $\gamma\delta$ T cells in osteoclastogenesis remained unexplored.

Zoledronate inhibits proliferation and growth of breast tumor cells and induce tumor cell apoptosis, but the mechanistic details have not been investigated. Earlier reports from our lab have shown that, $\gamma\delta$ T cells recognize and kill aminobisphosphate (Pamidronate and

Zoledronate) treated tumor cells. Expression of conventional molecules on tumor cells involved in the conjugate formation (MICA, NKG2D and ICAM1), of tumor cells with immune cells ($\gamma\delta$ T cells), were found unaltered upon Zoledronate treatment. It indicated potential involvement of other molecules that had not been identified. Zoledronate also acts as an immunomodulator, and has the ability to activate $\gamma\delta$ T cells and induce their expansion. Clinical trials conducted to investigate the effect Zoledronate in postmenopausal women have yielded controversial results (AZURE trial and ABCSG-12 trial). Thus, it was necessary to investigate if the therapeutic effect of Zoledronate is achieved through its ability to activate $\gamma\delta$ T cells in breast cancer patients with bone metastasis.

With this background, the objectives of the thesis were

1. To investigate the effect of $\gamma\delta$ T cells on osteoclastogenesis
2. To understand the effect of aminobisphosphonate (Zoledronate) on protein profiles of breast tumor cells
3. Immune profiling of breast cancer patients on Zoledronate treatment

We investigated the effect $\gamma\delta$ T cells on generation and function of osteoclasts. The findings suggest that $\gamma\delta$ T cells behave in both pro or anti-osteoclastogenic manner and it is the activation status (expression of CD69, CD25 and RANKL) and cytokine dynamics of $\gamma\delta$ T cells, which dictates their pro or anti osteoclastogenic behavior. “Non-activated” $\gamma\delta$ T cells enhanced osteoclastogenesis through IL6 production (a potent stimulator of osteoclast differentiation and activity). “Non-activated” $\gamma\delta$ T cells also secrete higher levels of TNF α , a proinflammatory cytokine, which may directly and indirectly enhance osteoclast generation and their resorptive activity. On the contrary, “activated” $\gamma\delta$ T cells inhibited osteoclast generation

and function through secretion of increased levels of IFN γ . Stimulation of $\gamma\delta$ T cells with phosphoantigens (bromohydrin pyrophosphate and Zoledronate) increased the expression of RANKL along with increase in IFN γ secretion. Increased RANKL expression on activated $\gamma\delta$ T cells assists their interaction with osteoclasts; while increased IFN γ disrupts RANK-RANKL signaling, thus inhibiting osteoclast survival. The present study has provided a new insight into understanding the dual role of $\gamma\delta$ T cells on osteoclastogenesis not reported earlier. Fine tuning the activation status and cytokine dynamics of $\gamma\delta$ T cells will help in designing future immunotherapeutic modalities for patients with primary breast, prostate cancer and multiple myeloma with bone metastasis.

In order to investigate the direct action of Zoledronate on tumor cells, we investigated the *in vitro* effect of aminobisphosphonate (Zoledronate) on breast tumor cells (MCF7) using proteomic approach (2D-PAGE/ MALDI-TOF TOF and LC-MS). Protein profiles of untreated and Zoledronate treated MCF7 cells were compared for differential protein expression. It was observed that, Zoledronate treatment in MCF7 cells inhibited crucial cellular pathways, which included fatty acid metabolism, mitochondrial respiration, cytoskeletal reorganization, cell cycle progression, protein synthesis- trafficking and degradation, copper homeostasis, while apoptosis induction and epidermal growth factor receptor (EGFR) degradation was found to be enhanced. Essentially, apart from inhibiting cholesterol synthesis pathway, Zoledronate also inhibited expression of proteins involved in biosynthesis of polyunsaturated fatty acid (fatty acid desaturase 2 enzyme) and degradation of glycosphingolipids (GM2AP), which constitute essential components of cell membrane. A significant downregulation in expression of proteins essential for peroxisomal biogenesis/ function (Pex19) and mitochondrial function (NADH: ubiquinone reductase enzyme subunit)

was found upon Zoledronate treatment in MCF7 cells. A remarkable reduction in actin nucleation core protein (ARP2/3) was observed, which resulted in actin derangement in Zoledronate treated MCF7 cells and abrupt actin derangement is known to induce apoptosis in these cells. Zoledronate treated MCF7 cells also showed thinning of keratin fibers. Expression of proteins involved in initiation of DNA replication and DNA repair were found reduced upon Zoledronate treatment. Proteins associated with cell cycle progression showed reduced expression in Zoledronate treated MCF7 cells, which resulted in S-phase arrest of cell cycle. Zoledronate treated MCF7 cells showed downregulation in proteins associated with protein synthesis, trafficking and degradation, which is indispensable for the normal cellular metabolism. Proteins associated with copper homeostasis (CutA and CutC) were found to be altered upon Zoledronate treatment, resulting in apoptosis of cells due to copper toxicity. Zoledronate treated MCF7 cells showed upregulation of proteins (RhoB and sortin nexin 1) involved in lysosomal degradation of EGFR. EGFR pathway is one of the crucial pathways in cell as it plays important role in proliferation, survival and migration. Expression of proteins associated with recruitment, activation of $\gamma\delta$ T cells (IPP synthesizing enzyme “diphosphomevalonate decarboxylase”, S100A8 and HSP60) and proteins involved in immune synapse formation were found significantly upregulated upon Zoledronate treatment of a MCF7 cells. Thus Zoledronate created a ‘metabolic crisis’ in the breast tumor cells and made them vulnerable to recognition by cytotoxic $\gamma\delta$ T cells. This is the first study showing in-depth analysis of the effect of Zoledronate treatment on breast tumor cells. The proteomics data has discovered novel therapeutic targets and has also highlighted the therapeutic effects of Zoledronate on cancer cells as well as on the immune system.

Further, immune profiling of breast cancer patients was carried out to analyze the *in vivo* effect of Zoledronate. Comparative immune profiling of healthy individuals, breast cancer patients on Zoledronate treatment and those who were not on Zoledronate treatment, was carried out using multicolor flow cytometry. It was observed that, Zoledronate treated breast cancer patients showed increased percentages of CD8⁺ T cells (Cytotoxic T), natural killer cells (CD3⁻CD56⁺) and B cells (CD19), while percentages of monocytes (CD14⁺) and $\gamma\delta$ T cells were found reduced in peripheral blood as compared to healthy individuals and untreated breast cancer patients. Despite having reduced percentages in peripheral blood, $\gamma\delta$ T cells were in highly activated state and showed increased expression of late activation marker CD25. In Zoledronate treated breast cancer patients, major subpopulation of $\gamma\delta$ T cells was of terminally differentiated effector memory (TEMRA) type. TEMRA memory subtype cells are highly cytotoxic in nature and produce higher levels of cytolytic granules and IFN γ . Intracellular cytokine profiling of $\gamma\delta$ T cells showed increased percentages of $\gamma\delta^+$ IFN γ^+ cells in peripheral blood of Zoledronate treated breast cancer patients as compared to untreated breast cancer patients and healthy individuals. $\gamma\delta$ T cells from Zoledronate treated breast cancer patients responded well to PMA+Ionomycin stimulation as compared to untreated breast cancer patients and showed a significant increase in percentages $\gamma\delta^+$ IFN γ^+ upon stimulation. IFN γ plays important role in promoting adaptive and innate immune responses. IFN γ modulates immunogenic properties of the tumors and prevents their proliferation. Analysis of cell free supernatants of activated $\gamma\delta$ T cells isolated from Zoledronate treated breast cancer patients showed reduced levels of IL6, which is a potent proinflammatory and pro-osteoclastogenic cytokine. It clearly indicated that Zoledronate treatment activates $\gamma\delta$ T cells, which in turn activates other immune cells and also reduces expression of pro-osteoclastogenic cytokines by $\gamma\delta$ T cells (Figure 40).

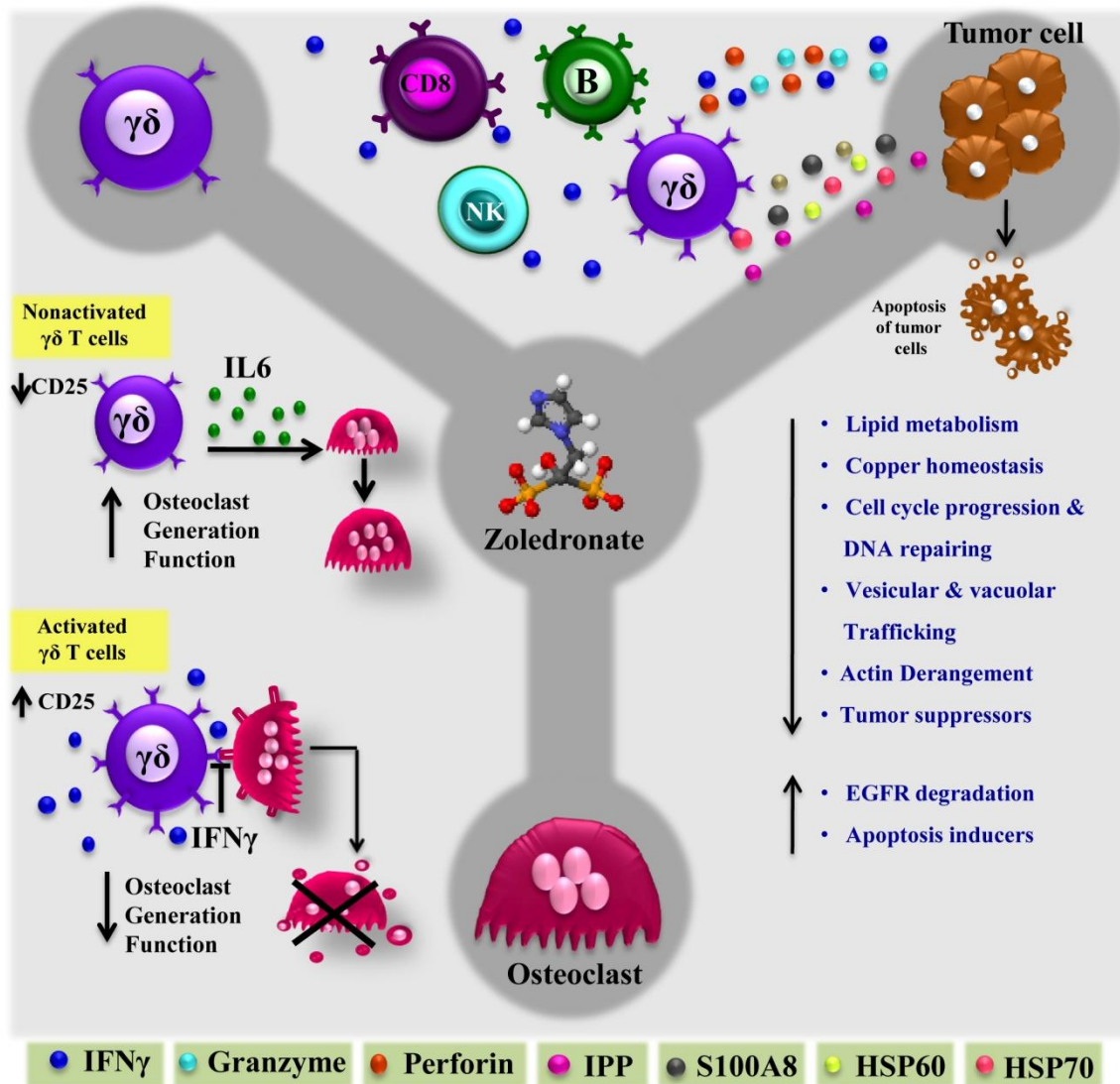


Figure 40: Crosstalk between bone and $\gamma\delta$ T lymphocytes in breast cancer patients mediated by Zoledronate

Zoledronate binds to bone due to its high affinity for calcium and gets embedded into bone matrix by osteoblasts. It is released into bone microenvironment by resorbing osteoclasts, where it activates $\gamma\delta$ T cells. Upon Zoledronate treatment, breast tumor cells show change in expression of proteins [upregulated (\uparrow) and downregulated (\downarrow)] associated with crucial cellular processes. Zoledronate treated breast cancer cells also upregulate expression of proteins associated recruitment and activation of $\gamma\delta$ T cells (heat shock protein (HSP) 60, HSP70, isopentenyl pyrophosphate (IPP), S100A8) and proteins associated with conjugate formation between tumor cells and immune cells. Thus, activated $\gamma\delta$ T cells release higher levels of interferon γ (IFN γ) and

cytolytic granules (perforin and granzyme), through which they exert antitumor effect. Upon activation, $\gamma\delta$ T cells activate other immune cells such as $CD8^+$ T cells, B cells and NK cells, thus expanding the antitumor effect. $IFN\gamma$ released by activated $\gamma\delta$ T cells also inhibit osteoclast generation and function by disruption of RANK-RANKL signaling. In “non-activated” state, $\gamma\delta$ T cells release higher concentrations of IL6 and enhance generation and activity of osteoclast.

In conclusion, the present study demonstrates that Zoledronate facilitates the tripartite crosstalk between the tumor cells, immune cells and bone cells. The study has highlighted the effect of Zoledronate in breast cancer patients, which is significantly different from its well defined anti-resorptive function. Given the development of new generation aminobisphosphonates, synthetic phosphoantigens, immobilized antigens and antibodies, it now appears practical to sculpt and expand $\gamma\delta$ T cells to achieve therapeutic effect in cancer patients. Results from Phase-I and Phase-II clinical trials indicate that the efficacy of $\gamma\delta$ T cell based cancer immunotherapy is comparable to conventional therapies. Combining agents (aminobisphosphonates) that promote $\gamma\delta$ T cell expansion and activation with cytolytic tumor specific antibodies that can mediate ADCC (antibody dependant cellular cytotoxicity) represents the new frontier of anticancer immunotherapy.

References

1. Ahn SG, Lee HM, Cho SH, Lee SA, Hwang SH, et al. (2013) Prognostic factors for patients with bone-only metastasis in breast cancer. *Yonsei Med J* 54: 1168-1177.
2. Soysa NS, Alles N, Aoki K, Ohya K (2012) Osteoclast formation and differentiation: an overview. *J Med Dent Sci* 59: 65-74.
3. Teitelbaum SL (2007) Osteoclasts: what do they do and how do they do it? *Am J Pathol* 170: 427-435.
4. Zheng Y, Zhou H, Dunstan CR, Sutherland RL, Seibel MJ (2013) The role of the bone microenvironment in skeletal metastasis. *J Bone Oncol* 2: 47-57.
5. Soki FN, Park SI, McCauley LK (2012) The multifaceted actions of PTHrP in skeletal metastasis. *Future Oncol* 8: 803-817.
6. Fournier PG, Stresing V, Ebetino FH, Clezardin P (2010) How do bisphosphonates inhibit bone metastasis in vivo? *Neoplasia* 12: 571-578.
7. Drake MT, Clarke BL, Khosla S (2008) Bisphosphonates: mechanism of action and role in clinical practice. *Mayo Clin Proc* 83: 1032-1045.
8. Kimachi K, Kajiya H, Nakayama S, Ikebe T, Okabe K (2011) Zoledronic acid inhibits RANK expression and migration of osteoclast precursors during osteoclastogenesis. *Naunyn Schmiedebergs Arch Pharmacol* 383: 297-308.
9. Green JR (2003) Antitumor effects of bisphosphonates. *Cancer* 97: 840-847.
10. Jagdev SP, Coleman RE, Shipman CM, Rostami HA, Croucher PI (2001) The bisphosphonate, zoledronic acid, induces apoptosis of breast cancer cells: evidence for synergy with paclitaxel. *Br J Cancer* 84: 1126-1134.
11. Chiplunkar S, Dhar S, Wesch D, Kabelitz D (2009) gammadelta T cells in cancer immunotherapy: current status and future prospects. *Immunotherapy* 1: 663-678.
12. Hayday AC (2000) [gamma][delta] cells: a right time and a right place for a conserved third way of protection. *Annu Rev Immunol* 18: 975-1026.
13. Caccamo N, Todaro M, Sireci G, Meraviglia S, Stassi G, et al. (2013) Mechanisms underlying lineage commitment and plasticity of human gammadelta T cells. *Cell Mol Immunol* 10: 30-34.
14. Beetz S, Marischen L, Kabelitz D, Wesch D (2007) Human gamma delta T cells: candidates for the development of immunotherapeutic strategies. *Immunol Res* 37: 97-111.
15. Konigshofer Y, Chien YH (2006) Gammadelta T cells - innate immune lymphocytes? *Curr Opin Immunol* 18: 527-533.
16. Kabelitz D, Kalyan S, Oberg HH, Wesch D (2013) Human Vdelta2 versus non-Vdelta2 gammadelta T cells in antitumor immunity. *Oncoimmunology* 2: e23304.
17. Sharp LL, Jameson JM, Cauvi G, Havran WL (2005) Dendritic epidermal T cells regulate skin homeostasis through local production of insulin-like growth factor 1. *Nat Immunol* 6: 73-79.
18. Jameson JM, Cauvi G, Sharp LL, Witherden DA, Havran WL (2005) Gammadelta T cell-induced hyaluronan production by epithelial cells regulates inflammation. *J Exp Med* 201: 1269-1279.
19. Havran WL, Jameson JM, Witherden DA (2005) Epithelial cells and their neighbors. III. Interactions between intraepithelial lymphocytes and neighboring epithelial cells. *Am J Physiol Gastrointest Liver Physiol* 289: G627-630.

20. Born WK, Reardon CL, O'Brien RL (2006) The function of gammadelta T cells in innate immunity. *Curr Opin Immunol* 18: 31-38.
21. Hayday AC (2009) Gammadelta T cells and the lymphoid stress-surveillance response. *Immunity* 31: 184-196.
22. Wu YL, Ding YP, Tanaka Y, Shen LW, Wei CH, et al. (2014) gammadelta T cells and their potential for immunotherapy. *Int J Biol Sci* 10: 119-135.
23. Wesch D, Marx S, Kabelitz D (1997) Comparative analysis of alpha beta and gamma delta T cell activation by Mycobacterium tuberculosis and isopentenyl pyrophosphate. *Eur J Immunol* 27: 952-956.
24. Gomes AQ, Correia DV, Grosso AR, Lanca T, Ferreira C, et al. (2010) Identification of a panel of ten cell surface protein antigens associated with immunotargeting of leukemias and lymphomas by peripheral blood gammadelta T cells. *Haematologica* 95: 1397-1404.
25. Gertner-Dardenne J, Castellano R, Mamessier E, Garbit S, Kochbati E, et al. (2012) Human Vgamma9Vdelta2 T cells specifically recognize and kill acute myeloid leukemic blasts. *J Immunol* 188: 4701-4708.
26. Dhar S, Chiplunkar SV (2010) Lysis of aminobisphosphonate-sensitized MCF-7 breast tumor cells by Vgamma9Vdelta2 T cells. *Cancer Immunol* 10: 10.
27. Thomas ML, Samant UC, Deshpande RK, Chiplunkar SV (2000) gammadelta T cells lyse autologous and allogenic oesophageal tumours: involvement of heat-shock proteins in the tumour cell lysis. *Cancer Immunol Immunother* 48: 653-659.
28. Pollinger B, Junt T, Metzler B, Walker UA, Tyndall A, et al. (2011) Th17 cells, not IL-17+ gammadelta T cells, drive arthritic bone destruction in mice and humans. *J Immunol* 186: 2602-2612.
29. Kotake S, Udagawa N, Hakoda M, Mogi M, Yano K, et al. (2001) Activated human T cells directly induce osteoclastogenesis from human monocytes: possible role of T cells in bone destruction in rheumatoid arthritis patients. *Arthritis Rheum* 44: 1003-1012.
30. Lee SJ, Nam KI, Jin HM, Cho YN, Lee SE, et al. (2011) Bone destruction by receptor activator of nuclear factor kappaB ligand-expressing T cells in chronic gouty arthritis. *Arthritis Res Ther* 13: R164.
31. Walsh MC, Kim N, Kadono Y, Rho J, Lee SY, et al. (2006) Osteoimmunology: interplay between the immune system and bone metabolism. *Annu Rev Immunol* 24: 33-63.
32. Sato K, Takayanagi H (2006) Osteoclasts, rheumatoid arthritis, and osteoimmunology. *Curr Opin Rheumatol* 18: 419-426.
33. Laemmli UK (1970) Cleavage of structural proteins during the assembly of the head of bacteriophage T4. *Nature* 227: 680-685.
34. Weil RJ, Palmieri DC, Bronder JL, Stark AM, Steeg PS (2005) Breast cancer metastasis to the central nervous system. *Am J Pathol* 167: 913-920.
35. Valastyan S, Weinberg RA (2011) Tumor metastasis: molecular insights and evolving paradigms. *Cell* 147: 275-292.
36. Tracey A, Martin LY, Andrew J, Sanders, Jane Lane, and Wen G. Jiang (2000) *Cancer Invasion and Metastasis: Molecular and Cellular Perspective*, .
37. Kozlow W, Guise TA (2005) Breast cancer metastasis to bone: mechanisms of osteolysis and implications for therapy. *J Mammary Gland Biol Neoplasia* 10: 169-180.
38. Suva LJ, Griffin RJ, Makhoul I (2009) Mechanisms of bone metastases of breast cancer. *Endocr Relat Cancer* 16: 703-713.

39. Raggatt LJ, Partridge NC (2010) Cellular and molecular mechanisms of bone remodeling. *J Biol Chem* 285: 25103-25108.
40. Feng X, McDonald JM (2011) Disorders of bone remodeling. *Annu Rev Pathol* 6: 121-145.
41. Roodman GD (2004) Mechanisms of bone metastasis. *N Engl J Med* 350: 1655-1664.
42. Bussard KM, Gay CV, Mastro AM (2008) The bone microenvironment in metastasis; what is special about bone? *Cancer Metastasis Rev* 27: 41-55.
43. Roodman GD (2001) Biology of osteoclast activation in cancer. *J Clin Oncol* 19: 3562-3571.
44. Takayanagi H (2007) Osteoimmunology: shared mechanisms and crosstalk between the immune and bone systems. *Nat Rev Immunol* 7: 292-304.
45. Horwood NJ, Kartsogiannis V, Quinn JM, Romas E, Martin TJ, et al. (1999) Activated T lymphocytes support osteoclast formation in vitro. *Biochem Biophys Res Commun* 265: 144-150.
46. Pang M, Martinez AF, Jacobs J, Balkan W, Troen BR (2005) RANK ligand and interferon gamma differentially regulate cathepsin gene expression in pre-osteoclastic cells. *Biochem Biophys Res Commun* 328: 756-763.
47. Kong YY, Feige U, Sarosi I, Bolon B, Tafuri A, et al. (1999) Activated T cells regulate bone loss and joint destruction in adjuvant arthritis through osteoprotegerin ligand. *Nature* 402: 304-309.
48. Kurihara N, Bertolini D, Suda T, Akiyama Y, Roodman GD (1990) IL-6 stimulates osteoclast-like multinucleated cell formation in long term human marrow cultures by inducing IL-1 release. *J Immunol* 144: 4226-4230.
49. Sato K, Suematsu A, Okamoto K, Yamaguchi A, Morishita Y, et al. (2006) Th17 functions as an osteoclastogenic helper T cell subset that links T cell activation and bone destruction. *J Exp Med* 203: 2673-2682.
50. Weitzmann MN, Cenci S, Rifas L, Haug J, Dipersio J, et al. (2001) T cell activation induces human osteoclast formation via receptor activator of nuclear factor kappaB ligand-dependent and -independent mechanisms. *J Bone Miner Res* 16: 328-337.
51. Takayanagi H, Ogasawara K, Hida S, Chiba T, Murata S, et al. (2000) T-cell-mediated regulation of osteoclastogenesis by signalling cross-talk between RANKL and IFN-gamma. *Nature* 408: 600-605.
52. Caraglia M, Santini D, Marra M, Vincenzi B, Tonini G, et al. (2006) Emerging anti-cancer molecular mechanisms of aminobisphosphonates. *Endocr Relat Cancer* 13: 7-26.
53. van Beek E, Pieterman E, Cohen L, Lowik C, Papapoulos S (1999) Farnesyl pyrophosphate synthase is the molecular target of nitrogen-containing bisphosphonates. *Biochem Biophys Res Commun* 264: 108-111.
54. Lipton A, Goessl C (2011) Clinical development of anti-RANKL therapies for treatment and prevention of bone metastasis. *Bone* 48: 96-99.
55. Roodman GD, Dougall WC (2008) RANK ligand as a therapeutic target for bone metastases and multiple myeloma. *Cancer Treat Rev* 34: 92-101.
56. Lee RJ, Saylor PJ, Smith MR (2011) Treatment and prevention of bone complications from prostate cancer. *Bone* 48: 88-95.
57. Neville-Webbe HL, Coleman RE (2010) Bisphosphonates and RANK ligand inhibitors for the treatment and prevention of metastatic bone disease. *Eur J Cancer* 46: 1211-1222.
58. Dhillon S, Lyseng-Williamson KA (2008) Zoledronic acid : a review of its use in the management of bone metastases of malignancy. *Drugs* 68: 507-534.

59. Croucher P, Jagdev S, Coleman R (2003) The anti-tumor potential of zoledronic acid. *Breast* 12 Suppl 2: S30-36.
60. Clezardin P (2005) Anti-tumour activity of zoledronic acid. *Cancer Treat Rev* 31 Suppl 3: 1-8.
61. Massaia M (2012) Aminobisphosphonates, statins and the mevalonate pathway: a cross-road to fine-tune the activation of NK and V γ 9V δ 2 T cells. *IBMS BoneKEy*.
62. Gober HJ, Kistowska M, Angman L, Jeno P, Mori L, et al. (2003) Human T cell receptor gammadelta cells recognize endogenous mevalonate metabolites in tumor cells. *J Exp Med* 197: 163-168.
63. Morita CT, Beckman EM, Bukowski JF, Tanaka Y, Band H, et al. (1995) Direct presentation of nonpeptide prenyl pyrophosphate antigens to human gamma delta T cells. *Immunity* 3: 495-507.
64. Wesch D, Glatzel A, Kabelitz D (2001) Differentiation of resting human peripheral blood gamma delta T cells toward Th1- or Th2-phenotype. *Cell Immunol* 212: 110-117.
65. Sireci G, Champagne E, Fournie JJ, Dieli F, Salerno A (1997) Patterns of phosphoantigen stimulation of human Vgamma9/Vdelta2 T cell clones include Th0 cytokines. *Hum Immunol* 58: 70-82.
66. Ness-Schwickerath KJ, Jin C, Morita CT (2010) Cytokine requirements for the differentiation and expansion of IL-17A- and IL-22-producing human Vgamma2Vdelta2 T cells. *J Immunol* 184: 7268-7280.
67. Caccamo N, La Mendola C, Orlando V, Meraviglia S, Todaro M, et al. (2011) Differentiation, phenotype, and function of interleukin-17-producing human Vgamma9Vdelta2 T cells. *Blood* 118: 129-138.
68. Casetti R, Agrati C, Wallace M, Sacchi A, Martini F, et al. (2009) Cutting edge: TGF-beta1 and IL-15 Induce FOXP3+ gammadelta regulatory T cells in the presence of antigen stimulation. *J Immunol* 183: 3574-3577.
69. Wrobel P, Shojaei H, Schittek B, Gieseler F, Wollenberg B, et al. (2007) Lysis of a broad range of epithelial tumour cells by human gamma delta T cells: involvement of NKG2D ligands and T-cell receptor- versus NKG2D-dependent recognition. *Scand J Immunol* 66: 320-328.
70. Todaro M, D'Asaro M, Caccamo N, Iovino F, Francipane MG, et al. (2009) Efficient killing of human colon cancer stem cells by gammadelta T lymphocytes. *J Immunol* 182: 7287-7296.
71. Laad AD, Thomas ML, Fakhri AR, Chiplunkar SV (1999) Human gamma delta T cells recognize heat shock protein-60 on oral tumor cells. *Int J Cancer* 80: 709-714.
72. Born WK, Kemal Aydintug M, O'Brien RL (2013) Diversity of gammadelta T-cell antigens. *Cell Mol Immunol* 10: 13-20.
73. Wang H, Sarikonda G, Puan KJ, Tanaka Y, Feng J, et al. (2011) Indirect stimulation of human Vgamma2Vdelta2 T cells through alterations in isoprenoid metabolism. *J Immunol* 187: 5099-5113.
74. Gogoi D, Chiplunkar SV (2013) Targeting gamma delta T cells for cancer immunotherapy: bench to bedside. *Indian J Med Res* 138: 755-761.
75. Kondo M, Izumi T, Fujieda N, Kondo A, Morishita T, et al. (2011) Expansion of human peripheral blood gammadelta T cells using zoledronate. *J Vis Exp*.
76. Das H, Wang L, Kamath A, Bukowski JF (2001) Vgamma2Vdelta2 T-cell receptor-mediated recognition of aminobisphosphonates. *Blood* 98: 1616-1618.

77. Fromigue O, Lagneaux L, Body JJ (2000) Bisphosphonates induce breast cancer cell death in vitro. *J Bone Miner Res* 15: 2211-2221.
78. Senaratne SG, Pirianov G, Mansi JL, Arnett TR, Colston KW (2000) Bisphosphonates induce apoptosis in human breast cancer cell lines. *Br J Cancer* 82: 1459-1468.
79. Roelofs AJ, Thompson K, Gordon S, Rogers MJ (2006) Molecular mechanisms of action of bisphosphonates: current status. *Clin Cancer Res* 12: 6222s-6230s.
80. Kunzmann V, Bauer E, Feurle J, Weissinger F, Tony HP, et al. (2000) Stimulation of gammadelta T cells by aminobisphosphonates and induction of antiplasma cell activity in multiple myeloma. *Blood* 96: 384-392.
81. Marten A, Lilienfeld-Toal M, Buchler MW, Schmidt J (2007) Zoledronic acid has direct antiproliferative and antimetastatic effect on pancreatic carcinoma cells and acts as an antigen for delta2 gamma/delta T cells. *J Immunother* 30: 370-377.
82. Sato K, Kimura S, Segawa H, Yokota A, Matsumoto S, et al. (2005) Cytotoxic effects of gammadelta T cells expanded ex vivo by a third generation bisphosphonate for cancer immunotherapy. *Int J Cancer* 116: 94-99.
83. Fredholm H, Eaker S, Frisell J, Holmberg L, Fredriksson I, et al. (2009) Breast cancer in young women: poor survival despite intensive treatment. *PLoS One* 4: e7695.
84. Anders CK, Johnson R, Litton J, Phillips M, Bleyer A (2009) Breast cancer before age 40 years. *Semin Oncol* 36: 237-249.
85. Agarwal G, Pradeep PV, Aggarwal V, Yip CH, Cheung PS (2007) Spectrum of breast cancer in Asian women. *World J Surg* 31: 1031-1040.
86. Mani SA, Guo W, Liao MJ, Eaton EN, Ayyanan A, et al. (2008) The epithelial-mesenchymal transition generates cells with properties of stem cells. *Cell* 133: 704-715.
87. Onder TT, Gupta PB, Mani SA, Yang J, Lander ES, et al. (2008) Loss of E-cadherin promotes metastasis via multiple downstream transcriptional pathways. *Cancer Res* 68: 3645-3654.
88. Peinado H, Olmeda D, Cano A (2007) Snail, Zeb and bHLH factors in tumour progression: an alliance against the epithelial phenotype? *Nat Rev Cancer* 7: 415-428.
89. Zeleniuch-Jacquotte A, Afanasyeva Y, Kaaks R, Rinaldi S, Scarmo S, et al. (2012) Premenopausal serum androgens and breast cancer risk: a nested case-control study. *Breast Cancer Res* 14: R32.
90. Harris TJ, McCormick F (2010) The molecular pathology of cancer. *Nat Rev Clin Oncol* 7: 251-265.
91. Caffarel MM, Pensa S, Wickenden JA, Watson CJ (2011) Molecular Biology of Breast Cancer. *Encyclopedia of life sciences*.
92. Singh V, Saunders C, Wylie L, Bourke A (2008) New diagnostic techniques for breast cancer detection. *Future Oncol* 4: 501-513.
93. . <http://www.cancer.org/cancer/breastcancer/detailedguide/breast-cancer-staging>
94. Malhotra GK, Zhao X, Band H, Band V (2010) Histological, molecular and functional subtypes of breast cancers. *Cancer Biol Ther* 10: 955-960.
95. Herschkowitz JI, Simin K, Weigman VJ, Mikaelian I, Usary J, et al. (2007) Identification of conserved gene expression features between murine mammary carcinoma models and human breast tumors. *Genome Biol* 8: R76.
96. Prat A, Parker JS, Karginova O, Fan C, Livasy C, et al. (2010) Phenotypic and molecular characterization of the claudin-low intrinsic subtype of breast cancer. *Breast Cancer Res* 12: R68.

97. Perou CM, Sorlie T, Eisen MB, van de Rijn M, Jeffrey SS, et al. (2000) Molecular portraits of human breast tumours. *Nature* 406: 747-752.
98. Sorlie T, Perou CM, Tibshirani R, Aas T, Geisler S, et al. (2001) Gene expression patterns of breast carcinomas distinguish tumor subclasses with clinical implications. *Proc Natl Acad Sci U S A* 98: 10869-10874.
99. Sorlie T, Tibshirani R, Parker J, Hastie T, Marron JS, et al. (2003) Repeated observation of breast tumor subtypes in independent gene expression data sets. *Proc Natl Acad Sci U S A* 100: 8418-8423.
100. Lam SW, Jimenez CR, Boven E (2014) Breast cancer classification by proteomic technologies: current state of knowledge. *Cancer Treat Rev* 40: 129-138.
101. Weigelt B, Peterse JL, van 't Veer LJ (2005) Breast cancer metastasis: markers and models. *Nat Rev Cancer* 5: 591-602.
102. Koscielny S, Tubiana M, Le MG, Valleron AJ, Mouriesse H, et al. (1984) Breast cancer: relationship between the size of the primary tumour and the probability of metastatic dissemination. *Br J Cancer* 49: 709-715.
103. Page DL (1991) Prognosis and breast cancer. Recognition of lethal and favorable prognostic types. *Am J Surg Pathol* 15: 334-349.
104. Ross JS, Fletcher JA, Linette GP, Stec J, Clark E, et al. (2003) The Her-2/neu gene and protein in breast cancer 2003: biomarker and target of therapy. *Oncologist* 8: 307-325.
105. Clemons M, Gelmon KA, Pritchard KI, Paterson AH (2012) Bone-targeted agents and skeletal-related events in breast cancer patients with bone metastases: the state of the art. *Curr Oncol* 19: 259-268.
106. Swain SM, Baselga J, Kim SB, Ro J, Semiglazov V, et al. (2015) Pertuzumab, trastuzumab, and docetaxel in HER2-positive metastatic breast cancer. *N Engl J Med* 372: 724-734.
107. Mundy GR (2002) Metastasis to bone: causes, consequences and therapeutic opportunities. *Nat Rev Cancer* 2: 584-593.
108. Paget S (1989) The distribution of secondary growths in cancer of the breast. 1889. *Cancer Metastasis Rev* 8: 98-101.
109. Boyce BF, Yoneda T, Guise TA (1999) Factors regulating the growth of metastatic cancer in bone. *Endocr Relat Cancer* 6: 333-347.
110. Vander Griend DJ, Rinker-Schaeffer CW (2004) A new look at an old problem: the survival and organ-specific growth of metastases. *Sci STKE* 2004: pe3.
111. Nguyen DX, Bos PD, Massague J (2009) Metastasis: from dissemination to organ-specific colonization. *Nat Rev Cancer* 9: 274-284.
112. Muller A, Homey B, Soto H, Ge N, Catron D, et al. (2001) Involvement of chemokine receptors in breast cancer metastasis. *Nature* 410: 50-56.
113. Yin JJ, Pollock CB, Kelly K (2005) Mechanisms of cancer metastasis to the bone. *Cell Res* 15: 57-62.
114. Kraljevic Pavelic S, Sedic M, Bosnjak H, Spaventi S, Pavelic K (2011) Metastasis: new perspectives on an old problem. *Mol Cancer* 10: 22.
115. Guise TA (2002) The vicious cycle of bone metastases. *J Musculoskelet Neuronal Interact* 2: 570-572.
116. Hess KR, Varadhachary GR, Taylor SH, Wei W, Raber MN, et al. (2006) Metastatic patterns in adenocarcinoma. *Cancer* 106: 1624-1633.

117. Clines GA, Guise TA (2005) Hypercalcaemia of malignancy and basic research on mechanisms responsible for osteolytic and osteoblastic metastasis to bone. *Endocr Relat Cancer* 12: 549-583.
118. Chirgwin JM, Guise TA (2000) Molecular mechanisms of tumor-bone interactions in osteolytic metastases. *Crit Rev Eukaryot Gene Expr* 10: 159-178.
119. Lerner UH (2006) Bone remodeling in post-menopausal osteoporosis. *J Dent Res* 85: 584-595.
120. Chen YC, Sosnoski DM, Mastro AM (2010) Breast cancer metastasis to the bone: mechanisms of bone loss. *Breast Cancer Res* 12: 215.
121. Caetano-Lopes J, Canhao H, Fonseca JE (2007) Osteoblasts and bone formation. *Acta Reumatol Port* 32: 103-110.
122. Wang RN, Green J, Wang Z, Deng Y, Qiao M, et al. (2014) Bone Morphogenetic Protein (BMP) signaling in development and human diseases. *Genes Dis* 1: 87-105.
123. Huang W, Yang S, Shao J, Li YP (2007) Signaling and transcriptional regulation in osteoblast commitment and differentiation. *Front Biosci* 12: 3068-3092.
124. Chen G, Deng C, Li YP (2012) TGF-beta and BMP signaling in osteoblast differentiation and bone formation. *Int J Biol Sci* 8: 272-288.
125. Ducy P, Zhang R, Geoffroy V, Ridall AL, Karsenty G (1997) *Osf2/Cbfa1*: a transcriptional activator of osteoblast differentiation. *Cell* 89: 747-754.
126. Datta HK, Ng WF, Walker JA, Tuck SP, Varanasi SS (2008) The cell biology of bone metabolism. *J Clin Pathol* 61: 577-587.
127. Hodge JM, Kirkland MA, Nicholson GC (2007) Multiple roles of M-CSF in human osteoclastogenesis. *J Cell Biochem* 102: 759-768.
128. Yagi M, Miyamoto T, Sawatani Y, Iwamoto K, Hosogane N, et al. (2005) DC-STAMP is essential for cell-cell fusion in osteoclasts and foreign body giant cells. *J Exp Med* 202: 345-351.
129. Arai F, Miyamoto T, Ohneda O, Inada T, Sudo T, et al. (1999) Commitment and differentiation of osteoclast precursor cells by the sequential expression of c-Fms and receptor activator of nuclear factor kappaB (RANK) receptors. *J Exp Med* 190: 1741-1754.
130. Leibbrandt A, Penninger JM (2008) RANK/RANKL: regulators of immune responses and bone physiology. *Ann N Y Acad Sci* 1143: 123-150.
131. Humphrey MB, Lanier LL, Nakamura MC (2005) Role of ITAM-containing adapter proteins and their receptors in the immune system and bone. *Immunol Rev* 208: 50-65.
132. Vaananen HK, Zhao H, Mulari M, Halleen JM (2000) The cell biology of osteoclast function. *J Cell Sci* 113 (Pt 3): 377-381.
133. Mulari M, Vaaraniemi J, Vaananen HK (2003) Intracellular membrane trafficking in bone resorbing osteoclasts. *Microsc Res Tech* 61: 496-503.
134. Luxenburg C, Geblinger D, Klein E, Anderson K, Hanein D, et al. (2007) The architecture of the adhesive apparatus of cultured osteoclasts: from podosome formation to sealing zone assembly. *PLoS One* 2: e179.
135. Saltel F, Destaing O, Bard F, Eichert D, Jurdic P (2004) Apatite-mediated actin dynamics in resorbing osteoclasts. *Mol Biol Cell* 15: 5231-5241.
136. Graves AR, Curran PK, Smith CL, Mindell JA (2008) The Cl⁻/H⁺ antiporter *ClC-7* is the primary chloride permeation pathway in lysosomes. *Nature* 453: 788-792.

137. Kornak U, Kasper D, Bosl MR, Kaiser E, Schweizer M, et al. (2001) Loss of the ClC-7 chloride channel leads to osteopetrosis in mice and man. *Cell* 104: 205-215.
138. Nesbitt SA, Horton MA (1997) Trafficking of matrix collagens through bone-resorbing osteoclasts. *Science* 276: 266-269.
139. Salo J, Lehenkari P, Mulari M, Metsikko K, Vaananen HK (1997) Removal of osteoclast bone resorption products by transcytosis. *Science* 276: 270-273.
140. Akiyama T, Bouillet P, Miyazaki T, Kadono Y, Chikuda H, et al. (2003) Regulation of osteoclast apoptosis by ubiquitylation of proapoptotic BH3-only Bcl-2 family member Bim. *EMBO J* 22: 6653-6664.
141. Xing L, Boyce BF (2005) Regulation of apoptosis in osteoclasts and osteoblastic cells. *Biochem Biophys Res Commun* 328: 709-720.
142. Coxon FP, Taylor A (2008) Vesicular trafficking in osteoclasts. *Semin Cell Dev Biol* 19: 424-433.
143. Coxon FP, Thompson K, Rogers MJ (2006) Recent advances in understanding the mechanism of action of bisphosphonates. *Curr Opin Pharmacol* 6: 307-312.
144. Bonewald LF (2011) The amazing osteocyte. *J Bone Miner Res* 26: 229-238.
145. Weitzmann MN, Pacifici R (2006) Estrogen deficiency and bone loss: an inflammatory tale. *J Clin Invest* 116: 1186-1194.
146. Bakker AD, Soejima K, Klein-Nulend J, Burger EH (2001) The production of nitric oxide and prostaglandin E(2) by primary bone cells is shear stress dependent. *J Biomech* 34: 671-677.
147. Seeman E, Delmas PD (2006) Bone quality--the material and structural basis of bone strength and fragility. *N Engl J Med* 354: 2250-2261.
148. Gu G, Hentunen TA, Nars M, Harkonen PL, Vaananen HK (2005) Estrogen protects primary osteocytes against glucocorticoid-induced apoptosis. *Apoptosis* 10: 583-595.
149. Sims NA, Martin TJ (2015) Coupling Signals between the Osteoclast and Osteoblast: How are Messages Transmitted between These Temporary Visitors to the Bone Surface? *Front Endocrinol (Lausanne)* 6: 41.
150. Thomas GP, Baker SU, Eisman JA, Gardiner EM (2001) Changing RANKL/OPG mRNA expression in differentiating murine primary osteoblasts. *J Endocrinol* 170: 451-460.
151. Baker PJ, Dixon M, Evans RT, Dufour L, Johnson E, et al. (1999) CD4(+) T cells and the proinflammatory cytokines gamma interferon and interleukin-6 contribute to alveolar bone loss in mice. *Infect Immun* 67: 2804-2809.
152. Lubberts E (2015) Role of T lymphocytes in the development of rheumatoid arthritis. Implications for treatment. *Curr Pharm Des* 21: 142-146.
153. Di Rosa F, Pabst R (2005) The bone marrow: a nest for migratory memory T cells. *Trends Immunol* 26: 360-366.
154. Weitzmann MN, Pacifici R (2005) The role of T lymphocytes in bone metabolism. *Immunol Rev* 208: 154-168.
155. Karaplis AC, Goltzman D (2000) PTH and PTHrP effects on the skeleton. *Rev Endocr Metab Disord* 1: 331-341.
156. Yamamoto I, Bringham FR, Potts JT, Jr., Segre GV (1988) Properties of parathyroid hormone receptors on circulating bovine lymphocytes. *J Bone Miner Res* 3: 289-295.
157. Atkinson MJ, Hesch RD, Cade C, Wadwah M, Perris AD (1987) Parathyroid hormone stimulation of mitosis in rat thymic lymphocytes is independent of cyclic AMP. *J Bone Miner Res* 2: 303-309.

158. Joseph Lorenzo MH, Yongwon Choi, Hiroshi Takayanagi, Georg Schett Osteoimmunology: Interactions of the Immune and Skeletal Systems.
159. Li H, Hong S, Qian J, Zheng Y, Yang J, et al. (2010) Cross talk between the bone and immune systems: osteoclasts function as antigen-presenting cells and activate CD4+ and CD8+ T cells. *Blood* 116: 210-217.
160. Roato I, Grano M, Brunetti G, Colucci S, Mussa A, et al. (2005) Mechanisms of spontaneous osteoclastogenesis in cancer with bone involvement. *FASEB J* 19: 228-230.
161. Colucci S, Brunetti G, Rizzi R, Zonno A, Mori G, et al. (2004) T cells support osteoclastogenesis in an in vitro model derived from human multiple myeloma bone disease: the role of the OPG/TRAIL interaction. *Blood* 104: 3722-3730.
162. Giuliani N, Colla S, Sala R, Moroni M, Lazzaretti M, et al. (2002) Human myeloma cells stimulate the receptor activator of nuclear factor-kappa B ligand (RANKL) in T lymphocytes: a potential role in multiple myeloma bone disease. *Blood* 100: 4615-4621.
163. Neville-Webbe HL, Cross NA, Eaton CL, Nyambo R, Evans CA, et al. (2004) Osteoprotegerin (OPG) produced by bone marrow stromal cells protects breast cancer cells from TRAIL-induced apoptosis. *Breast Cancer Res Treat* 86: 269-279.
164. Al-Rawi MA, Rmali K, Watkins G, Mansel RE, Jiang WG (2004) Aberrant expression of interleukin-7 (IL-7) and its signalling complex in human breast cancer. *Eur J Cancer* 40: 494-502.
165. Lee SK, Surh CD (2005) Role of interleukin-7 in bone and T-cell homeostasis. *Immunol Rev* 208: 169-180.
166. Ryan MR, Shepherd R, Leavey JK, Gao Y, Grassi F, et al. (2005) An IL-7-dependent rebound in thymic T cell output contributes to the bone loss induced by estrogen deficiency. *Proc Natl Acad Sci U S A* 102: 16735-16740.
167. Bendre MS, Margulies AG, Walser B, Akel NS, Bhattacharya S, et al. (2005) Tumor-derived interleukin-8 stimulates osteolysis independent of the receptor activator of nuclear factor-kappaB ligand pathway. *Cancer Res* 65: 11001-11009.
168. Casilli F, Bianchini A, Gloaguen I, Biordi L, Alesse E, et al. (2005) Inhibition of interleukin-8 (CXCL8/IL-8) responses by repertaxin, a new inhibitor of the chemokine receptors CXCR1 and CXCR2. *Biochem Pharmacol* 69: 385-394.
169. Siegel PM, Massague J (2003) Cytostatic and apoptotic actions of TGF-beta in homeostasis and cancer. *Nat Rev Cancer* 3: 807-821.
170. Park IK, Shultz LD, Letterio JJ, Gorham JD (2005) TGF-beta1 inhibits T-bet induction by IFN-gamma in murine CD4+ T cells through the protein tyrosine phosphatase Src homology region 2 domain-containing phosphatase-1. *J Immunol* 175: 5666-5674.
171. Huber S, Schramm C, Lehr HA, Mann A, Schmitt S, et al. (2004) Cutting edge: TGF-beta signaling is required for the in vivo expansion and immunosuppressive capacity of regulatory CD4+CD25+ T cells. *J Immunol* 173: 6526-6531.
172. Fantini MC, Becker C, Monteleone G, Pallone F, Galle PR, et al. (2004) Cutting edge: TGF-beta induces a regulatory phenotype in CD4+CD25- T cells through Foxp3 induction and down-regulation of Smad7. *J Immunol* 172: 5149-5153.
173. Thomas DA, Massague J (2005) TGF-beta directly targets cytotoxic T cell functions during tumor evasion of immune surveillance. *Cancer Cell* 8: 369-380.
174. Kotake S, Nanke Y, Mogi M, Kawamoto M, Furuya T, et al. (2005) IFN-gamma-producing human T cells directly induce osteoclastogenesis from human monocytes via the expression of RANKL. *Eur J Immunol* 35: 3353-3363.

175. Devlin RD, Reddy SV, Savino R, Ciliberto G, Roodman GD (1998) IL-6 mediates the effects of IL-1 or TNF, but not PTHrP or 1,25(OH)₂D₃, on osteoclast-like cell formation in normal human bone marrow cultures. *J Bone Miner Res* 13: 393-399.
176. Kudo O, Sabokbar A, Pocock A, Itonaga I, Fujikawa Y, et al. (2003) Interleukin-6 and interleukin-11 support human osteoclast formation by a RANKL-independent mechanism. *Bone* 32: 1-7.
177. Kim N, Kadono Y, Takami M, Lee J, Lee SH, et al. (2005) Osteoclast differentiation independent of the TRANCE-RANK-TRAF6 axis. *J Exp Med* 202: 589-595.
178. Cenci S, Weitzmann MN, Roggia C, Namba N, Novack D, et al. (2000) Estrogen deficiency induces bone loss by enhancing T-cell production of TNF-alpha. *J Clin Invest* 106: 1229-1237.
179. Zhang YH, Heulsmann A, Tondravi MM, Mukherjee A, Abu-Amer Y (2001) Tumor necrosis factor-alpha (TNF) stimulates RANKL-induced osteoclastogenesis via coupling of TNF type 1 receptor and RANK signaling pathways. *J Biol Chem* 276: 563-568.
180. Hofbauer LC, Lacey DL, Dunstan CR, Spelsberg TC, Riggs BL, et al. (1999) Interleukin-1beta and tumor necrosis factor-alpha, but not interleukin-6, stimulate osteoprotegerin ligand gene expression in human osteoblastic cells. *Bone* 25: 255-259.
181. Kurokouchi K, Kambe F, Yasukawa K, Izumi R, Ishiguro N, et al. (1998) TNF-alpha increases expression of IL-6 and ICAM-1 genes through activation of NF-kappaB in osteoblast-like ROS17/2.8 cells. *J Bone Miner Res* 13: 1290-1299.
182. Fujii T, Kitaura H, Kimura K, Hakami ZW, Takano-Yamamoto T (2012) IL-4 inhibits TNF-alpha-mediated osteoclast formation by inhibition of RANKL expression in TNF-alpha-activated stromal cells and direct inhibition of TNF-alpha-activated osteoclast precursors via a T-cell-independent mechanism in vivo. *Bone* 51: 771-780.
183. Owens JM, Gallagher AC, Chambers TJ (1996) IL-10 modulates formation of osteoclasts in murine hemopoietic cultures. *J Immunol* 157: 936-940.
184. Ooi LL, Zheng Y, Stalgis-Bilinski K, Dunstan CR (2011) The bone remodeling environment is a factor in breast cancer bone metastasis. *Bone* 48: 66-70.
185. Gillespie MT, Thomas RJ, Pu ZY, Zhou H, Martin TJ, et al. (1997) Calcitonin receptors, bone sialoprotein and osteopontin are expressed in primary breast cancers. *Int J Cancer* 73: 812-815.
186. Littlewood-Evans AJ, Bilbe G, Bowler WB, Farley D, Wlodarski B, et al. (1997) The osteoclast-associated protease cathepsin K is expressed in human breast carcinoma. *Cancer Res* 57: 5386-5390.
187. Mundy GR (1997) Mechanisms of bone metastasis. *Cancer* 80: 1546-1556.
188. Pederson L, Winding B, Foged NT, Spelsberg TC, Oursler MJ (1999) Identification of breast cancer cell line-derived paracrine factors that stimulate osteoclast activity. *Cancer Res* 59: 5849-5855.
189. Henderson MA, Danks JA, Slavin JL, Byrnes GB, Choong PF, et al. (2006) Parathyroid hormone-related protein localization in breast cancers predict improved prognosis. *Cancer Res* 66: 2250-2256.
190. Arima Y, Matsueda S, Yano H, Harada M, Itoh K (2005) Parathyroid hormone-related protein as a common target molecule in specific immunotherapy for a wide variety of tumor types. *Int J Oncol* 27: 981-988.
191. Yao A, Harada M, Matsueda S, Ishihara Y, Shomura H, et al. (2005) New epitope peptides derived from parathyroid hormone-related protein which have the capacity to induce

- prostate cancer-reactive cytotoxic T lymphocytes in HLA-A2+ prostate cancer patients. *Prostate* 62: 233-242.
192. Yin JJ, Selander K, Chirgwin JM, Dallas M, Grubbs BG, et al. (1999) TGF-beta signaling blockade inhibits PTHrP secretion by breast cancer cells and bone metastases development. *J Clin Invest* 103: 197-206.
193. Guise TA, Yin JJ, Taylor SD, Kumagai Y, Dallas M, et al. (1996) Evidence for a causal role of parathyroid hormone-related protein in the pathogenesis of human breast cancer-mediated osteolysis. *J Clin Invest* 98: 1544-1549.
194. Guise TA (1997) Parathyroid hormone-related protein and bone metastases. *Cancer* 80: 1572-1580.
195. Thomas RJ, Guise TA, Yin JJ, Elliott J, Horwood NJ, et al. (1999) Breast cancer cells interact with osteoblasts to support osteoclast formation. *Endocrinology* 140: 4451-4458.
196. Horwood NJ, Elliott J, Martin TJ, Gillespie MT (1998) Osteotropic agents regulate the expression of osteoclast differentiation factor and osteoprotegerin in osteoblastic stromal cells. *Endocrinology* 139: 4743-4746.
197. Fuller K, Wong B, Fox S, Choi Y, Chambers TJ (1998) TRANCE is necessary and sufficient for osteoblast-mediated activation of bone resorption in osteoclasts. *J Exp Med* 188: 997-1001.
198. Luo JL, Tan W, Ricono JM, Korchynskiy O, Zhang M, et al. (2007) Nuclear cytokine-activated IKKalpha controls prostate cancer metastasis by repressing Maspin. *Nature* 446: 690-694.
199. Sellers RS, LeRoy BE, Blomme EA, Tannehill-Gregg S, Corn S, et al. (2004) Effects of transforming growth factor-beta1 on parathyroid hormone-related protein mRNA expression and protein secretion in canine prostate epithelial, stromal, and carcinoma cells. *Prostate* 58: 366-373.
200. Serra R, Karaplis A, Sohn P (1999) Parathyroid hormone-related peptide (PTHrP)-dependent and -independent effects of transforming growth factor beta (TGF-beta) on endochondral bone formation. *J Cell Biol* 145: 783-794.
201. Chen YC, Sosnoski DM, Gandhi UH, Novinger LJ, Prabhu KS, et al. (2009) Selenium modifies the osteoblast inflammatory stress response to bone metastatic breast cancer. *Carcinogenesis* 30: 1941-1948.
202. Morgan H, Tumber A, Hill PA (2004) Breast cancer cells induce osteoclast formation by stimulating host IL-11 production and downregulating granulocyte/macrophage colony-stimulating factor. *Int J Cancer* 109: 653-660.
203. Ono K, Akatsu T, Murakami T, Kitamura R, Yamamoto M, et al. (2002) Involvement of cyclo-oxygenase-2 in osteoclast formation and bone destruction in bone metastasis of mammary carcinoma cell lines. *J Bone Miner Res* 17: 774-781.
204. de la Mata J, Uy HL, Guise TA, Story B, Boyce BF, et al. (1995) Interleukin-6 enhances hypercalcemia and bone resorption mediated by parathyroid hormone-related protein in vivo. *J Clin Invest* 95: 2846-2852.
205. Mutinga MJ (1975) Phlebotomus fauna in the cutaneous leishmaniasis focus of Mt. Elgon, Kenya. *East Afr Med J* 52: 340-347.
206. Siclari VA, Guise TA, Chirgwin JM (2006) Molecular interactions between breast cancer cells and the bone microenvironment drive skeletal metastases. *Cancer Metastasis Rev* 25: 621-633.

207. Hussein O, Tiedemann K, Komarova SV (2011) Breast cancer cells inhibit spontaneous and bisphosphonate-induced osteoclast apoptosis. *Bone* 48: 202-211.
208. Hiraga T, Nakamura H (2009) Imatinib mesylate suppresses bone metastases of breast cancer by inhibiting osteoclasts through the blockade of c-Fms signals. *Int J Cancer* 124: 215-222.
209. Body JJ, Facon T, Coleman RE, Lipton A, Geurs F, et al. (2006) A study of the biological receptor activator of nuclear factor-kappaB ligand inhibitor, denosumab, in patients with multiple myeloma or bone metastases from breast cancer. *Clin Cancer Res* 12: 1221-1228.
210. Lipton A, Steger GG, Figueroa J, Alvarado C, Solal-Celigny P, et al. (2007) Randomized active-controlled phase II study of denosumab efficacy and safety in patients with breast cancer-related bone metastases. *J Clin Oncol* 25: 4431-4437.
211. Lipton A, Steger GG, Figueroa J, Alvarado C, Solal-Celigny P, et al. (2008) Extended efficacy and safety of denosumab in breast cancer patients with bone metastases not receiving prior bisphosphonate therapy. *Clin Cancer Res* 14: 6690-6696.
212. Rogers MJ (2004) From molds and macrophages to mevalonate: a decade of progress in understanding the molecular mode of action of bisphosphonates. *Calcif Tissue Int* 75: 451-461.
213. Reinholz GG, Getz B, Sanders ES, Karpeisky MY, Padyukova N, et al. (2002) Distinct mechanisms of bisphosphonate action between osteoblasts and breast cancer cells: identity of a potent new bisphosphonate analogue. *Breast Cancer Res Treat* 71: 257-268.
214. Polascik TJ, Mouraviev V (2008) Zoledronic acid in the management of metastatic bone disease. *Ther Clin Risk Manag* 4: 261-268.
215. Kimmel DB (2007) Mechanism of action, pharmacokinetic and pharmacodynamic profile, and clinical applications of nitrogen-containing bisphosphonates. *J Dent Res* 86: 1022-1033.
216. Bukowski JF, Dascher CC, Das H (2005) Alternative bisphosphonate targets and mechanisms of action. *Biochem Biophys Res Commun* 328: 746-750.
217. Huang KC, Cheng CC, Chuang PY, Yang TY (2015) The effects of zoledronate on the survival and function of human osteoblast-like cells. *BMC Musculoskelet Disord* 16: 355.
218. Thurnher M, Nussbaumer O, Gruenbacher G (2012) Novel aspects of mevalonate pathway inhibitors as antitumor agents. *Clin Cancer Res* 18: 3524-3531.
219. Ilyas A, Hashim Z, Naeem N, Haneef K, Zarina S (2014) The effect of alendronate on proteome of hepatocellular carcinoma cell lines. *Int J Proteomics* 2014: 532953.
220. Kischel P, Guillonneau F, Dumont B, Bellahcene A, Stresing V, et al. (2008) Cell membrane proteomic analysis identifies proteins differentially expressed in osteotropic human breast cancer cells. *Neoplasia* 10: 1014-1020.
221. Susa M, Morii T, Yabe H, Horiuchi K, Toyama Y, et al. (2009) Alendronate inhibits growth of high-grade chondrosarcoma cells. *Anticancer Res* 29: 1879-1888.
222. Gupta S, Kim C, Yel L, Gollapudi S (2004) A role of fas-associated death domain (FADD) in increased apoptosis in aged humans. *J Clin Immunol* 24: 24-29.
223. Carding SR, Egan PJ (2002) Gammadelta T cells: functional plasticity and heterogeneity. *Nat Rev Immunol* 2: 336-345.
224. Kalyan S, Kabelitz D (2013) Defining the nature of human gammadelta T cells: a biographical sketch of the highly empathetic. *Cell Mol Immunol* 10: 21-29.

225. Thompson K, Rojas-Navea J, Rogers MJ (2006) Alkylamines cause Vgamma9Vdelta2 T-cell activation and proliferation by inhibiting the mevalonate pathway. *Blood* 107: 651-654.
226. Girlanda S, Fortis C, Belloni D, Ferrero E, Ticozzi P, et al. (2005) MICA expressed by multiple myeloma and monoclonal gammopathy of undetermined significance plasma cells Costimulates pamidronate-activated gammadelta lymphocytes. *Cancer Res* 65: 7502-7508.
227. Rincon-Orozco B, Kunzmann V, Wrobel P, Kabelitz D, Steinle A, et al. (2005) Activation of V gamma 9V delta 2 T cells by NKG2D. *J Immunol* 175: 2144-2151.
228. Cosman D, Mullberg J, Sutherland CL, Chin W, Armitage R, et al. (2001) ULBPs, novel MHC class I-related molecules, bind to CMV glycoprotein UL16 and stimulate NK cytotoxicity through the NKG2D receptor. *Immunity* 14: 123-133.
229. Lanca T, Correia DV, Moita CF, Raquel H, Neves-Costa A, et al. (2010) The MHC class Ib protein ULBP1 is a nonredundant determinant of leukemia/lymphoma susceptibility to gammadelta T-cell cytotoxicity. *Blood* 115: 2407-2411.
230. Kong Y, Cao W, Xi X, Ma C, Cui L, et al. (2009) The NKG2D ligand ULBP4 binds to TCRgamma9/delta2 and induces cytotoxicity to tumor cells through both TCRgammadelta and NKG2D. *Blood* 114: 310-317.
231. Qin G, Mao H, Zheng J, Sia SF, Liu Y, et al. (2009) Phosphoantigen-expanded human gammadelta T cells display potent cytotoxicity against monocyte-derived macrophages infected with human and avian influenza viruses. *J Infect Dis* 200: 858-865.
232. Dieli F, Troye-Blomberg M, Ivanyi J, Fournie JJ, Krensky AM, et al. (2001) Granulysin-dependent killing of intracellular and extracellular *Mycobacterium tuberculosis* by Vgamma9/Vdelta2 T lymphocytes. *J Infect Dis* 184: 1082-1085.
233. Bonneville M, O'Brien RL, Born WK (2010) Gammadelta T cell effector functions: a blend of innate programming and acquired plasticity. *Nat Rev Immunol* 10: 467-478.
234. Chen ZW, Letvin NL (2003) Vgamma2Vdelta2+ T cells and anti-microbial immune responses. *Microbes Infect* 5: 491-498.
235. O'Brien RL, Roark CL, Born WK (2009) IL-17-producing gammadelta T cells. *Eur J Immunol* 39: 662-666.
236. Kabelitz D, Bender A, Schondelmaier S, Schoel B, Kaufmann SH (1990) A large fraction of human peripheral blood gamma/delta + T cells is activated by *Mycobacterium tuberculosis* but not by its 65-kD heat shock protein. *J Exp Med* 171: 667-679.
237. Meuter S, Eberl M, Moser B (2010) Prolonged antigen survival and cytosolic export in cross-presenting human gammadelta T cells. *Proc Natl Acad Sci U S A* 107: 8730-8735.
238. Yuasa T, Sato K, Ashihara E, Takeuchi M, Maita S, et al. (2009) Intravesical administration of gammadelta T cells successfully prevents the growth of bladder cancer in the murine model. *Cancer Immunol Immunother* 58: 493-502.
239. Bryant NL, Suarez-Cuervo C, Gillespie GY, Markert JM, Nabors LB, et al. (2009) Characterization and immunotherapeutic potential of gammadelta T-cells in patients with glioblastoma. *Neuro Oncol* 11: 357-367.
240. Rey J, Veuillen C, Vey N, Bouabdallah R, Olive D (2009) Natural killer and gammadelta T cells in haematological malignancies: enhancing the immune effectors. *Trends Mol Med* 15: 275-284.
241. Deniger DC, Moyes JS, Cooper LJ (2014) Clinical applications of gamma delta T cells with multivalent immunity. *Front Immunol* 5: 636.

242. Van Acker HH, Anguille S, Van Tendeloo VF, Lion E (2015) Empowering gamma delta T cells with antitumor immunity by dendritic cell-based immunotherapy. *Oncoimmunology* 4: e1021538.
243. Gomes AQ, Martins DS, Silva-Santos B (2010) Targeting gammadelta T lymphocytes for cancer immunotherapy: from novel mechanistic insight to clinical application. *Cancer Res* 70: 10024-10027.
244. Meraviglia S, Eberl M, Vermijlen D, Todaro M, Buccheri S, et al. (2010) In vivo manipulation of Vgamma9Vdelta2 T cells with zoledronate and low-dose interleukin-2 for immunotherapy of advanced breast cancer patients. *Clin Exp Immunol* 161: 290-297.
245. Naoe M, Ogawa Y, Takeshita K, Morita J, Shichijo T, et al. (2010) Zoledronate stimulates gamma delta T cells in prostate cancer patients. *Oncol Res* 18: 493-501.
246. Godder KT, Henslee-Downey PJ, Mehta J, Park BS, Chiang KY, et al. (2007) Long term disease-free survival in acute leukemia patients recovering with increased gammadelta T cells after partially mismatched related donor bone marrow transplantation. *Bone Marrow Transplant* 39: 751-757.
247. Khan MW, Eberl M, Moser B (2014) Potential Use of gammadelta T Cell-Based Vaccines in Cancer Immunotherapy. *Front Immunol* 5: 512.
248. Cuetara BL, Crotti TN, O'Donoghue AJ, McHugh KP (2006) Cloning and characterization of osteoclast precursors from the RAW264.7 cell line. *In Vitro Cell Dev Biol Anim* 42: 182-188.
249. Gupta N, Barhanpurkar AP, Tomar GB, Srivastava RK, Kour S, et al. (2010) IL-3 inhibits human osteoclastogenesis and bone resorption through downregulation of c-Fms and diverts the cells to dendritic cell lineage. *J Immunol* 185: 2261-2272.
250. Shevchenko A, Wilm M, Vorm O, Mann M (1996) Mass spectrometric sequencing of proteins silver-stained polyacrylamide gels. *Anal Chem* 68: 850-858.
251. Takayanagi H (2007) Interaction between the immune system and bone metabolism: an emerging field of osteoimmunology. *Proc Jpn Acad Ser B Phys Biol Sci* 83: 136-143.
252. Terpos E, Dimopoulos MA (2011) Interaction between the skeletal and immune systems in cancer: mechanisms and clinical implications. *Cancer Immunol Immunother* 60: 305-317.
253. Gillespie MT (2007) Impact of cytokines and T lymphocytes upon osteoclast differentiation and function. *Arthritis Res Ther* 9: 103.
254. Kuzuyama T (2002) Mevalonate and nonmevalonate pathways for the biosynthesis of isoprene units. *Biosci Biotechnol Biochem* 66: 1619-1627.
255. Lange BM, Rujan T, Martin W, Croteau R (2000) Isoprenoid biosynthesis: the evolution of two ancient and distinct pathways across genomes. *Proc Natl Acad Sci U S A* 97: 13172-13177.
256. Benzaid I, Monkkonen H, Stresing V, Bonnelye E, Green J, et al. (2011) High phosphoantigen levels in bisphosphonate-treated human breast tumors promote Vgamma9Vdelta2 T-cell chemotaxis and cytotoxicity in vivo. *Cancer Res* 71: 4562-4572.
257. Ross FP, Teitelbaum SL (2005) alphavbeta3 and macrophage colony-stimulating factor: partners in osteoclast biology. *Immunol Rev* 208: 88-105.
258. Mizukami J, Takaesu G, Akatsuka H, Sakurai H, Ninomiya-Tsuji J, et al. (2002) Receptor activator of NF-kappaB ligand (RANKL) activates TAK1 mitogen-activated protein kinase kinase kinase through a signaling complex containing RANK, TAB2, and TRAF6. *Mol Cell Biol* 22: 992-1000.

259. Adams LM, Warburton MJ, Hayman AR (2007) Human breast cancer cell lines and tissues express tartrate-resistant acid phosphatase (TRAP). *Cell Biol Int* 31: 191-195.
260. Lopez-Aleman R, Suelves M, Munoz-Canoves P (2003) Plasmin generation dependent on alpha-enolase-type plasminogen receptor is required for myogenesis. *Thromb Haemost* 90: 724-733.
261. Tseng HY, Chen LH, Ye Y, Tay KH, Jiang CC, et al. (2012) The melanoma-associated antigen MAGE-D2 suppresses TRAIL receptor 2 and protects against TRAIL-induced apoptosis in human melanoma cells. *Carcinogenesis* 33: 1871-1881.
262. Desouza M, Gunning PW, Stehn JR (2012) The actin cytoskeleton as a sensor and mediator of apoptosis. *Bioarchitecture* 2: 75-87.
263. Cappello F, Conway de Macario E, Marasa L, Zummo G, Macario AJ (2008) Hsp60 expression, new locations, functions and perspectives for cancer diagnosis and therapy. *Cancer Biol Ther* 7: 801-809.
264. Itoh H, Komatsuda A, Ohtani H, Wakui H, Imai H, et al. (2002) Mammalian HSP60 is quickly sorted into the mitochondria under conditions of dehydration. *Eur J Biochem* 269: 5931-5938.
265. O'Brien RL, Fu YX, Cranfill R, Dallas A, Ellis C, et al. (1992) Heat shock protein Hsp60-reactive gamma delta cells: a large, diversified T-lymphocyte subset with highly focused specificity. *Proc Natl Acad Sci U S A* 89: 4348-4352.
266. Kaur I, Voss SD, Gupta RS, Schell K, Fisch P, et al. (1993) Human peripheral gamma delta T cells recognize hsp60 molecules on Daudi Burkitt's lymphoma cells. *J Immunol* 150: 2046-2055.
267. Wadia P, Atre N, Pradhan T, Mistry R, Chiplunkar S (2005) Heat shock protein induced TCR gammadelta gene rearrangements in patients with oral cancer. *Oral Oncol* 41: 175-182.
268. Adamson P, Paterson HF, Hall A (1992) Intracellular localization of the P21rho proteins. *J Cell Biol* 119: 617-627.
269. Wherlock M, Gampel A, Futter C, Mellor H (2004) Farnesyltransferase inhibitors disrupt EGF receptor traffic through modulation of the RhoB GTPase. *J Cell Sci* 117: 3221-3231.
270. Robertson D, Paterson HF, Adamson P, Hall A, Monaghan P (1995) Ultrastructural localization of ras-related proteins using epitope-tagged plasmids. *J Histochem Cytochem* 43: 471-480.
271. Kurten RC, Cadena DL, Gill GN (1996) Enhanced degradation of EGF receptors by a sorting nexin, SNX1. *Science* 272: 1008-1010.
272. Park HM, Cho HI, Shin CA, Shon HJ, Kim TG (2016) Zoledronic acid induces dose-dependent increase of antigen-specific CD8 T-cell responses in combination with peptide/poly-IC vaccine. *Vaccine* 34: 1275-1281.
273. Lambrinoudaki I, Vlachou S, Galapi F, Papadimitriou D, Papadias K (2008) Once-yearly zoledronic acid in the prevention of osteoporotic bone fractures in postmenopausal women. *Clin Interv Aging* 3: 445-451.
274. Berenson JR (2005) Recommendations for zoledronic acid treatment of patients with bone metastases. *Oncologist* 10: 52-62.
275. Coleman R, Cameron D, Dodwell D, Bell R, Wilson C, et al. (2014) Adjuvant zoledronic acid in patients with early breast cancer: final efficacy analysis of the AZURE (BIG 01/04) randomised open-label phase 3 trial. *Lancet Oncol* 15: 997-1006.

276. Coleman RE, Marshall H, Cameron D, Dodwell D, Burkinshaw R, et al. (2011) Breast-cancer adjuvant therapy with zoledronic acid. *N Engl J Med* 365: 1396-1405.
277. Gnant M, Mlineritsch B, Stoeger H, Luschin-Ebengreuth G, Heck D, et al. (2011) Adjuvant endocrine therapy plus zoledronic acid in premenopausal women with early-stage breast cancer: 62-month follow-up from the ABCSG-12 randomised trial. *Lancet Oncol* 12: 631-641.
278. Gnant M, Mlineritsch B, Stoeger H, Luschin-Ebengreuth G, Knauer M, et al. (2015) Zoledronic acid combined with adjuvant endocrine therapy of tamoxifen versus anastrozol plus ovarian function suppression in premenopausal early breast cancer: final analysis of the Austrian Breast and Colorectal Cancer Study Group Trial 12. *Ann Oncol* 26: 313-320.
279. Janeway CA Jr TP, Walport M, et al. (2001) *Immunobiology: The Immune System in Health and Disease*. 5th edition.
280. Hendriks J, Gravestien LA, Tesselaar K, van Lier RA, Schumacher TN, et al. (2000) CD27 is required for generation and long-term maintenance of T cell immunity. *Nat Immunol* 1: 433-440.
281. Sallusto F, Geginat J, Lanzavecchia A (2004) Central memory and effector memory T cell subsets: function, generation, and maintenance. *Annu Rev Immunol* 22: 745-763.
282. Mackay CR (1999) Dual personality of memory T cells. *Nature* 401: 659-660.
283. Lefrancois L, Marzo AL (2006) The descent of memory T-cell subsets. *Nat Rev Immunol* 6: 618-623.
284. Lopez RD (2002) Human gammadelta-T cells in adoptive immunotherapy of malignant and infectious diseases. *Immunol Res* 26: 207-221.
285. Kabelitz D, Wesch D, Pitters E, Zoller M (2004) Potential of human gammadelta T lymphocytes for immunotherapy of cancer. *Int J Cancer* 112: 727-732.
286. Di Mitri D, Azevedo RI, Henson SM, Libri V, Riddell NE, et al. (2011) Reversible senescence in human CD4+CD45RA+CD27- memory T cells. *J Immunol* 187: 2093-2100.
287. Chatila T, Silverman L, Miller R, Geha R (1989) Mechanisms of T cell activation by the calcium ionophore ionomycin. *J Immunol* 143: 1283-1289.
288. Hashimoto S, Takahashi Y, Tomita Y, Hayama T, Sawada S, et al. (1991) Mechanism of calcium ionophore and phorbol ester-induced T-cell activation. Accessory cell requirement for T-cell activation. *Scand J Immunol* 33: 393-403.
289. Roodman GD (2010) Pathogenesis of myeloma bone disease. *J Cell Biochem* 109: 283-291.
290. Lee SK, Lorenzo J (2006) Cytokines regulating osteoclast formation and function. *Curr Opin Rheumatol* 18: 411-418.
291. Cui Q, Shibata H, Oda A, Amou H, Nakano A, et al. (2011) Targeting myeloma-osteoclast interaction with Vgamma9Vdelta2 T cells. *Int J Hematol* 94: 63-70.
292. Meliconi R, Pitzalis C, Kingsley GH, Panayi GS (1991) Gamma/delta T cells and their subpopulations in blood and synovial fluid from rheumatoid arthritis and spondyloarthritis. *Clin Immunol Immunopathol* 59: 165-172.
293. Bank I, Cohen L, Mouallem M, Farfel Z, Grossman E, et al. (2002) gammadelta T cell subsets in patients with arthritis and chronic neutropenia. *Ann Rheum Dis* 61: 438-443.
294. Bodman-Smith MD, Anand A, Durand V, Youinou PY, Lydyard PM (2000) Decreased expression of FcgammaRIII (CD16) by gammadelta T cells in patients with rheumatoid arthritis. *Immunology* 99: 498-503.

295. Ono T, Okamoto K, Nakashima T, Nitta T, Hori S, et al. (2016) IL-17-producing gammadelta T cells enhance bone regeneration. *Nat Commun* 7: 10928.
296. Colburn NT, Zaal KJ, Wang F, Tuan RS (2009) A role for gamma/delta T cells in a mouse model of fracture healing. *Arthritis Rheum* 60: 1694-1703.
297. Ragab AA, Nalepka JL, Bi Y, Greenfield EM (2002) Cytokines synergistically induce osteoclast differentiation: support by immortalized or normal calvarial cells. *Am J Physiol Cell Physiol* 283: C679-687.
298. Wong PK, Quinn JM, Sims NA, van Nieuwenhuijze A, Campbell IK, et al. (2006) Interleukin-6 modulates production of T lymphocyte-derived cytokines in antigen-induced arthritis and drives inflammation-induced osteoclastogenesis. *Arthritis Rheum* 54: 158-168.
299. Kamolmatyakul S, Chen W, Li YP (2001) Interferon-gamma down-regulates gene expression of cathepsin K in osteoclasts and inhibits osteoclast formation. *J Dent Res* 80: 351-355.
300. Takayanagi H, Sato K, Takaoka A, Taniguchi T (2005) Interplay between interferon and other cytokine systems in bone metabolism. *Immunol Rev* 208: 181-193.
301. Haas W, Pereira P, Tonegawa S (1993) Gamma/delta cells. *Annu Rev Immunol* 11: 637-685.
302. Wang L, Kamath A, Das H, Li L, Bukowski JF (2001) Antibacterial effect of human V gamma 2V delta 2 T cells in vivo. *J Clin Invest* 108: 1349-1357.
303. Garcia VE, Sieling PA, Gong J, Barnes PF, Uyemura K, et al. (1997) Single-cell cytokine analysis of gamma delta T cell responses to nonpeptide mycobacterial antigens. *J Immunol* 159: 1328-1335.
304. Ziegler SF, Ramsdell F, Alderson MR (1994) The activation antigen CD69. *Stem Cells* 12: 456-465.
305. Rutella S, Rumi C, Lucia MB, Barberi T, Puggioni PL, et al. (1999) Induction of CD69 antigen on normal CD4+ and CD8+ lymphocyte subsets and its relationship with the phenotype of responding T-cells. *Cytometry* 38: 95-101.
306. Li EC, Davis LE (2003) Zoledronic acid: a new parenteral bisphosphonate. *Clin Ther* 25: 2669-2708.
307. Lunt SY, Vander Heiden MG (2011) Aerobic glycolysis: meeting the metabolic requirements of cell proliferation. *Annu Rev Cell Dev Biol* 27: 441-464.
308. Anitha A, Nakamura K, Thanseem I, Matsuzaki H, Miyachi T, et al. (2013) Downregulation of the expression of mitochondrial electron transport complex genes in autism brains. *Brain Pathol* 23: 294-302.
309. Fontanesi F, Soto IC, Barrientos A (2008) Cytochrome c oxidase biogenesis: new levels of regulation. *IUBMB Life* 60: 557-568.
310. Mick DU, Fox TD, Rehling P (2011) Inventory control: cytochrome c oxidase assembly regulates mitochondrial translation. *Nat Rev Mol Cell Biol* 12: 14-20.
311. Hakomori S (2003) Structure, organization, and function of glycosphingolipids in membrane. *Curr Opin Hematol* 10: 16-24.
312. Tettamanti G, Bassi R, Viani P, Riboni L (2003) Salvage pathways in glycosphingolipid metabolism. *Biochimie* 85: 423-437.
313. Kolter T, Sandhoff K (2010) Lysosomal degradation of membrane lipids. *FEBS Lett* 584: 1700-1712.

314. Conzelmann E, Burg J, Stephan G, Sandhoff K (1982) Complexing of glycolipids and their transfer between membranes by the activator protein for degradation of lysosomal ganglioside GM2. *Eur J Biochem* 123: 455-464.
315. Meier EM, Schwarzmann G, Furst W, Sandhoff K (1991) The human GM2 activator protein. A substrate specific cofactor of beta-hexosaminidase A. *J Biol Chem* 266: 1879-1887.
316. Werth N, Schuette CG, Wilkening G, Lemm T, Sandhoff K (2001) Degradation of membrane-bound ganglioside GM2 by beta -hexosaminidase A. Stimulation by GM2 activator protein and lysosomal lipids. *J Biol Chem* 276: 12685-12690.
317. Gotte K, Girzalsky W, Linkert M, Baumgart E, Kammerer S, et al. (1998) Pex19p, a farnesylated protein essential for peroxisome biogenesis. *Mol Cell Biol* 18: 616-628.
318. Matsuzono Y, Kinoshita N, Tamura S, Shimozawa N, Hamasaki M, et al. (1999) Human PEX19: cDNA cloning by functional complementation, mutation analysis in a patient with Zellweger syndrome, and potential role in peroxisomal membrane assembly. *Proc Natl Acad Sci U S A* 96: 2116-2121.
319. Sacksteder KA, Jones JM, South ST, Li X, Liu Y, et al. (2000) PEX19 binds multiple peroxisomal membrane proteins, is predominantly cytoplasmic, and is required for peroxisome membrane synthesis. *J Cell Biol* 148: 931-944.
320. Hettema EH, Girzalsky W, van Den Berg M, Erdmann R, Distel B (2000) *Saccharomyces cerevisiae* pex3p and pex19p are required for proper localization and stability of peroxisomal membrane proteins. *EMBO J* 19: 223-233.
321. Snyder WB, Koller A, Choy AJ, Subramani S (2000) The peroxin Pex19p interacts with multiple, integral membrane proteins at the peroxisomal membrane. *J Cell Biol* 149: 1171-1178.
322. Rucktaschel R, Thoms S, Sidorovitch V, Halbach A, Pechlivanis M, et al. (2009) Farnesylation of pex19p is required for its structural integrity and function in peroxisome biogenesis. *J Biol Chem* 284: 20885-20896.
323. Snyder WB, Faber KN, Wenzel TJ, Koller A, Luers GH, et al. (1999) Pex19p interacts with Pex3p and Pex10p and is essential for peroxisome biogenesis in *Pichia pastoris*. *Mol Biol Cell* 10: 1745-1761.
324. Buhaescu I, Izzedine H (2007) Mevalonate pathway: a review of clinical and therapeutical implications. *Clin Biochem* 40: 575-584.
325. Rogers MJ, Gordon S, Benford HL, Coxon FP, Luckman SP, et al. (2000) Cellular and molecular mechanisms of action of bisphosphonates. *Cancer* 88: 2961-2978.
326. Khosravi-Far R, Solski PA, Clark GJ, Kinch MS, Der CJ (1995) Activation of Rac1, RhoA, and mitogen-activated protein kinases is required for Ras transformation. *Mol Cell Biol* 15: 6443-6453.
327. Pruitt K, Der CJ (2001) Ras and Rho regulation of the cell cycle and oncogenesis. *Cancer Lett* 171: 1-10.
328. Westwick JK, Lambert QT, Clark GJ, Symons M, Van Aelst L, et al. (1997) Rac regulation of transformation, gene expression, and actin organization by multiple, PAK-independent pathways. *Mol Cell Biol* 17: 1324-1335.
329. Whitehead IP, Abe K, Gorski JL, Der CJ (1998) CDC42 and FGD1 cause distinct signaling and transforming activities. *Mol Cell Biol* 18: 4689-4697.

330. Bouzahzah B, Albanese C, Ahmed F, Pixley F, Lisanti MP, et al. (2001) Rho family GTPases regulate mammary epithelium cell growth and metastasis through distinguishable pathways. *Mol Med* 7: 816-830.
331. Jaffe AB, Hall A (2002) Rho GTPases in transformation and metastasis. *Adv Cancer Res* 84: 57-80.
332. Janda E, Lehmann K, Killisch I, Jechlinger M, Herzig M, et al. (2002) Ras and TGF[β] cooperatively regulate epithelial cell plasticity and metastasis: dissection of Ras signaling pathways. *J Cell Biol* 156: 299-313.
333. Keely PJ, Westwick JK, Whitehead IP, Der CJ, Parise LV (1997) Cdc42 and Rac1 induce integrin-mediated cell motility and invasiveness through PI(3)K. *Nature* 390: 632-636.
334. Liu A, Cerniglia GJ, Bernhard EJ, Prendergast GC (2001) RhoB is required to mediate apoptosis in neoplastically transformed cells after DNA damage. *Proc Natl Acad Sci U S A* 98: 6192-6197.
335. Du W, Lebowitz PF, Prendergast GC (1999) Cell growth inhibition by farnesyltransferase inhibitors is mediated by gain of geranylgeranylated RhoB. *Mol Cell Biol* 19: 1831-1840.
336. Du W, Prendergast GC (1999) Geranylgeranylated RhoB mediates suppression of human tumor cell growth by farnesyltransferase inhibitors. *Cancer Res* 59: 5492-5496.
337. Delarue FL, Taylor BS, Sebti SM (2001) Ras and RhoA suppress whereas RhoB enhances cytokine-induced transcription of nitric oxide synthase-2 in human normal liver AKN-1 cells and lung cancer A-549 cells. *Oncogene* 20: 6531-6537.
338. Delarue FL, Adnane J, Joshi B, Blaskovich MA, Wang DA, et al. (2007) Farnesyltransferase and geranylgeranyltransferase I inhibitors upregulate RhoB expression by HDAC1 dissociation, HAT association and histone acetylation of the RhoB promoter. *Oncogene* 26: 633-640.
339. Adnane J, Muro-Cacho C, Mathews L, Sebti SM, Munoz-Antonia T (2002) Suppression of rho B expression in invasive carcinoma from head and neck cancer patients. *Clin Cancer Res* 8: 2225-2232.
340. Forget MA, Desrosiers RR, Del M, Moumdjian R, Shedid D, et al. (2002) The expression of rho proteins decreases with human brain tumor progression: potential tumor markers. *Clin Exp Metastasis* 19: 9-15.
341. Mazieres J, Antonia T, Daste G, Muro-Cacho C, Berchery D, et al. (2004) Loss of RhoB expression in human lung cancer progression. *Clin Cancer Res* 10: 2742-2750.
342. Jiang K, Sun J, Cheng J, Djeu JY, Wei S, et al. (2004) Akt mediates Ras downregulation of RhoB, a suppressor of transformation, invasion, and metastasis. *Mol Cell Biol* 24: 5565-5576.
343. Jiang K, Delarue FL, Sebti SM (2004) EGFR, ErbB2 and Ras but not Src suppress RhoB expression while ectopic expression of RhoB antagonizes oncogene-mediated transformation. *Oncogene* 23: 1136-1145.
344. Martinelli E, De Palma R, Orditura M, De Vita F, Ciardiello F (2009) Anti-epidermal growth factor receptor monoclonal antibodies in cancer therapy. *Clin Exp Immunol* 158: 1-9.
345. Schneider MR, Wolf E (2009) The epidermal growth factor receptor ligands at a glance. *J Cell Physiol* 218: 460-466.
346. McNiven MA, Cao H, Pitts KR, Yoon Y (2000) The dynamin family of mechanoenzymes: pinching in new places. *Trends Biochem Sci* 25: 115-120.

347. Felder S, Miller K, Moehren G, Ullrich A, Schlessinger J, et al. (1990) Kinase activity controls the sorting of the epidermal growth factor receptor within the multivesicular body. *Cell* 61: 623-634.
348. Futter CE, Pearse A, Hewlett LJ, Hopkins CR (1996) Multivesicular endosomes containing internalized EGF-EGF receptor complexes mature and then fuse directly with lysosomes. *J Cell Biol* 132: 1011-1023.
349. Burke P, Schooler K, Wiley HS (2001) Regulation of epidermal growth factor receptor signaling by endocytosis and intracellular trafficking. *Mol Biol Cell* 12: 1897-1910.
350. Yarden Y, Sliwkowski MX (2001) Untangling the ErbB signalling network. *Nat Rev Mol Cell Biol* 2: 127-137.
351. Masuda H, Zhang D, Bartholomeusz C, Doihara H, Hortobagyi GN, et al. (2012) Role of epidermal growth factor receptor in breast cancer. *Breast Cancer Res Treat* 136: 331-345.
352. Kirisits A, Pils D, Krainer M (2007) Epidermal growth factor receptor degradation: an alternative view of oncogenic pathways. *Int J Biochem Cell Biol* 39: 2173-2182.
353. Elledge SJ (1996) Cell cycle checkpoints: preventing an identity crisis. *Science* 274: 1664-1672.
354. Champeris Tsaniras S, Kanellakis N, Symeonidou IE, Nikolopoulou P, Lygerou Z, et al. (2014) Licensing of DNA replication, cancer, pluripotency and differentiation: an interlinked world? *Semin Cell Dev Biol* 30: 174-180.
355. Veltman DM, Insall RH (2010) WASP family proteins: their evolution and its physiological implications. *Mol Biol Cell* 21: 2880-2893.
356. Veltman D (2014) Actin dynamics: cell migration takes a new turn with arpin. *Curr Biol* 24: R31-33.
357. Kulms D, Dussmann H, Poppelmann B, Stander S, Schwarz A, et al. (2002) Apoptosis induced by disruption of the actin cytoskeleton is mediated via activation of CD95 (Fas/APO-1). *Cell Death Differ* 9: 598-608.
358. White SR, Williams P, Wojcik KR, Sun S, Hiemstra PS, et al. (2001) Initiation of apoptosis by actin cytoskeletal derangement in human airway epithelial cells. *Am J Respir Cell Mol Biol* 24: 282-294.
359. Genesca M, Sola A, Hotter G (2006) Actin cytoskeleton derangement induces apoptosis in renal ischemia/reperfusion. *Apoptosis* 11: 563-571.
360. Rao JY, Jin YS, Zheng Q, Cheng J, Tai J, et al. (1999) Alterations of the actin polymerization status as an apoptotic morphological effector in HL-60 cells. *J Cell Biochem* 75: 686-697.
361. Boldogh IR, Yang HC, Nowakowski WD, Karmon SL, Hays LG, et al. (2001) Arp2/3 complex and actin dynamics are required for actin-based mitochondrial motility in yeast. *Proc Natl Acad Sci U S A* 98: 3162-3167.
362. Simon VR, Karmon SL, Pon LA (1997) Mitochondrial inheritance: cell cycle and actin cable dependence of polarized mitochondrial movements in *Saccharomyces cerevisiae*. *Cell Motil Cytoskeleton* 37: 199-210.
363. Suria H, Chau LA, Negrou E, Kelvin DJ, Madrenas J (1999) Cytoskeletal disruption induces T cell apoptosis by a caspase-3 mediated mechanism. *Life Sci* 65: 2697-2707.
364. Yamazaki Y, Tsuruga M, Zhou D, Fujita Y, Shang X, et al. (2000) Cytoskeletal disruption accelerates caspase-3 activation and alters the intracellular membrane reorganization in DNA damage-induced apoptosis. *Exp Cell Res* 259: 64-78.

365. Krupanidhi S, Sreekumar A, Sanjeevi CB (2008) Copper & biological health. *Indian J Med Res* 128: 448-461.
366. Li Y, Du J, Zhang P, Ding J (2010) Crystal structure of human copper homeostasis protein CutC reveals a potential copper-binding site. *J Struct Biol* 169: 399-405.
367. Tanaka Y, Tsumoto K, Nakanishi T, Yasutake Y, Sakai N, et al. (2004) Structural implications for heavy metal-induced reversible assembly and aggregation of a protein: the case of *Pyrococcus horikoshii* CutA. *FEBS Lett* 556: 167-174.
368. Arnesano F, Banci L, Benvenuti M, Bertini I, Calderone V, et al. (2003) The evolutionarily conserved trimeric structure of CutA1 proteins suggests a role in signal transduction. *J Biol Chem* 278: 45999-46006.
369. Yang J, Li Q, Yang H, Yan L, Yang L, et al. (2008) Overexpression of human CUTA isoform2 enhances the cytotoxicity of copper to HeLa cells. *Acta Biochim Pol* 55: 411-415.
370. Kunjunni R, Sathianathan S, Behari M, Chattopadhyay P, Subbiah V (2016) Silencing of Human CutC Gene (hCutC) Induces Apoptosis in HepG2 Cells. *Biol Trace Elem Res* 172: 120-126.
371. Gunther MR, Hanna PM, Mason RP, Cohen MS (1995) Hydroxyl radical formation from cuprous ion and hydrogen peroxide: a spin-trapping study. *Arch Biochem Biophys* 316: 515-522.
372. White AR, Multhaup G, Maher F, Bellingham S, Camakaris J, et al. (1999) The Alzheimer's disease amyloid precursor protein modulates copper-induced toxicity and oxidative stress in primary neuronal cultures. *J Neurosci* 19: 9170-9179.
373. Liang Q, Zhou B (2007) Copper and manganese induce yeast apoptosis via different pathways. *Mol Biol Cell* 18: 4741-4749.
374. Raikonen J, Crockett JC, Rogers MJ, Monkkonen H, Auriola S, et al. (2009) Zoledronic acid induces formation of a pro-apoptotic ATP analogue and isopentenyl pyrophosphate in osteoclasts in vivo and in MCF-7 cells in vitro. *Br J Pharmacol* 157: 427-435.
375. Raikonen J, Monkkonen H, Auriola S, Monkkonen J (2010) Mevalonate pathway intermediates downregulate zoledronic acid-induced isopentenyl pyrophosphate and ATP analog formation in human breast cancer cells. *Biochem Pharmacol* 79: 777-783.
376. Chen H, Xu C, Jin Q, Liu Z (2014) S100 protein family in human cancer. *Am J Cancer Res* 4: 89-115.
377. Sedaghat F, Notopoulos A (2008) S100 protein family and its application in clinical practice. *Hippokratia* 12: 198-204.
378. Santamaria-Kisiel L, Rintala-Dempsey AC, Shaw GS (2006) Calcium-dependent and -independent interactions of the S100 protein family. *Biochem J* 396: 201-214.
379. Paleja B, Anand A, Chaukar D, D'Cruz A, Chiplunkar S (2013) Decreased functional response to Toll like receptor ligands in patients with oral cancer. *Hum Immunol* 74: 927-936.
380. Pietschmann K, Beetz S, Welte S, Martens I, Gruen J, et al. (2009) Toll-like receptor expression and function in subsets of human gammadelta T lymphocytes. *Scand J Immunol* 70: 245-255.
381. Becker J, Craig EA (1994) Heat-shock proteins as molecular chaperones. *Eur J Biochem* 219: 11-23.
382. Campanella C, Bucchieri F, Merendino AM, Fucarino A, Burgio G, et al. (2012) The odyssey of Hsp60 from tumor cells to other destinations includes plasma membrane-

- associated stages and Golgi and exosomal protein-trafficking modalities. *PLoS One* 7: e42008.
383. Merendino AM, Bucchieri F, Campanella C, Marciano V, Ribbene A, et al. (2010) Hsp60 is actively secreted by human tumor cells. *PLoS One* 5: e9247.
384. Chen T, Guo J, Han C, Yang M, Cao X (2009) Heat shock protein 70, released from heat-stressed tumor cells, initiates antitumor immunity by inducing tumor cell chemokine production and activating dendritic cells via TLR4 pathway. *J Immunol* 182: 1449-1459.
385. Barreto A, Gonzalez JM, Kabingu E, Asea A, Fiorentino S (2003) Stress-induced release of HSC70 from human tumors. *Cell Immunol* 222: 97-104.
386. Chang GC, Liu KJ, Hsieh CL, Hu TS, Charoenfuprasert S, et al. (2006) Identification of alpha-enolase as an autoantigen in lung cancer: its overexpression is associated with clinical outcomes. *Clin Cancer Res* 12: 5746-5754.
387. Wygrecka M, Marsh LM, Morty RE, Henneke I, Guenther A, et al. (2009) Enolase-1 promotes plasminogen-mediated recruitment of monocytes to the acutely inflamed lung. *Blood* 113: 5588-5598.
388. Kondo M, Sakuta K, Noguchi A, Ariyoshi N, Sato K, et al. (2008) Zoledronate facilitates large-scale ex vivo expansion of functional gammadelta T cells from cancer patients for use in adoptive immunotherapy. *Cytotherapy* 10: 842-856.
389. Dieli F, Gebbia N, Poccia F, Caccamo N, Montesano C, et al. (2003) Induction of gammadelta T-lymphocyte effector functions by bisphosphonate zoledronic acid in cancer patients in vivo. *Blood* 102: 2310-2311.
390. Green DR, Droin N, Pinkoski M (2003) Activation-induced cell death in T cells. *Immunol Rev* 193: 70-81.
391. Gioia C, Agrati C, Casetti R, Cairo C, Borsellino G, et al. (2002) Lack of CD27-CD45RA-V gamma 9V delta 2+ T cell effectors in immunocompromised hosts and during active pulmonary tuberculosis. *J Immunol* 168: 1484-1489.
392. Welton JL, Marti S, Mahdi MH, Boobier C, Barrett-Lee PJ, et al. (2013) gammadelta T cells predict outcome in zoledronate-treated breast cancer patients. *Oncologist* 18: e22-23.
393. Erika P Hamilton¹ KKH, Amy C Hobeika², Jeffrey Peppercorn³, Michael A Morse³, H Kim Lyster⁴, Kouros Owzar⁵, Gretchen Kimmick³, P Kelly Marcom³, Kimberly L Blackwell³ (2015) Zoledronic acid induces an immune response through increased central memory and effector memory gamma/delta T cells in early and metastatic breast cancer patients. *Clinical communication-oncology* 2: 1.
394. Poli A, Michel T, Theresine M, Andres E, Hentges F, et al. (2009) CD56bright natural killer (NK) cells: an important NK cell subset. *Immunology* 126: 458-465.
395. Zamai L, Ponti C, Mirandola P, Gobbi G, Papa S, et al. (2007) NK cells and cancer. *J Immunol* 178: 4011-4016.
396. Munz C, Steinman RM, Fujii S (2005) Dendritic cell maturation by innate lymphocytes: coordinated stimulation of innate and adaptive immunity. *J Exp Med* 202: 203-207.
397. Yang Q, Goding SR, Hokland ME, Basse PH (2006) Antitumor activity of NK cells. *Immunol Res* 36: 13-25.
398. Dahlberg CI, Sarhan D, Chrobok M, Duru AD, Alici E (2015) Natural Killer Cell-Based Therapies Targeting Cancer: Possible Strategies to Gain and Sustain Anti-Tumor Activity. *Front Immunol* 6: 605.

399. Maniar A, Zhang X, Lin W, Gastman BR, Pauza CD, et al. (2010) Human gammadelta T lymphocytes induce robust NK cell-mediated antitumor cytotoxicity through CD137 engagement. *Blood* 116: 1726-1733.
400. Brandes M, Willimann K, Moser B (2005) Professional antigen-presentation function by human gammadelta T Cells. *Science* 309: 264-268.
401. Himoudi N, Morgenstern DA, Yan M, Vernay B, Saraiva L, et al. (2012) Human gammadelta T lymphocytes are licensed for professional antigen presentation by interaction with opsonized target cells. *J Immunol* 188: 1708-1716.
402. Brandes M, Willimann K, Bioley G, Levy N, Eberl M, et al. (2009) Cross-presenting human gammadelta T cells induce robust CD8+ alphabeta T cell responses. *Proc Natl Acad Sci U S A* 106: 2307-2312.
403. Schmidt M, Bohm D, von Torne C, Steiner E, Puhl A, et al. (2008) The humoral immune system has a key prognostic impact in node-negative breast cancer. *Cancer Res* 68: 5405-5413.
404. Fowler DW, Copier J, Dalgleish AG, Bodman-Smith MD (2014) Zoledronic acid causes gammadelta T cells to target monocytes and down-modulate inflammatory homing. *Immunology* 143: 539-549.
405. Shang B, Liu Y, Jiang SJ (2015) Prognostic value of tumor-infiltrating FoxP3+ regulatory T cells in cancers: a systematic review and meta-analysis. *Sci Rep* 5: 15179.
406. Abo-Elenein A, Elgohary SE, Hashish A, El-Halaby E (2008) Significance of immunoregulatory T cells in different stages of breast cancer patients. *Egypt J Immunol* 15: 145-152.
407. Okita R, Saeki T, Takashima S, Yamaguchi Y, Toge T (2005) CD4+CD25+ regulatory T cells in the peripheral blood of patients with breast cancer and non-small cell lung cancer. *Oncol Rep* 14: 1269-1273.
408. Wolf AM, Wolf D, Steurer M, Gastl G, Gunsilius E, et al. (2003) Increase of regulatory T cells in the peripheral blood of cancer patients. *Clin Cancer Res* 9: 606-612.
409. Castella B, Riganti C, Fiore F, Pantaleoni F, Canepari ME, et al. (2011) Immune modulation by zoledronic acid in human myeloma: an advantageous cross-talk between Vgamma9Vdelta2 T cells, alphabeta CD8+ T cells, regulatory T cells, and dendritic cells. *J Immunol* 187: 1578-1590.
410. Boyman O, Sprent J (2012) The role of interleukin-2 during homeostasis and activation of the immune system. *Nat Rev Immunol* 12: 180-190.
411. Toka FN, Kenney MA, Golde WT (2011) Rapid and transient activation of gammadelta T cells to IFN-gamma production, NK cell-like killing, and antigen processing during acute virus infection. *J Immunol* 186: 4853-4861.
412. Anderson DM, Maraskovsky E, Billingsley WL, Dougall WC, Tometsko ME, et al. (1997) A homologue of the TNF receptor and its ligand enhance T-cell growth and dendritic-cell function. *Nature* 390: 175-179.
413. Pappalardo A, Thompson K (2013) Activated gammadelta T cells inhibit osteoclast differentiation and resorptive activity in vitro. *Clin Exp Immunol* 174: 281-291.
414. Kanamaru F, Iwai H, Ikeda T, Nakajima A, Ishikawa I, et al. (2004) Expression of membrane-bound and soluble receptor activator of NF-kappaB ligand (RANKL) in human T cells. *Immunol Lett* 94: 239-246.

415. Wong BR, Rho J, Arron J, Robinson E, Orlinick J, et al. (1997) TRANCE is a novel ligand of the tumor necrosis factor receptor family that activates c-Jun N-terminal kinase in T cells. *J Biol Chem* 272: 25190-25194.
416. Phalke S CS (2015) Activation status of $\gamma\delta$ T cells dictates their effect on osteoclast generation and bone resorption. *Bone Reports* 1: 8.
417. Schroder K, Hertzog PJ, Ravasi T, Hume DA (2004) Interferon-gamma: an overview of signals, mechanisms and functions. *J Leukoc Biol* 75: 163-189.
418. Yi JS, Cox MA, Zajac AJ (2010) T-cell exhaustion: characteristics, causes and conversion. *Immunology* 129: 474-481.
419. Guo Y, Xu F, Lu T, Duan Z, Zhang Z (2012) Interleukin-6 signaling pathway in targeted therapy for cancer. *Cancer Treat Rev* 38: 904-910.

Publications



Activation status of $\gamma\delta$ T cells dictates their effect on osteoclast generation and bone resorption



Swati P. Phalke, Shubhada V. Chiplunkar *

Chiplunkar Laboratory, Advanced Centre for Treatment, Research and Education in Cancer (ACTREC), Tata Memorial Centre, Navi Mumbai, India

ARTICLE INFO

Article history:

Received 20 June 2015

Received in revised form 20 September 2015

Accepted 14 October 2015

Available online 23 October 2015

Keywords:

$\gamma\delta$ T cells

Activation status

Phosphoantigen

Cytokines

Osteoclasts

ABSTRACT

$\gamma\delta$ T cells, a small subset of T cell population (5–10%), forms a bridge between innate and adaptive immunity. Although the role of $\gamma\delta$ T cells in infectious diseases and antitumor immunity is well investigated, their role in bone biology needs to be explored. Aminobisphosphonates are used as a standard treatment modality for bone related disorders and are potent activators of $\gamma\delta$ T cells. In the present study, we have compared the effect of “activated” and “freshly isolated” $\gamma\delta$ T cells on osteoclast generation and function. We have shown that “activated” (α CD3/CD28 + rhIL2 or BrHPP + rhIL2 stimulated) $\gamma\delta$ T cells inhibit osteoclastogenesis, while “freshly isolated” $\gamma\delta$ T cells enhance osteoclast generation and function. Upon stimulation with phosphoantigen (BrHPP), “freshly isolated” $\gamma\delta$ T cells were also able to suppress osteoclast generation and function. Cytokine profiles of these cells revealed that, “freshly isolated” $\gamma\delta$ T cells secrete higher amounts of IL6 (pro-osteoclastogenic), while “activated” $\gamma\delta$ T cells secrete high IFN γ levels (anti-osteoclastogenic). Neutralization of IFN γ and IL6 reversed the “inhibitory” or “stimulatory” effect of $\gamma\delta$ T cells on osteoclastogenesis. In conclusion, we have shown that, activation status and dynamics of IL6 and IFN γ secretion dictate pro and anti-osteoclastogenic role of $\gamma\delta$ T cells.

© 2015 The Authors. Published by Elsevier Inc. This is an open access article under the CC BY-NC-ND license (<http://creativecommons.org/licenses/by-nc-nd/4.0/>).

1. Introduction

$\gamma\delta$ T cells represent a unique subset of immune cells accounting for 5–10% of total T cell population in peripheral blood of humans. $\gamma\delta$ T cells are unique as compared to $\alpha\beta$ T cells due to their T-cell receptor (TCR) gene usage, tissue tropism and MHC independent antigen recognition (Chiplunkar et al., 2009; Hayday, 2000). Major subtype of $\gamma\delta$ T cells in human peripheral blood express V γ 9V δ 2 TCR (also called as V γ 2V δ 2) and are typically of Th1 type secreting copious amount of IFN γ upon stimulation (Caccamo et al., 2013; Beetz et al., 2007). Similar to $\alpha\beta$ T cells, $\gamma\delta$ T cells exhibit plasticity and can differentiate into Th2 (Wesch et al., 2001; Sireci et al., 1997), Th17 (Ness-Schwickerath et al., 2010; Caccamo et al., 2011), Tfh (Caccamo et al., 2013) and T

regulatory (Casetti et al., 2009) type. $\gamma\delta$ T cells play an important role in antitumor cytotoxicity (Konigshofer and Chien, 2006; Kabelitz et al., 2013), wound healing and tissue repair (Sharp et al., 2005; Jameson et al., 2005; Havran et al., 2005). These cells express natural killer receptors (Born et al., 2006; Hayday, 2009) and recognize stressed/tumour cells expressing MICA/B and ULBPs (Wu et al., 2014). $\gamma\delta$ T cells are increased in bacterial, viral and parasitic infections (Born et al., 2006). Antitumor ability of $\gamma\delta$ T cells against solid tumours and leukaemia's has been widely reported (Wrobel et al., 2007; Todaro et al., 2009; Gomes et al., 2010; Gertner-Dardenne et al., 2012; Dhar and Chiplunkar, 2010; Thomas et al., 2000; Laad et al., 1999). A unique set of antigens recognized by $\gamma\delta$ T cells include intermediate products of eukaryotic mevalonate pathway (isopentenyl pyrophosphate or its synthetic analogue bromohydrin pyrophosphate) and bacterial Rohmer pathway (HMBPP [(E)-4-hydroxy-3-methyl-but-2-enylpyrophosphate]). Plant derived alkylamines and aminobisphosphonates are also known to activate $\gamma\delta$ T cells (Born et al., 2006). Aminobisphosphonates and anti-RANKL therapies are used to treat patients with bone metastasis to reduce the skeletal complications and tumour burden (Lipton and Goessl, 2011; Roodman and Dougall, 2008; Lee et al., 2011a; Neville-Webbe and Coleman, 2010). The meta-analysis done to analyse the safety and efficacy of V γ 9V δ 2 based immunotherapy has shown improved overall survival in patients compared to conventional therapies (Buccheri et al., 2014).

Though bone appears to be static in nature, it is a dynamic structure which undergoes continuous remodelling. The process of bone

Abbreviations: PBMCs, peripheral blood mononuclear cells; FH, Ficoll-Hypaque; RPMI, Roswell Park Memorial Institute medium; BrHPP, bromohydrin pyrophosphate; OPCs, osteoclast precursor cells; TRAP, tartarate resistant acid phosphatase; rhIL2, recombinant human interleukin 2; IL6, interleukin 6; IFN γ , interferon gamma; α IL6, anti-interleukin 6; α IFN γ , anti-interferon gamma; rhMCSF, recombinant human macrophage-colony stimulating factor; rhRANKL, recombinant human receptor activator of nuclear factor kappa-B ligand; α MEM, complete minimum essential medium with alpha modification; FCS, Fetal calf serum; PBS, phosphate buffered saline; CBA, cytometric bead array; OAA5, osteoclast activity assay substrate; MACS, magnetic-activated cell sorting; MFI, mean fluorescent intensity; SEM, standard error of mean.

* Corresponding author at: Chiplunkar Laboratory, Advanced Centre for Treatment, Research and Education in Cancer (ACTREC), Tata Memorial Centre, Kharghar, Navi Mumbai 410210, India.

E-mail address: schiplunkar@actrec.gov.in (S.V. Chiplunkar).

remodelling is under the tight control of osteoblasts and osteoclasts. Osteoblasts are derived from mesenchymal cells, secrete bone matrix proteins and promote mineralization. Osteoclasts are large multinucleated cells generated by fusion of monocyte-macrophage precursor cells (Soysa et al., 2012) and are known to decalcify and degrade the bone by secreting the lysosomal proteases (Teitelbaum, 2007). In normal conditions, osteoclasts and osteoblasts work in coordinated manner to maintain normal bone physiology, while their imbalance results in pathological conditions, such as osteoporosis, rheumatoid arthritis (RA), Paget's disease and osteopetrosis. Immune system and skeletal system are influenced by a number of common cytokines, chemokines, signalling molecules and transcription factors (Takayanagi, 2007). Activated T lymphocytes support osteoclastogenesis through production of IL6 (Kurihara et al., 1990), IL17 (Sato et al., 2006), RANKL (Horwood et al., 1999; Weitzmann et al., 2001; Takayanagi et al., 2000) and TNF α (Lam et al., 2000). Inflamed synovial joints of rheumatoid arthritic patients showed presence of $\gamma\delta$ T cells (Keystone et al., 1991), though $\gamma\delta$ T cells were not recognized as major contributors of arthritic bone destruction (Pollinger et al., 2011). It was recently demonstrated that activated $\gamma\delta$ T cells inhibit osteoclast differentiation and their resorptive function hence have important implications in understanding pathogenesis of rheumatoid arthritis (Pappalardo and Thompson, 2013). In disease free breast cancer patients, a single dose of aminobisphosphonate (zoledronic acid) induces a long lasting activation of effector subsets of $\gamma\delta$ T cells (Santini et al., 2009). These studies indicate that activation status of $\gamma\delta$ T cells is responsible for their antiosteoclastogenic activity. The objective of the present study was to have a comparative analysis of "activated" and "freshly isolated" $\gamma\delta$ T cells with respect to their effect on generation and function of osteoclasts. Our results demonstrate that "activated" $\gamma\delta$ T cells inhibit generation and resorptive ability of osteoclasts, while "freshly isolated" $\gamma\delta$ T cells promote osteoclast formation and function.

2. Materials and methods

2.1. Study group

Peripheral blood from healthy volunteers (age, 25–45 years) was collected in heparin containing vacutainers. The present study was approved by the Institutional Ethics Committee and informed consents were taken from the healthy volunteers before collecting the blood sample.

2.2. Expansion and isolation of $\gamma\delta$ T cells

$\gamma\delta$ T cells were either directly isolated from peripheral blood mononuclear cells (PBMCs) or from ex-vivo expanded PBMC cultures. Briefly, PBMCs were separated from heparinised peripheral blood of healthy individuals by Ficoll-Hypaque (Sigma-Aldrich, USA) density gradient centrifugation. PBMCs (5×10^6), resuspended in 5 ml cRPMI (10% heat-inactivated human AB serum, 2 mM glutamine, and antibiotics) were stimulated for 12 days with rhIL-2 (30 IU/ml) in 25 mm² tissue culture flasks precoated with α CD3 (1 μ g) + α CD28 (1 μ g), with intermediate feedings with rhIL2. These cells were subcultured after 6 days. On the 12th day, cultures were terminated and $\gamma\delta$ T cells were immunomagnetically separated (positive selection) by using $\gamma\delta$ -TCR MACS kit (magnetic activated cell sorting, Milteney Biotech, Germany) as per the kit instructions. On the 12th day, $13 \pm 2.5 \times 10^6$ $\gamma\delta$ T cells were obtained from α CD3/CD28 expanded PBMCs ($150 \pm 40 \times 10^6$). "Freshly isolated" $\gamma\delta$ T cells were obtained from PBMCs without expansion. About $3.8 \pm 1.6 \times 10^6$ $\gamma\delta$ T cells were isolated directly from PBMCs ($130 \pm 52 \times 10^6$) by MACS purification. The purity of the MACS separated $\gamma\delta$ T cells (FITC labelled) was analysed by flow cytometry and ranged from 95 to 98%. The $\gamma\delta$ T cells were rested overnight in medium before using them for further experiments. $\gamma\delta$ T cells purified from α CD3/CD28 + rhIL2 expanded PBMCs are termed as "activated" $\gamma\delta$ T cells,

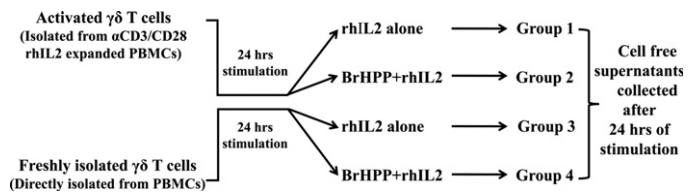
while $\gamma\delta$ T cells isolated directly from PBMCs are referred as "freshly isolated" $\gamma\delta$ T cells.

2.3. Flow cytometry

Expression of CD69, CD25 and RANKL was analysed on "activated" and "freshly isolated" $\gamma\delta$ T cells. To analyse expression of CD69, CD25 and RANKL on "activated" $\gamma\delta$ T cells, PBMCs (1×10^6 /ml) were cultured in cRPMI supplemented with either rhIL2 (30 IU/ml) alone, BrHPP (200 nM) + rhIL2 or α CD3/CD28 (1 μ g) + rhIL2 for 12 days in 24 well plate at 37 °C in 5% CO₂ incubator. BrHPP is a synthetic analogue of isopentenyl pyrophosphate (Espinosa et al., 2001) and is used as antigen for $\gamma\delta$ T cells. The cells were fed with rhIL2 every 3rd day and subcultured on the 6th day. PBMCs without any stimulation (Day 0) were kept as control. On termination of culture on the 12th day, expanded PBMCs were collected, washed in cold $1 \times$ PBS (4 °C) and resuspended in cold FACS buffer ($1 \times$ PBS, 2% FCS, 0.01% sodium azide) as 1×10^6 PBMCs/50 μ l. These PBMCs were then stained for markers like $\gamma\delta$ -TCR-APC (BD Pharmingen, USA), CD25-PECy7 (BD Pharmingen, USA), CD69-FITC (BD Pharmingen, USA), RANKL-PE (Biolegend, USA) at 4 °C for 30 min in dark, followed by fixing in 1% paraformaldehyde at 4 °C for 15 min in dark. For "freshly isolated" $\gamma\delta$ T cells (directly separated from PBMCs on Day 0), purified $\gamma\delta$ T cells were rested overnight and then were stimulated either with rhIL2 (0.5 IU) alone, α CD3/CD28 (1 μ g) + rhIL2, BrHPP (200 nM) + rhIL2 or left unstimulated (control) for 24 h at 37 °C in 5% CO₂ incubator. 50,000 events were acquired on a FACS Aria (Becton Dickinson, USA) flow cytometer and data was analysed using FlowJo Software (Version 10, Tree Star, USA). For the above experiments, lymphocytes were gated on the basis of their forward and side scatter. Further $\gamma\delta$ T cells were gated on the basis of the fluorescence intensity versus forward scatter and expression of CD69, CD25 and RANKL was analysed on the gated $\gamma\delta$ T cell population.

2.4. Cytometric bead array

"Activated" (separated from α CD3/CD28 expanded PBMCs) and "freshly isolated" $\gamma\delta$ T cells (5×10^4), resuspended in cRPMI (200 μ l), were stimulated with rhIL2 (0.5 IU) alone or BrHPP (200 nM) + rhIL2 (0.5 IU), in round bottom 96 well plate (Nunc) for 24 h at 37 °C in 5% CO₂ incubator. The experimental groups were as represented below (Groups 1 to 4).



After 24 h, cells free supernatants from Groups 1–4 were collected and were stored at -80 °C. As experimental controls, cell free supernatants were collected from "activated" and "freshly isolated" $\gamma\delta$ T cells incubated in medium only (unstimulated) for 24 h. Th1/Th2/Th17 cytokines (IL2, IL4, IL6, IL10, TNF α , IFN γ and IL17A) in these supernatants were analysed using cytometric bead array kit (BD Biosciences) as per the kit instructions. In brief, 50 μ l test samples and PE detection antibody were incubated with capture bead reagent for 3 h at room temperature in dark, followed by washing with wash buffer. Samples were acquired on BD FACS Aria cytometer (BD Bioscience, San Jose, CA, USA) and data was analyzed using FCAP Array software version 1.0 (BD Biosciences).

2.5. Generation of human osteoclasts

Human osteoclasts were generated from CD14⁺ cells (monocytes) in the presence of rhM-CSF and rhRANKL (Gupta et al., 2010). In brief,

CD14⁺ cells were separated from healthy PBMCs by positive selection method using CD14 MACS kit (Milteney Biotech). CD14⁺ cells (1×10^5) were cultured on thermax coverslips (Nunc) in flat bottom 96 well plate containing 200 μ l α MEM (10% heat inactivated FCS (Invitrogen Life Technologies, USA), 2 mM L-glutamine and antibiotics) at 37 °C in 5% CO₂ incubator. These cultures were supplemented with 30 ng/ml rhMCSF (R&D Systems) and 40 ng/ml rhRANKL (R&D Systems) and were replenished on every 3rd day. On the 21st day, mature multinucleated osteoclasts were characterized by staining for expression of vitronectin receptor (α V β 3 integrin) using monoclonal antibody for CD51/61 (Biologend), also known as 23c6 antibody along with nuclear stain DAPI. 23c6⁺ cells having >3 nuclei were considered as mature osteoclasts (Supplementary Fig. 1A).

2.6. CD14⁺ and $\gamma\delta$ T cell coculture assay

Effect of $\gamma\delta$ T cells on osteoclastogenesis was analysed by generating osteoclasts from CD14⁺ cells in the presence of autologous “activated” (ACT) or “freshly isolated” (FI) $\gamma\delta$ T cells. On Day 0, CD14⁺ cells (1×10^5) were cocultured with unstimulated “activated” or “freshly isolated” $\gamma\delta$ T cells (1×10^4) in α MEM (200 μ l) containing rhMCSF (30 ng/ml), rhRANKL (40 ng/ml) and rhIL2 (0.5 IU). As a positive control, osteoclasts were generated from CD14⁺ cells in the presence of rhMCSF and rhRANKL only. To analyse the effect of phosphoantigen stimulated “freshly isolated” $\gamma\delta$ T cells on osteoclastogenesis, BrHPP (200 nM) was also added to cocultures along with rhMCSF and rhRANKL on Day 0. For 21 days, CD14: $\gamma\delta$ T cells (10:1) were nourished with rhMCSF, rhRANKL and rhIL2 on every 3rd day. On the 21st day, multinucleated (>3 nuclei) 23c6⁺ osteoclasts generated in an entire well were quantified and the effect of $\gamma\delta$ T cells on osteoclastogenesis was determined by analysing increase or decrease in the total number of osteoclast generated per well as compared to control wells.

2.7. In vitro bone resorption assay using osteoclast activity assay substrate (OAAS)

“Activated” and “freshly isolated” $\gamma\delta$ T cells were stimulated with rhIL2 or BrHPP + rhIL2 for 24 h and cell free supernatants were collected (Groups 1–4) as described above (Section 2.4). Osteoclast precursor cells were generated from CD14⁺ cells (1×10^5) in the presence of rhMCSF and rhRANKL for 12 days in OAAS module (BD Biosciences). OAAS is a 16 well module, with thin calcium-phosphate coated wells and is used to evaluate functional activity of osteoclasts in vitro. From the 12th day onwards, every 3rd day, the cultures were supplemented with pretitrated volumes of cell free supernatant (50 μ l) from Groups 1–4 along with rhMCSF and rhRANKL. Osteoclasts generated in the presence of rhMCSF and rhRANKL were kept as positive control. On the 21st day, the cells were bleached out using 6% sodium hypochlorite and 5.2% sodium chloride. OAAS plates were air dried and resorption area/pits generated by mature resorbing osteoclasts were imaged using light microscopy (Supplementary Fig. 1B). The resorptive ability of osteoclasts was assessed by quantifying the total resorbed area generated in OAAS well using ImageJ Software.

2.8. Cytokine neutralization

Osteoclast precursor cells were generated from CD14⁺ cells (1×10^5) in the presence of rhMCSF and rhRANKL for 12 days in OAAS module as described above. From the 12th day onwards, every 3rd day, along with rhMCSF and rhRANKL, the cultures were supplemented with 50 μ l cell free supernatant of unstimulated “activated” and “freshly isolated” $\gamma\delta$ T cells, with or without monoclonal mouse antihuman α IFN γ or α IL6 neutralization antibody (10 μ g/ml/well) respectively. Osteoclasts generated in the presence of rhMCSF and rhRANKL were kept as positive control. On the 21st day, the cultures were terminated and resorption area was calculated using ImageJ software.

2.9. Statistical analysis

The data was analysed using student's unpaired t test. p values ≤ 0.05 were considered statistically significant [$p < 0.05$ (*), $p < 0.005$ (**), $p < 0.0005$ (***)]. Error bar indicates mean \pm SEM.

3. Results

3.1. Expression of activation markers (CD69, CD25 and RANKL) on $\gamma\delta$ T cells

Expression of activation markers (CD69, CD25 and RANKL) on $\gamma\delta$ T cells were analysed by stimulating these cells with two distinct TCR signals (α CD3/CD28 or BrHPP) in the presence of rhIL2.

As shown in Fig. 1A, unstimulated PBMCs (Day 0) showed lower expression levels of CD69 (3.62% [percent positive], MFI = 72.5 [mean fluorescent intensity]), CD25 (16.2%, MFI = 405) and RANKL (4.06%, MFI = 115) on gated $\gamma\delta$ T cells. However, a marked increase in expression of CD25 and RANKL was observed on $\gamma\delta$ T cells upon stimulation of PBMCs with α CD3/CD28 + rhIL2 (100%, MFI = 134,379 and 53.5%, MFI = 641 respectively) or BrHPP + rhIL2 (99.1%, MFI = 17,740 and 36.4%, MFI = 654 respectively) for 12 days. Almost all $\gamma\delta$ T cells were positive for CD25 expression after stimulation, indicating that these cells were in highly activated state. Expression of CD69 (early activation marker) on $\gamma\delta$ T cells was found marginal changed upon stimulation of PBMCs with α CD3/CD28 + rhIL2 (0.9%, MFI = -714) and BrHPP + rhIL2 (2.82%, MFI = 211) for 12 days compared to unstimulated PBMCs (3.62%, MFI = 72.5).

Expression of these activation markers were also analysed on immunomagnetically purified $\gamma\delta$ T cells (Fig. 1B). Purified (“freshly isolated”) $\gamma\delta$ T cells were either left unstimulated (control) or were stimulated with rhIL2 alone or a combination of α CD3/CD28 + rhIL2 or BrHPP + rhIL2 for 24 h. As shown in Fig. 1B, in an unstimulated state, “freshly isolated” $\gamma\delta$ T cells showed lower levels of CD69 (5.04%, MFI = 126), CD25 (2.48%, MFI = 103) and RANKL (1.72%, MFI = 41.4). Upon stimulation with rhIL2 for 24 h, increase in the expression of CD69 (29.2%, MFI = 295), CD25 (9.10% MFI = 354) and RANKL (3.79% MFI = 81.3) was observed. “Freshly isolated” $\gamma\delta$ T cells stimulated with α CD3/CD28 + rhIL2 or BrHPP + rhIL2 showed markedly higher levels of CD69 (39.8%, MFI = 344 and 52.4%, MFI = 335 respectively), CD25 (13.2%, MFI = 512 and 18.3%, MFI = 677 respectively) and RANKL (7.38%, MFI = 106 and 9.49%, MFI = 77.6 respectively) as compared to unstimulated and rhIL2 stimulated $\gamma\delta$ T cells. Thus on the basis of expression of activation markers (CD69, CD25 and RANKL) $\gamma\delta$ T cells were considered as “non-activated” (freshly isolated) and “activated” (isolated from α CD3/CD28 + rhIL2 stimulated PBMCs) $\gamma\delta$ T cells.

3.2. Direct effect of $\gamma\delta$ T cells on generation of osteoclast

CD14⁺ cells (1×10^5 /well, osteoclast precursor cells) were cocultured with “activated” or “freshly isolated” $\gamma\delta$ T cells (1×10^4 /well, 10:1) in the presence of rhMCSF, rhRANKL and rhIL2 for 21 days (described in material and methods Section 2.6), with intermediate feedings on every 3rd day. Osteoclasts generated in the presence of rhMCSF and rhRANKL served as a positive control. Osteoclasts showing multinucleation (≥ 3 nuclei) and 23c6 positivity (vitronectin receptor) were considered as mature osteoclasts. Number of osteoclasts generated (25 ± 4 osteoclasts/well) in the presence of rhMCSF and rhRANKL (positive control) were normalized to 100% and data has been represented as relative increase or decrease in number of osteoclasts generated per well compared to positive control. Coculture of “activated” $\gamma\delta$ T cells with CD14⁺ cells in the presence of rhMCSF and rhRANKL showed significant reduction (1.5 ± 0.5 osteoclasts/well, 93.6% reduction, $p = 0.0012$) in 23c6⁺ multinucleated osteoclasts compared to positive control (Fig. 2). In contrast, generation of osteoclasts in the presence of “freshly isolated” $\gamma\delta$ T cells showed marked increase in the number of 23c6⁺ multinucleated osteoclasts (53.5 ± 14.5 osteoclasts/well, 110%

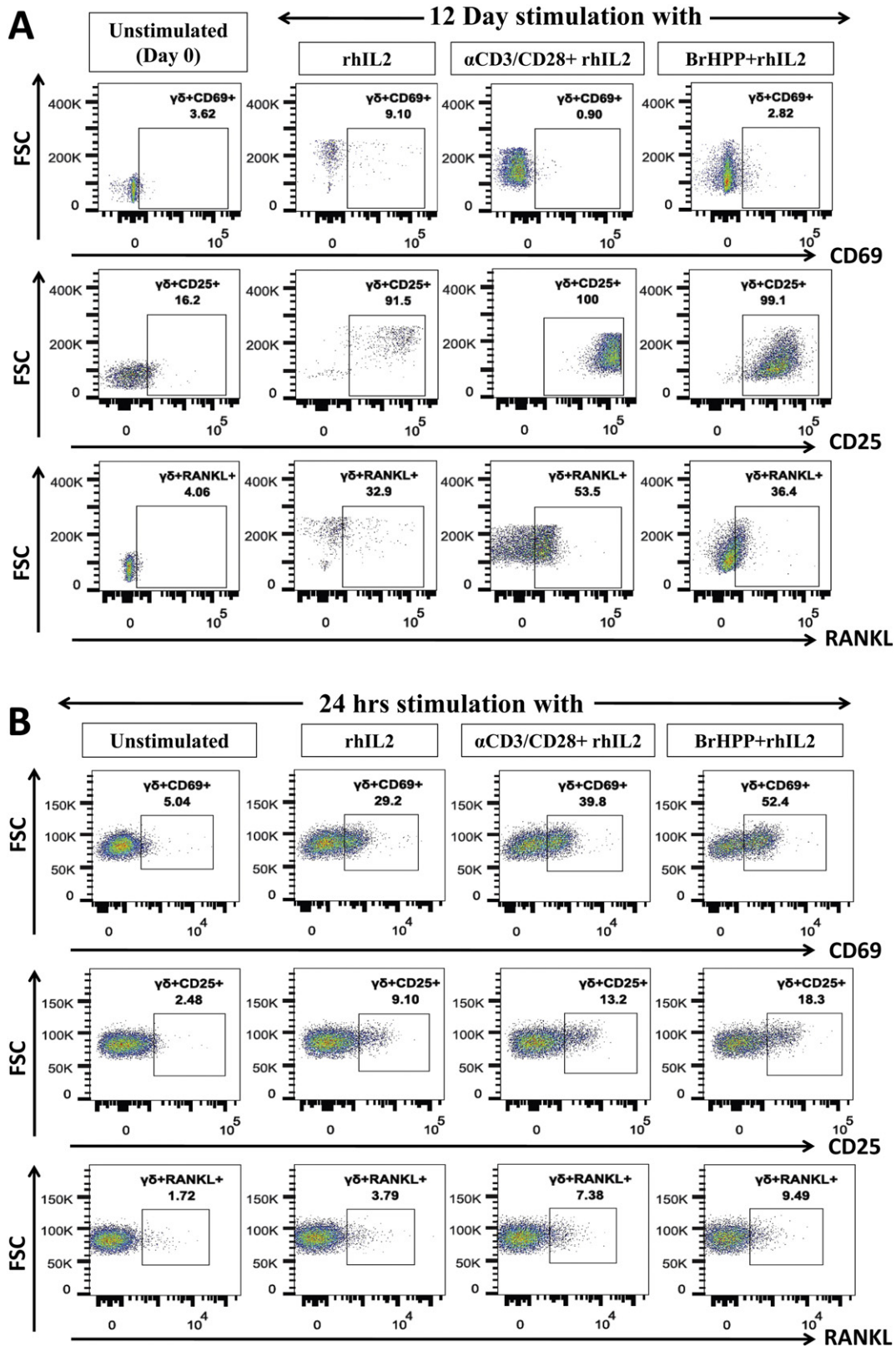


Fig. 1. Analysis of activation markers (CD69, CD25, and RANKL) on $\gamma\delta$ T cells. **A)** Expression of activation markers (CD69, CD25, and RANKL) was analysed on $\gamma\delta$ T cells in unstimulated PBMCs (1×10^6 /ml/well) or PBMCs expanded with rhIL2 (30 IU/ml) alone, α CD3/CD28 (1μ g) + rhIL2 or BrHPP (200 nM) + rhIL2 for 12 days. After the 12th day, PBMCs were stained using $\gamma\delta$ -APC, CD69-FITC, CD25-PeCy7, and RANKL-PE. Baseline expression of these markers on $\gamma\delta$ T cells was analysed by staining unstimulated PBMCs (Day 0, control). The gating strategy used was as follows: Lymphocytes were gated based on their forward and side scatter. Depending on the fluorescence intensity of $\gamma\delta$ -APC, $\gamma\delta$ T cells were gated. Further percentages of $\gamma\delta$ T cells expressing CD69, CD25 and RANKL were analysed on gated $\gamma\delta$ T cells. The gates have been set according to only cell controls for respective stimulation. **B)** Purified $\gamma\delta$ T cells were also stimulated with rhIL2 alone, α CD3/CD28 + rhIL2 or BrHPP + rhIL2 for 24 h or left unstimulated (medium alone) and were analysed for the expression of CD69, CD25 and RANKL. The gating strategy used was as described above. (Three independent experiments were carried out and the representative figure is given.)

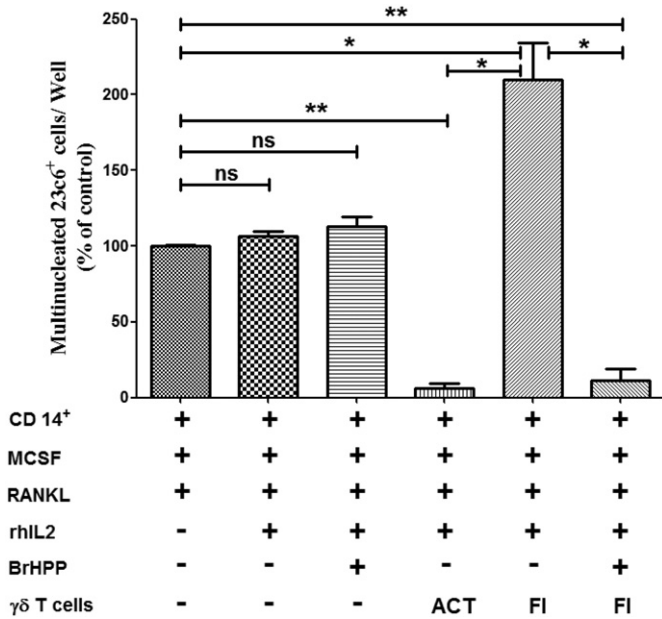


Fig. 2. Effect of “activated” and “freshly isolated” $\gamma\delta$ T cells on generation of osteoclasts. CD14⁺ cells (1×10^5 /well) were co-cultured with “activated” (ACT) or “freshly isolated” (FI) $\gamma\delta$ T cells (1×10^4) in α MEM supplemented with rhMCSF (30 ng/ml), rhRANKL (40 ng/ml) and rhIL2 (0.5 IU/well) on thermanox coverslips (Nunc) in flat bottom 96 well plate. Osteoclasts generated in the presence of rhMCSF and rhRANKL were kept as positive control. “Freshly isolated” $\gamma\delta$ T cells were stimulated with phosphoantigen by supplementing the cultures with BrHPP (200 nM) along with rhMCSF, rhRANKL and rhIL2 on Day 0. The CD14⁺: $\gamma\delta$ T cell cocultures were fed with rhMCSF, rhRANKL, rhIL2 every 3rd day for 21 days. On the 21st day, osteoclasts were characterized by staining them for vitronectin receptor (anti-human-CD51/CD61-AF488) and total number of osteoclasts (multinucleated 23c6⁺ cells) generated per well were quantitated. Number of osteoclasts generated in the presence of rhMCSF and rhRANKL (positive control) were normalized to 100% and data has been represented as relative increase or decrease in number of osteoclasts generated per well compared to positive control. Three independent experiments were carried out and the data is represented as mean \pm SEM. [$p < 0.05$ (*), $p < 0.005$ (**), $p < 0.0005$ (***)].

increase, $p = 0.0458$). These results indicated that “activated” $\gamma\delta$ T cells inhibit osteoclastogenesis, while “freshly isolated” $\gamma\delta$ T cells tend to increase the number of osteoclasts upon coculture. In order to confirm this observation “freshly isolated” $\gamma\delta$ T cells were cocultured with CD14⁺ cells in the presence of phosphoantigen BrHPP along with rhMCSF, rhRANKL and rhIL2. It was interesting to observe that generation of osteoclasts in the presence of “freshly isolated” $\gamma\delta$ T cells that were stimulated with BrHPP showed significant reduction (2.5 ± 1.5 osteoclasts/well, 88.8% reduction, $p = 0.0078$) in the total number of 23c6⁺ osteoclasts, confirming that “activation status” of $\gamma\delta$ T cells govern their function to regulate osteoclastogenesis. CD14⁺ cells cultured in the presence of rhMCSF and rhRANKL in the presence of rhIL2 (26.5 ± 3.5 osteoclasts/well) or BrHPP + rhIL2 (28 ± 3 osteoclasts/well) showed osteoclast numbers that were comparable to that observed in positive control (25 ± 4 osteoclasts/well), indicating that rhIL2 or BrHPP + rhIL2 had no effect on osteoclast generation.

3.3. Effect of soluble factors secreted by phosphoantigen stimulated $\gamma\delta$ T cells on function of osteoclasts

In order to investigate the indirect effect of $\gamma\delta$ T cells on osteoclast function mediated through secretion of soluble factors upon phosphoantigenic stimuli, osteoclast precursor cells (OPCs, generated on OAAS using rhMCSF and rhRANKL for 12 days) were cultured in the presence of pretitrated volumes of cell free supernatants of “activated” and “freshly isolated” $\gamma\delta$ T cells, stimulated with rhIL2 or BrHPP + rhIL2 (Groups 1–4), along with rhMCSF and rhRANKL. Osteoclasts cultured in the presence of rhMCSF and rhRANKL were kept as positive control. Total resorbed area generated by resorbing osteoclasts

in OAAS well was used as end point measurement of assay. Total resorption area generated per well by osteoclasts cultured in the presence of rhMCSF and rhRANKL (positive control) was normalized to 100% and data has been represented as relative increase or decrease in resorption area compared to positive control. As shown in Fig. 3, OPCs, supplemented with supernatants of “activated” $\gamma\delta$ T cells which were stimulated with rhIL2 alone (Group 1) or BrHPP + rhIL2 (Group 2) showed 72% and 70.4% reduction ($p = 0.0001$ and $p = 0.0011$ respectively) in the total resorbed area as compared to positive control. Similarly, effect of soluble factors secreted by “freshly isolated” $\gamma\delta$ T cells which were stimulated with rhIL2 alone (Group 3) or BrHPP + rhIL2 (Group 4) on osteoclast function showed significant increase (184.1%, $p = 0.002$ and 42.6%, $p = 0.0192$ respectively) in total resorbed area as compared to positive control. The results clearly indicated that soluble factors secreted by “activated” $\gamma\delta$ T cells potentially suppress osteoclast mediated bone resorption, whereas soluble factors secreted by “freshly isolated” $\gamma\delta$ T cells increase bone resorption.

3.4. Cytokine profiling of supernatants of antigen activated $\gamma\delta$ T cells

Cell free supernatants were collected from “activated” (ACT) and “freshly isolated” (FI) $\gamma\delta$ T cells. The various groups are described in materials and methods, Section 2.4. “Activated” and “freshly isolated” $\gamma\delta$ T cells were either left unstimulated (medium only control) or were stimulated with rhIL2 alone (Group 1, Group 3), BrHPP + rhIL2 (Group 2, Group 4). Cell free supernatants of these cells were collected and analysed for Th1/Th2/Th17 cytokines by CBA, as represented in Supplementary data, Table 1. Analysis of cell free supernatants of “activated” and “freshly isolated” $\gamma\delta$ T cells in the unstimulated control group interestingly showed significant differences in levels of two cytokines- IL6 (pro-osteoclastogenic) and IFN γ (anti-osteoclastogenic) compared to other cytokines (Supplementary data, Table 1). As shown in Fig. 4, in

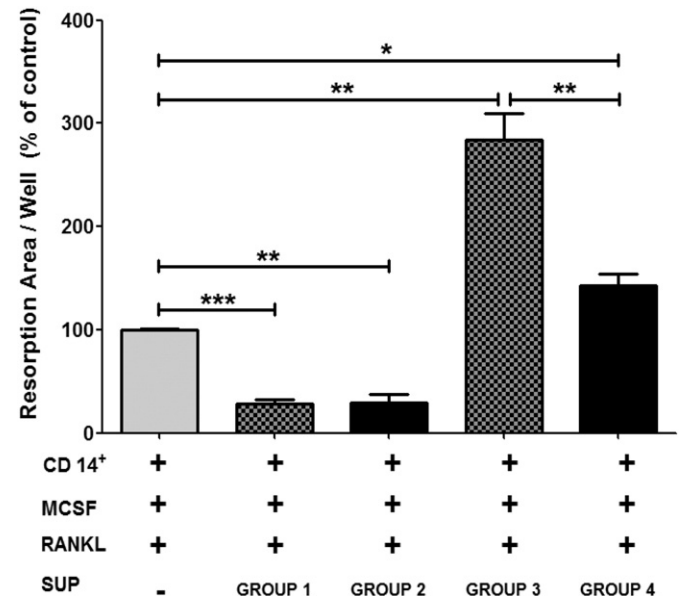


Fig. 3. Effect of supernatants of $\gamma\delta$ T cells on resorptive ability of osteoclasts. Osteoclasts were generated from CD14⁺ cells (1×10^5 /well) in the presence of rhMCSF (30 ng/ml) and rhRANKL (40 ng/ml) for 12 days on osteoclast activity assay substrate. From the 12th day onwards, the cultures were fed with cell free supernatants of “activated” and “freshly isolated” $\gamma\delta$ T cells, stimulated with rhIL2 (Group 1 and Group 3) or BrHPP + rhIL2 (Group 2 and Group 4) respectively, along with rhMCSF and rhRANKL on every 3rd day. Osteoclasts generated in the presence of rhMCSF and rhRANKL were kept as positive control. The cultures were terminated on the 21st day and the area resorbed by mature osteoclasts was calculated using ImageJ software. Total resorption area generated per well by osteoclasts cultured in the presence of rhMCSF and rhRANKL (positive control) was normalized to 100% and data has been represented as relative increase or decrease in resorption area compared to positive control. The data shown is mean \pm SEM of three independent experiments. [$p < 0.05$ (*), $p < 0.005$ (**), $p < 0.0005$ (***)].

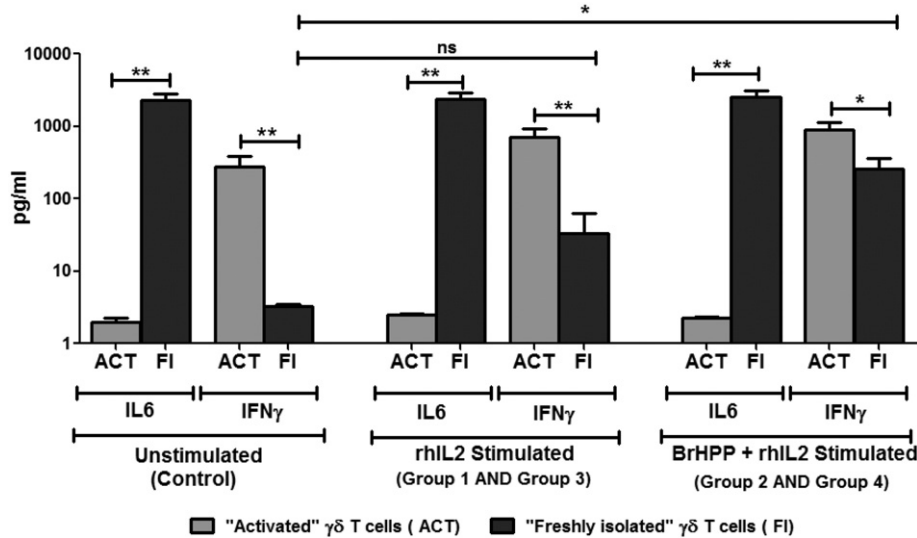


Fig. 4. Estimation of IL6 and IFN γ levels in cell free supernatants of “activated” (ACT) and “freshly isolated” (FI) $\gamma\delta$ T cells. “Activated” (purified from α CD3/CD28 + rhIL2 expanded PBMCs) or “freshly isolated” (directly purified from PBMCs on Day 0) $\gamma\delta$ T cells (5×10^4 /well) were stimulated with rhIL2 (0.5 IU/well) or BrHPP (200 nM) + rhIL2 for 24 h at 37 °C in CO $_2$ incubator. Both “activated” and “freshly isolated” $\gamma\delta$ T cells, which were unstimulated (incubated in culture medium alone), were kept as control. After 24 h, the cell free supernatants were collected. Th1/Th2/Th17 cytokines of these cell free supernatants were quantified by cytometric bead array (CBA). In an unstimulated state, supernatants of “activated” and “freshly isolated” $\gamma\delta$ T cells showed marked differences in IL6 and IFN γ levels. Stimulation of “activated” and “freshly isolated” $\gamma\delta$ T cells with rhIL2 (Group 1, Group 3 respectively) or BrHPP + rhIL2 (Group 2, Group 4 respectively) showed enhanced IFN γ secretion. Levels of IL6 remained higher in cell free supernatants of “freshly isolated” $\gamma\delta$ T cells. (“Activated” $\gamma\delta$ T cells (n = 5), “freshly isolated” $\gamma\delta$ T cells (n = 7)). [p < 0.05 (*), p < 0.005 (**), p < 0.0005 (***)].

an unstimulated state, “freshly isolated” $\gamma\delta$ T cells showed higher levels of IL6 (Mean \pm SEM 2318 ± 471 pg/ml), while “activated” $\gamma\delta$ T cells showed significantly ($p = 0.005$) lower levels of IL6 (1.9 ± 0.3 pg/ml). Comparison of IFN γ levels showed that, “freshly isolated” $\gamma\delta$ T cells secreted very low (3.2 ± 0.27 pg/ml) levels of IFN γ , while “activated” $\gamma\delta$ T cells showed significantly ($p = 0.008$) higher levels of IFN γ (274.1 ± 111.2 pg/ml).

Upon stimulation with rhIL2, supernatant of “activated” $\gamma\delta$ T cells (Group 1) showed significantly higher levels of IFN γ (706.5 ± 211.8 pg/ml, $p = 0.0044$) compared to “freshly isolated” $\gamma\delta$ T cells (33.5 ± 29.1 pg/ml, Group 3). Similarly, upon stimulation with BrHPP + rhIL2, “activated” $\gamma\delta$ T cells (Group 2) showed significantly higher levels of IFN γ (879.7 ± 240 pg/ml, $p = 0.0264$) compared to “freshly isolated” $\gamma\delta$ T cells (260.7 ± 101.2 pg/ml Group 4). Freshly isolated $\gamma\delta$ T cells upon stimulation with rhIL2 showed a progressive increase in IFN γ production that further enhanced with BrHPP + rhIL2 stimulation ($p = 0.01$) compared to unstimulated $\gamma\delta$ T cells.

The levels of IL6 secreted by “activated” (Group 1 and Group 3) and “freshly isolated” (Group 2 and Group 4) $\gamma\delta$ T cells were not significantly different compared to supernatants of unstimulated $\gamma\delta$ T cells (control).

Results indicate that “freshly isolated” $\gamma\delta$ T cells secrete higher levels of IL6, thus have pro-osteoclastogenic effect, while “activated” $\gamma\delta$ T cells maintain higher levels of IFN γ playing an anti-osteoclastogenic role.

3.5. Effect of IFN γ or IL6 neutralization in cell free supernatants of $\gamma\delta$ T cells on osteoclast function

To validate that the effect of $\gamma\delta$ T cells on osteoclastogenesis is mediated through cytokines (IFN γ and IL6), functional assays were carried out using neutralizing antibodies to these cytokines. Osteoclasts were generated in the presence of cell free supernatants of unstimulated “activated” and “freshly isolated” $\gamma\delta$ T cells in the presence or absence of α IFN γ or α IL6 antibody. As shown in Fig. 5, osteoclasts generated in presence of cell free supernatants of “activated” $\gamma\delta$ T cells showed significant (57.4%) reduction in resorption area ($10.78 \pm 1 \mu\text{m}^2$) compared to positive control ($25.4 \pm 0.5 \mu\text{m}^2$, 100%). After addition of α IFN γ antibody to these cultures the inhibition was reversed and brought to 89.7% ($22.7 \pm 0.3 \mu\text{m}^2$), which was comparable to that observed in positive

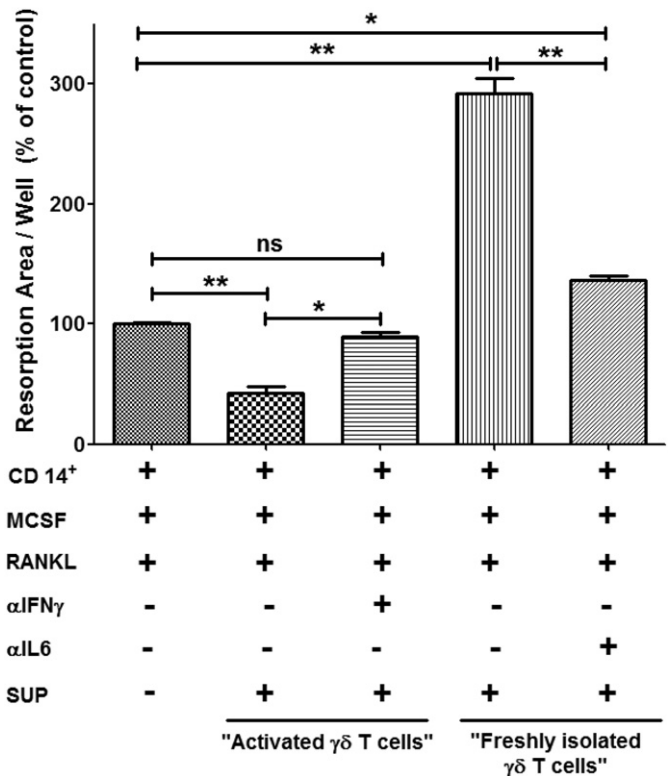


Fig. 5. Effect of IFN γ and IL6 neutralization in cell free supernatants of “activated” (ACT) and “freshly isolated” (FI) $\gamma\delta$ T cells on osteoclast function. CD14 $^+$ cells (1×10^5) were cultured in the presence of rhMCSF and rhRANKL for 12 days in OAAS module to generate OPCs. After which, every 3rd day, the cultures were supplemented with 50 μ l supernatants of unstimulated “activated” and “freshly isolated” $\gamma\delta$ T cells, rhMCSF, and rhRANKL with or without monoclonal mouse α IFN γ or α IL6 neutralization antibody (10 μ g/ml/well). Osteoclasts generated in the presence of rhMCSF and rhRANKL were kept as positive control. On the 21st day, the cultures were terminated and resorption area was calculated. Resorption area generated in positive control was normalized to 100% and data has been represented as relative increase or decrease in resorption area compared to positive control. The data shown is mean \pm SEM of two independent experiments. [p < 0.05 (*), p < 0.005 (**), p < 0.0005 (***)].

control, confirming our observation that IFN γ is a major cytokine generated by “activated” $\gamma\delta$ T cells that inhibits osteoclastogenesis.

Similarly, osteoclasts generated in the presence of cell free supernatants of “freshly isolated” $\gamma\delta$ T cells showed increase in resorption area by 191.9% ($74.1 \pm 1.6 \mu\text{m}^2$) over positive control (100%). Upon addition of α IL6 antibody to the cultures, there was a marked reduction in the resorption area ($34.5 \pm 0.2 \mu\text{m}^2$, $p = 0.0068$) reducing from 191.9% to 36.1% over positive control (100%). Our results suggest that the dynamics of IFN γ and IL6 play a major role in mediating the pro and anti-osteoclastogenic effects of “activated” $\gamma\delta$ T cells and “freshly isolated” $\gamma\delta$ T cells respectively.

4. Discussion

Bone is a common site of metastasis in breast cancer (Suva et al., 2009), prostate cancer and multiple myeloma (Roodman, 2010). Metastatic tumour cells disturb the bone metabolism by releasing factors which induce differentiation and activation of osteoclasts (Roodman, 2001). It has also been reported that cytokines secreted by lymphocytes present in the bone microenvironment affect bone metabolism (Gillespie, 2007). Investigations are focused on understanding how T lymphocytes interact with osteoclasts and influence their function. Activated CD4⁺ T cells express RANKL and secrete cytokines such as IL1 β , IL6, IL17, TNF α and RANKL that support osteoclastogenesis (Horwood et al., 1999; Kotake et al., 2001; Lee et al., 2011b; Kong et al., 1999). Interestingly, it has also been reported that activated T lymphocytes secrete cytokines such as IFN γ , IL4, IL10 and GM-CSF that inhibit osteoclastogenesis (Walsh et al., 2006; Sato and Takayanagi, 2006). It is still not understood what dictates the pro and anti-osteoclastogenic behaviour of the lymphocytes. Although the role of CD4⁺ $\alpha\beta$ T cells in osteoclastogenesis has been investigated, the role of $\gamma\delta$ T cells is not well understood. In the present study, we have made an attempt to analyze the effect of “activated” and “freshly isolated” $\gamma\delta$ T cells on osteoclast generation and function.

We used $\gamma\delta$ T cells from two sources; those that were isolated directly from PBMCs (“freshly isolated” $\gamma\delta$ T cells) and those that were isolated from PBMCs stimulated with α CD3/CD28 + rhIL2 (“activated” $\gamma\delta$ T cells). Coculture of “freshly isolated” $\gamma\delta$ T cells with CD14⁺ cells enhanced the generation of osteoclasts and stimulated their resorptive ability. On the contrary, “activated” $\gamma\delta$ T cells showed inhibitory effect on generation and function of osteoclasts. The process of osteoclastogenesis is majorly influenced by cytokine milieu in the microenvironment, where IL6, IL17, TNF α , TGF β , IFN γ and RANKL play indispensable role. Analysis of cell free supernatants of “freshly isolated” $\gamma\delta$ T cells at baseline levels (unstimulated) showed marked difference in their IL6 and IFN γ levels. In an unstimulated state, “freshly isolated” $\gamma\delta$ T cells were major producers of IL6, with negligible levels of IFN γ . On the contrary, “activated” $\gamma\delta$ T cells showed higher IFN γ levels with low IL6 production.

IL6 is a potent pro-osteoclastogenic cytokine, with the capacity to induce osteoclastogenesis in RANKL independent manner (Kudo et al., 2003) and it also acts in synergistic manner with TNF α to induce osteoclastogenesis (Ragab et al., 2002). IL6 has been reported to stimulate formation of osteoclast like multinucleated cells in long term cultures of human bone marrow through induction of IL1 β (Kurihara et al., 1990). T lymphocytes from IL6^{-/-} mice have shown lesser production of IL17 (pro-osteoclastogenic) and also affected RANKL/OPG production by T lymphocytes (Wong et al., 2006). Cultures of osteoclasts from bone marrow cells of IL6^{-/-} mice in the presence of M-CSF and RANKL produced ~50% lesser osteoclasts as compared to wild type mice (Wong et al., 2006). On the contrary, IFN γ has been appreciated for its protective role in osteoclastogenesis by inhibiting osteoclast formation and bone resorption in vitro (Takayanagi et al., 2000; Kamolmatyakul et al., 2001). Mice lacking one of the components of IFN γ receptor (IFN γ R1) showed enhanced osteoclastogenesis from bone marrow derived monocyte/macrophage precursor cells (BMMs) and bone loss

(Takayanagi et al., 2000). Also, IFN γ producing activated T cells showed osteoclast generation from BMMs in the absence of RANKL in IFN γ R^{-/-} mice (Takayanagi et al., 2000). IFN γ either downregulates TRAF6 (TNF receptor associated factor 6) expression or activates/enhances ubiquitin dependent proteosomal systems whose direct target is TRAF6 (Takayanagi et al., 2000; Takayanagi et al., 2005), which results in disruption of RANK–RANKL signalling.

In order to confirm that IL6 and IFN γ are the key cytokines involved in the pro and anti-osteoclastogenic effects mediated by “freshly isolated” and “activated” $\gamma\delta$ T cells respectively, neutralization experiment was carried out using α IL6 and α IFN γ antibodies. Addition of α IL6 antibody to the supernatants of “freshly isolated” $\gamma\delta$ T cells showed a marked reduction in the resorption area. However, the resorption area remained marginally above that was observed with positive control (rhM-CSF + rhRANKL). The data indicates that other cytokines like TNF α and IL17 may also contribute to the pro-osteoclastogenic effect, which may be present in the supernatants after blocking IL6 (Supplementary Table 1). Similarly blocking of IFN γ significantly reversed (89.74%) the anti-osteoclastogenic effect, indicating that IFN γ is the dominant cytokine inhibiting osteoclastogenesis.

Human $\gamma\delta$ T cells are Th1 type cells which produce copious amounts of IFN γ upon stimulation (Haas et al., 1993; Wang et al., 2001; Garcia et al., 1997). BrHPP, an analogue of IPP, known to be a potent antigen of $\gamma\delta$ T cells was used to stimulate “freshly isolated” $\gamma\delta$ T cells in the presence of rhIL2. Upon stimulation with BrHPP + rhIL2, the activation markers (CD69, CD25 and RANKL) on these cells were found to be increased compared to unstimulated $\gamma\delta$ T cells. CD69, an early activation marker, is expressed on T cells upon triggering through TCR complex (Ziegler et al., 1994). T cell activation through CD69 results in upregulation of CD25 and induction of Th1 cytokine (IL2 and IFN γ), ultimately triggering proliferation of the lymphocytes (Rutella et al., 1999). As expected, higher levels of IFN γ along with increased expression of activation markers (CD25 and RANKL) were observed on “activated” $\gamma\delta$ T cells (which were expanded using α CD3/CD28 + rhIL2), while no significant change was observed in early activation marker CD69. “Freshly isolated” $\gamma\delta$ T cells upon stimulation with BrHPP + rhIL2 showed increase in IFN γ production, along with significant increase in early activation markers like CD69 and RANKL. Compared to rhIL2 stimulated, “freshly isolated” $\gamma\delta$ T cells stimulated with BrHPP + rhIL2, irrespective of short or long term activation, showed inhibitory effect on generation (vitronectin receptor expression) and resorptive ability (resorption area on OAS plates) of osteoclasts. Thus, “freshly isolated” $\gamma\delta$ T cells stimulated with phosphoantigen (BrHPP + rhIL2) exhibited the characteristics of “activated” $\gamma\delta$ T cells to suppress osteoclast generation and function.

To best of our knowledge, this is the first study to show that activation status and the cytokines released by $\gamma\delta$ T cells dictates their effect on osteoclastogenesis. Aminobisphosphonates, the new generation bisphosphonates, are used as standard treatment modality in patients with breast cancer, prostate cancer and multiple myeloma patients exhibiting skeletal metastasis (Dhar and Chiplunkar, 2010; Roodman and Dougall, 2008). Aminobisphosphonates inhibit activity and survival of osteoclasts (Caraglia et al., 2006). Besides their antitumor and anti-resorptive ability, aminobisphosphonate (Zoledronic acid) are potent activators of $\gamma\delta$ T cells. IL6, dominantly secreted by “freshly isolated” $\gamma\delta$ T cells (low CD25, CD69 expression) promote osteoclastogenesis, while antigen (BrHPP) activated $\gamma\delta$ T cells (high CD25, CD69 expression) inhibit osteoclastogenesis through increased IFN γ production. This data adds a new dimension towards understanding the mechanism of action of aminobisphosphonate in patients receiving this treatment for skeletal metastasis. Although antitumor and anti-resorptive roles of aminobisphosphonates are reported, the present study further demonstrates the crosstalk of immune cells and osteoclasts mediated by aminobisphosphonates. Future immunotherapeutic approaches can utilize aminobisphosphonates activated $\gamma\delta$ T cells for treatment of skeletal metastasis.

5. Conclusion

Effect of $\gamma\delta$ T cells on osteoclastogenesis depends on their activation status. Phosphoantigen “activated” $\gamma\delta$ T cells express higher levels of activation markers (CD25 and RANKL expression) and secrete higher levels of IFN γ (anti-osteoclastogenic), thus inhibiting osteoclast generation and function. On the contrary, “freshly isolated” $\gamma\delta$ T cells, in an unstimulated state (low CD25, CD69 and RANKL expression) secrete higher levels of IL6 (pro-osteoclastogenic) and enhance osteoclast generation and function. “Freshly isolated” $\gamma\delta$ T cells, when stimulated with phosphoantigen (BrHPP) showed increased IFN γ secretion and attained anti-osteoclastogenic potential. Neutralization of IFN γ and IL6 using blocking antibodies majorly diminished the “inhibitory” or “stimulatory” effect of “freshly isolated” and “activated” $\gamma\delta$ T cells respectively on osteoclastogenesis. In conclusion, activation status and dynamics of IL6/IFN γ dictates pro or anti-osteoclastogenic role of $\gamma\delta$ T cells.

Supplementary data to this article can be found online at <http://dx.doi.org/10.1016/j.bonr.2015.10.004>.

Conflict of interest statement

The author (s) declare(s) that there is no conflict of interest.

Acknowledgements

The present study was funded through the intramural funding of the Tata Memorial Centre, India (Grant – “Seed in Air-2700”). We thank the “Department of Biotechnology, India” for providing fellowship to Ms. Swati P. Phalke. We are thankful to all the healthy volunteers for providing blood samples for this study.

References

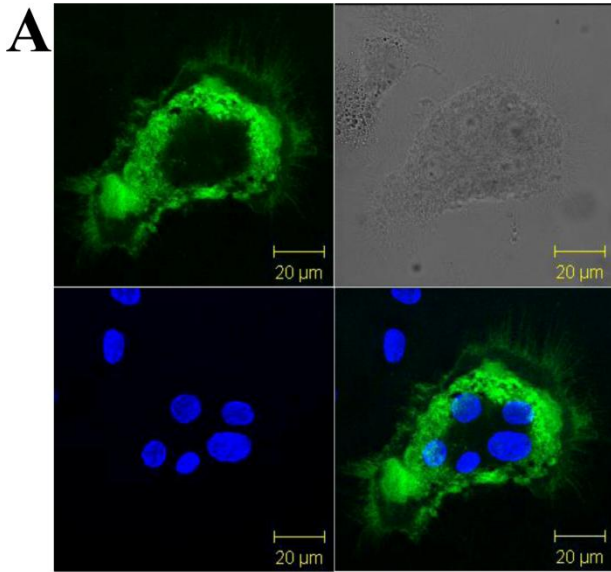
- Beetz, S., Marischen, L., Kabelitz, D., Wesch, D., 2007. Human gamma delta T cells: candidates for the development of immunotherapeutic strategies. *Immunol. Res.* 37, 97–111.
- Born, W.K., Reardon, C.L., O'Brien, R.L., 2006. The function of gammadelta T cells in innate immunity. *Curr. Opin. Immunol.* 18, 31–38.
- Buccheri, S., Guggino, G., Caccamo, N., Li Donni, P., Dieli, F., 2014. Efficacy and safety of gammadelta T cell-based tumor immunotherapy: a meta-analysis. *J. Biol. Regul. Homeost. Agents* 28, 81–90.
- Caccamo, N., La Mendola, C., Orlando, V., Meraviglia, S., Todaro, M., Stassi, G., Sireci, G., Fournie, J.J., Dieli, F., 2011. Differentiation, phenotype, and function of interleukin-17-producing human Vgamma9Vdelta2 T cells. *Blood* 118, 129–138.
- Caccamo, N., Todaro, M., Sireci, G., Meraviglia, S., Stassi, G., Dieli, F., 2013. Mechanisms underlying lineage commitment and plasticity of human gammadelta T cells. *Cell. Mol. Immunol.* 10, 30–34.
- Caraglia, M., Santini, D., Marra, M., Vincenzi, B., Tonini, G., Budillon, A., 2006. Emerging anti-cancer molecular mechanisms of aminobisphosphonates. *Endocr. Relat. Cancer* 13, 7–26.
- Casetti, R., Agrati, C., Wallace, M., Sacchi, A., Martini, F., Martino, A., Rinaldi, A., Malkovsky, M., 2009. Cutting edge: TGF-beta1 and IL-15 induce FOXP3+ gammadelta regulatory T cells in the presence of antigen stimulation. *J. Immunol.* 183, 3574–3577.
- Chiplunkar, S., Dhar, S., Wesch, D., Kabelitz, D., 2009. Gammadelta T cells in cancer immunotherapy: current status and future prospects. *Immunotherapy* 1, 663–678.
- Dhar, S., Chiplunkar, S.V., 2010. Lysis of aminobisphosphonate-sensitized MCF-7 breast tumor cells by Vgamma9Vdelta2 T cells. *Cancer Immunol.* 10, 10.
- Espinosa, E., Belmont, C., Pont, F., Luciani, B., Poupot, R., Romagne, F., Brailly, H., Bonneville, M., Fournie, J.J., 2001. Chemical synthesis and biological activity of bromohydrin pyrophosphate, a potent stimulator of human gamma delta T cells. *J. Biol. Chem.* 276, 18337–18344.
- Garcia, V.E., Sieling, P.A., Gong, J., Barnes, P.F., Uyemura, K., Tanaka, Y., Bloom, B.R., Morita, C.T., Modlin, R.L., 1997. Single-cell cytokine analysis of gamma delta T cell responses to nonpeptide mycobacterial antigens. *J. Immunol.* 159, 1328–1335.
- Gertner-Dardenne, J., Castellano, R., Mamessier, E., Garbit, S., Kochbati, E., Etienne, A., Charbonnier, A., Collette, Y., Vey, N., Olive, D., 2012. Human Vgamma9Vdelta2 T cells specifically recognize and kill acute myeloid leukemic blasts. *J. Immunol.* 188, 4701–4708.
- Gillespie, M.T., 2007. Impact of cytokines and T lymphocytes upon osteoclast differentiation and function. *Arthritis Res. Ther.* 9, 103.
- Gomes, A.Q., Correia, D.V., Grosso, A.R., Lanca, T., Ferreira, C., Lacerda, J.F., Barata, J.T., Silva, M.G., Silva-Santos, B., 2010. Identification of a panel of ten cell surface protein antigens associated with immunotargeting of leukemias and lymphomas by peripheral blood gammadelta T cells. *Haematologica* 95, 1397–1404.
- Gupta, N., Barhanpurkar, A.P., Tomar, G.B., Srivastava, R.K., Kour, S., Pote, S.T., Mishra, G.C., Wani, M.R., 2010. IL-3 inhibits human osteoclastogenesis and bone resorption through downregulation of c-Fms and diverts the cells to dendritic cell lineage. *J. Immunol.* 185, 2261–2272.
- Haas, W., Pereira, P., Tonegawa, S., 1993. Gamma/delta cells. *Annu. Rev. Immunol.* 11, 637–685.
- Havran, W.L., Jameson, J.M., Witherden, D.A., 2005. Epithelial cells and their neighbors. III. Interactions between intraepithelial lymphocytes and neighboring epithelial cells. *Am. J. Physiol. Gastrointest. Liver Physiol.* 289, G627–G630.
- Hayday, A.C., 2000. [Gamma][delta] cells: a right time and a right place for a conserved third way of protection. *Annu. Rev. Immunol.* 18, 975–1026.
- Hayday, A.C., 2009. Gammadelta T cells and the lymphoid stress-surveillance response. *Immunity* 31, 184–196.
- Horwood, N.J., Kartsogiannis, V., Quinn, J.M., Romas, E., Martin, T.J., Gillespie, M.T., 1999. Activated T lymphocytes support osteoclast formation in vitro. *Biochem. Biophys. Res. Commun.* 265, 144–150.
- Jameson, J.M., Cauvi, G., Sharp, L.L., Witherden, D.A., Havran, W.L., 2005. Gammadelta T cell-induced hyaluronan production by epithelial cells regulates inflammation. *J. Exp. Med.* 201, 1269–1279.
- Kabelitz, D., Kalyan, S., Oberg, H.H., Wesch, D., 2013. Human Vdelta2 versus non-Vdelta2 gammadelta T cells in antitumor immunity. *Oncimmunology* 2, e23304.
- Kamolmatyakul, S., Chen, W., Li, Y.P., 2001. Interferon-gamma down-regulates gene expression of cathepsin K in osteoclasts and inhibits osteoclast formation. *J. Dent. Res.* 80, 351–355.
- Keystone, E.C., Rittershaus, C., Wood, N., Snow, K.M., Flatow, J., Purvis, J.C., Poplonski, L., Kung, P.C., 1991. Elevation of a gamma delta T cell subset in peripheral blood and synovial fluid of patients with rheumatoid arthritis. *Clin. Exp. Immunol.* 84, 78–82.
- Kong, Y.Y., Feige, U., Sarosi, I., Bolon, B., Tafuri, A., Morony, S., Capparelli, C., Li, J., Elliott, R., McCabe, S., Wong, T., Campagnuolo, G., Moran, E., Bogoch, E.R., Van, G., Nguyen, L.T., Ohashi, P.S., Lacey, D.L., Fish, E., Boyle, W.J., Penninger, J.M., 1999. Activated T cells regulate bone loss and joint destruction in adjuvant arthritis through osteoprotegerin ligand. *Nature* 402, 304–309.
- Konigshofer, Y., Chien, Y.H., 2006. Gammadelta T cells –innate immune lymphocytes? *Curr. Opin. Immunol.* 18, 527–533.
- Kotake, S., Udagawa, N., Hakoda, M., Mogi, M., Yano, K., Tsuda, E., Takahashi, K., Furuya, T., Ishiyama, S., Kim, K.J., Saito, S., Nishikawa, T., Takahashi, N., Togari, A., Tomatsu, T., Suda, T., Kamatani, N., 2001. Activated human T cells directly induce osteoclastogenesis from human monocytes: possible role of T cells in bone destruction in rheumatoid arthritis patients. *Arthritis Rheum.* 44, 1003–1012.
- Kudo, O., Sabokbar, A., Pocock, A., Itonaga, I., Fujikawa, Y., Athanasou, N.A., 2003. Interleukin-6 and interleukin-11 support human osteoclast formation by a RANKL-independent mechanism. *Bone* 32, 1–7.
- Kurihara, N., Bertolini, D., Suda, T., Akiyama, Y., Roodman, G.D., 1990. IL-6 stimulates osteoclast-like multinucleated cell formation in long term human marrow cultures by inducing IL-1 release. *J. Immunol.* 144, 4226–4230.
- Laad, A.D., Thomas, M.L., Fakhri, A.R., Chiplunkar, S.V., 1999. Human gamma delta T cells recognize heat shock protein-60 on oral tumor cells. *Int. J. Cancer* 80, 709–714.
- Lam, J., Takahashi, S., Barker, J.E., Kanagawa, O., Ross, F.P., Teitelbaum, S.L., 2000. TNF-alpha induces osteoclastogenesis by direct stimulation of macrophages exposed to permissive levels of RANK ligand. *J. Clin. Invest.* 106, 1481–1488.
- Lee, R.J., Saylor, P.J., Smith, M.R., 2011a. Treatment and prevention of bone complications from prostate cancer. *Bone* 48, 88–95.
- Lee, S.J., Nam, K.I., Jin, H.M., Cho, Y.N., Lee, S.E., Kim, T.J., Lee, S.S., Kee, S.J., Lee, K.B., Kim, N., Park, Y.W., 2011b. Bone destruction by receptor activator of nuclear factor kappaB ligand-expressing T cells in chronic gouty arthritis. *Arthritis Res. Ther.* 13, R164.
- Lipton, A., Goessl, C., 2011. Clinical development of anti-RANKL therapies for treatment and prevention of bone metastasis. *Bone* 48, 96–99.
- Ness-Schwickerath, K.J., Jin, C., Morita, C.T., 2010. Cytokine requirements for the differentiation and expansion of IL-17A- and IL-22-producing human Vgamma2Vdelta2 T cells. *J. Immunol.* 184, 7268–7280.
- Neville-Webbe, H.L., Coleman, R.E., 2010. Bisphosphonates and RANK ligand inhibitors for the treatment and prevention of metastatic bone disease. *Eur. J. Cancer* 46, 1211–1222.
- Pappalardo, A., Thompson, K., 2013. Activated gammadelta T cells inhibit osteoclast differentiation and resorptive activity in vitro. *Clin. Exp. Immunol.* 174, 281–291.
- Pollinger, B., Jung, T., Smetzer, B., Walker, U.A., Tyndall, A., Allard, C., Bay, S., Keller, R., Raulf, F., Di Padova, F., O'Reilly, T., Horwood, N.J., Patel, D.D., Littlewood-Evans, A., 2011. Th17 cells, not IL-17+ gammadelta T cells, drive arthritic bone destruction in mice and humans. *J. Immunol.* 186, 2602–2612.
- Ragab, A.A., Nalepka, J.L., Bi, Y., Greenfield, E.M., 2002. Cytokines synergistically induce osteoclast differentiation: support by immortalized or normal calvarial cells. *Am. J. Physiol. Cell Physiol.* 283, C679–C687.
- Roodman, G.D., 2001. Biology of osteoclast activation in cancer. *J. Clin. Oncol.* 19, 3562–3571.
- Roodman, G.D., 2010. Pathogenesis of myeloma bone disease. *J. Cell. Biochem.* 109, 283–291.
- Roodman, G.D., Dougall, W.C., 2008. RANK ligand as a therapeutic target for bone metastases and multiple myeloma. *Cancer Treat. Rev.* 34, 92–101.
- Rutella, S., Rumi, C., Lucia, M.B., Barberi, T., Puggioni, P.L., Lai, M., Romano, A., Cuda, R., Leone, G., 1999. Induction of CD69 antigen on normal CD4+ and CD8+ lymphocyte subsets and its relationship with the phenotype of responding T-cells. *Cytometry* 38, 95–101.
- Santini, D., Martini, F., Fratto, M.E., Galluzzo, S., Vincenzi, B., Agrati, C., Turchi, F., Piacentini, P., Rocci, L., Manavalan, J.S., Tonini, G., Poccia, F., 2009. In vivo effects of zoledronic acid on peripheral gammadelta T lymphocytes in early breast cancer patients. *Cancer Immunol. Immunother.* 58, 31–38.
- Sato, K., Takayanagi, H., 2006. Osteoclasts, rheumatoid arthritis, and osteoimmunology. *Curr. Opin. Rheumatol.* 18, 419–426.

- Sato, K., Suematsu, A., Okamoto, K., Yamaguchi, A., Morishita, Y., Kadono, Y., Tanaka, S., Kodama, T., Akira, S., Iwakura, Y., Cua, D.J., Takayanagi, H., 2006. Th17 functions as an osteoclastogenic helper T cell subset that links T cell activation and bone destruction. *J. Exp. Med.* 203, 2673–2682.
- Sharp, L.L., Jameson, J.M., Cauvi, G., Havran, W.L., 2005. Dendritic epidermal T cells regulate skin homeostasis through local production of insulin-like growth factor 1. *Nat. Immunol.* 6, 73–79.
- Sireci, G., Champagne, E., Fournie, J.J., Dieli, F., Salerno, A., 1997. Patterns of phosphoantigen stimulation of human Vgamma9/Vdelta2 T cell clones include Th0 cytokines. *Hum. Immunol.* 58, 70–82.
- Soysa, N.S., Alles, N., Aoki, K., Ohya, K., 2012. Osteoclast formation and differentiation: an overview. *J. Med. Dent. Sci.* 59, 65–74.
- Suva, L.J., Griffin, R.J., Makhoul, I., 2009. Mechanisms of bone metastases of breast cancer. *Endocr. Relat. Cancer* 16, 703–713.
- Takayanagi, H., 2007. Osteoimmunology: shared mechanisms and crosstalk between the immune and bone systems. *Nat. Rev. Immunol.* 7, 292–304.
- Takayanagi, H., Ogasawara, K., Hida, S., Chiba, T., Murata, S., Sato, K., Takaoka, A., Yokochi, T., Oda, H., Tanaka, K., Nakamura, K., Taniguchi, T., 2000. T-cell-mediated regulation of osteoclastogenesis by signalling cross-talk between RANKL and IFN-gamma. *Nature* 408, 600–605.
- Takayanagi, H., Sato, K., Takaoka, A., Taniguchi, T., 2005. Interplay between interferon and other cytokine systems in bone metabolism. *Immunol. Rev.* 208, 181–193.
- Teitelbaum, S.L., 2007. Osteoclasts: what do they do and how do they do it? *Am. J. Pathol.* 170, 427–435.
- Thomas, M.L., Samant, U.C., Deshpande, R.K., Chiplunkar, S.V., 2000. Gammadelta T cells lyse autologous and allogenic oesophageal tumours: involvement of heat-shock proteins in the tumour cell lysis. *Cancer Immunol. Immunother.* 48, 653–659.
- Todaro, M., D'Asaro, M., Caccamo, N., Iovino, F., Francipane, M.G., Meraviglia, S., Orlando, V., La Mendola, C., Gulotta, G., Salerno, A., Dieli, F., Stassi, G., 2009. Efficient killing of human colon cancer stem cells by gammadelta T lymphocytes. *J. Immunol.* 182, 7287–7296.
- Walsh, M.C., Kim, N., Kadono, Y., Rho, J., Lee, S.Y., Lorenzo, J., Choi, Y., 2006. Osteoimmunology: interplay between the immune system and bone metabolism. *Annu. Rev. Immunol.* 24, 33–63.
- Wang, L., Kamath, A., Das, H., Li, L., Bukowski, J.F., 2001. Antibacterial effect of human V gamma 2V delta 2 T cells in vivo. *J. Clin. Invest.* 108, 1349–1357.
- Weitzmann, M.N., Cenci, S., Rifas, L., Haug, J., Dipersio, J., Pacifici, R., 2001. T cell activation induces human osteoclast formation via receptor activator of nuclear factor kappaB ligand-dependent and -independent mechanisms. *J. Bone Miner. Res.* 16, 328–337.
- Wesch, D., Glatzel, A., Kabelitz, D., 2001. Differentiation of resting human peripheral blood gamma delta T cells toward Th1- or Th2-phenotype. *Cell. Immunol.* 212, 110–117.
- Wong, P.K., Quinn, J.M., Sims, N.A., van Nieuwenhuijze, A., Campbell, I.K., Wicks, I.P., 2006. Interleukin-6 modulates production of T lymphocyte-derived cytokines in antigen-induced arthritis and drives inflammation-induced osteoclastogenesis. *Arthritis Rheum.* 54, 158–168.
- Wrobel, P., Shojaei, H., Schitteck, B., Gieseler, F., Wollenberg, B., Kalthoff, H., Kabelitz, D., Wesch, D., 2007. Lysis of a broad range of epithelial tumour cells by human gamma delta T cells: involvement of NKG2D ligands and T-cell receptor- versus NKG2D-dependent recognition. *Scand. J. Immunol.* 66, 320–328.
- Wu, Y.L., Ding, Y.P., Tanaka, Y., Shen, L.W., Wei, C.H., Minato, N., Zhang, W., 2014. Gammadelta T cells and their potential for immunotherapy. *Int. J. Biol. Sci.* 10, 119–135.
- Ziegler, S.F., Ramsdell, F., Alderson, M.R., 1994. The activation antigen CD69. *Stem Cells* 12, 456–465.

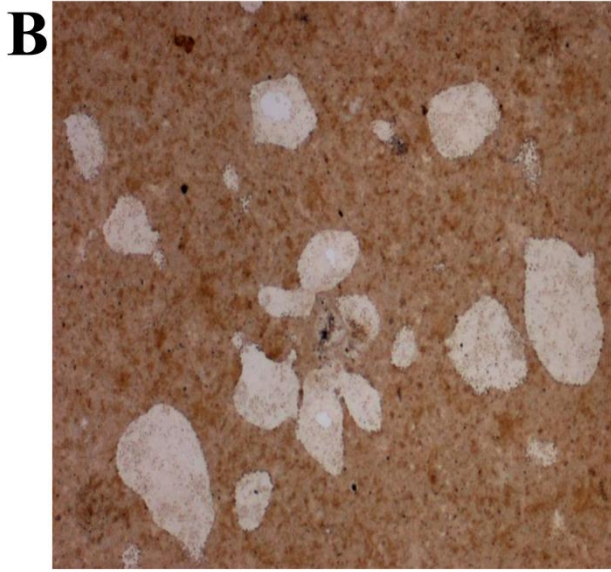
Supplementary Table 1

	<u>Unstimulated</u> <u>$\gamma\delta$ T cells</u>			<u>IL2 stimulated</u> <u>$\gamma\delta$ T cells</u>			<u>BrHPP stimulated</u> <u>$\gamma\delta$ T cells</u>		
	Cytokine Concentration (pg/ml)			Cytokine Concentration (pg/ml)			Cytokine Concentration(pg/ml)		
	<i>ACT</i> (n=5)	<i>FI</i> (n=7)	P value	<i>ACT</i> (n=5)	<i>FI</i> (n=7)	P value	<i>ACT</i> (n=5)	<i>FI</i> (n=7)	P value
IL2	2.7 ± 0.9	17.2 ± 9.4	ns	13.7 ± 3.4	680.2±412	ns	14.1 ± 5.0	366.9±330.4	ns
IL4	5.4 ± 0.8	2.6 ± 0.6	*	18.3 ± 5.4	3.1 ± 0.6	**	20.2 ± 4.6	2.3 ± 0.7	***
IL6	1.9 ± 0.3	2318±471	**	2.4 ± 0.09	2375±537.8	**	2.24 ± 0.07	2563±498.7	**
IL10	3.8 ± 0.6	10.6 ± 3.2	ns	3.3 ± 0.6	12.2 ± 4.5	ns	3.9 ± 0.5	12.3 ± 3.8	ns
TNFα	67.5 ± 37	205.7± 38.3	*	165.5±82	254.9±48.9	ns	188.1±90.9	547.1±104.9	*
IFNγ	274.1±111	3.2 ± 0.2	**	706.5±211	33.5±29.21	**	879.7±240	260.7±101.2	*
IL17	4.5 ± 4.1	2.0 ± 0.9	ns	0.3 ± 0.3	1.4 ± 0.5	ns	0.3 ± 0.3	1.4 ± 0.6	ns

Supplementary Figure 1



23c6-AF 488 DAPI



Resorption pits

Cytokine Dynamics of $\gamma\delta$ T Cells: A Double Edged Sword in Osteoclastogenesis

Swati Phalke and Shubhada V. Chiplunkar*

Chiplunkar Laboratory, Advanced Centre for Treatment, Research and Education in Cancer (ACTREC), Tata Memorial Centre, Navi Mumbai, India

*Corresponding author: Shubhada V. Chiplunkar, Chiplunkar Laboratory, Advanced Centre for Treatment, Research and Education in Cancer (ACTREC), Tata Memorial Centre, Kharghar, Navi Mumbai – 410210, India, Tel: +91-022-27405075; Fax: +91-022-27405080; E-mail: schiplunkar@actrec.gov.in

Received date: June 28, 2016; Accepted date: September 28, 2016; Published date: October 05, 2016

Copyright: © 2016 Phalke S, et al. This is an open-access article distributed under the terms of the Creative Commons Attribution License, which permits unrestricted use, distribution, and reproduction in any medium, provided the original author and source are credited.

Key words

$\gamma\delta$ T cells; Aminobisphosphonates; Cytokines; Osteoclastogenesis; IL6; IFN γ

Short Communication

Bone remodelling is necessary to maintain mineral homeostasis and structural integrity of bone. It is a continuous and highly coordinated process, which is essentially carried out by osteoblasts (bone forming cells) and osteoclasts (bone resorbing cells) through release of cytokines or soluble factors. Number of reports suggests that, tumor cells, immune cells and bone cells share cytokines, chemokines and signalling molecules. Conventional T cells ($\alpha\beta$ T cells) are known to enhance osteoclast generation and function through release of pro-osteoclastogenic factors like IL17 and RANKL. Although the presence of $\gamma\delta$ T cells in bone microenvironment has been reported, their role in bone biology is not well understood. Studies from our lab suggest that, depending on the activation status and cytokine dynamics, $\gamma\delta$ T cells can function in a pro or anti-osteoclastogenic manner. Activated $\gamma\delta$ T cells secrete higher levels of IFN γ (anti-osteoclastogenic cytokine) and inhibit the process of osteoclastogenesis, while non-activated $\gamma\delta$ T cells produce increased levels of IL6 (anti-osteoclastogenic cytokine) and were found to enhance osteoclast generation and function. Aminobisphosphonate Zoledronate has potent antiresorptive activity and is used for the treatment of postmenopausal osteoporosis and skeletal malignancies associated with metastatic cancer. Zoledronate is also known to be a potent activator of $\gamma\delta$ T cells. Aminobisphosphonates are embedded in bone due to their high affinity for calcium and get released in the bone microenvironment by resorbing osteoclasts. These Aminobisphosphonates activate $\gamma\delta$ T cells, which have antitumor and antiresorptive activity. The present review highlights the new role played by aminobisphosphonates in cancer patients through activation of effector functions of $\gamma\delta$ T cells and other immune cells, which extends beyond their well-defined antiresorptive function.

Bone is a dynamic structure and is continuously remodelled. To maintain the quality of the bone, it is necessary to replace old / damaged bone with new bone and this process is carried out by osteoblasts and osteoclasts. Osteoblasts are bone forming cells, which differentiate from mesenchymal stem cells, while osteoclasts are bone resorbing cells which are formed by fusion of monocyte-macrophage precursor cells under the influence of macrophage colony stimulating factor (M-CSF) and receptor activator of nuclear factor κ B ligand (RANKL). M-CSF is crucial for proliferation and survival of macrophages and osteoclast precursor cells [1] while RANKL is essential for differentiation of osteoclasts [2]. Osteoblasts and osteoclasts work in a tightly regulated manner to maintain the normal bone physiology, while imbalance results in pathological conditions such as osteopetrosis, osteoporosis, Paget's diseases, rheumatoid arthritis (RA), periodontal disease [3,4]. The process of bone

remodelling is regulated by cytokines present in the bone microenvironment.

There is enough data suggesting that immune cells influence skeletal system through cytokines, chemokines, signalling molecules and surface receptors [5]. Cytokines and chemokines released by macrophages, T lymphocytes, bone marrow cells and B cells present in the bone microenvironment mediate crosstalk between immune cells and bone cells. There is an increasing interest in studying how T cells are involved in bone metabolism and how they influence the generation and resorptive activity of osteoclasts [2,6,7]. Immune cells secrete an array of cytokines like IL6, IL17, TGF β , TNF α and RANKL which induce osteoclast formation and function, while cytokines like IL4, IL10, IL12, IL13, IL18 and IFN γ inhibit the process of osteoclastogenesis [8]. Conventional CD4+ T cells upon activation increase expression of RANKL and are known to be pro-osteoclastogenic [9]. IL17 producing CD4+ T cells cause bone destruction by inducing RANKL expression on synovial fibroblasts and osteoblasts. Although $\alpha\beta$ T cells are studied with respect to their role in bone biology, role of $\gamma\delta$ T cells has not been explored in detail.

$\gamma\delta$ T cells are a unique subset of T cells, which harbor properties of both innate and adaptive immune cells. They represent <10% of the total T cell population, where >90% population resides in peripheral blood and expresses V γ 9V δ 2 TCR. $\gamma\delta$ T cells possess unique properties with respect to antigen recognition, tissue tropism, MHC-independent antigen recognition and antitumor response. $\gamma\delta$ T cells recognize unique antigens, different from conventional $\alpha\beta$ T cells, which include small phosphoantigens such as isopentenyl pyrophosphate (IPP) and (E)-4-Hydroxy-3-methyl-but-2-enyl pyrophosphate (HMBPP), phospholipids, heat shock proteins, alkyl amines and aminobisphosphonates [10]. IPP is an intermediate molecule in eukaryotic mevalonate/ cholesterol pathway, while HMBPP is an intermediate molecule in bacterial non-mevalonate/ rohmer pathway. Aminobisphosphonates (Zoledronate), a class of potent antiresorptive drug, are used as a standard treatment modality to treat postmenopausal osteoporosis and cancer patients with bone metastasis [11,12]. $\gamma\delta$ T cells are Th1 type cells but are extensively plastic and differentiate into different subsets like Th2, Th17, T-follicular helper and T-regulatory cells under different pathological conditions, producing different sets of cytokines [13]. $\gamma\delta$ T cells have been appreciated for their role in antitumor cytotoxicity [14,15], wound healing and tissue repair [16-18] and thus have generated much interest in recent years. These cells produce several cytokines like IL17, IL6, IL10, TNF α , IFN γ and RANKL depending on their activation status. Many of these factors are known to influence bone metabolism. Most of the $\gamma\delta$ T cell based studies, in context of osteoimmunology, have been done in patients of rheumatoid arthritis (RA) and multiple myeloma [19,20]. Their presence has been demonstrated in bone microenvironment, in synovial fluids of rheumatoid arthritis patients and at bone fracture sites [19,21]. Various groups have also shown

presence of chemokine receptors like CCL5 and CCR1 on $\gamma\delta$ T cells, which indicate their propensity to migrate to bone. It has been reported that, Th17+ cells, and not IL17+ $\gamma\delta$ T cells drive arthritic bone destruction in RA patients [19]. In contrast, another report shows that, IL17+ producing $\gamma\delta$ T cells are increased in synovial fluids and peripheral blood of RA patients [21]. Also, RA patients have shown

changes in $\gamma\delta$ T cell subpopulations and their phenotypes [22,23]. Recently, IL17 producing $\gamma\delta$ T cells were shown to promote bone formation and facilitate bone fracture healing [24]. However, role of $\gamma\delta$ T cells in fracture healing has remained controversial as $\gamma\delta$ T cell deficient mice had shown stable fracture repair and better biochemical strength of bone [25].

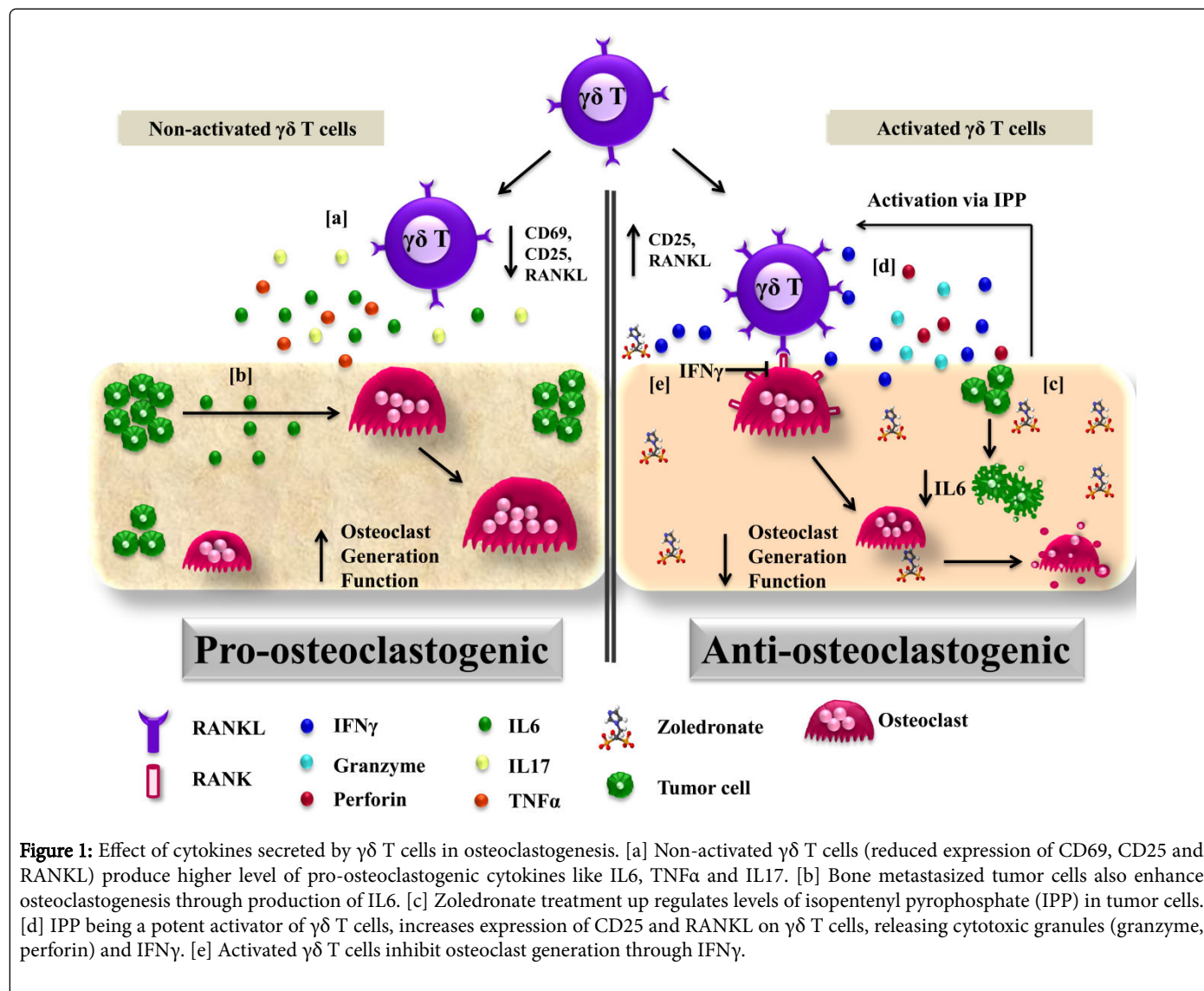


Figure 1: Effect of cytokines secreted by $\gamma\delta$ T cells in osteoclastogenesis. [a] Non-activated $\gamma\delta$ T cells (reduced expression of CD69, CD25 and RANKL) produce higher level of pro-osteoclastogenic cytokines like IL6, TNF α and IL17. [b] Bone metastasized tumor cells also enhance osteoclastogenesis through production of IL6. [c] Zoledronate treatment up regulates levels of isopentenyl pyrophosphate (IPP) in tumor cells. [d] IPP being a potent activator of $\gamma\delta$ T cells, increases expression of CD25 and RANKL on $\gamma\delta$ T cells, releasing cytotoxic granules (granzyme, perforin) and IFN γ . [e] Activated $\gamma\delta$ T cells inhibit osteoclast generation through IFN γ .

We believe that the functional differences observed with $\gamma\delta$ T cells may be attributed to their activation status. Studies from our lab investigated the role of non-activated and activated $\gamma\delta$ T cells in osteoclastogenesis. We have shown that $\gamma\delta$ T cells behave in both pro or anti-osteoclastogenic manner and it is the activation status (expression of CD69, CD25 and RANKL) and cytokine dynamics of $\gamma\delta$ T cells which dictates their ultimate behaviour [26]. Non-activated $\gamma\delta$ T cells produced higher levels of IL6 and were found to enhance osteoclastogenesis [26]. IL6 is a potent stimulator of osteoclast differentiation and activity [8]. IL6, TNF α and IL1 β work in a synergistic manner to stimulate osteoclast differentiation [27]. IL6 together with IL11 supports osteoclast formation and resorption [28]. Non-activated $\gamma\delta$ T cells were also found to secrete higher levels of TNF α , a proinflammatory cytokine, which directly and indirectly

enhances osteoclast generation and its resorptive activity [29,30]. TNF along with RANKL increases expression of RANK on osteoclast precursor cells [31]. TNF α and TGF β synergistically can induce osteoclastogenesis in the absence of TRAF6 or RANK, which explains potential role of TNF α in bone pathologies [29]. TNF and IL1 β synergistically promote expression of osteoprotegerin ligand (osteoprotegerin is a decoy receptor for RANKL) in osteoblasts [32], up regulates expression of RANKL on osteoblasts and stromal cells, stimulates differentiation of osteoclast precursor cells and increases activity and survival of osteoclasts by preventing apoptosis [33]. TNF α stimulates production of IL6 in osteoblasts and osteoblast-like osteosarcoma cells [34].

We demonstrated that, activated $\gamma\delta$ T cells inhibited osteoclast generation and function through secretion of increased levels of IFN γ

[26]. IFN γ inhibits generation (degradation of TRAF6 adaptor protein in RANKL signalling) and function (down regulated expression of cathepsin-k) in osteoclasts [35]. Stimulation of $\gamma\delta$ T cells with phosphoantigens (bromohydrin pyrophosphate) and Zoledronate increased the expression of RANKL along with increase in IFN γ secretion. Increased RANKL expression on activated $\gamma\delta$ T cells assists their interaction with osteoclasts; while increased IFN γ disrupts RANK-RANKL signalling, thus inhibiting osteoclast survival (Figure 1).

The present study has provided a new insight into understanding the crosstalk of $\gamma\delta$ T cells with osteoclasts that can be extrapolated to patients with bone metastasis such as multiple myeloma, breast and prostate cancer. Through a vicious cycle, metastasized tumor cells increase osteoclast generation, activity and survival by releasing cytokines such as IL6, PTHrP, TNF α and prostaglandin E2. These tumor cells recruit immune cells at bone microenvironment by releasing IL7, IL8 and parathyroid hormone related protein (PTHrP). Memory T cells have been detected in bone microenvironment but their proliferation and function are inhibited by increased levels of TGF β , released upon bone resorption by osteoclasts [36]. Blocking of TGF β at metastatic sites activates local antitumor immune responses by these T cells [37]. Thus, in case of bone metastasis, metastasized tumor cells exacerbate the situation by enhancing osteoclastogenesis and compromising the immune system.

Anti-IL6 or anti-RANKL therapies have shown effective results in control of bone metastasis. Zoledronate, a third generation aminobisphosphonate, is a most potent antiresorptive drug, with antitumor activity [38]. It has high affinity for bone minerals and thus gets incorporated into bone and is slowly released in the bone microenvironment by resorbing osteoclasts. Zoledronate inhibits farnesyl pyrophosphate synthase (FPPS), a key enzyme in mevalonate pathway/ cholesterol pathway, which causes osteoclast and tumor cell apoptosis. Inhibition of FPPS causes accumulation of IPP, which in turn activates $\gamma\delta$ T cells. $\alpha\beta$ T cells remain unaffected upon amino bisphosphonate treatment [38,39].

In this scenario, Zoledronate treatment to breast cancer patients provides a favorable environment for the consistent activation of the $\gamma\delta$ T cells in bone microenvironment. Activation of $\gamma\delta$ T cells through aminobisphosphonates could exert a potent inhibitory effect on osteoclasts and tumor cells. Activated $\gamma\delta$ T cells mediate their cytotoxic effects through release of perforin, granzyme and cytokines (IFN γ and TNF α). IFN γ alone has an ability to up regulate expression of MHC I and II molecules and promote activation of CD4+, CD8+ T cells, B cells, dendritic cells and monocyte-macrophage precursor cells and thus increase antigen presentation by these cells [40]. Activated CD4+ T cells secrete pro-osteoclastogenic cytokines like IL17, TNF α , IL1 β and IL6 which support and enhance osteoclastogenesis. Unlike $\alpha\beta$ T cells, $\gamma\delta$ T cells are Th1 cells and predominantly produce copious amount of IFN γ upon activation. IFN γ has multiple antitumor effects like direct inhibition of tumor growth, inhibition of angiogenesis and macrophage stimulation. It has also been reported that, metastatic breast cancer cells produce factors which promote survival of osteoclasts and block the apoptotic effects of bisphosphonates [41]. Aminobisphosphonates can activate $\gamma\delta$ T cells that are capable of exhibiting antitumor effects. This action of aminobisphosphonates may counteract the inhibitory effects of tumor derived factors.

A growing body of evidence points towards the role of $\gamma\delta$ T cells as an anticancer immunotherapeutic treatment modality. Bisphosphonates are known to activate $\gamma\delta$ T cells and therefore, their

use in cancer therapy warrants further investigation. Bisphosphonates can be used as bone targeting anticancer agent that have direct effect on tumor cell proliferation, invasion and bone metastasis. The interesting aspect is that cytokines (IFN γ) released by bisphosphonate activated $\gamma\delta$ T cells has anti-osteoclastogenic effect. Fine tuning the activation status and cytokine dynamics of $\gamma\delta$ T cells may pave way for development of future immunotherapeutic modalities for patients with primary breast, prostate cancer and multiple myeloma and bone metastasis.

References

1. Takayanagi H (2007) Osteoimmunology: shared mechanisms and crosstalk between the immune and bone systems. *Nat Rev Immunol* 7: 292-304.
2. Takayanagi H, Ogasawara K, Hida S, Chiba T, Murata S, et al. (2000) T-cell-mediated regulation of osteoclastogenesis by signalling cross-talk between RANKL and IFN-gamma. *Nature* 408: 600-605.
3. Drake MT (2013) Osteoporosis and cancer. *Curr Osteoporos Rep* 11: 163-170.
4. Boyle WJ, Simonet WS, Lacey DL (2003) Osteoclast differentiation and activation. *Nature* 423: 337-342.
5. Lee SK, Lorenzo J (2006) Cytokines regulating osteoclast formation and function. *Curr Opin Rheumatol* 18: 411-418.
6. Rifas L, Weitzmann MN (2009) A novel T cell cytokine, secreted osteoclastogenic factor of activated T cells, induces osteoclast formation in a RANKL-independent manner. *Arthritis Rheum* 60: 3324-3335.
7. Weitzmann MN, Cenci S, Rifas L, Haug J, Dipersio J, et al. (2001) T cell activation induces human osteoclast formation via receptor activator of nuclear factor kappaB ligand-dependent and -independent mechanisms. *J Bone Miner Res* 16: 328-337.
8. Datta HK, Ng WF, Walker JA, Tuck SP, Varanasi SS (2008) The cell biology of bone metabolism. *J Clin Pathol* 61: 577-587.
9. Kotake S, Nanke Y, Mogi M, Kawamoto M, Furuya T, et al. (2005) IFN-gamma-producing human T cells directly induce osteoclastogenesis from human monocytes via the expression of RANKL. *Eur J Immunol* 35: 3353-3363.
10. Born WK, Kemal Aydintug M, O'Brien RL (2013) Diversity of gammadelta T-cell antigens. *Cell Mol Immunol* 10: 13-20.
11. Rizzoli R (2010) Zoledronic Acid for the treatment and prevention of primary and secondary osteoporosis. *Ther Adv Musculoskelet Dis* 2: 3-16.
12. Drake MT, Clarke BL, Khosla S (2008) Bisphosphonates: mechanism of action and role in clinical practice. *Mayo Clin Proc* 83: 1032-1045.
13. Caccamo N, Todaro M, Sireci G, Meraviglia S, Stassi G, et al. (2013) Mechanisms underlying lineage commitment and plasticity of human gammadelta T cells. *Cell Mol Immunol* 10: 30-34.
14. Konigshofer Y, Chien YH (2006) Gammadelta T cells - innate immune lymphocytes? *Curr Opin Immunol* 18: 527-533.
15. Kabelitz D, Kalyan S, Oberg HH, Wesch D (2013) Human Vdelta2 versus non-Vdelta2 gammadelta T cells in antitumor immunity. *Oncoimmunology* 2: e23304.
16. Sharp LL, Jameson JM, Cauvi G, Havran WL (2005) Dendritic epidermal T cells regulate skin homeostasis through local production of insulin-like growth factor 1. *Nat Immunol* 6: 73-79.
17. Jameson JM, Cauvi G, Sharp LL, Witherden DA, Havran WL (2005) Gammadelta T cell-induced hyaluronan production by epithelial cells regulates inflammation. *J Exp Med* 201: 1269-1279.
18. Havran WL, Jameson JM, Witherden DA (2005) Epithelial cells and their neighbors. III. Interactions between intraepithelial lymphocytes and neighboring epithelial cells. *Am J Physiol Gastrointest Liver Physiol* 289: G627-630.

19. Pollinger B, Junt T, Metzler B, Walker UA, Tyndall A, et al. (2011) Th17 cells, not IL-17+ gammadelta T cells, drive arthritic bone destruction in mice and humans. *J Immunol* 186: 2602-2612.
20. Cui Q, Shibata H, Oda A, Amou H, Nakano A, et al. (2011) Targeting myeloma-osteoclast interaction with Vgamma9Vdelta2 T cells. *Int J Hematol* 94: 63-70.
21. Meliconi R, Pitzalis C, Kingsley GH, Panayi GS (1991) Gamma/delta T cells and their subpopulations in blood and synovial fluid from rheumatoid arthritis and spondyloarthritis. *Clin Immunol Immunopathol* 59: 165-172.
22. Bank I, Cohen L, Mouallem M, Farfel Z, Grossman E, et al. (2002) gammadelta T cell subsets in patients with arthritis and chronic neutropenia. *Ann Rheum Dis* 61: 438-443.
23. Bodman-Smith MD, Anand A, Durand V, Youinou PY, Lydyard PM (2000) Decreased expression of FcgammaRIII (CD16) by gammadelta T cells in patients with rheumatoid arthritis. *Immunology* 99: 498-503.
24. Ono T, Okamoto K, Nakashima T, Nitta T, Hori S, et al. (2016) IL-17-producing gammadelta T cells enhance bone regeneration. *Nat Commun* 7: 10928.
25. Colburn NT, Zaal KJ, Wang F, Tuan RS (2009) A role for gamma/delta T cells in a mouse model of fracture healing. *Arthritis Rheum* 60: 1694-1703.
26. Phalke SP (2015) Activation status of $\gamma\delta$ T cells dictates their effect on osteoclast generation and bone resorption. *Bone Reports* 1: 8.
27. Devlin RD, Reddy SV, Savino R, Ciliberto G, Roodman GD (1998) IL-6 mediates the effects of IL-1 or TNF, but not PTHrP or 1,25(OH)2D3, on osteoclast-like cell formation in normal human bone marrow cultures. *J Bone Miner Res* 13: 393-399.
28. Kudo O, Sabokbar A, Pocock A, Itonaga I, Fujikawa Y, et al. (2003) Interleukin-6 and interleukin-11 support human osteoclast formation by a RANKL-independent mechanism. *Bone* 32: 1-7.
29. Kim N, Kadono Y, Takami M, Lee J, Lee SH, et al. (2005) Osteoclast differentiation independent of the TRANCE-RANK-TRAF6 axis. *J Exp Med* 202: 589-595.
30. Cenci S, Weitzmann MN, Roggia C, Namba N, Novack D, et al. (2000) Estrogen deficiency induces bone loss by enhancing T-cell production of TNF-alpha. *J Clin Invest* 106: 1229-1237.
31. Zhang YH, Heulsmann A, Tondravi MM, Mukherjee A, Abu-Amer Y (2001) Tumor necrosis factor-alpha (TNF) stimulates RANKL-induced osteoclastogenesis via coupling of TNF type 1 receptor and RANK signaling pathways. *J Biol Chem* 276: 563-568.
32. Hofbauer LC, Lacey DL, Dunstan CR, Spelsberg TC, Riggs BL, et al. (1999) Interleukin-1beta and tumor necrosis factor-alpha, but not interleukin-6, stimulate osteoprotegerin ligand gene expression in human osteoblastic cells. *Bone* 25: 255-259.
33. Weitzmann MN, Pacifici R (2006) Estrogen deficiency and bone loss: an inflammatory tale. *J Clin Invest* 116: 1186-1194.
34. Kurokouchi K, Kambe F, Yasukawa K, Izumi R, Ishiguro N, et al. (1998) TNF-alpha increases expression of IL-6 and ICAM-1 genes through activation of NF-kappaB in osteoblast-like ROS17/2.8 cells. *J Bone Miner Res* 13: 1290-1299.
35. Kamolmatyakul S, Chen W, Li YP (2001) Interferon-gamma down-regulates gene expression of cathepsin K in osteoclasts and inhibits osteoclast formation. *J Dent Res* 80: 351-355.
36. D'Amico L, Roato I (2012) Cross-talk between T cells and osteoclasts in bone resorption. *Bonekey Rep* 1: 82.
37. Wrzesinski SH, Wan YY, Flavell RA (2007) Transforming growth factor-beta and the immune response: implications for anticancer therapy. *Clin Cancer Res* 13: 5262-5270.
38. Dhar S, Chiplunkar SV (2010) Lysis of aminobisphosphonate-sensitized MCF-7 breast tumor cells by Vgamma9Vdelta2 T cells. *Cancer Immunol* 10: 10.
39. Fournier PG, Chirgwin JM, Guise TA (2006) New insights into the role of T cells in the vicious cycle of bone metastases. *Curr Opin Rheumatol* 18: 396-404.
40. Schroder K, Hertzog PJ, Ravasi T, Hume DA (2004) Interferon-gamma: an overview of signals, mechanisms and functions. *J Leukoc Biol* 75: 163-189.
41. Hussein O, Tiedemann K, Komarova SV (2011) Breast cancer cells inhibit spontaneous and bisphosphonate-induced osteoclast apoptosis. *Bone* 48: 202-211.

Understanding the crosstalk between $\gamma\delta$ T cells and osteoclasts in patients with breast cancer

Shubhada Chiplunkar^{1*}, Swati P. Phalke¹, Vani Parmar² and Rajendra A. Badwe²

¹ ACTREC-TMC, India

² Tata Memorial Hospital, India

Bone metastasis is a common cause of morbidity in breast cancer patients. Aminobisphosphonates are widely used in treatment of bone metastasis and skeletal disorders. Aminobisphosphonates increase endogenous pool of isopentenyl pyrophosphate (IPP) of mevalonate pathway in tumor cells, which acts as potent antigen for $\gamma\delta$ T cells. $\gamma\delta$ T cells are unique subsets of T-lymphocytes that are activated by aminobisphosphonates and phosphoantigens (bromohydrin pyrophosphate, IPP). The present study aims at understanding the crosstalk between $\gamma\delta$ T cells and osteoclasts in patients with breast cancer metastasis. Multicolor flow cytometry showed higher expression of RANKL on $\gamma\delta$ T cells of breast cancer patients. Stimulation with aminobisphosphonate (zoledronate) increased RANKL expression on $\gamma\delta$ T cells. Osteoclasts generated from CD14⁺ monocytes of breast cancer patients and healthy individuals in the presence of zoledronate activated $\gamma\delta$ T cells showed reduced osteoclastogenesis as analysed by 23c6 mAb (CD51/61) and DAPI staining. Osteoclasts generated in the presence of cell free supernatants of activated $\gamma\delta$ T cells showed reduced resorption area (pits) on Osteoclast Activity Assay Substrate. Cytokine analysis of activated $\gamma\delta$ T cells showed presence of IFN- γ , antiosteoclastogenic cytokine. Zoledronate activated $\gamma\delta$ T cells have high propensity to migrate to bone and inhibit osteoclastogenesis. Aminobisphosphonate activated $\gamma\delta$ T cell based immunotherapy would be a promising approach to treat bone metastasis in breast cancer.

Keywords: Aminobisphosphonates, $\gamma\delta$ T cells, Osteoclasts, bone metastasis, breast cancer

Conference: 15th International Congress of Immunology (ICI), Milan, Italy, 22 Aug - 27 Aug, 2013. **Presentation Type:** Abstract **Topic:** Innate immunity

Citation: Chiplunkar S, Phalke SP, Parmar V and Badwe RA (2013). Understanding the crosstalk between $\gamma\delta$ T cells and osteoclasts in patients with breast cancer. *Front. Immunol. Conference Abstract: 15th International Congress of Immunology (ICI)*. doi: 10.3389/conf.fimmu.2013.02.01017

Received: 30 Jun 2013; **Published Online:** 22 Aug 2013.

* **Correspondence:** Prof. Shubhada Chiplunkar, ACTREC-TMC, Navi Mumbai, Maharashtra, 410210, India, schiplunkar@actrec.gov.in

